# Studying face individualization through Event Related and Steady State Visual Evoked Potentials techniques in healthy and prosopagnosic individuals

Esther Alonso Prieto

Institute of Research in Psychology (IPSY)
Center for Cognitive and Systems Neuroscience

Université catholique de Louvain

A thesis submitted for the degree of

*PhilosophiæDoctor*

2011 October

# Abstract

Discriminating the identity of a person by the facial appearance is a ubiquitous facet of daily life supported by a distributed network of brain areas. This neural network has been divided into two distinct subsystems: a core system, which supports the visual analysis of faces, and an extended system, concerned with the construal of person knowledge.

It is widely accepted that three main anatomical structures compose the face perception core system: the occipital face area (OFA), the fusiform face area (FFA) and the posterior superior temporal sulcus (STS). However, the temporal activation course of these structures during face perception is not fully understood. Event Related Potential (ERP) studies of prosopagnosic patients can help to clarify this issue.

In the first part of the current thesis (Study 1) this approach was adopted to:

1. characterize the electrophysiological profile of a well known case of prosopagnosia (patient PS);
2. determine whether the N170 face effect (the amplitude increase exhibited by the N170 component when faces are presented compared to other object categories) and the N170 face inversion effect (amplitude and latency increases of this component in response to inverted faces compared to upright faces) are present in this patient despite extensive damages in the territory of the right inferior occipital gyrus that encompasses the territory of the OFA;
3. determine whether the obtained outcome is replicable across techniques (i.e., studying Event Related Fields (ERF) by means of magnetoencephalogram (MEG)).

The results demonstrated that:

1. PS electrophysiological profile exhibits differences compared to healthy controls, which might be due to changes in brain volume conductive properties after the lesion;

2. despite these differences, she exhibits an N170 face effect and an N170 face inversion effect similar to that exhibited by healthy controls;
3. all results can be replicated using MEG.

While the first result is of usefulness to future EEG/MEG studies of patient PS, the second result helps to clarify the timing of the face selective FFA activations observed in this patient using functional Magnetic Resonance Imaging (fMRI). It also brings support to non-hierarchical models of face perception and sheds light on the debate about the neural sources of the face selective component N170 and its magnetic counterpart, the M170.

Motivated by result # 1 obtained in Study 1, the second part of this thesis, Studies 2 to 4, focused on the introduction of the Steady State Visual Evoked Potentials (SSVEP) technique in the study of face perception in healthy and prosopagnosic individuals. In contrast to ERPs, SSVEPs have a higher signal to noise ratio and can be objectively quantified. As a result, SSVEP measures are less influenced by possible changes to brain volume conductive properties.

Study 2 presents an experiment aimed at:

1. demonstrating that the SSVEP sensitivity to facial identity appears despite variations in several dimensions of the stimuli such as face gender, skin color and presence of hair.

Study 3 presents another experiment aimed at:

1. determining the range of stimulation frequencies for which the SSVEP sensitivity to facial identity is highest.

The results demonstrated that:

1. the sensitivity of the SSVEP to facial identity can be observed despite the modifications introduced to the facial stimuli;
2. those modifications can produce subtle changes in the efficiency of face individualization processes, which can be captured by the SSVEP;
3. the stimulation frequency at which the SSVEP sensitivity to facial identity is highest ranges between 4 and 9.09 Hz (the optimal frequency is 5.88 Hz).

These results have important methodological implications for future SSVEP studies of face perception as well as for current theories about the temporal dynamics of brain processes.

Going a step further, Study 4 presents two experiments aimed at:

1. demonstrating that the optimal testing conditions identified in Study 2 and 3 can be extrapolated to patient PS.

This study demonstrated that indeed, patient PS can be tested under the same conditions as healthy individuals. Additionally, it gives further support to the demonstration that the SSVEP technique is sensitive to changes in the efficiency of face perception processes.

Summarizing, this thesis brings further theoretical knowledge about the functional organization of the face perception neuronal network. It also demonstrates that ERPs and especially SSVEPs, are useful measures to study how the brain processes facial identity and provides important methodological guidelines for future research in this field.

To my parents

# Acknowledgements

I once heard that places are as special as the persons we meet in them: I totally agree. For me, Brussels will always be a wonderful city not because of its medieval palaces and its chocolate stores but because of all the colleagues and friends who extended their hands and hearts to me during all these three years and knew how to support me and criticize me during the preparation of this thesis. They include Dana Kuefner, Adriano Boremanse, Goedelle Van Belle, Susanne Quadflieg, Joan Liu, Meike Ramon, Renaud Laguesse, Waldo Rosales and Dr. Rik Henson.

D. Kuefner, A. Boremanse and J. Liu assisted me with great enthusiasm during EEG recording and data analysis.

G. Van Belle provided wise recommendations on the statistical analysis of the data.

S. Quadflied gave constructive advice on how to write this thesis.

M. Ramon and R. Laguesse helped me to prepare the facial stimuli used in the experiments.

Dr. R. Henson provided invaluable contributions to the completion of Study 1.

W. Rosales, besides invested his time generously to write efficient MATLAB codes for the analysis of the data and teach me during the process; also stoically endured long hours of discussions on the theoretical implications of the experimental results. *More importantly, you simply knew how to be there when I cried, when I was irritated, when I forgot to eat, when I needed you most.*

I am also indebted to my supervisor, Prof. B. Rossion for his scientific guidance but specially for his unconditional support during times of darkness.

Further thanks go to all individuals who participated in the experiments, especially prosopagnosic patients PS, LR and GG. Without their patience and professional behavior the experiments presented in this thesis would not have been possible.

# Contents

**List of Figures** **vii**

**List of Tables** **xiii**

**Glossary** **xv**

**1 General Introduction** **1**
1.1 EEG and MEG . . . . . 5
1.1.1 Event Related Potentials . . . . . 10
1.1.2 Steady State Potentials . . . . . 12
1.1.3 Steady state and transient responses: similar or different phenomena? . . . . . 17
1.2 Brain lesion studies: when the damaged brain speaks . . . . . 20
1.2.1 Prosopagnosia . . . . . 23
1.2.2 Patient PS . . . . . 25

**2 Early FFA activation in a prosopagnosic patient with damage to the OFA: an N170 study** **29**
2.1 Functional and anatomical breakdown of face individualization . . . . . 29
2.1.1 Identification of face-selective brain regions . . . . . 30
2.1.2 Specialization within face-responsive areas: linking structure to function . . . . . 31
2.1.3 Functional relations among face selective areas: a distributed, hierarchical model of face perception . . . . . 35
2.1.4 The N170/M170 components and face perception . . . . . 38
2.1.4.1 Nature of the facial information encoded by the N170 . 38
2.1.4.2 The magnetic counterpart of the N170, the M170 . . . 44
2.1.4.3 Neuronal sources of the N170/M170 . . . . . 44
2.2 Study 1: Early (N170) face-sensitivity despite right lateral occipital brain damage in acquired prosopagnosia . . . . . 46

2.2.1 Introduction . . . 47
2.2.2 Methods . . . 51
2.2.2.1 Participants . . . 51
2.2.2.2 Stimuli . . . 51
2.2.2.3 Procedure . . . 54
2.2.3 Results . . . 57
2.2.3.1 EEG Data. Experiment 1: Faces vs. Objects . . . 57
2.2.3.2 EEG data. Experiment 2: Face Inversion . . . 71
2.2.3.3 MEG data. Experiment 1: faces vs. objects . . . 73
2.2.3.4 MEG data. Experiment 2: Face Inversion . . . 79
2.2.4 Discussion . . . 84
2.2.4.1 Generic face sensitive processes as reflected in the N170/M170 face effect . . . 84
2.2.4.2 The right inferior occipital cortex is not necessary to generate the right N170 / M170 effect . . . 85
2.2.4.3 The absence of left N170 following the left middle fusiform lesion . . . 87
2.2.4.4 The effect of face inversion on the N170 and M170 without right inferior occipital cortex . . . 88
2.2.5 Conclusions . . . 89

**3 Characterization of the SSVEP sensitivity to facial identity in healthy humans 91**
3.1 Relation between stimulus characteristics and the steady state brain response . . . 91
3.2 Study 2: SSVEP sensitivity to facial identity across variations in face appearance . . . 96
3.2.1 Introduction . . . 97
3.2.2 Materials and methods . . . 99
3.2.2.1 Participants . . . 99
3.2.2.2 Stimuli . . . 99
3.2.2.3 Procedure . . . 101
3.2.2.4 EEG recording . . . 103
3.2.2.5 EEG analysis . . . 103
3.2.3 Results . . . 105
3.2.3.1 Behavior . . . 105
3.2.3.2 Frequency domain analysis: entrainment and SSFRE at the stimulation frequency . . . 105
3.2.3.3 Time-frequency analysis . . . 106

3.2.3.4 Narrow-band filtering . . . 123
3.2.4 Discussion . . . 125
3.3 Study 3: Defining the fundamental stimulation frequency for individual face perception . . . 128
3.3.1 Introduction . . . 129
3.3.2 Materials and methods . . . 131
3.3.2.1 Participants . . . 131
3.3.2.2 Stimuli . . . 131
3.3.2.3 Experimental procedure, EEG recording and analysis . 131
3.3.3 Results . . . 133
3.3.3.1 Behavior . . . 133
3.3.3.2 Entrainment of the scalp signal to the stimulation frequency . . . 133
3.3.3.3 SSFRE at the fundamental frequency . . . 133
3.3.3.4 SSFRE at harmonics of the fundamental frequency . . 154
3.3.4 Discussion . . . 157
3.3.4.1 Optimal stimulus presentation rate to process individual face information in the human brain . . . 157
3.3.4.2 SSFRE as a function of harmonic frequencies . . . 162
3.3.5 Conclusions . . . 163

**4 Characterization of the SSVEP sensitivity to facial identity in prosopagnosic patient PS 165**
4.1 Study 4: Steady State Visual Potentials to individual faces in acquired prosopagnosia . . . 165
4.1.1 Introduction . . . 166
4.1.2 Materials and methods . . . 167
4.1.2.1 Participants . . . 167
4.1.2.2 Experimental procedure and EEG recording . . . 168
4.1.2.3 EEG recording . . . 168
4.1.3 Results . . . 169
4.1.3.1 Experiment 1 . . . 169
4.1.3.2 Experiment 2 . . . 176
4.1.4 Discussion . . . 178
4.1.5 Conclusions . . . 180

**5 General discussion and future perspectives 181**

**References 185**

# List of Figures


1.1 SSVEP elicited by the rhythmic presentation of identical and different faces. . . . 4
1.2 Schematic representation of the biophysical mechanisms underlying the generation of the EEG. . . . 7
1.3 Schematic representation of ERP recording and analysis procedures. . . . 9
1.4 Schematic representation of transient and steady state electrophysiological responses. . . . 10
1.5 Schematic representation of the FFT technique. . . . 14
1.6 Comparison of sinusoidal and square stimulation. . . . 15
1.7 Comparison of the frequency spectrum of sinusoidal and square waveforms. 16
1.8 Schematic representation of the superposition hypothesis about the generation of the steady state brain response. . . . 18
1.9 Entrainment of neural oscillations in a simple phase oscillator model. . . . 21
1.10 Location of the brain lesions that lead to prosopagnosia. . . . 24
1.11 Pattern of lesions in PS brain. . . . 25
1.12 Summary of PS visual functions. . . . 27

2.1 FMRI face selective activations on an inflated brain of one subject. . . . 32
2.2 Distributed model for face perception proposed by Haxby and colleagues. 35
2.3 Nonhierarchical organization of human face perception as proposed by Rossion (2008). . . . 37
2.4 Typical VPP and N170. . . . 39
2.5 Mooney and Arcimboldo faces. . . . 41
2.6 Adaptation phenomenon in the N170 . . . . 42
2.7 The composite face effect and the inversion face effect . . . . 43
2.8 Brain damage profile of the acquired prosopagnosia patient PS. . . . 52
2.9 Experimental design applied in Study 1. . . . 53
2.10 Electrodes layout used for data recording in Study 1 . . . . 55
2.11 Results obtained by healthy participants in experiment 1 (faces vs. objects), Study 1. . . . 59

2.12 Averaged waveforms of the age-matched participants in response to faces, cars and their scrambled counterparts. . . . . 60
2.13 Scalp voltage distribution of P1 and N170 components for age-matched participants. . . . . 61
2.14 Evolution of electrophysiological responses to visual stimulation at the back of the head of patient PS. . . . . 64
2.15 Waveforms recorded over PS' scalp following visual stimulation in experiment 1 (faces vs. objects). . . . . 65
2.16 PS' EEG waveforms for each of the experimental repetitions of experiment 1 (faces vs. objects) and 2 (face inversion). . . . . 68
2.17 PS' waveforms re-referenced to Fz. . . . . 69
2.18 Normalized Face Effect Index and Normalized Face Inversion Effect Index 70
2.19 Results obtained by PS and age-matched healthy participants in experiment 2 (face inversion). . . . . 72
2.20 Results obtained by the group of young participants in experiment 2 (face inversion). . . . . 72
2.21 M100 component for patient PS in experiment 1 (faces vs. objects) as recorded by MEG magnetometers. . . . . 74
2.22 M170 component for patient PS in experiment 1 (faces vs. objects) as recorded by MEG magnetometers. . . . . 75
2.23 M170 component for patient PS in experiment 1 (faces vs. objects) as recorded by MEG gradiometers. . . . . 76
2.24 MEG superior left and right ROIs in experiment 1 (faces vs. objects). . 77
2.25 Evoked responses averaged across three channels for the more inferior left and right ROIs in experiment 1 (faces vs. objects). . . . . 78
2.26 M100 component for PS in experiment 2 (face inversion) as recorded by MEG magnetometers. . . . . 80
2.27 M170 component for PS in Experiment 2 (face inversion) as recorded by MEG magnetometers. . . . . 80
2.28 M170 component for PS in experiment 2 (face inversion) as recorded by MEG gradiometers. . . . . 81
2.29 Evoked responses averaged across three channels for the more superior left and right ROIs in experiment 2 (face inversion). . . . . 82
2.30 Evoked responses averaged across three channels for the more inferior left and right ROIs in experiment 2 (face inversion). . . . . 83

3.1 Frequency subsystems. . . . . 92
3.2 Facial stimuli employed in the experiment . . . . . 100
3.3 Schematic view of the experiment used in Study 2 . . . . . 102
3.4 128 electrodes layout used for EEG recording . . . . . 104

3.5 SNR values for all stimuli employed in Study 2 . . . . . 107
3.6 SSFRE scalp distribution for each stimulus type presented at 4.00 Hz . 108
3.7 SSFRE scalp distribution for each stimulus type presented at 5.88 Hz . 109
3.8 **Entrainment to the stimulation frequency (male and female real cropped faces, R - m and R - f, presented at 4.00 Hz).** . . 110
3.9 **Entrainment to the stimulation frequency (male and female real, gray, cropped faces, RG - m and RG - f, presented at 4.00 Hz).** . . . . . 111
3.10 **Entrainment to the stimulation frequency (male and female Max Planck faces, MP - m and MP - f, presented at 4.00 Hz).** 112
3.11 **Entrainment to the stimulation frequency (male and female KDEF faces, KDEF - m and KDEF - f, presented at 4.00 Hz).** 113
3.12 **Entrainment to the stimulation frequency (male and female real cropped faces, R - m and R - f, presented at 5.88 Hz).** . . 114
3.13 **Entrainment to the stimulation frequency (male and female real cropped faces, RG - m and RG - f presented at 5.88 Hz).** . 115
3.14 **Entrainment to the stimulation frequency (male and female Max Planck faces, MP - m and MP - f presented at 5.88 Hz).** . 116
3.15 **Entrainment to the stimulation frequency (male and female real cropped faces, KDEF - m and KDEF - f presented at 5.88 Hz).** . . . . . 117
3.16 Mean and standard deviation of the SSFRE for each stimulus type presented at 4.00 Hz . . . . . 118
3.17 Mean and standard deviation of the SSFRE for each stimulus type presented at 5.88Hz . . . . . 118
3.18 SSFRE obtained after collapsing across stimulus type . . . . . 119
3.19 Time frequency analysis of the EEG signal recorded in response to different faces presented at 4.00 Hz for electrode P8 . . . . . 120
3.20 Time frequency analysis of the EEG signal recorded in response to identical faces presented at 4.00 Hz for electrode P8 . . . . . 121
3.21 Subtraction of the time frequency decomposition of the EEG signal recorded in response to different - identical faces presented at 4.00 Hz for electrode P8 . . . . . 122
3.22 The amplitude of the EEG signal is displayed as a function of time for both conditions . . . . . 123
3.23 The EEG signal is displayed between 10 and 20 s post-stimulus for both conditions . . . . . 124
3.24 The EEG signal is displayed between 2 s before the stimulation and 10 s after for both conditions in electrode P8 . . . . . 125

3.25 Changes in the EEG signal across time in response to different faces . . 126
3.26 Schematic view of the experiment applied in Study 3 . . . . . 132
3.27 FFT power spectrum: 1.00 to 3.03 Hz . . . . . 134
3.28 FFT power spectrum: 4.00 to 5.88 Hz . . . . . 135
3.29 FFT power spectrum: 7.14 to 9.09 Hz . . . . . 136
3.30 FFT power spectrum: 10.00 to 12.48 Hz . . . . . 137
3.31 FFT power spectrum: 14.28 to 16.66 Hz . . . . . 138
3.32 SNR for stimulation frequencies 1.00 to 3.03 Hz. . . . . 139
3.33 SNR for stimulation frequencies 4.00 to 5.88 Hz. . . . . 140
3.34 SNR for stimulation frequencies 7.14 to 9.09 Hz. . . . . 141
3.35 SNR for stimulation frequencies 10.00 to 12.48 Hz. . . . . 142
3.36 SNR for stimulation frequencies 14.28 to 16.66 Hz. . . . . 143
3.37 SSFRE topographical distribution scaled for each frequency independently.144
3.38 SSFRE topographical distribution scaled according to the stimulation frequency that provoked the highest effect. . . . . 145
3.39 SSFRE between 4 and 11.11 Hz for each electrode . . . . . 146
3.40 Entrainment to the stimulation frequency (1.00 and 2.00 Hz). . . . . 147
3.41 Entrainment to the stimulation frequency (3.00 and 4.00 Hz). . . . . 148
3.42 Entrainment to the stimulation frequency (5.00 and 5.88 Hz). . . . . 149
3.43 Entrainment to the stimulation frequency (7.14 and 8.33 Hz). . . . . 150
3.44 Entrainment to the stimulation frequency (9.09 and 10.00 Hz). . . . . 151
3.45 Entrainment to the stimulation frequency (11.11 and 12.48 Hz). . . . . 152
3.46 Entrainment to the stimulation frequency (14.28 to 16.66 Hz). . . . . 153
3.47 SSFRE frequency sensitivity curve . . . . . 155
3.48 SSFRE frequency sensitivity curve for each participant . . . . . 156
3.49 The SSFRE scalp distribution for each stimulation frequency and corresponding harmonics for fundamental frequencies 1.00 to 5.00 Hz . . . . 158
3.50 The SSFRE scalp distribution for each stimulation frequency and corresponding harmonics for fundamental frequencies 5.88 to 10.00 Hz . . . 159
3.51 The SSFRE scalp distribution for each stimulation frequency and corresponding harmonics for fundamental frequencies 11.11 to 16.66 Hz . . . 160

4.1 SNR values obtained for patient PS: 1.00 to 3.03 Hz . . . . . 170
4.2 SNR values obtained for patient PS: 4.00 to 5.88 Hz . . . . . 171
4.3 SNR values obtained for patient PS: 7.14.00 to 9.09 Hz . . . . . 172
4.4 SNR values obtained for patient PS: 10.00 to 12.48 Hz . . . . . 173
4.5 SNR values obtained for patient PS: 14.28 to 16.66 Hz . . . . . 174
4.6 SSFRE topographic distribution for patient PS . . . . . 175
4.7 PS SSFRE frequency sensitivity curve . . . . . 176

4.8 SSFRE topographic distribution for healthy controls, sex and age matched with PS. . . . . 177
4.9 SSFRE frequency sensitivity curve of PS and age matched controls together with confidence intervals. . . . . 178
4.10 SSFRE topographic distribution for PS in response to the different types of facial stimuli used in this study. . . . . 179

## LIST OF FIGURES

# List of Tables


2.1 Behavioral results experiment 1 (faces vs. objects) . . . . . 58
2.2 Mean amplitude and latency values of P1 component for younger participants. . . . . 60
2.3 Mean amplitude and latency values of P1 component for PS. . . . . 63
2.4 Mean amplitude and latency values of N170 component for younger participants. . . . . 63
2.5 Mean amplitude and latency values of N170 component for PS. . . . . 66
2.6 Behavioral results experiment 2 (face inversion) . . . . . 71

# Glossary

**AP** Acquired Prosopagnosia

**EEG** Electroencephalogram

**ERP** Event Related Potential

**EPSP** Excitatory Postsynaptic Potential

**FFA** Fusiform Face Area

**FG** Fusiform Gyrus

**FFT** Fast Fourier Transform

**IPSP** Inhibitory Postsynaptic Potential

**LOC** Lateral Occipital Complex

**LGN** Lateral Geniculate Nucleus

**MEG** Magnetoencephalogram

**OFA** Occipital Face Area

**PET** Positron Emission Tomography

**SSFRE** Steady State Face Repetition Effect

**SSVEP** Steady State Visual Evoked Potential

**STS** Superior Temporal Sulcus

**TMS** Transcranial Magnetic Stimulation

**VPP** Visual Positive Potential

# Chapter 1

# General Introduction

Faces fascinate us. On a daily basis we identify our relatives, friends, even the strangers that walk the street alongside us based on their facial appearance. We are such experts in face perception that, in fact, we need less than a few seconds to determine a person's identity, gender and age, to recognize their emotions and appreciate their beauty. It is an effortlessly and yet extremely accurate act, which has always been there and which we take for granted.

The prominence of faces in our lives and the striking, face-specific impairments often found in the context of damage to particular brain areas have awaken scientists interest in the neuro-cognitive nature of face perception. Thus, research efforts have been directed to determine the anatomical structures that support these processes and the temporal course of their activations.

Concerning the neuroanatomy of face perception, data accumulated during the last decades have revealed a constellation of face-selective regions that respond more strongly to faces than to nonface objects. These regions are the lateral middle fusiform gyrus, encompassing the so-called fusiform face area (FFA), especially in the right hemisphere (Halgren *et al.*, 1999; Haxby *et al.*, 2000; Kanwisher *et al.*, 1997; McCarthy *et al.*, 2011; Rossion *et al.*, 2000a); and the inferior occipital gyrus, encompassing the so-called occipital face area (OFA) (Gauthier *et al.*, 2000). Although less consistently, larger activation for faces than objects has also been found in the superior temporal sulcus (STS) (Haxby *et al.*, 2000; Kanwisher & Yovel, 2006; Sergent & Signoret, 1992).

The precise function of these regions is still a matter of debate. It has been suggested that the OFA is concerned with the extraction of information about basic face features (Pitcher *et al.*, 2007); that the FFA is concerned with the integration of those features in a complex, holistic facial representation that lead to the identification of the face bearer (Atkinson & Adolphs, 2011; Grill-Spector *et al.*, 2004; Haxby *et al.*, 2000; Ishai *et al.*, 1999; Kanwisher & Yovel, 2006; Kanwisher *et al.*, 1997; Liu *et al.*, 2010; Pitcher *et al.*, 2011; Rossion, 2008) and that the STS is involved in the analysis of changeable

aspects of the face such as expression, gaze direction and speech related movements (Hasselmo *et al.*, 1989; Haxby *et al.*, 2000; Hoffman & Haxby, 2000; Oram & Perrett, 1996; Perrett *et al.*, 1985; Puce *et al.*, 2003).

Concerning the time course of face processes, intracranial studies of epileptic patients undergoing brain surgery have identified a series of Event Related Potentials (ERPs) whose amplitude increases when faces are presented. A sharp, negative component has been recorded around 200 ms with electrodes implanted in the lateral fusiform gyrus (FG) and also in the inferior temporal or inferior occipital gyri (Allison *et al.*, 1999; McCarthy *et al.*, 1999; Puce *et al.*, 1999). A sequence of ERPs between 130 and 250 ms (N130-P180-N240) has also been observed using face recognition tasks. While the P180 has been registered with electrodes placed in the ventral posterior temporal region, the N130 and N240 components have been observed in the temporal, parietal and frontal lobes (Allison *et al.*, 1999; Barbeau *et al.*, 2008; McCarthy *et al.*, 1999; Puce *et al.*, 1999).

On the scalp, a face selective negative component with a latency of about 170 ms has been identified (Bentin *et al.*, 1996; Boetzel *et al.*, 1995; George *et al.*, 1996; Rossion *et al.*, 2000b). The sensitivity of this scalp ERP to face perception processes is suggested by the observation that its amplitude increases when faces are presented compared to other object categories, the so-called N170 face effect (Bentin *et al.*, 1996; Boetzel *et al.*, 1995; Jacques *et al.*, 2007; Rossion & Caharel, 2011; Rossion *et al.*, 2000b). Additionally, both, the N170 amplitude and latency, increase when faces are presented upside down, the so-called N170 face inversion effect (Eimer, 2000a,b; Goffaux *et al.*, 2003; Itier & Taylor, 2002; Jeffreys, 1993, 1996; Rossion *et al.*, 1999, 2003a; Sagiv & Bentin, 2001). Last but not least, the N170 amplitude increases when different faces are presented compared to when identical faces are presented (Caharel *et al.*, 2009a; Ewbank *et al.*, 2008; Heisz *et al.*, 2006; Itier & Taylor, 2002; Jacques *et al.*, 2007).

Relating both dimensions in the healthy human brain, e.g., which areas do what and when, has proved to be elusive mainly because none of the available research methods provide anatomical and temporal information simultaneously and non-invasively. One possible way to overcome this limitation is studying individuals with acquired prosopagnosia (AP) by means of the electroencephalogram (EEG) or magnetoencephalogram (MEG). AP is a neurological syndrome that refers to the inability to recognize individual faces after the occurrence of damage to specific brain areas (Bodamer, 1947). The EEG/MEG detect the electric (EEG) and magnetic (MEG) fields produced by the electric potentials generated by neural currents and, as a result, both techniques are able to measure changes in neural activity on a millisecond time-scale. The lesional profile of prosopagnosic patients could inform us about the anatomical regions that are relevant for the processes under study whereas her/his electrophysiological or magnetoencephalographic profile would inform us about the activation time course of

the relevant anatomical structures. To put it more concretely, the presence or absence of face specific components, such as the N170 and its magnetic counterpart M170, in a prosopagnosic patient could tell us whether the damaged region is related with the processes that underlie the generation of the component during the latency window of its appearance.

In Chapter 2, this approach will be employed to address particular issues about the activation time course of the FFA and the neural generators of the N170/M170 components. Specifically, the face selectivity of the N170/M170 will be studied in a prosopagnosic patient with damage to the territory of the right OFA to demonstrate that: (1) the right OFA activation is not necessary to cause either the N170/M170 face effect nor the N170/M170 face inversion effect; (b) that face selective brain activations can take place within the first 170 ms after stimulus presentation even in absence of feedforward inputs from the OFA, which suggest that face preferential FFA responses observed in this patient using fMRI might be due to bottom-up early visual processes instead of top-down processes.

ERP studies in prosopagnosic patients are not exempt of difficulties, as it will be shown also in the study presented in Chapter 2. The difficulties are due to the fact that brain lesions can modify the volume conductive properties of the brain, which in turn might change the morphology of the ERP wave (van den Broek *et al.*, 1998). Such variations can be mistakenly interpreted as alterations in the cognitive processes underlying the component. In addition, changes in brain conductivity can result in an augment in the signal noise. Increasing the amount of trials does not fully solve this problem because it leads to long experiment times and participants fatigue. To overcome these difficulties, this thesis will also focus on the introduction and validation of another technique, the Steady State Visual Evoked Potential (SSVEP), in the field of face perception [1].

At least three advantages of SSVEP over transient ERPs and neuroimaging techniques justify the interest in using it to study face perception in healthy and diseased populations. First, in a brief period of time one can obtain data with an extremely high signal-to-noise ratio. This is due mainly to the fact that the experimenter can choose the stimulation frequency avoiding the ranges at which spontaneous EEG fluctuations and artifacts, e.g., alpha waves, blinks, and muscle potentials, tend to take place. Second, in SSVEP experiments, the brain electrical response to the stimulus occur at the same frequency as the stimulus. It implies that the variable of interest can be unequivocally selected and quantified in the frequency domain. Third, by presenting different stimulus features at distinct frequencies simultaneously (frequency tagging) it is possible to differentiate the brain response to each feature and determine the importance of the stimulus properties for a given process in the context of the same experiment.

[1] For a more detailed explanation on the SSVEP technique, the reader is referred to Section 1.1.

Recently, Rossion & Boremanse (2011) showed that, as for other stimulus types, SSVEP can also be obtained when neutral faces are presented to healthy individuals at a temporal rate of 3.5 Hz. Most importantly, they also showed that the amplitude of this response increases when the identity of the faces is varied compared to when it remains the same. These two observations demonstrated the sensitivity of the SSVEP to face individualization processes. Hence, the SSVEP can be used as a marker to study which facial features are particularly diagnostic during face individualization as well as the properties of the cognitive processes involved.

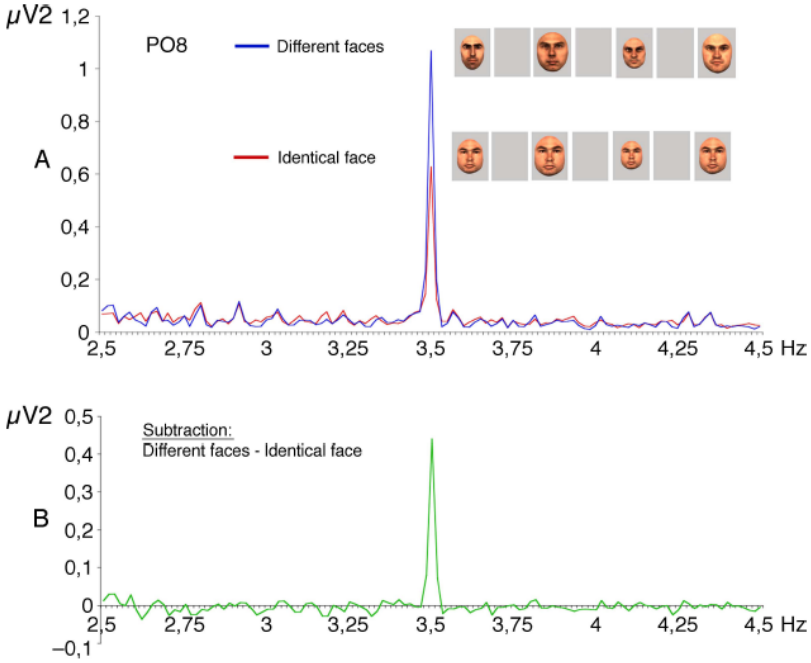


**Figure 1.1: SSVEP elicited by the rhythmic presentation of identical and different faces.** - (A) Power values obtained at different frequency points that range from 2.5 to 4.5 Hz centered on the fundamental stimulation frequency (3.5 Hz) in response to the presentation of different and identical faces (grand averaged of 12 participants). Note that different upright faces elicited a significantly larger response than identical upright faces. This difference between the two conditions of interest arises only at the frequency of stimulation. (B) Subtraction between the two conditions (different faces − identical face). Reproduced from Rossion & Boremanse (2011).

As the authors used only one type of facial stimuli, it is not known whether their results can be generalized to facial stimuli which, for example, present or not skin color, hair, face shape line etc. Manipulating such face features is common in face perception studies, which justifies the importance of determining whether they influence the sensitivity of the SSVEP technique to face perception brain processes.

Aditionally, in the study of Rossion & Boremanse (2011) only one stimulus presentation rate (3.5 Hz) was used. Consequently, it is still not known whether the sensitivity of the SSVEP to facial identity changes varies as a function of stimulation frequency and, thus, which experimental conditions should be employed in future studies to guarantee optimal results.

Chapters 3 and 4 of this thesis will focus on the above mentioned issues. Study 2 presented in Chapter 3 will aim to determine whether changes to features of the facial stimulus such as skin color and hair can influence the amplitude difference between SSVEPs elicited in response to different and identical faces. Specifically, it will be seen that although such SSVEP differential response can be elicited by different types of facial stimulus, it is higher for faces that present all external and internal features. Study 3 also presented in Chapter 3 will aim to determine the temporal presentation rate at which the SSVEP to a facial stimuli of varying identity is highest. It will be demonstrated that stimulus presentation rates between 4.00 and 9.09 Hz elicit the highest increase in the SSVEP amplitude when different faces are presented compared to when identical faces are presented and that this effect is highest at 5.88 Hz.

Finally, Chapter 4 will introduce a study aimed at determining whether the effect of varying the identity of a face on the SSVEP is also observed in prosopagnosic patient PS. Specifically, it will be demonstrated that the SSVEP technique is sensitive to variations in the efficiency of face individualization processes and thus, it can be used in the future to investigate face perception mechanisms in prosopagnosic patients. Additionally, it will show that at least in the case of patient PS, this technique can be employed under experimental conditions identical to those that are optimal to test healthy individuals.

This thesis is organized as follows. The remainder of Chapter 1 will provide a basic introduction to the most important aspects of the experimental techniques employed in all the studies presented here: EEG/MEG and brain lesion approach. Chapter 2, 3 and 4 will present the experimental contributions of this thesis: an ERP study of a very special case of prosopagnosia and three SSVEP studies of face discrimination in healthy and prosopagnosic individuals. These chapters will summarize the theoretical background needed to interpret the experimental results before presenting the studies themselves. Chapter 5 will present a general summary of the main experimental findings as well as of the conclusions that can be drawn from them.

## 1.1 EEG and MEG: Unique Windows into the Temporal Realm of Cognition

Hans Berger performed the first recording of the electrical activity of the human brain from the scalp in 1924, based on the pioneering work on electricity of animal bodies

by Luigi Galvani (1737-1798) and on exposed animal cortex by Richard Caton (1842-1926). Since its introduction and due to its high temporal resolution, the EEG has become an important technique to study the time evolution of sensory, cognitive and motor brain processes.

The exact nature of the voltage changes that can be recorded on the scalp is still not fully understood. There are two main types of electrical activity associated with neurons: action potentials and postsynaptic excitatory and inhibitory potentials (EPSP and IPSP). Action potentials are short-lasting, discrete voltage spikes generated along the cell, from its beginning to the terminals. They are triggered by the opening and closing of ion channels thereby altering the flux of ions and, as a consequence, the voltage difference across the cell membrane. The whole process takes about a millisecond, a time scale that restricts the maximum firing rate of the neuron (limited to a few hundred events per second) as well as the speed of action potentials propagation (limited to 0.5-50 meters per second depending on the caliber and insulation type of the axon cable). This time scale, together with the physical arrangement of axons in the brain, might prevent the observation of action potentials on the scalp: they could be registered by electrodes placed at great distances only under the rare circumstances that they occur synchronously in neurons whose axons run parallel to each other (Buzsaki, 2006; Nunez & Srinivasan, 2005).

IPSP and EPSP arise when the neurotransmitters bind onto specialized receptors on the membrane of the postsynaptic cell causing ion channels to open, if an excitatory neurotransmitter is released; or close, if an inhibitory neurotransmitter is released. In the first case, current will flow from the extracellular space into the cell (yielding a net negativity on the outside of the cell apical dendrites) and out of the cell body and basal dendrites (yielding a net positivity in this area). The opposite occurs in the second case. The combination of a negativity at one end of the neuron and a positivity at the other end creates a small dipole (a pair of opposite charges separated by a small distance) as it is shown in Figure 1.2 (Buzsaki, 2006; Nunez & Srinivasan, 2005).

Because of the long duration of postsynaptic potentials and because they are displayed by many more neurons than, e.g., action potentials, they have a high chance of summation. These chances increase if they are generated in the cortical pyramidal cells, which are aligned perpendicularly to the surface of the cortex (Figure 1.2). Because of these reasons, it has been suggested that the scalp EEG might reflect mainly the contribution of IPSP and EPSP along the apical dendrites of large clusters of pyramidal neurons. The contribution of the action potentials should be negligible (Buzsaki, 2006; Nunez & Srinivasan, 2005).

Besides running directly between the two poles of the dipole, electricity can travel through conductive mediums, e.g., the brain. When it reaches the scalp surface it can

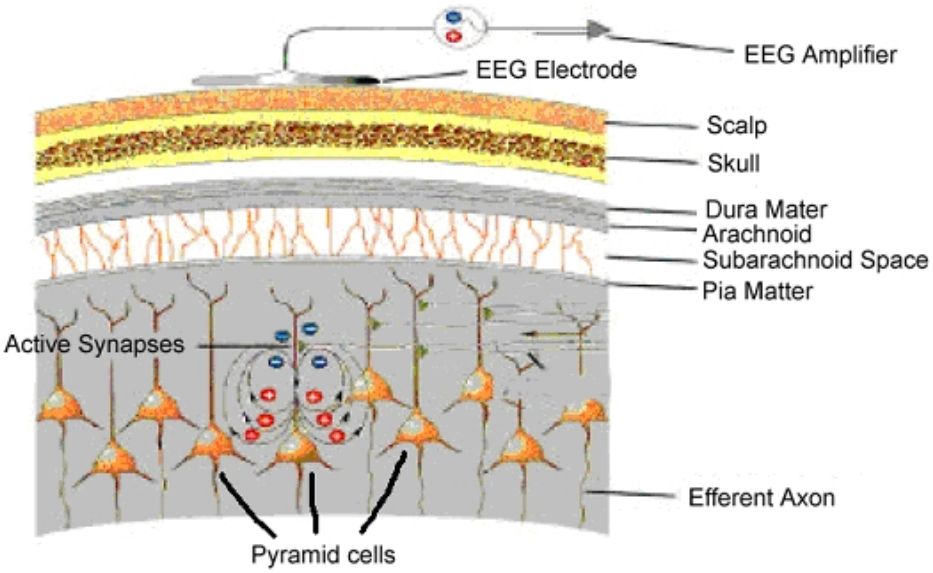


**Figure 1.2: Schematic representation of the biophysical mechanisms underlying the generation of the EEG.** - When postsynaptic potentials are generated within groups of pyramidal cells, a neuronal current dipole is created. Under the proper circumstances, the dipoles from individual neurons can summate and the produced voltage can be registered by the measuring instrument, e.g., electrode, placed on the scalp. The position and orientation of the neuronal dipoles determine the distribution of positive and negative voltages observed on the scalp signal.

be recorded as voltage or difference between electric potentials registered at two different points. As a result, not only the position and orientation of the generating dipoles but also the conductivity values of the brain, the skull and the scalp will influence the registered signal. Additionally, the electricity spreads out through the conductors and tends to follow the path of least resistance spreading laterally when it encounters the high resistance of the skull. Consequently, the surface or topographical distribution of the scalp signal lacks spatial resolution: it can not be assured that the voltage registered at a given electrode was generated by the anatomical structures located directly beneath (Nunez & Srinivasan, 2005). However, it does not lack temporal resolution. The scalp signal registers changes in the brain activity with a temporal resolution of milliseconds, a time scale closely related to cognition and behavior (Buzsaki, 2006; Nunez & Srinivasan, 2005).

The EEG is not the only technique able to measure the neuronal activity in the millisecond time scale. Electrical currents create an orthogonally oriented magnetic field which can also reach the scalp and be registered by means of superconductive quantum interference devices (SQUIDS). This is the functioning principle of another high temporal resolution technique, the magnetoencephalogram (MEG).

EEG and MEG are sensitive to different neuronal sources: while the former can capture the tangential as well as the radial components of a current source; the latter appears to be more sensitive only to the tangential components. Therefore, EEG is sensitive to the activation of neurons located at the top of the cortical gyri and in the sulci whereas MEG selectively measures the activity in the sulci (Nunez & Srinivasan, 2005).

To elicit the sensory, motor and cognitive brain processes of interest EEG/MEG researchers present subjects with particular stimuli, e.g., sounds, pictures, words etc., while registering their EEG/MEG scalp signal under standardized experimental conditions (Figure 1.3).

The obtained electrophysiological response can be classified as either transient or steady-state (Figure 1.4). The transient response implies that the brain mechanisms elicited by the external events are in a resting state when the stimulus is presented and comes back to such state before the arrival of the next stimuli (Regan, 1989). Given that the electric potentials generated this way display a stable time relation to the definable external event they have been called Event Related Potentials (ERPs) (Vaughan, 1972). The steady state potentials or responses imply that the constituent frequency components of the repetitive evoked potential remain constant in amplitude and phase during the stimulation (Regan, 1966, 1989). The next two sections will explain the main characteristics of both types of responses.

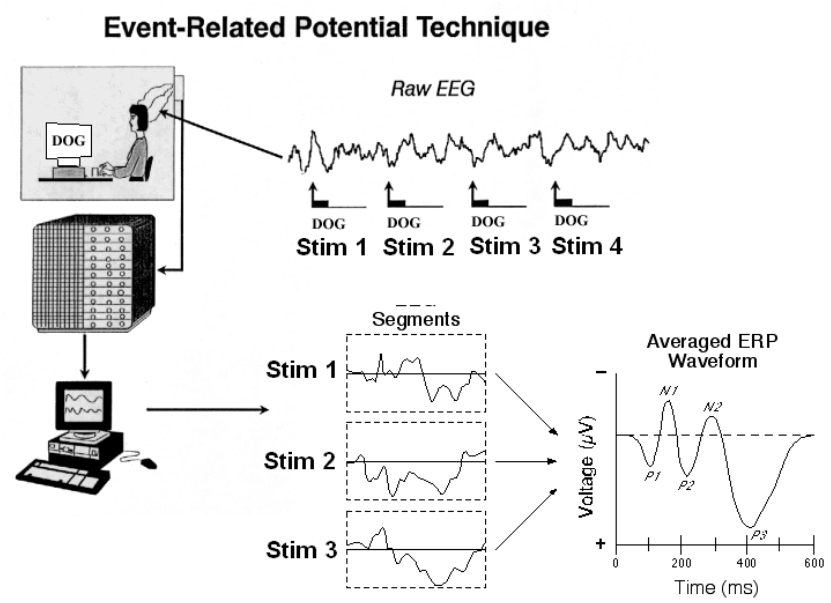


**Figure 1.3: Schematic representation of ERP recording and analysis procedures.** - ERPs are obtained by presenting subjects with a repetitive stimulation (e.g., the word 'dog') while registering their EEG/MEG scalp signal on a computer. The signal obtained in response to each of the stimulus is extracted in time segments and averaged together. The brain activity that did not occur at a consistent time relative to the stimuli is cancelled out. Only the activity related to the stimulation remains. The averaged waveform consist of a series of peaks (also called ERPs, potentials or components) that have been linked to specific cognitive processes.

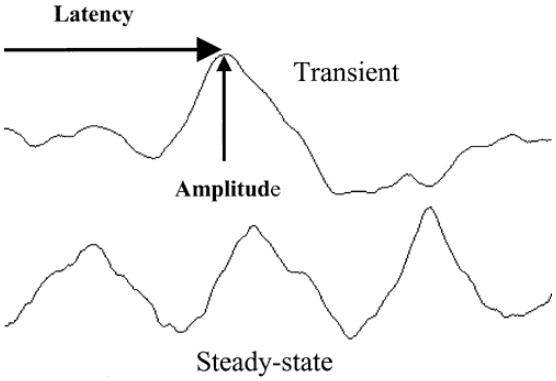


**Figure 1.4: Schematic representation of transient and steady state electrophysiological responses.** - Averaging the individual brain responses to the presentation of a pattern reversal visual stimulus can produce a transient waveform with a single major positive peak (figure top). If the stimulus is presented at a constant rhythmic rate a steady state response consisting of a cyclic waveform with positive and negative peaks can also be obtained (figure bottom). The main frequency component of such response will correspond to the stimulus presentation frequency. (Reproduced from Tasman & Jaeger (2001).

### 1.1.1 Event Related Potentials

As already mentioned, ERPs are changes in the ongoing electrical neural activity due to the occurrence of brain processes associated to specific external events (Luck & Handy (2005),2005). They are traditionally named according to their polarity (negative or positive) and latency. For example, the ERP (or component) P100 (also called P1 for abbreviation) corresponds to a positive deflection of the EEG signal whose amplitude is maximal around 100 ms after the presentation of the stimulus.

The association between the occurrence of an ERP and the presentation of an external stimulus makes the ERPs a good indicator of how the experimental manipulations might affect a given information processing stage. In other words, by determining their latency, amplitude and scalp topographical distribution, it can be inferred whether there was a change in the timing, intensity or nature of the cognitive process of interest.

Because ERPs are embedded within a background EEG noise of much larger amplitude, researchers have relied on the averaging procedure to enhance them. This procedure uses prior knowledge of the exact instant at which the stimulus is presented and extracts stimulus locked epochs that are later averaged together in a point-by-point manner (Figure 1.3) (Dawson, 1954; Luck, 2005). It relies on two assumptions. First, the EEG data collected on single trials is assumed to consist of an ERP waveform plus random noise. Second, whereas the ERP waveform is assumed to be identical on each trial, the noise is assumed to be completely random. Consequently, through averaging

it is possible to enhance the same waveform that was present on individual trials, while canceling the random noise (Dawson, 1954; Luck, 2005; Regan, 1989).

As mentioned earlier, one of the fundamental properties of ERPs is that after the presentation of the stimulus, the system always returns to its resting state. Consequently, the averaged response can be regarded as the averaged transient response of the sensory system stimulated (Regan, 1989).

### Some major ERP components

Decades of research have allowed the characterization of several ERPs. Among them, the earliest visual components are:

**C1**: In response to the presentation of simple visual stimuli such as light flashes or checkerboards, a negative deflection can be observed on the scalp, which reaches its highest amplitude between 60 and 90 ms (Di Russo *et al.*, 2003). Its polarity can change according to the part of the visual field where the stimulus is presented, i.e., it is positive for stimuli in the lower visual field and negative for stimuli in the upper visual field (Hillyard & Anllo-Vento, 1998). This property, together with evidence from imaging studies and source analysis approaches, have led some authors to conclude that C1 neural generators are probably located in deep structures of the primary visual cortex, specifically the calcarine sulcus (Di Russo *et al.*, 2002; Pourtois *et al.*, 2004). However, recent studies have demonstrated that ERPs generated outside the primary visual cortex, in V2 and V3, can also reverse polarity for upper and lower field stimuli (Ales *et al.*, 2010). This observation qualifies the suggestion that C1 reflects the initial response of the primary visual cortex to a stimulus (Ales *et al.*, 2010). When the stimulus is presented in the horizontal midline, the amplitude of the component decreases making difficult to distinguish it from the next visual component, the P100 (also named P1).

**P100 or P1** [2]: This is one of the most studied visual components (Figure 1.3). It appears between 60-90 ms and peaks around 100 ms over lateral occipital electrodes. Its amplitude can be affected by the direction of spatial attention (Di Russo *et al.*, 2003) and low-level stimulus features such as contrast and frequency content (Rossion & Caharel, 2011). It has been suggested that the early part of this component (72 to 110 ms) is generated by dorsal extrastriate cortex in the middle occipital gyrus whereas the later part (110 to 146 ms) is generated more ventrally in the fusiform gyrus (Di Russo *et al.*, 2002).

**N100 or N1**: The P1 is followed by the N1 wave (Figure 1.3). This negative deflection can be detected at several recording sites (occipital, parietal, central, and frontal electrodes) with slight variations in latency. As a result, it has been proposed

[2] See Section 2.1.4.1 for more information on the relation between P1 and face perception processes.

to differentiate between several N1 subcomponents (e.g., see Itier & Taylor (2004)). The earliest subcomponent peaks between 100 and 150 ms poststimulus at anterior electrode sites. The latest subcomponents peak between 150 and 200 ms poststimulus at parietal electrodes and at lateral occipital electrodes. Spatial attention (Hillyard *et al.*, 1998; Mangun, 1995) as well as the nature of the cognitive task (e.g., discrimination vs. detection tasks) (Hopf *et al.*, 2002; Ritter *et al.*, 1979; Vogel & Luck, 2000) influence the amplitude of the N1.

**N170 and Vertex Positive Potential (VPP)**: Faces elicit a more negative N1 than other objects categories at lateral occipital electrodes sites at around 170 ms (Bentin *et al.*, 1996; Jeffreys, 1989). This component, traditionally known as N170, was initially observed using a few electrodes that covered mainly the central midline sites. It appeared as a strong positivity and so it was initially named the Vertex Positive Potential (VPP) (Boetzel & Gruesser, 1989; Jeffreys, 1989). Due to its relevance for this thesis, the characteristics of the N170 will be discussed in more detail in Chapter 2, section 2.1.4. The next section will summarize the main characteristics of the steady state brain response.

### 1.1.2 Steady State Potentials

The ability of the brain to follow a rhythm imposed by an external sensory event was observed for the first time using visual stimulation by Regan and colleagues (Regan, 1966). Specifically, the authors demonstrated that when subjects were continuously stimulated with a light flash, flickering at a constant frequency, the main frequency component of the response registered on the scalp was equal to the stimulation frequency (Regan, 1966, 1989, 2009; Regan & Regan, 1988). Additional harmonics responses at frequencies multiple of the stimulus presentation rate have also been observed (Fawcett *et al.*, 2004; Herrmann, 2001; Pei *et al.*, 2002; Rager & Singer, 1998).

Steady state potentials have been described not only for visual stimuli (Baker *et al.*, 2011; Brown & Norcia, 1997; Regan, 1966, 1968a; Shea *et al.*, 1999), but also for auditory (Galambos, 1982; Galambos *et al.*, 1981) and somatosensory stimuli (Noss *et al.*, 1996). In this thesis we will focus on the visual modality (Steady State Visual Evoked Potential, SSVEP).

As mentioned in the previous section, the discrete frequency components of the steady state potentials remain roughly constant in amplitude and phase over the stimulation period. In other words, shortly after the initiation of repetitive stimulation, the relevant sensory system attains a steady state that lasts throughout the duration of the stimulation (without returning to its resting state) (Regan, 1966, 1989, 2009; Regan & Regan, 1988).

In order to enhance the signal-to-noise ratio and extract the brain response of interest from the background EEG, researchers use prior knowledge of the exact frequency

at which the response must occur, which corresponds to the stimulation frequency (Regan, 1989). In other words, if the stimulus is presented at a temporal rate of 2 Hz, it is expected that the main frequency component of the EEG signal is also 2 Hz. In order to extract such frequency components from the signal, researchers can perform either time domain or frequency domain analysis.

In the time domain analysis, the difference between the maximum positive and the maximum negative amplitudes of the waveform is measured usually after band pass filtering the data around the frequency of interest, e.g. if the frequency of interest is 2 Hz the data can be filtered between 1 and 3 Hz. If the analysis is performed with respect to frequency, in the frequency domain, mathematical algorithms are employed to decompose the time domain signal into its frequency components (Regan, 1989). Two of these mathematical algorithms are the Fourier Transform and the Wavelet Transform.

The Fourier Transform relies on the principle that any periodic signal can be represented as the sum of sinusoidal waves with appropriate amplitude and phase (Figure 1.5) (Enslein & etc, 1977). It transforms a discrete signal in the time domain into a set of sine waves of different frequencies, phases and amplitudes. In other words, it calculates the frequency, amplitude and phase of each sine wave needed to make up any given signal (Figure 1.5). Unfortunately, the Fourier Transform does not provide information about the frequency variations in time, which can be a problem for the analysis of non-stationary signals.

The Wavelet Transform captures both the frequency and time information present in the signal by using a wavelet function (a wave-like oscillation with an amplitude that starts out at zero, increases, and then decreases back to zero) instead of sines and cosines functions to decompose the time domain signal into time/frequency space simultaneously. One gets information on both the amplitude of any "periodic" signal within the series, and how this amplitude varies with time. Wavelet transforms have advantages over traditional Fourier transforms for representing functions that have discontinuities and sharp peaks, and for accurately deconstructing and reconstructing finite, non-periodic and/or non-stationary signals.

In general, the frequency domain analysis is usually preferred over the time domain analysis because besides being faster, it does not depend on subjective criteria to identify peaks of interest in a noisy trace (Regan, 1989).

To control the sequence of stimulus presentation across time two types of temporal modulations have been traditionally used: square and sinusoidal stimulations. When the square stimulation is used, the external event appears and disappears abruptly. As a result, when the stimulus intensity is represented with respect to time the obtained function corresponds to a square waveform. In the sinusoidal stimulation, the external

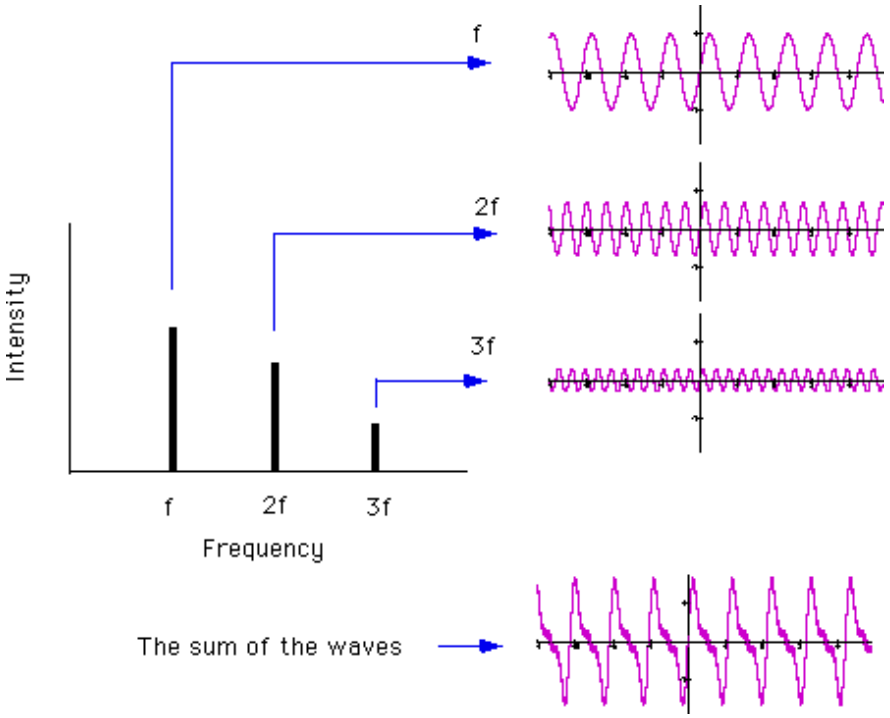


**Figure 1.5: Schematic representation of the FFT technique.** - Three sinusoidal waves (shown at the right of the figure) with different amplitudes and constituent frequency components (as evidenced by the frequency vs. intensity plot shown at the left of the figure) are added together to form the complex waveform (shown at the bottom of the figure). This is the principle of the FFT technique: sinusoidal waves can be added together to produce more complex waves.

event appears and disappears gradually and thus, variations in the stimulus intensity across time describe a sinusoidal waveform (Figure 1.6).

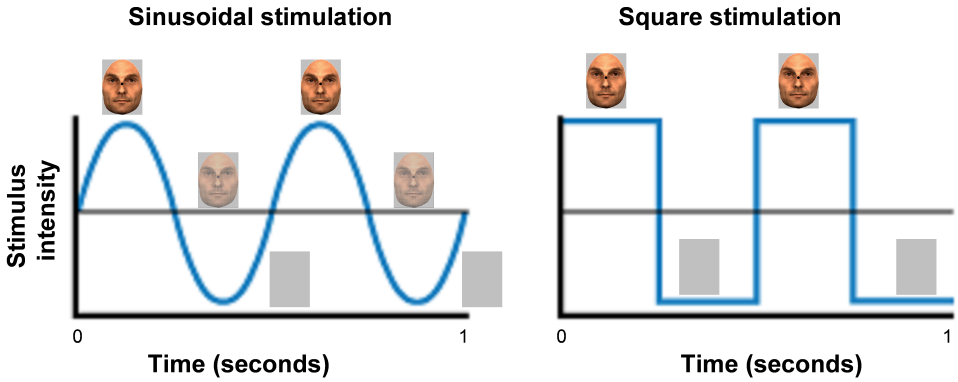


**Figure 1.6: Comparison of sinusoidal and square stimulation.** - The appearance of a facial image on the screen is controlled with a sinusoidal and a square waves of 2 Hz. In the first case, the stimulus appears and disappears gradually: it is fully displayed at the waveform peaks, partially displayed at zero crossing and absent at waveform throughs. With the square wave, the stimulus appears (waveform peaks) and disappears (waveform through) abruptly.

Even when both, the sinusoidal and the square waveforms correspond to identical stimulus presentation rates or stimulation frequencies, their descriptions in the frequency domain (their frequency spectrums) differ. The frequency spectrum of a square wave consists of a series of sinusoids at the fundamental frequency plus the odd harmonics decreasing in size (Figure 1.7). All these frequency components can be manifested in the brain steady state response, making difficult to distinguish between frequency modulations due to the stimulation and those due to brain physiological mechanisms. In contrast, the frequency spectrum of a sinusoidal wave consists of a single frequency (Figure 1.7). As a result, the appearance of distinct frequency components at higher harmonics are evidence of nonlinear brain processing or asynchrony between the activation of neural populations (Pastor *et al.*, 2007; Regan, 1989).

The strength of the brain steady state signal in response to a square or a sinusoidal stimuli might also diverge. This issue was directly addressed in a recent study using a light flickering at different frequencies (Nicol *et al.*, 2011). The authors showed that for lower frequencies (below 7.52 Hz) the response functions at the fundamental, the second and third harmonics were highest for square-wave flicker modulation than for sine-wave flicker modulation. This result was interpreted as a consequence of the fact that at such slow frequencies the visual system can distinguish better the abrupt onset and offset of the stimulus, which is emphasized by the square-wave stimulus modulation (Nicol *et al.*, 2011).

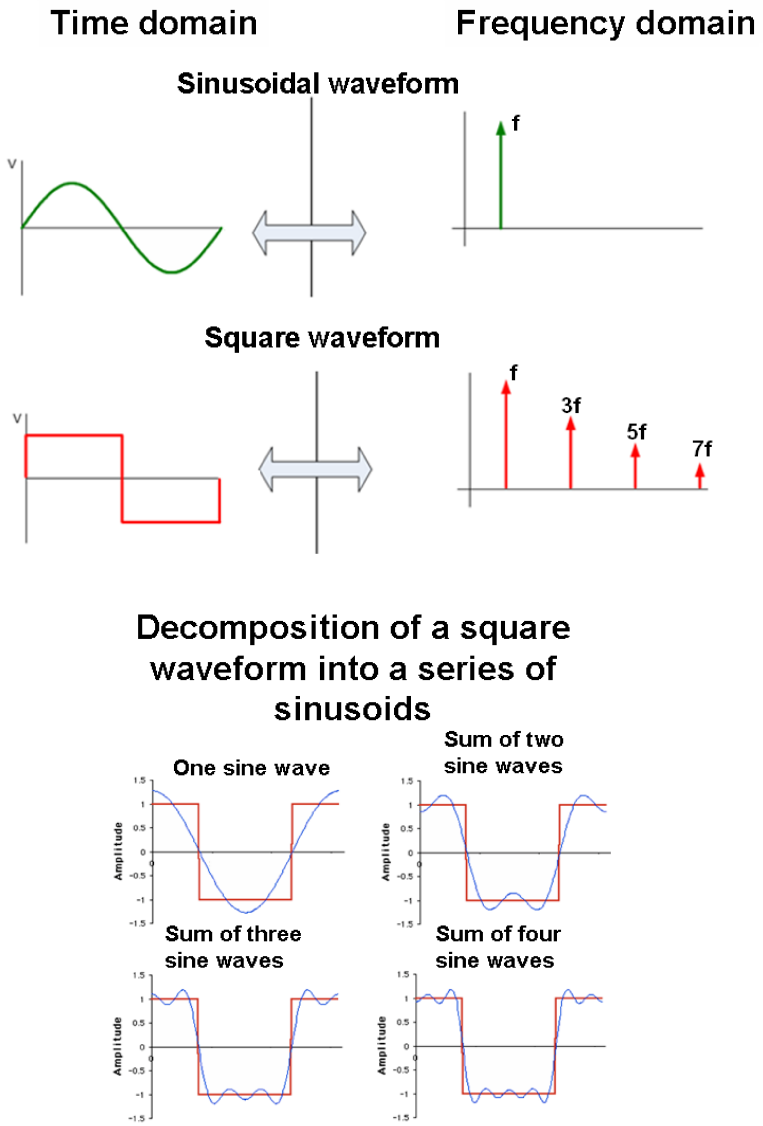


**Figure 1.7: Comparison of the frequency spectrum of sinusoidal and square waveforms.** - A sinusoidal waveform can be fully described by a component at the fundamental frequency. In contrast, the frequency spectrum of a square wave includes components at the fundamental frequency and odd harmonics (figure top). This is due to the fact that in the frequency domain a square wave has to be expressed as a sum of a large series of sinusoids (figure bottom).

Given that a sinusoidal wave can be described more accurately than the square wave in the frequency domain and that the experiments presented here employed a wide range of stimulation frequencies, including low frequencies at which the visual system can distinguish abrupt stimulus onset and offset, in this thesis the stimulus presentation will be controlled using a sinusoidal function.

### 1.1.3 Steady state and transient responses: similar or different phenomena?

Intense research has been devoted to determine the nature of the relation between the steady state and the transient responses: is the steady state just a manifestation of the same mechanisms underlying the generation of the transient response and, thus, both provide equivalent information about the brain processes or, on the contrary they reflect different brain properties? Two opposing hypotheses have been proposed to answer this question. Each of them will be briefly introduced in the next paragraphs.

The starting point of the first hypothesis comes from the observation that there is an evident relationship between the 40 Hz steady state auditory component and the middle latency auditory transient potentials (Galambos *et al.*, 1981). This observation led the authors to propose that superposition of independent transient responses was the mechanism underlying the steady state auditory potential (Galambos *et al.*, 1981). Afterwards, several authors have tried to extrapolate this findings to the visual (Capilla *et al.*, 2011) and somatosensory domains (Azzena *et al.*, 1995; Bohorquez & Ozdamar, 2008; Santarelli *et al.*, 1995; Stapells *et al.*, 1988).

Response superposition implies that the steady state signal arises from the addition of independent transient responses elicited by the rhythmic presentation of the external event (Figure 1.8) (Azzena *et al.*, 1995; Bohorquez & Ozdamar, 2008; Capilla *et al.*, 2011; Heinrich, 2010; Santarelli *et al.*, 1995; Stapells *et al.*, 1988), a feature that characterizes linear systems (Illingworth, 1991). For example, if a late negative deflection evoked by the first stimulus coincide with an early negative deflection evoked by the second or third stimulus, both can add each other. Similarly, if they do not coincide, they can attenuate or even cancel each other (Heinrich, 2010). Whereas response canceling can led to the wrong conclusion that the brain is not responding to the stimulation, response addition would yield to the observation of sinusoidal-like waveforms on the scalp and, as a result, well defined peaks at certain frequencies, e.g., the stimulation frequency and/or particular harmonics (Figure 1.8), (Bohorquez & Ozdamar, 2008; Capilla *et al.*, 2011; Galambos *et al.*, 1981; Heinrich, 2010).

The experiments aimed at demonstrating that the steady state response emerges from the linear superposition of transient responses average together either artificial or real transient responses and measure how well the reconstructed and the real steady state responses correlate. While some studies have obtained a relatively high correlation

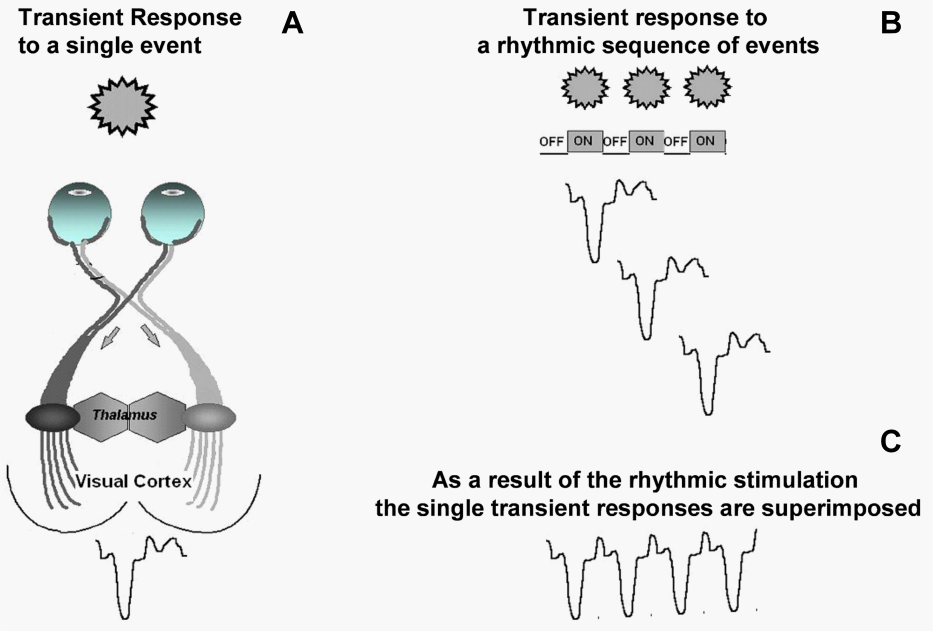


**Figure 1.8: Schematic representation of the superposition hypothesis about the generation of the steady state brain response.** - (A) An hypothetical transient response to the presentation of a single event is presented. (B) Transient responses elicited by several stimuli presented continuously and rhythmically are displayed. (C) The rhythmically produced transient responses are superimposed yielding to a quasi-sinusoidal steady state response.

between observed and predicted responses (Hari *et al.*, 1989; Plourde & Villemure, 1996; Suzuki *et al.*, 1994), other studies, which used computer simulations to attain a more detailed reconstruction of the steady state response have obtained weak correlations or no correlation at all (Azzena *et al.*, 1995; Conti *et al.*, 1999; Santarelli *et al.*, 1995).

To explain this failure, some authors argued that the transient base response used to reconstruct the steady state signal was poorly designed because it did not consider the influence of adaptation (a decrease in the strength of the neuronal response after repeated stimulation) and neuronal refractoriness (inability of the neuron to respond to a second stimulus during the course of an action potential) on the steady state signal (Bohorquez & Ozdamar, 2008).

To corroborate this hypothesis, Bohorquez & Ozdamar (2008) simulated the steady state auditory response at 40 Hz using stimulation sequences with jittered interval inter-stimulus using the Continuous Loop Averaging Deconvolution method. The authors found that the obtained base responses were able to predict the 40 Hz auditory steady state especially when low-jitter sequences were employed (Bohorquez & Ozdamar, 2008). Using similar methods, Capilla *et al.* (2011) have arrived to identical conclusions in the visual domain.

When evaluating the evidence just reviewed one has to consider that it might be always possible to find a combination of transient waves, e.g, varying the interval inter-stimulus, that reproduces the steady state response to a certain extent (Azzena *et al.*, 1995). As a result, finding that the linear superposition of transient responses that have been manipulated to some extent reproduces with relative accuracy a steady state response is a necessary but not sufficient criteria to confirm the superposition hypothesis.

The second hypothesis proposed to explain the nature of the relation between the event related and the steady state potentials states that the brain does not necessarily behave as a linear system: the information contained in the afferent input can experience modifications in a way that relates to the overall goals of the organism. As a result the responses to a single transient input may differ from the response to a repetitive input (Regan, 1989).

Abundant evidence has been gathered to support the suggestion that the steady state response is a manifestation of the non-linear properties of the brain. For example, Spekreyse & Tweel (1965) found that a 5.6 Hz flickering stimulus provoked a main response at 11.2 Hz while an 11.2 Hz flicker provoked a response at a similar frequency indicating the presence of strong non-linearity. Superimposing noise-modulated light on the flickering stimulus abolished the frequency-doubled response but did not affect the linear 11.2 Hz response. Similar results have been replicated in the goldfish retinal ganglion cells (Spekreijse, 1969), in the monkey lateral geniculate body (Spekreijse *et al.*, 1971) and in humans (Regan & Regan, 1988).

Some authors have gone a step further in defining the non-linear mechanisms that generate the steady state response and have proposed that such response reflects the ability of the neurons to oscillate at particular frequencies and get synchronized to an external periodic event (see, e.g., Basar (1980, 1998); Galambos (1982); Herrmann (2001)). Synchronization means that the neuron oscillating period is equal to that of the external event: the neuron becomes entrained, the oscillation phase is adjusted to the phase of the periodic external force (phase resetting) while the oscillation amplitude increases (Figure 1.9) (Basar, 1980; Jansen *et al.*, 2003; Pikovsky *et al.*, 2003; Sayers *et al.*, 1974).

Unfortunately, the role played by such phase resetting mechanism in the generation of brain electrical activity is still a matter of great controversy in the literature (see, e.g., Fuentemilla *et al.* (2006); Hanslmayr *et al.* (2007); Klimesch *et al.* (2004); Makeig *et al.* (2002) for evidence in favor of the existence of the phase resetting mechanism and see, e.g., Mazaheri & Jensen (2006); Shah *et al.* (2004) for evidence against it). In a recent review on the topic, Sauseng *et al.* (2007) concluded that currently there are no methods which can unambiguously dissociate between a real phase reset and artificial phase concentration due to an additive evoked response.

Summarizing, the gathered data concerned with the hypothesis proposed to explain the relation between the steady state and the transient responses is not conclusive. The strongest evidence suggests that the steady state reflects the non-linear properties of the brain. Additionally, it seems plausible to think that several mechanisms might underlie the generation of steady state response and that not for all stimulation frequencies or in all cognitive domains the same mechanisms have to be at play. The current controversy on this topic, however, does not limit the utility of either the event related potential or the steady state potential techniques in the study of the brain cognitive mechanisms. Each technique allow extracting information about different aspects of cognition, e.g., while the event related potentials technique provides accurate time information, the steady state potential technique allows tracking the neural responses to different features of the same stimulus. Thus, the information yielded by each method is complementary rather than contradictory.

## 1.2 Brain lesion studies: when the damaged brain speaks

This thesis will apply both, the ERP and the SSVEP techniques to the study of face perception not only in healthy individuals but also in brain damage prosopagnosic patients. That is why the next paragraphs will focus on explaining some important aspects of brain lesion studies in general and prosopagnosia syndrome in particular.

Finding that a brain damaged patient -or group of patients- shows impaired performance in certain tasks but not others allow establishing a relation between the damaged

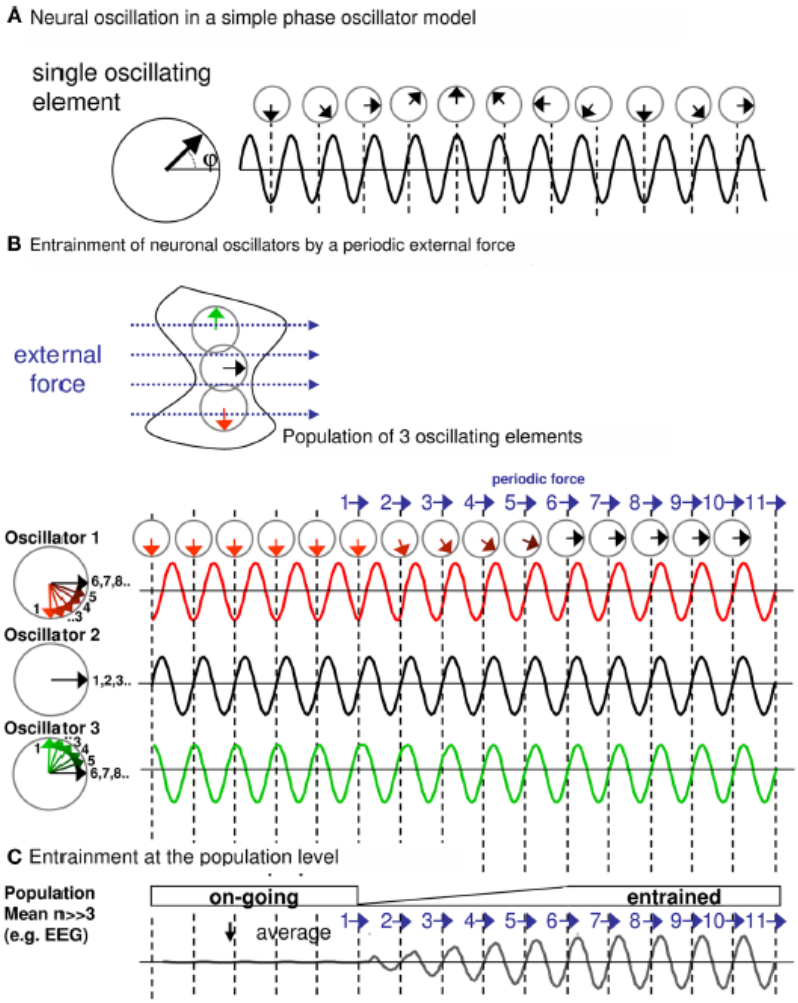


**Figure 1.9: Entrainment of neural oscillations in a simple phase oscillator model.** - (A) Neurons oscillate independently, the phases of such oscillations are not synchronized with respect to each other. (B) An external force entrains the neural oscillators realigning the oscillation phase. All oscillators become synchronized among them and with respect to the external force. (C) At the population level the entrainment increases progressively together with the amplitude of the oscillation. Reproduced from Thut & Gross (2011).

area and the functions needed to complete the affected tasks. This is the essence of the brain lesion approach, which has proved to be particularly beneficial for the field of cognitive neuroscience, in general, and face perception, in particular. For example, using this method Broca and Wernicke revealed the importance of the frontal and temporal lobes in speech production and language comprehension in the late 19th century (Broca, 1865; Wernicke, 1874). In the 1940s, the method was employed to reveal the role of the occipito-temporal region for face recognition (Bodamer, 1947). In the 1960s, the work of Sperry and colleagues with split brain patients helped establishing the dominance of the left hemisphere in language and arithmetic and the dominance of the right hemisphere in visuo-spatial skills (Vinken, 1983). More recently, studying patients with lesions to the amygdala, the left insula and basal ganglia have helped determining the involvement of those areas in recognizing whether faces are expressing fear or disgust (Adolphs *et al.*, 1995; Calder *et al.*, 2000).

However, using the brain lesion approach to draw specific conclusions about brain functions is not an easy task since there are several factors that may confound the interpretation of results. First, natural brain lesions do not occur randomly, on the contrary, they often follow a pattern of location that is determined by certain neurophysiological constraints such as the position of the cerebral arteries. As a result, quite different disorders may occur consistently together and spuriously look as if they are part of the same syndrome with a common underlying mechanism. Second, the fact that damages to a given area cause a specific dysfunction does not necessarily mean that in the normal brain the function is fully localized in that solely area. There is abundant evidence showing that cognitive functions are distributed across a network of regions that are heavily interconnected (see Haxby *et al.* (2000) for a review on face perception). Consequently, lesions to any of these regions or to the connections between them can disrupt the whole cognitive function by affecting one of its information processing stages. Third, the researcher has also to take into account that plastic changes take place within the healthy tissue to cope with the consequences of the lesion. These changes can lead to the development of new, relatively successful strategies when carrying out the task. Eventually, the new strategies can become natural and automatic as they gain a more dominant brain representation. Fourth, the lesion approach frequently relies on reporting single cases in order to prove specific theoretical points, call the attention towards deficits that were previously disregarded and counteract the effect of possible differences between patients with dissimilar patterns of lesions. However, single cases may be unusual and not representative of other cases, which will limit the generality of the drawn conclusion.

With all these things in mind, the next section will provide a brief introduction to prosopagnosia, the brain lesion syndrome that has contributed significantly to our current knowledge about face perception.

### 1.2.1 Prosopagnosia

Although the first reports describing cases of inability to recognize people from faces date back to the mid-19th century (see, for example, Wigan (2007); Wilbrand (2011)) it was not until the 1947 that this disorder was proposed as a specific form of visual agnosia and formally coined as prosopagnosia (Bodamer, 1947).

Prosopagnosia, derived from the Greek words *prosopon*, which means face, and *agnosia*, which means not knowing, is defined as the inability to recognize familiar faces in absence of other low level perceptual difficulties or high level cognitive dysfunctions such as aphasia, amnesia or general mental deterioration (Bodamer, 1947). Patients suffering this deficit are usually able to use non-facial cues such as voice, gesture, distinctive physical characteristics or clothes to recognize the face bearer and retrieve semantic information about him/her (Godefroy & Bogousslavsky, 2007). They are also able to judge his/her age, gender, emotional expressions or gaze direction (Tranel *et al.*, 1988).

The appearance of prosopagnosia has been ascribed to three different etiologies: *congenital*, *neurodegenerative* or *acquired*. The *congenital* (also called developmental) prosopagnosia manifests during the first years of life (Behrmann *et al.*, 2005) in absence of any known cause. This observation, together with recent reports of families with multiple prosopagnosic members, have lead to the suggestion that it has a genetic origin (Behrmann *et al.*, 2005; De Haan, 1999; Duchaine *et al.*, 2003; Kennerknecht *et al.*, 2006). In recent years, a growing amount of studies about developmental prosopagnosia has been published leading to the acceptance of the syndrome. The *neurodegenerative* (or progressive) prosopagnosia is observed as part of neurodegenerative diseases. It progresses slowly and concomitantly with other general symptoms (Evans *et al.*, 1995; George & Jose, 2009). The *acquired* prosopagnosia, the one that is relevant in this context, is observed after focal brain lesions. These lesions are commonly caused by ischemic processes, head traumas, hematomas of unknown pathogenesis, viral encephalitis or tumors (Goldsmith & Liu, 2001).

Acquired prosopagnosia is classically subdivided in two subtypes, apperceptive and associative, although their neuropsychological characterization is not clear cut. Patients suffering the first subtype have problems to make sense of faces, to say whether or not two faces are identical and to judge the age or gender of the person in the picture (Goldsmith & Liu, 2001). These abilities are preserved in those suffering the second subtype and yet they cannot identify the face bearer (Goldsmith & Liu, 2001).

The lesions causing acquired prosopagnosia are more frequently found in the occipital or temporal lobes and rarely in the frontal or parietal lobes (Busigny, 2010). Within the temporal lobe, the structure more frequently damaged is the fusiform gyrus (FG) followed by the inferior temporal gyrus and the parahippocampal gyrus. Less frequently, the lesions are located in the middle temporal gyrus, the superior temporal

gyrus, the temporal pole, the amygdale, the hippocampal gyrus and the superior temporal sulcus (STS). Within the occipital lobe, the structures more frequently damaged are the lingual gyrus, the inferior occipital gyrus followed by the middle occipital gyrus, the superior occipital gyrus, the primary visual cortex and the cuneus (Barton, 2008b; Barton *et al.*, 2002; Bouvier & Engel, 2006) (Figure 1.10).

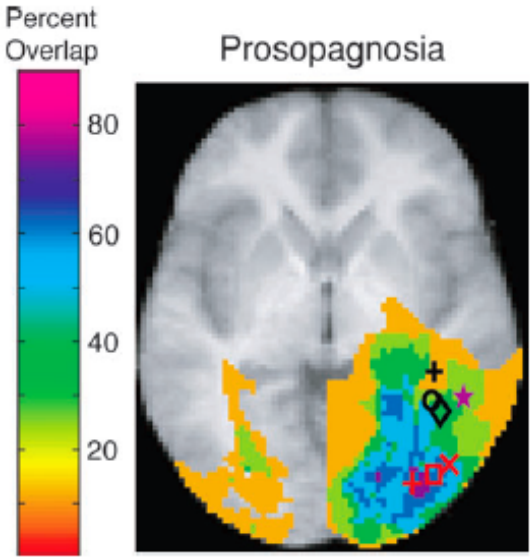


**Figure 1.10: Location of the brain lesions that lead to prosopagnosia.** - The image represents the percentage of overlap in the location of the brain lesions that lead to prosopagnosia in eight cases reported in the literature. Representative neuroimaging peak activations are also superimposed: black symbols indicate responses near the face-sensitive area FFA, red symbols indicate responses near the face-sensitive area OFA, and the purple symbol indicates a response near the face-sensitive area STS. Reproduced from (Bouvier & Engel, 2006).

In the majority of cases the injuries involve both hemispheres, which agrees with initial post-mortem observations of patients who presented left hemisphere silent damages together with clear right hemisphere lesions (Damasio *et al.*, 1982). However, the literature is not exempt of cases presenting unilateral injuries (see, e.g., Barton (2008a); Benton (1980); De Renzi *et al.* (1994); Eimer & McCarthy (1999); Mattson *et al.* (2000); Wright *et al.* (2006)). The vast majority of unilateral lesions are located in the right hemisphere (Benton, 1980; De Renzi *et al.*, 1994), which agrees with electrophysiological and neuroimaging studies showing that face selective activations are stronger in the right than in the left hemisphere (Barton *et al.*, 2002; Bouvier & Engel, 2006; Sergent & Signoret, 1992). Unilateral left hemisphere lesions have to be interpreted more cautiously because of the presence of some confounding variables in the

reported cases. For example, the patients PHD (Eimer & McCarthy, 1999), DN (Mattson *et al.*, 2000), and 015 (Barton, 2008a) are left handed and thus they may exhibit an uncommon pattern of hemispheric specialization. The patient described by Wright and colleagues presented generalized epileptic seizures that may have compromised the right hemisphere (Wright *et al.*, 2006).

Summarizing, the pathology underlying the appearance of prosopagnosia involves lesions that affect mainly the fusiform gyrus, the lingual gyrus and the inferior occipital gyrus. Damage to the right hemisphere seems to be both necessary and sufficient to cause prosopagnosia (at least in right handers).

### 1.2.2 Patient PS

The experiments presented in this thesis are focused on one case of prosopagnosia, patient PS. Studying this patient has been crucial to demonstrate specific theoretical points about face perception processes in the healthy brain (see e.g., Busigny *et al.* (2010); Caldara *et al.* (2005); Dricot *et al.* (2008a,b); Ramon & Rossion (2010); Ramon *et al.* (2009, 2010a,b); Rossion (2003, 2008); Rossion *et al.* (2000a, 2003b, 2011)).

PS is a female, right handed patient, born in 1950, who suffered a traffic accident in 1992. As a result of the accident, she sustained a traumatic intracranial hemorrhage that provoked damages to the left fusiform gyrus and the right inferior lateral occipital cortex encompassing the territory of the OFA (Sorger *et al.*, 2007). Minor lesions in the left posterior cerebellum and in the right middle temporal gyrus were also provoked (Figure 1.11), (Sorger *et al.*, 2007).

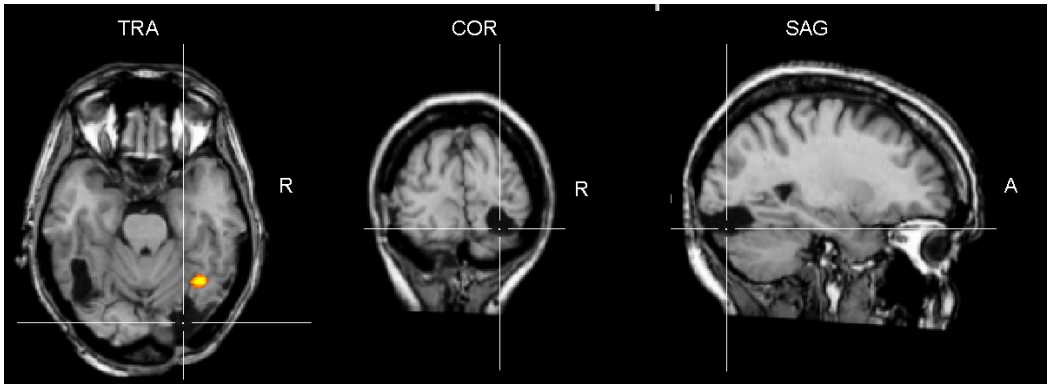


**Figure 1.11: Pattern of lesions in PS brain.** - PS has damage to the left middle fusiform gyrus and a small lesion to the right middle temporal gyrus, but her main lesion, thought to be instrumental in causing her prosopagnosia, concerns the right inferior occipital cortex (line crossing). (TRA: transverse plane; COR: coronal plane; SAG: sagittal plane; R: right; A: anterior)

Following medical treatment, PS recovered all cognitive functions except for the persistent inability to recognize familiar faces, including family members or even her own image in a photograph (Godefroy & Bogousslavsky, 2007; Sorger *et al.*, 2007). To identify the persons around her, she relies on non-facial cues such as hairstyle, gesture, characteristic features etc. (Sorger *et al.*, 2007).

Extensive neuropsychological evaluations (see Figure 1.12 for a summary of her neuropsychological profile) demonstrated that the patient does not present low-level perceptual difficulties, except for a small left paracentral scotoma. She also behaves normally in all cognitive tasks not related with faces (Rossion, 2003; Schiltz *et al.*, 2006). Similarly, she performs normally in high level perceptual tasks and is able to name the 260 items of the Snodgrass and Vanderwart Battery (Snodgrass & Vanderwart, 1980) within normal time limits. She is capable of recognizing non-facial object categories such as birds, chairs, boats and cars (Schiltz *et al.*, 2006) and learning even novel, imaginary objects (Rossion *et al.*, 2003b). Strong deficits are evident when the patient is confronted with face recognition tasks. Specifically, her performance is severely impaired in the Benton Facial Recognition Test (Benton *et al.*, 1994; Rossion, 2003) and in face matching tasks that present the stimuli from different view points (Rossion, 2003). Some studies have showed that, in contrast to normal individuals, PS does not rely on the information contained in the eye area to identify faces but on the information contained in the mouth area (Caldara *et al.*, 2005; Orban de Xivry *et al.*, 2008; Ramon & Rossion, 2010; Sorger *et al.*, 2007).

fMRI studies have allowed relating these neuropsychological deficits with dysfunctional activations of the FFA. In other words, despite the anatomical integrity of this area and its preserved ability to respond preferentially to faces (Rossion, 2003), this region does not exhibit the classic release from adaptation response when the face identity is changed (Dricot *et al.*, 2008b; Schiltz *et al.*, 2006). This observation suggests that the connections between the FFA and the OFA are indispensable for face individualization.

In contrast, such release from adaptation is observed in the lateral occipital complex (LOC) (Dricot *et al.*, 2008b), an area involved in objects perception and identification (Vinberg & Grill-Spector, 2008). Connections between the LOC and the FFA may subserve the preserved ability of the patient to discriminate between faces and objects (Dricot *et al.*, 2008b).

In summary, ERPs and SSVEPs are valuable tools to study the brain mechanisms underlying face perception. Both techniques provide high temporal resolution indexes that can help not only to elucidate the activation course of face perception processes but also to determine how different facial features are coded by the brain. When combined with the study of brain lesion patients, especifically prosopagnosic patients, useful information about the anatomical structures involved in face perception can be obtained. The next Chapters will introduce four studies that will demonstrate how

*Summary of visual functions of patient P.S.*

| | |
|---|---|
| Basic perceptual processes | |
| Visual field | Slower than normals on left superior field |
| Acuity | 0.7 bilaterally |
| Contrast | Nicolet contrast sensitivity test: OK |
| Colour perception (Ishihara) | 12/17, lower range |
| Low-level visual processing | |
| Benton line orientation | Normal (57/60) |
| Birmingham Object Recognition Battery (BORB) | |
| Object copying test 1 | OK |
| Line length (test 2) | OK |
| Size (test 3) | OK |
| Orientation (test 4) | OK |
| Gap position (test 5) | OK |
| Overlapping shapes (test 6) | OK, slowed down for three subtests |
| Minimal feature match (test 7) | OK |
| Foreshortened views (test 8) | OK |
| Object recognition | |
| BORB (test 10) Object decision task | OK |
| Object decision task on computer | OK (98%)<br>Objects: 946 ms; non-objects: 1626 ms |
| BORB (test 11) Item match (class recognition) | OK |
| BORB (test 12) Semantic association | OK |
| Object naming (Colorized Snodgrass and Vanderwart) | OK |
| Short-term visual memory | |
| Test de la ruche (French) | OK |
| Long-term visual memory | |
| Doors test | OK |
| Rey complex drawing | OK |
| Face processing | |
| Benton face recognition test | 27/54 (strongly impaired); 32 s |
| Warrington face recognition battery | 18/25 (impaired, percentile 3) |
| Reading | Slow but accurate |
| Visual imagery | |
| Object Drawings (test 9: BORB) | OK |
| Reaction Time (phasic alert) | Slower than normals, percentile 5 |

**Figure 1.12: Summary of PS visual functions.** - Results obtained by patient PS in several visual tasks. Reproduced from Rossion (2003).

ERPs and SSVEPs can be used to study face mechanisms in healthy and diseased populations and will laid the foundations for future research in this field.

# Chapter 2

# Early FFA activation in a prosopagnosic patient with damage to the OFA: an N170 study

This chapter presents Study 1, which characterized PS' electrophysiological profile and demonstrated that the OFA is a necessary structure to produce neither the N170/M170 face effect nor the N170/M170 face inversion effect. The study also suggested that the face selective activation observed in the FFA of prosopagnosic patient PS using fMRI may occur around 170 ms post-stimulus. These results are discussed in relation to current models of face perception.

The chapter is organized as follows. The first section will provide a general overview of the current knowledge about the anatomo-functional basis of face perception, on one hand, and the main characteristics of the N170/M170 components, on the other. Both topics are relevant in the context of Study 1, which will be presented in the last section.

## 2.1 Functional and anatomical breakdown of face individualization

Given the diversity and complexity of the information contained in a face, we might expect that a distributed neuronal network supports face detection or categorization (i.e., it is a face not a car), discrimination (i.e., face A and B are different) and identification (i.e., it is Robin). In fact, converging evidence from neuroimaging, neuropsychology and neurophysiology studies have identified several areas lying outside the retinotopic

cortex that respond selectively to faces compared to other object categories. These studies also indicate that those structures might be organized in interdependent functional stages. The next sections will review such evidence.

### 2.1.1 Identification of face-selective brain regions

The existence of anatomical regions directly involved in face perception was first suggested by brain lesion studies (Bodamer, 1947); followed by the recording of single neurons in the monkey brain (Gross *et al.*, 1972).

As it was explained in previous sections, the neurobehavioral syndrome called prosopagnosia affects the ability to recognize familiar faces in absence of other low and high level cognitive disorders and it is due to relatively well localized brain lesions in the ventral occipito-temporal cortex involving the lingual and fusiform gyri bilaterally but with a right hemisphere dominance (Damasio *et al.*, 1982; Sergent & Signoret, 1992), as well as the anterior temporal cortex (Bukach *et al.*, 2006).

In the monkey brain, neuronal patches in the superior temporal sulcus (STS) and in the inferior temporal gyrus respond selectively or exclusively to faces compared to other types of visual stimuli (Desimone, 2011; Desimone *et al.*, 1984; Gross *et al.*, 1972; Perrett *et al.*, 1982). Around 97% of the visually responsive cells of one of this face selective STS patches, which includes a structure possibly homologue to the human FFA, respond strongly to faces, which supports the existence of entire cortical areas dedicated to face processing (Tsao *et al.*, 2006).

Given that changes in basic stimulus characteristics such as face position, color or size do not affect the face selectivity of STS cells in the monkey brain, it can be concluded that such selectivity is driven by complex, more abstract visual attributes which allow encoding a stimulus as a face (Desimone, 2011; Perrett *et al.*, 1982). Further support for this conclusion comes from studies aimed to determine whether other stimulus types are also able to produce a response as strong as a face. To this end, some authors have tested over 1,000 natural images using rapid serial visual presentation (Foeldiak *et al.*, 2004). They have found that faces were contained in the 70 stimuli that produced the strongest responses in specific cell groups of the macaque temporal cortex (Foeldiak *et al.*, 2004). The next best stimuli produced less than one-fifth of the response produced by the facial stimuli (Foeldiak *et al.*, 2004).

The above mentioned findings have been corroborated by studies of evoked potentials recorded with electrodes placed on the cortical surface in epileptic patients. Specifically, two face-specific brain responses, the negative components N200 (maximal around 200 ms) and N700 (maximal around 690 ms) have been recorded from electrodes implanted on the ventral occipitotemporal cortex and on the inferior occipital gyri (Allison *et al.*, 1999; McCarthy *et al.*, 1999; Puce *et al.*, 1999). The ventral occipitotemporal recording sites have been located mainly in the lateral fusiform and adjacent

inferior temporal gyri. Additional sites have been placed in the middle fusiform gyrus (Allison *et al.*, 1999; McCarthy *et al.*, 1999; Puce *et al.*, 1999).

The development of functional brain imaging has allowed to gather further evidence in support of the existence of a distributed neural system for face perception in the healthy human brain. Face selective activations have been found in the lateral middle fusiform gyrus often bilaterally but stronger in the right than in the left hemisphere (Grill-Spector *et al.*, 2004; Halgren *et al.*, 1999; Haxby *et al.*, 1999; Kanwisher & Yovel, 2006; Kanwisher *et al.*, 1997; McCarthy *et al.*, 2011; Rossion *et al.*, 2000a, 2011). This area has been coined the fusiform face area (FFA) (Kanwisher *et al.*, 1997). Posterior to the FFA, in the inferior occipital gyrus, another area has exhibited face selective fMRI activations (Gauthier *et al.*, 2000; Halgren *et al.*, 1999; Haxby *et al.*, 1999; Rossion *et al.*, 2000a; Sergent *et al.*, 1992). This region has been coined the occipital face area (OFA) (Gauthier *et al.*, 2000) and, together with the FFA, defined as a the two core structures of the face perception network (Haxby *et al.*, 2000). Activation in the posterior part of the superior temporal sulcus have also been found although less consistently (Haxby *et al.*, 1999; Puce *et al.*, 1998).

Summarizing, converging evidence supports the view that ventro-medial regions of both hemispheres, especially the middle fusiform gyrus, the inferior occipital gyri and the superior temporal sulcus are critical for the successful perception and identification of faces (Figure 2.1). The functional role of each of these structures and the nature of their interactions during face processing will be the topic of the next section.

### 2.1.2 Specialization within face-responsive areas: linking structure to function

Faces convey a high amount of information not only about the identity of the person, but also about how she/he is feeling or where she/he is directing her/his attention. Are the face selective areas specialized for the analysis of particular types of information?

The main experimental evidence gathered to answer this question comes from studies of healthy and prosopagnosic individuals. In healthy individuals it has been shown that attending to face identity or changing the identity of faces increase the magnitude of the fMRI BOLD response in the FFA (see, e.g., Gauthier *et al.* (2000); Loffler *et al.* (2005); Schiltz *et al.* (2006); Winston *et al.* (2004)). In contrast, attending to the eye gaze direction or changing the viewpoint or expression of identical faces increase the magnitude of the response in the STS (Calder *et al.*, 2007; Grill-Spector *et al.*, 2004; Hasselmo *et al.*, 1989; Haxby *et al.*, 2000; Hoffman & Haxby, 2000; Sander *et al.*, 2004; Winston *et al.*, 2004). Interestingly, some authors have found that the activity in the STS also increases for facial identity changes when facial expression is changed or when subjects are attending to facial expression (Fox *et al.*, 2009; Winston *et al.*, 2004). Moving eyes and mouths also have been found to activate a bilateral region centered in

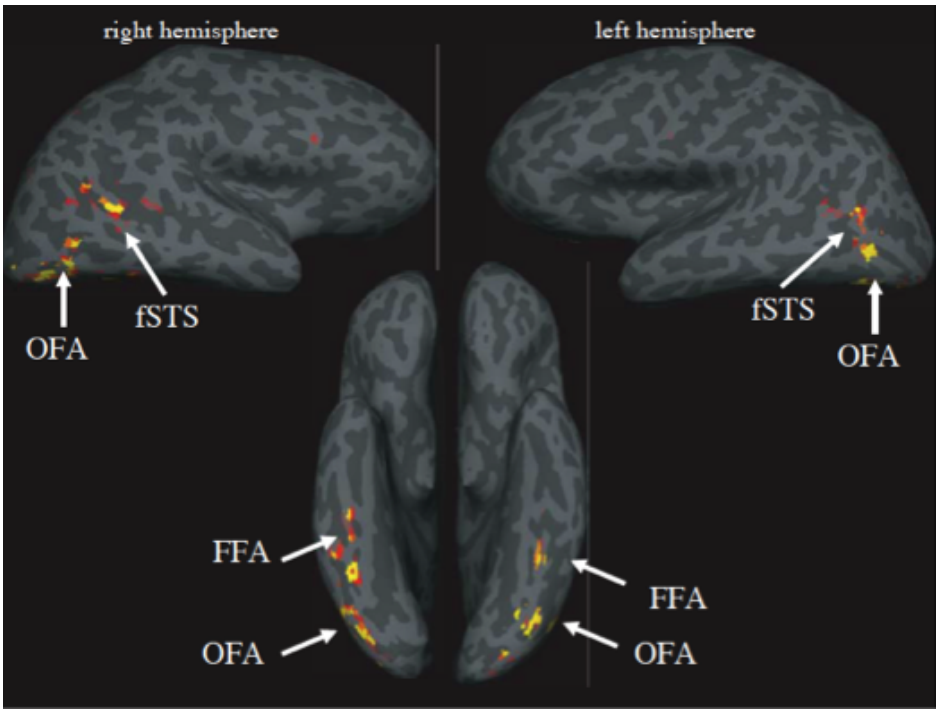


**Figure 2.1: FMRI face selective activations on an inflated brain of one subject.** - The figure shows the three brain regions that respond stronger to faces than to other object categories as it has been found in fMRI studies of healthy humans. These regions are the FFA in the fusiform gyrus along the ventral part of the brain, the OFA in the lateral occipital area and the face STS (fSTS) in the posterior region of the superior temporal sulcus. Reproduced from Kanwisher & Yovel (2006).

the posterior STS (Puce *et al.*, 1998). These findings have led some authors to suggest that there is a functional dissociation between areas that respond to invariant aspects of the face (e.g., identity) and areas that respond to changeable aspects of the face (e.g., expression, speech related movements, eye gaze) (Haxby *et al.*, 2000).

The involvement of the FFA in processing face identity has been further corroborated by prosopagnosia studies. These studies has also suggested that the OFA may play a critical role in identifying the face bearer. As discussed in Chapter 1, section 1.2, patients suffering prosopagnosia are unable to identify a person by his/her facial appearance, a deficit that appears after damages to the ventral part of the occipital and temporal cortex bilaterally (Damasio *et al.*, 1982; Sergent & Signoret, 1992), encompassing the FFA and the OFA (Barton *et al.*, 2002; Bouvier & Engel, 2006; Rossion, 2003). More recent neuroimaging studies of patient PS, who has damage to the right inferior occipital cortex encompassing the OFA, have shown that the fMRI signal in the right FFA, despite showing a normal range of preferential activation to faces, does not show any evidence of sensitivity to discrimination of individual faces (Dricot *et al.*, 2008b; Schiltz *et al.*, 2006). Specifically, the fMRI response in this area fails to show a larger response for faces of different identities (presented in a block or as pairs of face stimuli) compared to the presentation of faces of the same identity (Dricot *et al.*, 2008b; Schiltz *et al.*, 2006).

Besides conveying a high amount of information that tributes to the execution of different face perception processes such as those mentioned above, faces also contain a very specific arrangement of features: a frontal configuration that includes two horizontally and symmetrically placed parts, the eyes; located above two vertically placed parts, the nose and the mouth; framed by a roughly oval contour with hair on the top and sides. What is driving the response of the face selective areas: the facial features per-se or the interrelationship between them, the overall face configuration?

Positron emission tomography (PET) studies aimed to answer this question have reported that the activation of the right fusiform gyrus decreases when human subjects have to focus their attention on particular features to discriminate between faces but not when they had to use the configural information (Rossion *et al.*, 2000a). However, other studies have reported that the FFA exhibits either feature based sensitivity (Harris & Aguirre, 2010) or both, feature based and configuration based sensitivity (Liu *et al.*, 2010; Yovel & Kanwisher, 2004). Similarly, intracranial recordings in humans have shown that a region both lateral and medial to those responding to whole faces in ventral IT cortex responds preferentially to face parts (McCarthy *et al.*, 1999).

Using either fMRI adaptation or Transcranial Magnetic Stimulation (TMS), some authors have found that the OFA is sensitive to manipulations of face parts (e.g. removing vs. presenting the eyes, mouth or nose, modifying its appearance or arrangement) but not to manipulations to face overall configuration (e.g. changing the face shape or

the spacing between its parts) (Fox *et al.*, 2009; Liu *et al.*, 2010; Pitcher *et al.*, 2007). In contrast, other authors have reported that the right OFA is sensitive to changes in face shape (Jiang *et al.*, 2009) and in the spatial relation between face features (Rhodes *et al.*, 2009).

Methodological issues might be responsible for the apparent disparity of results. For example, manipulating the properties of face features may introduce some degree of changes in the configuration of the face while asking subjects to attend to particular features or configurations may influence the natural processing strategy of a given area. Additionally, some of the studies reviewed above differ with respect to the definition of regions of interest. While some authors used functional localizers to delineate the OFA and the FFA in each participant (e.g., Liu *et al.* (2010)) other authors relied on group average whole brain contrast (e.g., Rotshtein *et al.* (2005)) or in previously reported anatomical coordinates (Pitcher *et al.*, 2007). In the last two cases, the individual differences in brain anatomy may difficult the determination of face selective voxels included in the final analysis.

Summarizing, the predominant interpretation of the evidence reviewed here, is that to individualize a face, the OFA performs a fine-grained analysis of the facial features. In contrast, the FFA, where neurons would presumably have bigger receptive fields than in the OFA, performs both a features based and configuration based analysis. The STS seems to use features based information to analyze changeable facial aspects such as gaze direction or expression. The fact that some structures seem to be preferentially tuned to particular facial properties does not exclude the possibility that, for example, the OFA responds to configural aspects of the face or that the STS responds to identity changes. However, the ability to respond to such properties might emerge after receiving modulatory feedback inputs from other face preferential regions.

The existence of such modulatory feed-forward and feedback connections has been undoubtedly proved by Moeller and colleagues using fMRI-guided electrical microstimulation of the macaque brain (Moeller *et al.*, 2008). In brief, the authors found that stimulation of face selective regions located in the fundus and in the middle lateral region of the STS activated three anterior face patches. Furthermore, stimulation of these anterior regions led to feedback activation in the STS comparable in strength and spatial precision to the feed-forward activations (Moeller *et al.*, 2008).

In the human brain similar functional connections have been proposed. The next section will focus on the most widely accepted face perception model that systematizes the current knowledge on this topic.

### 2.1.3 Functional relations among face selective areas: a distributed, hierarchical model of face perception

Nearly one decade ago, Haxby and colleagues proposed a model of human face perception that systematized the increasing and diverse knowledge accumulated in relation to the neuroanatomy of face perception and the functional role of each of the face selective regions (Haxby *et al.*, 2000). This model proposes that face perception is mediated by a distributed neural system that compromises multiple regions grouped in a core and an extended subsystems.

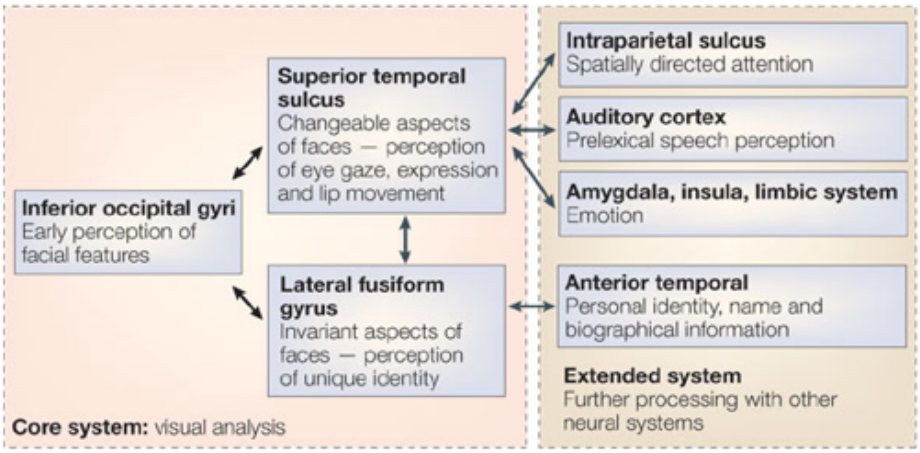


**Figure 2.2: Distributed model for face perception proposed by Haxby and colleagues.** - Schematic representation of the functional interconnections established among face selective areas of the core and extended subsystems during face processes. Reproduced from Haxby *et al.* (2000).

The core system includes three regions: the occipitotemporal in extrastriate visual cortex, the fusiform gyrus and the STS. The inferior occipital gyrus is proposed to be concerned with an initial structural encoding stage in which information about face parts is extracted (Haxby *et al.*, 2000, 1999; Hoffman & Haxby, 2000). The lateral fusiform gyrus is thought to be involved in the analysis of the invariant aspects of the face that define its unique identity, e.g. its holistic configuration (George *et al.*, 1999; Haxby *et al.*, 2000, 1999; Hoffman & Haxby, 2000; Sergent *et al.*, 1992). Finally, the STS is thought to be related to the extraction of changeable aspects of the face that allow the analysis of social information, e.g. speech, expression or direction of eye gaze (Haxby *et al.*, 2000, 1999; Hoffman & Haxby, 2000).

The extended part of the system involves the intraparietal sulcus, recruited when changes in the gaze direction of the face bearer elicits a shift in spatial attention (Haxby *et al.*, 2000, 1999; Hoffman & Haxby, 2000); the auditory cortex, involved in prelexical

speech perception (Haxby *et al.*, 2000; Hoffman & Haxby, 2000; Puce *et al.*, 2003); the limbic system, insula and amygdala, where facial expressions and emotions are processed (Breiter *et al.*, 1996; Ishai *et al.*, 2004; Morris *et al.*, 1996; Phillips *et al.*, 1998) and the anterior temporal region, where biographic information, personal identity and name are retrieved (Ellis, 1992; Haxby *et al.*, 2000). The components of the extended system are not primarily face selective but they process facial stimuli in concert with other neural systems (Haxby *et al.*, 2000).

This model echoes the traditional notion of the visual system functional organization in which information processing proceeds along the feedforward hierarchy of areas, leading to increasingly complex representations of the stimuli (Hubel & Wiesel, 1962; Van Essen *et al.*, 1986). Thus, it proposes that the flow of information processing during face perception goes from a posterior visual area that occupies an intermediate level in the anatomical hierarchy (e.g., the inferior occipital gyri which encompasses the OFA) to more anterior areas (e.g., the lateral fusiform gyrus encompassing the FFA and the STS). Both, the FFA and the STS are able to analyze increasingly complex aspects of the image. The activation of the OFA precedes all subsequent face processing operations, including individualization and identification. However, the notion of the OFA as the necessary entry point to the face perception system has been recently challenged by two fMRI studies in which prosopagnosic patients PS and DF present face selective activations in the right FFA despite lesions in the right OFA (Schiltz *et al.*, 2006; Steeves *et al.*, 2006).

Based on these findings, Rossion and colleagues have suggested that the finer-grained perceptual analysis of faces in the right OFA may be guided by the activation of a generic face template in the right FFA (Rossion *et al.*, 2011). In other words, configural information might be encoded at an early stage of face processing in the FFA. This process might prepare destination areas such as the OFA, which is preferentially sensitive to the properties of the facial features, for receiving more detailed information and for integrating this information into a global, facial representation (Figure 2.3), (Rossion, 2008).

However, it can also be hypothesized that the face selective activation observed in PS' and DFs' FFA is the result of feedback connections from the frontal cortex or from areas of the extended face perception system. The fMRI simply lacks the temporal resolution needed to determine whether or not the FFA is activated within early stages of face processing. In contrast, the EEG can help to solve this issue, given its high temporal resolution. As introduced in the previous section, there is an ERP, N170, which marks the earliest and most reliable face selective activation that can be observed on the human EEG signal and whose neural generators have been located mainly in the OFA and FFA. It follows that the appearance of this component in the EEG signal of prosopagnosic patient PS could be related to an early activation of the

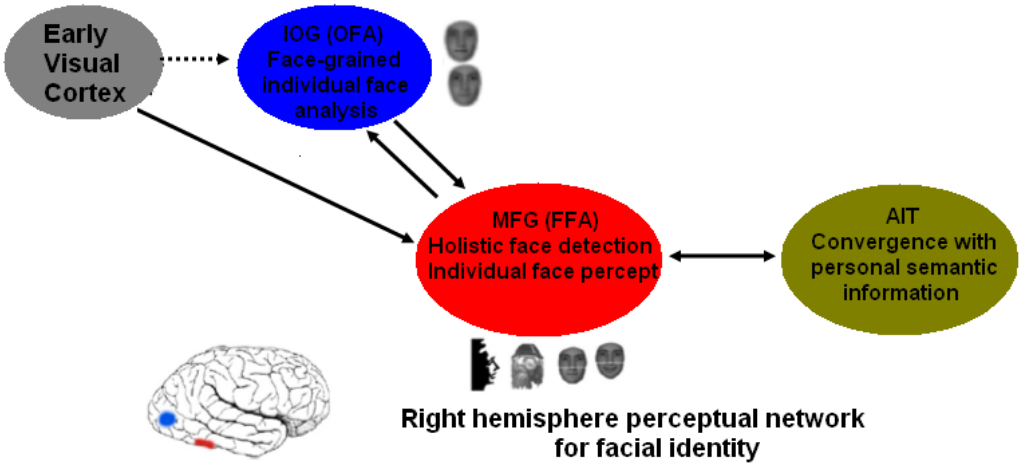


**Figure 2.3: Nonhierarchical organization of human face perception as proposed by Rossion (2008).** - The figure illustrates the organization of information processing by the human face perception system based on recent findings on prosopagnosic patients PS and DF. Following early visual analysis, the facial stimuli would be categorized in the middle fusiform gyrus (mFG) leading to face preferential activations (FFA). This direct pathway is independent form the posteriorly located OFA which might (or might not) show face preferential responses following early visual input (dotted line). The initial, crude, face representation in the FFA would be later refined through reentrant interactions with the IOG, leading or increasing the face preferential activation of this region. Processes in the OFA, where neurons have smaller receptive fields, are tuned to finer-grained analyses of face features. Initial process in the FFA is holistic in nature but after reentrant interactions with the OFA, detailed feature-based analysis is included. In the anterior infero-temporal cortex, personal semantic information is retrieved. Reproduced from Rossion (2008).

FFA or STS. The following section will review what is currently known about the N170 face specificity.

### 2.1.4 The N170/M170 components and face perception

The use of the EEG to study face perception experienced a significant advance in the late 1980s when several authors reported the existence of the Vertex Positive Potential (VPP). This component of positive polarity was highest around 170 ms over central electrodes and increased amplitude when subjects were confronted with facial stimuli (Boetzel & Gruesser, 1989; Jeffreys, 1989, 1993, 1996). The authors also noted that the VPP presented a negative counterpart at bilateral occipito-temporal electrodes, which was later coined N170 by Bentin and colleagues (Bentin *et al.*, 1996).

As indicated in its name, the N170 is negative in amplitude and peaks between 130-200 ms after the presentation of the stimulus. It follows the early posterior visual components C1 (maximal around 70 ms) and P1 (maximal around 100 ms). It is most prominent over occipito-temporal electrodes and although it can be observed in response to any visual stimulus, it is larger in response to faces than to any other stimulus. (Bentin *et al.*, 1996; Boetzel & Gruesser, 1989; Boetzel *et al.*, 1995; Rossion *et al.*, 2000b) (Figure 2.4). This last observation, increased N170 amplitude for faces compared to other object categories, is what has been called the N170 face effect.

Trying to understand this effect and its relation to human face perception has been the focus of several studies. Questions as to which face processes the N170 is concerned with; what is the nature of the facial information it encodes and which brain areas underlie its generation are still a matter of debate, although to different extent. The next paragraphs will develop each of these topics.

#### 2.1.4.1 Nature of the facial information encoded by the N170

The N170 face selectivity is suggested by the observation that the amplitude of this component increases when faces are presented. However, it is well known that low-level properties of the visual stimuli such as luminance, contrast and spatial frequency spectrum can influence the amplitude of early visual potentials and these properties can differ between all faces, on one hand, and all other types of objects, on the other. Consequently, one may wonder which stimulus properties (low level properties or the elaboration of a facial representation) drive the N170 face effect.

The answer to this question comes from studies which show that the N170 face effect does not disappear when low level stimulus properties are controlled (Rossion & Caharel, 2011; Rousselet *et al.*, 2007). Similarly, it does not disappear when the elements of the facial stimulus are rearranged, reoriented, divided in halves, removed or isolated (Bentin *et al.*, 1996; George *et al.*, 1996; Itier & Taylor, 2002; Sagiv &

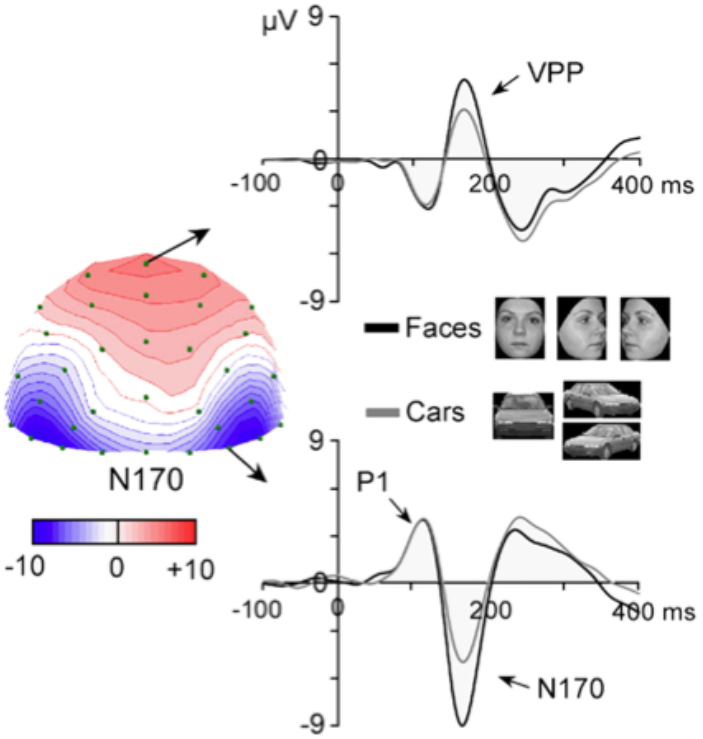


**Figure 2.4: Typical VPP and N170.** - The figure presents a typical waveform obtained in response to the presentation of faces and non-face objects (cars) at posterior lateral electrode sites. While the amplitude of the P1 is equal in both cases, the amplitude of the N170 noticeably increases in response to faces. The topography of the component is also shown. Note the bilateral, occipito-temporal negative distribution together with the central positive distribution (VPP).Reproduced from Rossion & Jacques (2010).

Bentin, 2001). In contrast, the N170 face effect does disappear when the stimulus can not be categorized as a face by the visual system. For example, when "Mooney" and "Arcimboldo" faces (Figure 2.5) are presented upside down, an arrangement that prevent the stimulus to be interpreted as a face (George *et al.*, 2005; Jeffreys, 1993); when subjects are unaware of the physiognomic content of a non-facial image (Bentin & Golland, 2002); when information critical to interpret a stimulus as a face is removed, e.g., presenting the eyes or mouth in isolation (Bentin *et al.*, 1996) or when noise in the frequency bands critical for face perception (11-16 cycles/image) is superimposed on the image (Tanskanen *et al.*, 2005). These results suggest that, indeed, the N170 face effect reflects the elaboration of a facial representation by the visual system.

This conclusion leads to two additional problems about the nature of the facial representation activated at the level of this component: Does it include identity information? Is it based in holistic or features-based facial processing?

Concerning the first question, abundant evidence suggest that the facial representation manifested by the N170 already contains identity information. For example, using a face identity reversal paradigm in which ERPs are recorded in response to an individual face that immediately follows another face, Jacques & Rossion (2006) have observed that the N170 amplitude is larger for the condition where the two faces represented different identities compared to a condition where the two faces represented the same identity. Interestingly, similar results have been obtained when a face is presented repeatedly and then it is followed by a new face demonstrating that it takes around 160 ms to observe the first repetition or adaptation effect to identity on the scalp EEG signal (Figure 2.6) (Jacques *et al.*, 2007). This result parallels those obtained in fMRI adaptation experiments (Grill-Spector & Malach, 2001), which show that the response of face selective areas significantly decreases when identical faces are repeated and increases (the neuronal group is released from adaptation) when different faces are presented (see, e.g., Fox *et al.* (2009); Mur *et al.* (2010); Ramon *et al.* (2009); Winston *et al.* (2004)).

To answer the second question, several studies have tried to find out whether the distinctive signatures of holistic face processing, the composite face effect and the face inversion effect, are manifested in the N170. The former effect refers to the observation that subjects judge as different the identity of two faces which are composed by identical top parts and different bottom parts only when both parts are presented in alignment. In contrast, when both parts are misaligned, subjects recognize the similarity in the top parts and the difference in the bottom parts. This indicate that all face features, although distributed along a top and a bottom part, are integrated holistically in order to discriminate the identity of the face bearer (Figure 2.7). The later effect refers to the observation that inverted faces are more difficult to discriminate and identify than upright faces because the visual system ability to process the image holistically

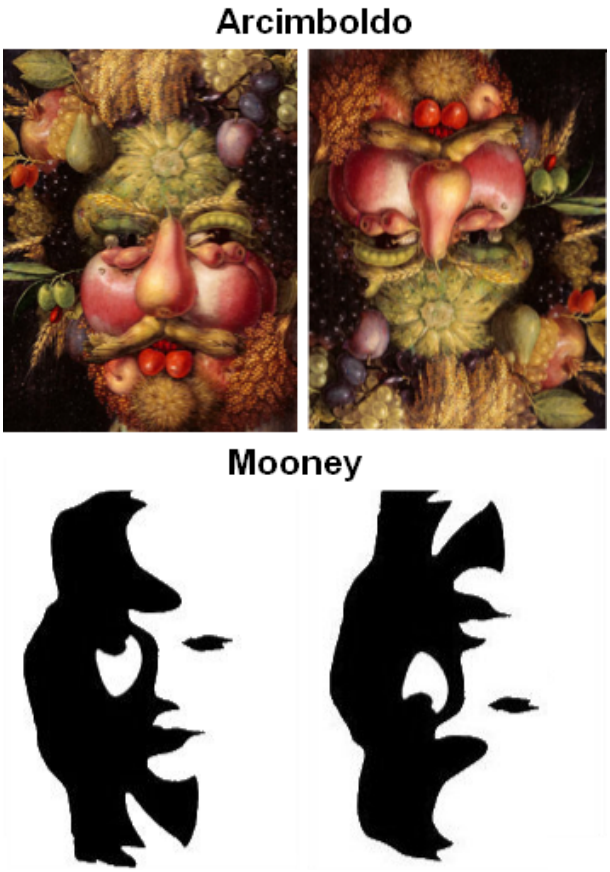


**Figure 2.5: Mooney and Arcimboldo faces.** - The figure presents two typical Mooney and Arcimboldo faces. Note that a face can be distinguished in this type of stimuli only when the stimuli are displayed in their upright position (left side of the image) but not in their inverted position (right side of the image).

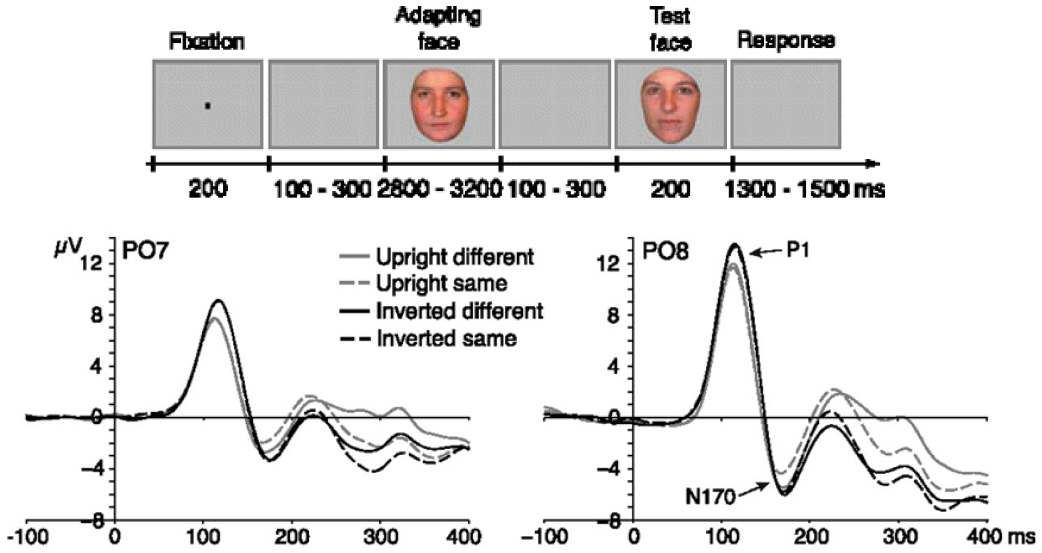


**Figure 2.6: Adaptation phenomenon in the N170** - The top part of the image represents the time line of the stimulus sequence employed to demonstrate that the N170 amplitude adapts when identical faces are repeated. A first face was presented for about 3 seconds (adapting face) followed by a test face which could be either identical or different to the test face. In the bottom part of the image it is shown the grand average ERP waveforms elicited by the second face of the trial sequence (test face) at two occipitotemporal electrodes (PO7, left hemisphere; PO8, right hemisphere). These waveforms are presented as a function of orientation (upright vs. inverted) and adaptation (same vs. different). Note how for the upright condition the test face elicited a higher N170 amplitude when it was different to the adapting face than when they were identical. Reproduced from Jacques *et al.* (2007).

is disrupted by inversion (Figure 2.7) (Freire *et al.*, 2000; Yin, 1969). Both effects are manifested in the N170 since the amplitude of this component increases when composite faces are presented in alignment -and perceived as different- (Jacques & Rossion, 2009) and both, the amplitude and the latency, increase when faces are presented upside down (Lewis & Edmonds, 2003; Rousselet *et al.*, 2003).

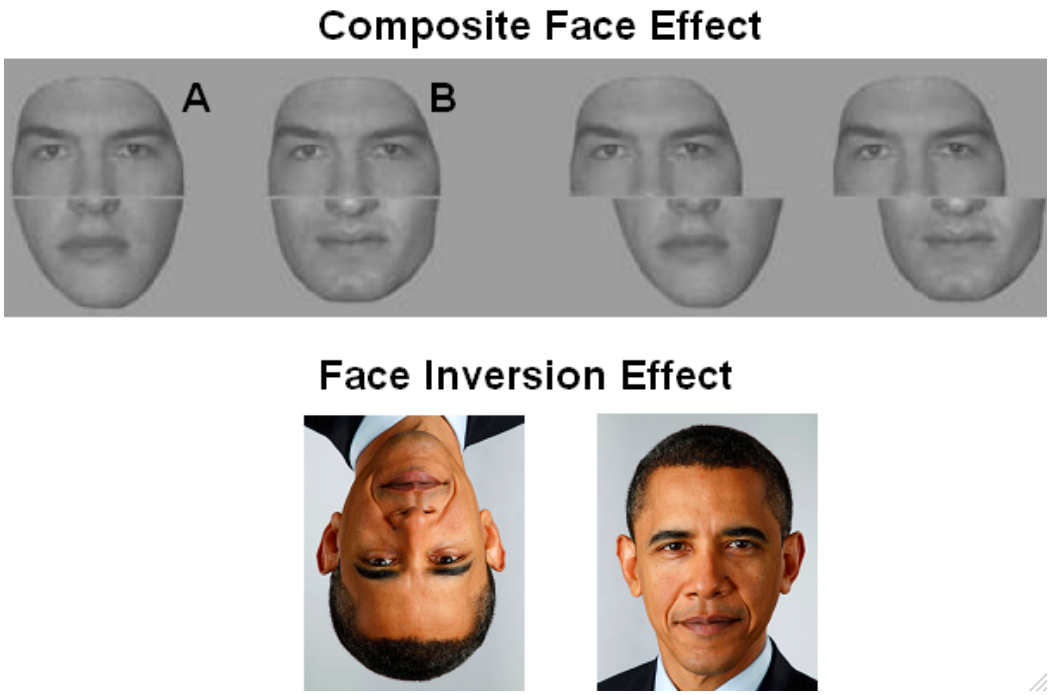


**Figure 2.7: The composite face effect and the inversion face effect** - The composite face effect refers to the observation that, for example, faces A and B are judged as different individuals when the top and the bottom face halves are aligned despite de fact that they are composed of identical top parts. This similarity in the top part of the faces is realized only when both halves are misaligned. The inversion face effect refers to the difficulties people experience to recognize the identity of a face when it is presented upside down.

However, the N170 is not the only ERP that exhibits an amplitude increase in response to faces. In fact, another component, which appears before the N170 and also exhibits some degree of face selectivity, has been observed. This component is the P1, a positive potential that is most prominent on electrodes near the medial occipital pole at about 100 ms following stimulus onset (Eimer, 1998, 2000a; Goffaux *et al.*, 2003; Herrmann *et al.*, 2005a,b; Itier & Taylor, 2004; Liu *et al.*, 2002).

In contrast to the N170 face effect, the P1 face effect does not correlate with the amount of face information contained in the image and is not affected by the addition of noise in the frequency bands that are critical for face perception (Tanskanen *et al.*,

2005). Additionally, the P1 face effect can be reversed by the manipulation of low-level visual parameters such as contrast or even canceled by removing surface information such as color and texture (Halgren *et al.*, 2000). Furthermore, when all low-level visual properties are properly controlled the P1 face effect disappears (Rossion & Caharel, 2011). These results suggest that the P1 amplitude increase in response to faces is based on the extraction of low-level information contained in the stimuli (Rossion & Caharel, 2011).

Summarizing, the accumulated data demonstrate that the N170 is the earliest and most reliable face selective response that can be observed on the scalp EEG. It appears to mark the generation of a holistic face representation that allows categorizing a stimulus as a face and discriminating its identity.

#### 2.1.4.2 The magnetic counterpart of the N170, the M170

Using MEG, it is also possible to record a strong response whose amplitude increases for faces compared to non-face stimulus over occipito-temporal sensors. This event related field (ERF), named M170, peaks around 170 ms after stimulus onset. Given that EEG and MEG do not exhibit the same level of sensitivity to all neuronal sources (Nunez & Srinivasan, 2005) it is plausible to question whether the M170 component reflects the same processes that underlie the generation of the N170.

In an attempt to answer this question, Liu *et al.* (2000) tested subjects with 13 object pictures representative of the stimuli usually employed in intracranial and scalp EEG studies of faces, e.g, human faces, animal faces, animal and human body parts, different types of objects, outlined faces and gray scale faces (Liu *et al.*, 2000). It was shown that the M170 response profile is equivalent to that of the N170. Specifically, the M170 amplitude was larger for faces compared to other objects, including animal and humans body parts and this amplitude increase remained despite task requirements of categorizing both, faces and non-face stimuli, at the subordinate level. It also remained for outline and gray scale faces. When faces where inverted, the M170 latency, but not its amplitude, increased by 13 ms (Liu *et al.*, 2000), a result that has been later replicated (Itier & Taylor, 2002).

Concluding, the gathered evidence is rather consistent in showing that the M170 and the N170 reflect similar processes. As a result, both event related components provide supplementary information and results replicated using both techniques make a robust case in favor of their validity.

#### 2.1.4.3 Neuronal sources of the N170/M170

Determining the brain areas that generate the N170, and its magnetic counterpart the M170, has been the focus of several studies which can be grouped according to the

inverse solution algorithm they have employed: dipolar (ECD) (Scherg & Ebersole, 1994) or distributed (LAURA, LORETA, sLORETA) (Grave de Peralta Menendez *et al.*, 2001; Pascual-Marqui *et al.*, 1994).

In the first case, using dipolar methods, N170 and M170 sources have been located in the lateral occipito-temporal cortex or slightly more medial, in the posterior part of the fusiform gyurs (Boetzel *et al.*, 1995; Deffke *et al.*, 2007; Halgren *et al.*, 2000; Pizzagalli *et al.*, 2002; Rossion *et al.*, 2003a; Schweinberger *et al.*, 2002; Swithenby *et al.*, 1998; Tarkiainen *et al.*, 2002; Watanabe *et al.*, 1999). This region is compatible with the location of the OFA, as identified with fMRI. However, other authors have found the N170/M170 sources in the middle fusiform gyurs, a region that is more compatible with the location of the FFA (Linkenkaer-Hansen *et al.*, 1998; Sams *et al.*, 1997). Additional sources have been placed in the lingual gyrus (Taylor *et al.*, 2001).

In the second case, using distributed inverse algorithms, N170 sources have been located in the posterior part of the STS (Itier & Taylor, 2004; Watanabe *et al.*, 2003), in the anterior part of the fusiform gyrus (BA 20) and in a parieto-temporal network of areas (Herrmann *et al.*, 2005b). In the case of the M170, the neuronal generators have been located quite anteriorly in the fusiform gyrus with a strong right hemispheric dominance (Henson *et al.*, 2007).

Some studies have tried to determine whether the amplitude increase observed in response to faces compared to other object categories is due to a stronger activation of the same sources for faces or to the addition of one or more sources but the results are far from conclusive. For example, Rossion *et al.* (2003a) found that the sources in response to faces and cars differ only in the strength and orientation of the dipoles but not in their location while Itier & Taylor (2004) found that faces recruit an additional pSTS source.

Important differences in methodology might explain the contrasting results. Just to remind the reader, the spatial information provided by the EEG/MEG is severely limited. Due to the geometry of the neuronal sources, the volume conductive properties of the brain and the characteristics of the measurement instrument not all currents produced by the neuronal groups at any give time can reach the scalp. As a result, the recorded signal is compatible with multiple configurations of known and unknown sources. To select one of these configurations, the inverse algorithms introduce mathematical and anatomo-physiologic constraints (Nunez & Srinivasan, 2005). It follows that the adequacy of the final solution will depend on how well the introduced constraints reflect the physiologic mechanisms under study. For example, the dipolar method assume that the EEG/MEG signal has been generated by a limited amount of concentrated, point-like sources whose initial coordinates are approximately known and can be feed to the algorithm (Scherg & Ebersole, 1994). This will necessary bias some dipole configurations in detriment of others, which is particularly dangerous when one

is dealing with a high level cognitive process such as face perception that can provoke the activation of an unknown number of anatomical structures distributed across different brain regions. Distributed algorithms have the capability to deal with an unknown amount of distributed sources that are simultaneously active. At first glance, they appear to be suitable for localizing the brain areas that generated face specific event related components. Unfortunately, two of the possible face selective areas involved in the generation of the N170/M170 are the OFA and the FFA. These regions are located 2 cm apart and the distributed methods will have problems to disentangle their specific contributions.

All facts considered, the most cautious interpretation of the above mentioned results suggest that the N170/M170 might be generated by multiple cortical sources: primary sources located in face selective clusters, mainly the occipital gyrus and the fusiform gyrus, and secondary sources in visual areas that respond to object shapes e.g. the lateral occipital complex.

## 2.2 Study 1: Early (N170) face-sensitivity despite right lateral occipital brain damage in acquired prosopagnosia

*Esther Alonso Prieto*[1], *Stephanie Caharel*[1], *Richard Henson*[2] *and Bruno Rossion*[1]

[1] Université catholique de Louvain, Louvain-la-Neuve, Belgium
[2] MRC Cognition and Brain Sciences Unit, Cambridge, England

(This article is under review at the journal "Frontiers in Neuroscience".)

**Abstract**

The amplitude of the N170 event related potential increases when pictures of faces are presented compared to other objects categories. This so-called N170 face effect is larger over occipito-temporal sites, especially in the right hemisphere, peaks around 170 ms and has been associated with the early categorization of the visual stimulus as a face. Here we tested whether this N170 face effect can be observed despite damages to the visual areas that show a preferential response to faces as typically identified in neuroimaging. Event related potentials (128 electrodes) were recorded in response to faces, cars and their phase-scrambled versions in a well-known brain-damaged case of prosopagnosia (PS). Despite the patient's right inferior occipital gyrus lesion encompassing the most posterior cortical area that shows preferential activations to faces (i.e., the so-called occipital face area, OFA), we observed a clear early face-sensitive

component over the right occipito-temporal hemisphere of the patient that was identified as the N170. A second experiment supported the association of this component with the N170, showing the typical increase of latency and amplitude in response to inverted faces. In contrast, there was no N170 in the left hemisphere, where PS has a lesion to the middle fusiform gyrus and shows no evidence of face-preferential response in neuroimaging (no left fusiform face area, or FFA). These results were replicated by a magneto-encephalographic investigation of the patient with the same experiments, disclosing an M170 component. These observations indicate that face preferential activation in the inferior occipital cortex is not necessary to elicit early visual responses associated with face perception (N170/M170) on the human scalp. These results further suggest that when the right inferior occipital cortex is damaged, the integrity of the middle fusiform gyrus and/or the superior temporal sulcus, two areas that show face preferential responses in the patient's right hemisphere - might be enough to generate the face-sensitive N170. Finally, the results suggest that the face preferential activations observed in fMRI studies of this patient might occur within the first 170 ms after stimulus onset.

**Keywords:**

prosopagnosia, N170/M170, OFA, FFA

### 2.2.1 Introduction

Faces are the most frequent and important stimuli we encounter in our social life and the question of how they are perceived has received considerable interest in cognitive neuroscience. Although the extensive research during the last decades has advanced our understanding of the neural mechanisms underlying face perception, still little is known about the functional role of the brain areas involved and the temporal dynamics of the process. Studies of patients with acquired prosopagnosia, who are unable to recognize faces after brain injury (Bodamer, 1947), are useful in this endeavor. Together with electrophysiological and neuroimaging research in animals and healthy humans, such lesion studies have helped to demonstrate the importance of a wide set of areas responding specifically or preferentially to faces in the occipito-temporal cortex, with a dominance of the right hemisphere (e.g., Allison *et al.* (1994, 1999); Barton *et al.* (2002); Bouvier & Engel (2006); Damasio *et al.* (1982); Gauthier *et al.* (2000); Haxby *et al.* (2000); Kanwisher *et al.* (1997); Rossion (2003); Sergent & Signoret (1992); Sergent *et al.* (1992)).

The combination of neuroimaging with the study of brain-damaged patients provides important further constraints on the functional organization of this set of areas (Marotta *et al.*, 2001; Rossion, 2008). For instance, in the normal brain, preferential

activation to faces is generally observed concomitantly at least in the inferior occipital gyrus (so-called Occipital Face Area, OFA) (see Pitcher *et al.* (2011) for a review), the middle fusiform gyrus (the so-called Fusiform Face Area, FFA) (Kanwisher *et al.* (1997) and see Kanwisher & Yovel (2006) for a review), and the posterior section of the superior temporal sulcus (pSTS) (Puce *et al.* (1998) and see Haxby *et al.* (2000) for a review). Interestingly, despite a right hemisphere lesion to the inferior occipital gyrus leading to prosopagnosia, and thus no evidence of an OFA activation, one can still observe right FFA and pSTS activation (see Rossion (2003); Sorger *et al.* (2007) for evidence on patient PS and Steeves *et al.* (2006) for evidence in patient DF). This latter observation challenges a strictly hierarchical view of the neural basis of face perception (Fairhall & Ishai, 2007; Haxby *et al.*, 2000; Ishai, 2008; Pitcher *et al.*, 2007). Instead, it suggests that in the intact human brain there may be direct pathways from early visual areas to the middle fusiform gyrus and pSTS, bypassing a face-preferential activation in the inferior occipital cortex (i.e., in particular to FFA bypassing OFA (Atkinson & Adolphs, 2011; Rossion, 2003, 2008). One purpose of a hypothetical direct ventral pathway to the middle fusiform gyrus might be to categorize the visual stimulus as a face based on an initial, coarse, holistic/configural representation (Goffaux *et al.*, 2011; Rossion, 2008; Rossion *et al.*, 2011).

According to this view, preferential activation to faces should have an early onset time, irrespective of the integrity of the inferior occipital cortex (i.e., any OFA activation). To corroborate this hypothesis, knowledge about the activation time course of face preferential areas in normal observers and brain-damaged patients could be useful. Unfortunately, the time course of activation cannot be directly measured in these areas in the normal human brain. Currently, recordings of electrical (electroencephalogram, EEG) and magnetic fields (magnetoencephalography, MEG) on the human scalp are the only non-invasive methods that provide information at sufficient temporal resolution (i.e. milliseconds), albeit with a poor spatial resolution. These studies have identified on the human scalp an occipito-temporal event related potential (ERP) of negative polarity, the N170, which appears between 130 and 170 ms after stimulus onset and increases its amplitude when faces are presented compared to other object categories (e.g., Bentin *et al.* (1996); Boetzel *et al.* (1995); for earlier studies on the positive counterpart of N170, see Jeffreys (1989); for a review of N170 face-sensitivity, see Rossion & Jacques (2010)).

Although MEG is sensitive to only a subset of the sources generating the EEG scalp components (i.e., tangential sources), MEG studies have also reported an increased M170 in response to faces (e.g., Halgren *et al.* (2000); Linkenkaer-Hansen *et al.* (1998)).

This increased amplitude has been named the N170/M170 face effect and represents a temporal marker of the first and most consistent electrophysiological response to faces

in the human brain (Jacques & Rossion, 2006; Rossion & Jacques, 2010) a response that cannot be accounted for by low-level visual features (Rossion & Caharel, 2011).

Even though there is no agreement about the exact neural sources of this component, the posterior and middle sections of the fusiform gyrus have been identified as primary contributors of the scalp component in many source localization studies (e.g., Boetzel *et al.* (1995); Deffke *et al.* (2007); Henson *et al.* (2009); Linkenkaer-Hansen *et al.* (1998); Watanabe *et al.* (1999)) possibly with an additional contribution of the pSTS (Itier & Taylor, 2004).

Although confronting the anatomical, neuropsychological and electrophysiological profiles of patients with acquired prosopagnosia can help to determine the neurofunctional dynamics of face perception, such studies are scarce and their implications generally remain at the functional level (for ERP studies on patients with congenital/developmental prosopagnosia, see e.g., Bentin *et al.* (1999, 2007)). For instance, Renault *et al.* (1989) showed evidence for covert (i.e., non-conscious) recognition of faces in a case of prosopagnosia using the P300 amplitude and latency difference for familiar and unfamiliar face processing (for similar evidence in another case using a face identity matching paradigm see Bobes *et al.* (2003)). Eimer & McCarthy (1999) reported an absence of N170 component in their case of acquired prosopagnosia, providing ERP evidence that the patient's encoding of face representations was impaired. However, most recently, Dalrymple *et al.* (2011) reported the ERP data of 5 patients with acquired prosopagnosia whose lesions and face-sensitive cortical areas had been well defined. Two patients with lesions sparing the cortical territory of the posterior face-sensitive areas (FFA, OFA, pSTS) presented with normal N170 face effect in the right hemisphere. In contrast, two patients with lesions encompassing both the right OFA and FFA did not present with a N170 face effect. Interestingly, a fifth patient who had brain damage encompassing the right FFA but not the OFA presented with a N170 face effect. The authors concluded that at least two of the 3 major functional areas must be functionally intact to generate the N170 face effect. However, to be correct, this claim still has to be substantiated by the demonstration of a normal N170 face effect when damage concerns the right inferior occipital gyrus, with no OFA activation, while the 2 main anterior components of the right hemisphere cortical face network (FFA, pSTS) are spared. More generally, to our knowledge, there is no report of a right N170 face effect in a patient with acquired prosopagnosia who has a right hemisphere lesion limited to the inferior occipital gyrus while sparing both the middle fusiform gyrus and pSTS. That is, one cannot exclude from previous studies that the integrity of the right inferior occipital gyrus alone, encompassing the right OFA, is necessary for observing early face-sensitive responses on the scalp.

This issue was addressed in the present study. Here, electromagnetic scalp recordings of the brain-damaged patient PS are reported for the first time when the patient

is stimulated with faces, objects and visual stimuli while controlling for low-level visual features. According to the introduction section above, this endeavor is important for at least two reasons. First, to test the hypothesis that a lesion of the right inferior occipital cortex (i.e., no right OFA, rOFA), which removes any face preferential response in this region, does not prevent the observation of early face-preferential responses (N170/M170) over the right hemisphere (Rossion, 2003). Such an observation would provide indirect evidence that face-sensitive activation as recorded in fMRI in high-level areas (FFA and pSTS) may have an early onset time of activation despite no relay in the inferior occipital gyrus, and therefore may arise through direct feedforward inputs from early visual areas. Alternatively, if an early face preferential potential cannot be observed over PS's right hemisphere, it might be argued that FFA and pSTS activation to faces in the patient's brain as described in previous studies is rather driven by top-down processes, as could be alternatively hypothesized (e.g., Kleinschmidt & Cohen (2006); Reddy *et al.* (2007); Righart *et al.* (2010)).

Second, patient PS has a lesion in the left hemisphere showing the reverse pattern to the right hemisphere damage: it encompasses the whole left middle fusiform gyrus, without evidence of left FFA activation, while the left inferior occipital cortex remains structurally intact (Figure 2.8). Hence, comparing the N170 recorded on the right versus the left hemisphere in this patient might be particularly informative as to the contribution of the FFA to the N170 recorded on the scalp. In other words, the presence of an N170 on the right but not on the left hemisphere would strongly suggest that the FFA plays a major role in generating the N170 face effect.

In addition, with respect to the previous ERP studies of cases of acquired prosopagnosia cited above, the present study presents with several particular interests. First, it focuses on a patient whose impairment in face perception/recognition is well characterized and restricted to faces (e.g. Busigny *et al.* (2010)), who has been studied extensively in fMRI (e.g., Rossion (2003); Sorger *et al.* (2007)) and for whom a demonstration of early face-sensitive responses would have theoretical implications for the neural dynamics of face perception, as explained above. Second, the single-case tested here was stimulated with visual images matched for low-level properties with faces and objects and several EEG recordings (8 in total) were made to ensure replicability of the findings. Third, PS was also tested in a MEG experiment for converging evidence since MEG is less affected by signal distortions caused by the skull and scalp than is EEG, an important consideration when studying patients with brain damage. Finally, since one of the most characteristic signatures of the N170 as recorded in the normal adult brain is its increased latency and amplitude to inverted faces (e.g.,Linkenkaer-Hansen *et al.* (1998); Rossion *et al.* (1999)) a second experiment was performed on PS in which upright and inverted faces were presented, in order to help identifying the component in the patient's brain and characterize its response properties.

## 2.2.2 Methods

### 2.2.2.1 Participants

**Patient PS:**

PS' neuropsychological profile was already presented in chapter 2, section 1.4. Briefly, she was born in 1950 and sustained a closed head injury in 1992 that left her with extensive lesions of the left mid-ventral (mainly fusiform gyrus) and the right inferior occipital cortex (Figure 2.8). Her visual field is almost full (she has a small left para-central scotoma) (Sorger *et al.*, 2007) and her visual acuity is below normal but good (0.8 for both eyes as tested in August 2003 (Sorger *et al.*, 2007)). PS' only continuing complaint is a profound difficulty in recognizing familiar faces, including those of her family when they are presented out of context. This impairment in face recognition and individual face discrimination has been formally established in several behavioral studies with classical neuropsychological tests as well as individual face matching and recognition computer tasks (see Busigny *et al.* (2010); Rossion *et al.* (2003b); Schiltz *et al.* (2006)). Importantly, PS does not present any difficulty in recognizing and discriminating non-face objects, even when fine-grained discrimination is required and considering both accuracy rates and response times (Busigny *et al.*, 2010; Rossion *et al.*, 2003b; Schiltz *et al.*, 2006).

**Normal controls:**

In EEG experiment 1, faces vs. objects, the sample of control participants consisted of 11 paid female volunteers (mean age = 23 ± 2.45 years), with the data of 4 of them having been included in a larger sample of males and females subjects in a recent study (Rossion & Caharel, 2011). In experiment 2, inverted faces, 8 paid female volunteers were tested (mean age = 21.43 ± 2.57 years). Four age-matched female controls (mean age = 59.33 ± 2.52 years) were also tested in each experiment to account for potential age-related effects on early visual ERPs that were of interest in the present study. All participants but one were right handed and all had normal or corrected-to-normal vision. They gave their informed consent after detailed information about the experiment was provided. The study was approved by the ethical committee of the Catholic University of Louvain and was in agreement with the Declaration of Helsinki.

### 2.2.2.2 Stimuli

**Experiment 1. Faces vs. objects and scrambled stimuli:**

Two sets of 43 colored photographs of full front faces and cars were used (Figure 2.9). Two additional sets of stimuli were built by scrambling the faces and the cars using a

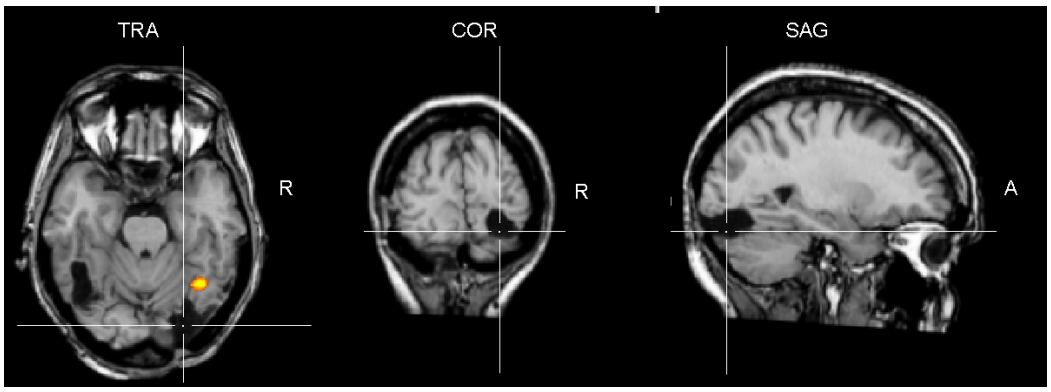


**Figure 2.8: Brain damage profile of the acquired prosopagnosia patient PS.** - This patient has damage to the left middle fusiform gyrus and a small lesion to the right middle temporal gyrus, but her main lesion, thought to be instrumental in causing her prosopagnosia, concerns the right inferior occipital cortex (line crossing). This lesion does not prevent a preferential activation for faces in the right middle fusiform gyrus (FFA; here as the result of a combined analysis of 6 functional localizer runs, contrasting faces and object pictures in a face localizer contrast, see Sorger *et al.* (2007) for details). Although this region responds preferentially to faces, it does not show the normal release from adaptation to different facial identities, in line with the difficulties of the patient in individualizing faces. (TRA: transverse plane; COR: coronal plane; SAG: sagittal plane; R: right; A: anterior.)

Fourier phase randomization procedure (Figure 2.9) ,(Naesaenen, 1999)). This procedure leads to different scrambled stimuli than used in several previous ERP studies, in which face components are swapped (e.g.,George *et al.* (1996)) or pieces of the stimuli are exchanged so that the faces and objects are not recognizable (e.g., Allison *et al.* (1994); Bentin *et al.* (1996)). Here, as in a few previous studies (e.g., Rousselet *et al.* (2005); Watanabe *et al.* (2003)) the phase spectrum of the images is replaced with random values, keeping their amplitude spectrum unaltered. It yields images that preserve the global low-level properties of the originals (i.e., luminance, global contrast, color, spatial frequency) while destroying their shape (Rossion & Caharel, 2011).

This particular set of stimuli (faces, cars, and their scrambled counterparts) has been used in recent studies in order to localize the human brain areas responding preferentially or selectively to faces in fMRI and disentangle low-level from high-level visual factors as contributing to differences between faces and other stimuli on early visual ERPs (e.g., Rossion & Caharel (2011)). All stimuli subtended 3.72 x 4.24 degrees of visual angle and they were displayed using E-prime 1.1 on a light grey background.

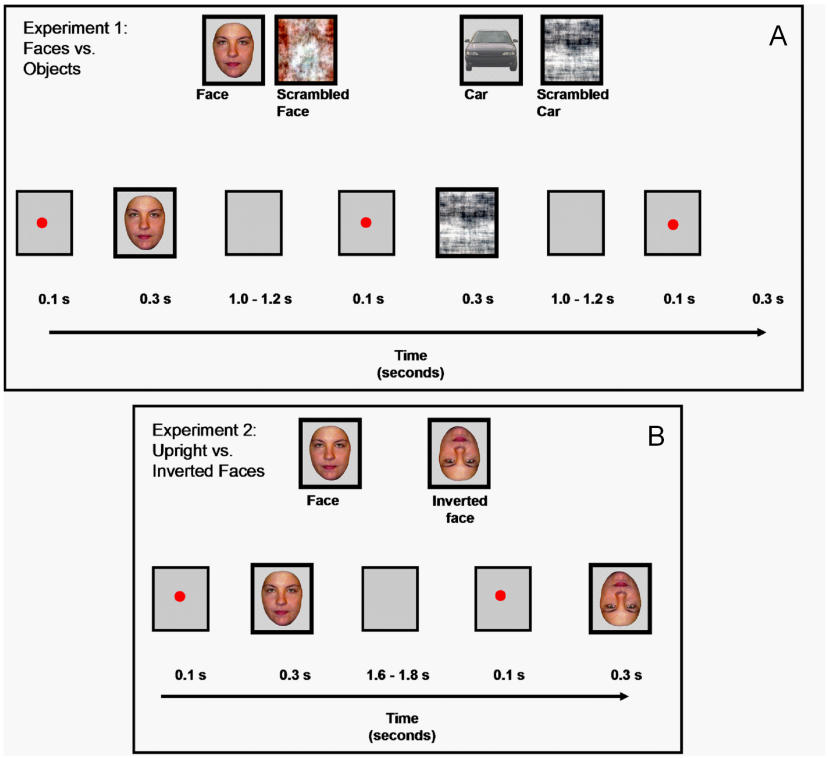


**Figure 2.9: Experimental design applied in Study 1.** - (A): Experiment 1, faces vs. objects. (B): Experiment 2, upright vs. inverted faces.

**Experiment 2. Face inversion:**

Photographs of thirty front view faces (15 females) without glasses, facial hair, or make-up, and with neutral expression were used. Inverted (flipped) versions of the 30 faces were also presented during the experiment (Figure 2.9). These cropped faces were equated for mean pixel luminance. They were shown in full color and subtended approximately 2.95 x 4.02 degrees of visual angle.

#### 2.2.2.3 Procedure

Two times forty-three instances of each of the 4 kinds of stimuli (86 x 4 trials in total) were presented in random order (Figure 2.9A) and participants had to judge whether the stimulus was an object (face or car) or a 'texture' (scrambled versions). To ensure that PS' results were replicable and also to increase signal-to-noise ratio, she performed the experiment 8 times in total (2 recording sessions in December, 2008; December, 2009; March 2010 and June 2010) leading to a total of 688 trials for each condition. Grand averages of all sessions are reported, and the data of each individual session are also displayed.

The timeline of events in experiment 2 is shown in Figure 2.9B, in which upright and inverted faces (random order) were presented and participants had to press one key if the stimulus was upright and another key if the stimulus was inverted. They performed 90 trials per condition in one session (30 stimuli in each set repeated 3 times each). Again, to ensure that her results were replicable and to increase signal-to-noise ratio, PS performed the experiment 8 times in total, always following experiment 1 (in December, 2008; December, 2009, March and June, 2010) leading to a total of 720 trials for each condition. The MEG data were acquired during a two-day visit to the MRC Cognition and Brain Sciences unit in Cambridge, UK, from 29th-30th November, 2007. Three runs of Experiment 1 were applied consecutively on Day 1, and one run of Experiment 2 on Day 2.

**EEG recording and data analysis:**

Scalp EEG was recorded from 128 Ag/AgCl electrodes mounted in an electrode cap (Wavegard, ANT Inc.) (Figure 2.10) with a left mastoid reference. Electrodes were positioned according to the standard 10-20 system with additional intermediate positions. Two pairs of bipolar electrodes were used to record vertical and horizontal eye movements. Electrode impedances were maintained below 10 kΩ during recording. EEG analog signal was digitized at a 1000 Hz sample rate and a digital analog-aliasing filter of 0.27* sampling rate was applied at recording (at 1000 Hz sampling rate the usable bandwidth is 0 to approximately 270 Hz). EEG data were analyzed using ASA 4.6 (ANT, Inc.), Brain Vision Analyzer (2.0), and custom-made routines in Matlab 7.0.

EEG was filtered with a bandpass filter of 0.1 to 30 Hz. Time points in the filtered data at which the absolute amplitude of the EEG exceeded ± 120 $\mu$V were marked as EEG artifact or blink artifacts. Trials containing EEG artifacts were rejected from further analysis, as were trials containing an incorrect behavioral response. Data was then averaged in epochs from 200 ms pre-stimulus onset to 800 ms post-stimulus onset. Averages were baseline corrected using the 200 ms pre-stimulus epoch and re-referenced to a common average reference.

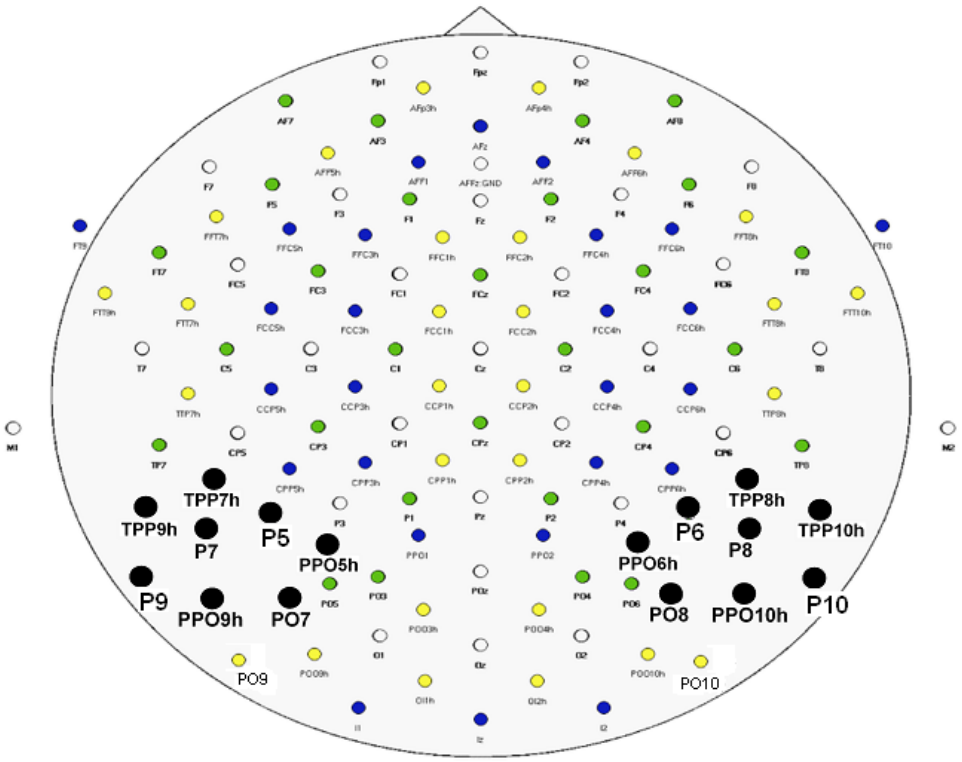


**Figure 2.10: Electrodes layout used for data recording in Study 1** - The figures showed a representation of the electrodes distribution used for EEG recording. The electrodes where PS presented the highest N170 for all conditions (P6, P8, PO8, PPO10h and PPO6h) as well as the electrodes where she exhibited the highest difference between faces and cars (P8, P10, TPP8h and TPP10h) are indicated (see text for further details). Note that the equivalent electrodes in the left hemisphere are also displayed.

### MEG recording and analysis:

MEG data were acquired using a whole-head, 306-sensors (102 magnetometers and 102 pairs of orthogonally oriented planar gradiometers) VectorView system (Elekta

Neuromag Oy). The MEG unit was housed in a light magnetically shielded room (MSR). Signals were sampled at 1 kHz within on-line band-pass filtering 0.03-330 Hz. The position of PS' head was monitored continuously by four head-position indicators (HPI) coils. To measure eye movements and blinks, electrooculogram (EOG) was recorded from two pairs of bipolar electrodes placed above and below one eye (VEOG) and on the outer canthus of each eye (HEOG). Experiment 1 was run three times in a single session, though HPI problems towards the end of the second run resulted in loss of about 20% of those trials. Experiment 2 was run once during a separate session on the following day.

Initial preprocessing of the MEG data used Signal Space Separation (SSS) (Taulu & Simola, 2006) as implemented in the MaxFilter 2.0 software (Elekta Neuromag, Helsinki). This approach re-expresses the data in terms of linear combinations of spherical-harmonic basis functions describing two separable subspaces that reflect sources originating inside and outside the sensor array. The origin was set to the centre of the head, defined as the best-fitting sphere to the digitized scalp points (excluding points on the face and nose). This SSS representation was then used in three steps. First, 'bad' channels were detected using the initial 20 seconds of data from each session, which were uncontaminated by HPI signal (no bad channels were detected). In the second step, head-movement correction was applied every 200 ms (estimated total translation within each session was less than 3 mm), and noise from sources beyond the outer sphere, or from within the space between the inner and outer spheres (that would produce components in inner and outer spheres that are temporally correlated) was removed using the temporal extension of SSS (Taulu & Simola, 2006). In a third step, the movement-corrected head position in each session was virtually transformed to a common location across sessions relative to the default device space. This was achieved by moving the origin of the sphere fit to PS' headpoints to a point (0, 13, -6) in device coordinates (appropriate for the typical head-size according to the Elekta Neuromag Users Manual), and rotated such that the head coordinate system, defined by the pre-auricular and nasion fiducial markers, was aligned to the device coordinate system. Data were downsampled to 250 Hz (with anti-aliasing filter).

The SSS-processed continuous data were then analyzed with SPM5 and custom-made routines in MATLAB, emulating the same pre-processing steps as for PS' EEG data, i.e. filtered within a band of 0.1 to 30 Hz, epoched from -200ms to +800ms (baseline-corrected from -200ms to 0ms), and then epochs containing EOG deflections above $\pm 120 \mu V$ rejected prior to averaging over epochs for each condition to create event-related fields (ERFs) for each condition (resulting in at least 146 artifact-free trials for each of the 4 conditions in Experiment 1, and at least 83 trials for each of the 2 conditions in Experiment 2).

#### Statistical analysis of ERP and ERF data

In normal participants, two clear visual ERP components elicited by the different sets of stimuli were analyzed: the P1 (maximal at approximately 100 ms), and the N170 (maximal at approximately 150 ms). Amplitude values of these components were measured at the different pairs of occipito-temporal electrodes in the left and right hemisphere where they were the most prominent. Amplitudes were quantified for each condition as the mean voltage measured within 30 ms windows centered on the grand average peak latencies of the components maximum. Peak latency of both components were extracted automatically at the maximum amplitude between 70 and 140 ms for the P1, and at the minimum value between 120 and 190 ms for the N170 at the pairs of occipito-temporal electrodes where these components were the largest. A similar approach was taken to the ERFs recorded from the MEG magnetometers (the root-mean square (RMS) of the planar gradiometer data showed similar results). The amplitude and latency values of each component were then submitted to separate repeated-measures analysis of variance (ANOVA). Three within-subject factors were used: Shape (non-scrambled, scrambled), Category (faces, cars) and Hemisphere (right and left). Post-hoc comparisons were performed using post-hoc t-tests ($p<0.05$). All effects with two or more degrees of freedom were adjusted for violations of sphericity according to the Greenhouse-Geisser correction.

For the ERP data, this analysis was performed for the younger control group and for PS, although the electrodes selected were slightly different for PS because the topography was not identical to control participants (see results). For PS we used the 8 repetitions of the experiment. The 4 age-matched controls performed only one repetition of the experiment and were not analyzed as a group, but their individual data were compared to PS. The comparison between PS (once again using all 8 experiment repetitions averaged together) and the control group was performed using the Crawford and Howell's method (Crawford *et al.*, 2009).

### 2.2.3 Results

#### 2.2.3.1 EEG Data. Experiment 1: Faces vs. Objects

#### Behavioral data

Mean accuracy and response time to correct responses for each experimental group are reported in Table 2.1. Performance was almost flawless in this easy task, with PS and age-matched controls scoring above 99% in all conditions. Young controls performed between 95.5% and 97.8%. PS' average RTs in the first session did not differ from those of controls (Faces: $t(14) = 0.14$, $p > 0.05$; Cars: $t(14) = 0.79$, $p > 0.05$; Scrambled Faces: $t(14) = 0.48$, $p > 0.05$; Scrambled Cars: $t(14) = 0.57$, $p > 0.05$).

| | Accuracy (%) | | | | Reaction Time (ms) | | | |
|---|---|---|---|---|---|---|---|---|
| | Faces | Cars | Scramb. Faces | Scramb. Cars | Faces | Cars | Scramb. Faces | Scramb. Cars |
| Young Controls | 97.8 ±3.73 | 95.57 ± 4.95 | 97.64 ± 2.78 | 97.86 ± 3.58 | 626.19 ± 169.6 | 585.15 ± 102.1 | 614.78 ± 125.6 | 589.68 ±91.54 |
| Age matched Controls | 99.6 ± 0.56 | 99.38 ± 1.14 | 99.70 ± 0.57 | 99.99 ± 0.00 | 499.67 ± 83.83 | 526.43 ± 87.59 | 526.41 ± 81.94 | 521.53 ± 78.32 |
| PS | 100.00 ± 0.00 | 99.27 ± 1.64 | 99.13 ± 1.35 | 99.42 ± 0.88 | 721.10 ± 71.93 | 742.52 ± 65.39 | 733.08 ± 66.98 | 730.61 ± 62.65 |

**Table 2.1: Behavioral results experiment 1 (faces vs. objects)** - Mean accuracy and response time achieved by each experimental group in experiment 1, faces vs objects.

**Electrophysiological data: P1 component**

*Young controls:* In young controls the first electrophysiological component observed in response to all 4 stimuli, the P1, peaked at about 100 ms (Table 2.2, Figure 2.11 A) and reached its highest amplitude at P8/P7 and lower channels. Similar pattern was observed in the group of age-matched controls (Figures 2.12 and 2.13). In the group of younger controls, there was a main effect of Category on P1 amplitude (ANOVA, $F(1, 10) = 8.31$, $p<0.05$), reflecting the larger response to faces and scrambled faces than cars and scrambled cars (Figure 2.11 A) (see also Rossion & Caharel (2011)). There was no effect of Shape or interaction between the two factors ($ps>0.05$). All other effects were non-significant (all $ps>0.05$). Regarding P1 latency, the ANOVA analysis revealed a significant interaction between Category and Shape (ANOVA, $F(1, 10) = 7.83$, $p < 0.05$). This result was due to slower responses to scrambled faces than faces (t-test, $t(10) = 2.28$, $p < 0.05$) and scrambled cars (t-test, $t(10) = 2.50$, $p < 0.05$).

*PS:* Patient PS exhibited a first positive electrophysiological response between 80 and 114 ms in all experimental conditions, identified as the P1. It reached its largest amplitude between 100 and 120 ms, about 10 ms earlier in the left than in the right hemisphere. In all cases, it was delayed and slightly larger for scrambled stimuli (Table 2.3, Figures 2.14 and 2.15). When the P1 component reached its largest amplitude, there was a simultaneous increase in amplitude at some of the lowest, right occipital electrodes, with a much later peak (around 140 ms). These right posterior electrodes were located on the skull over the right lateral occipital cortex, where the brain structure is damaged. This unusual visual component had a positive polarity and was present in all conditions during the late P1 peak. Interestingly, before the rise of the P1, between

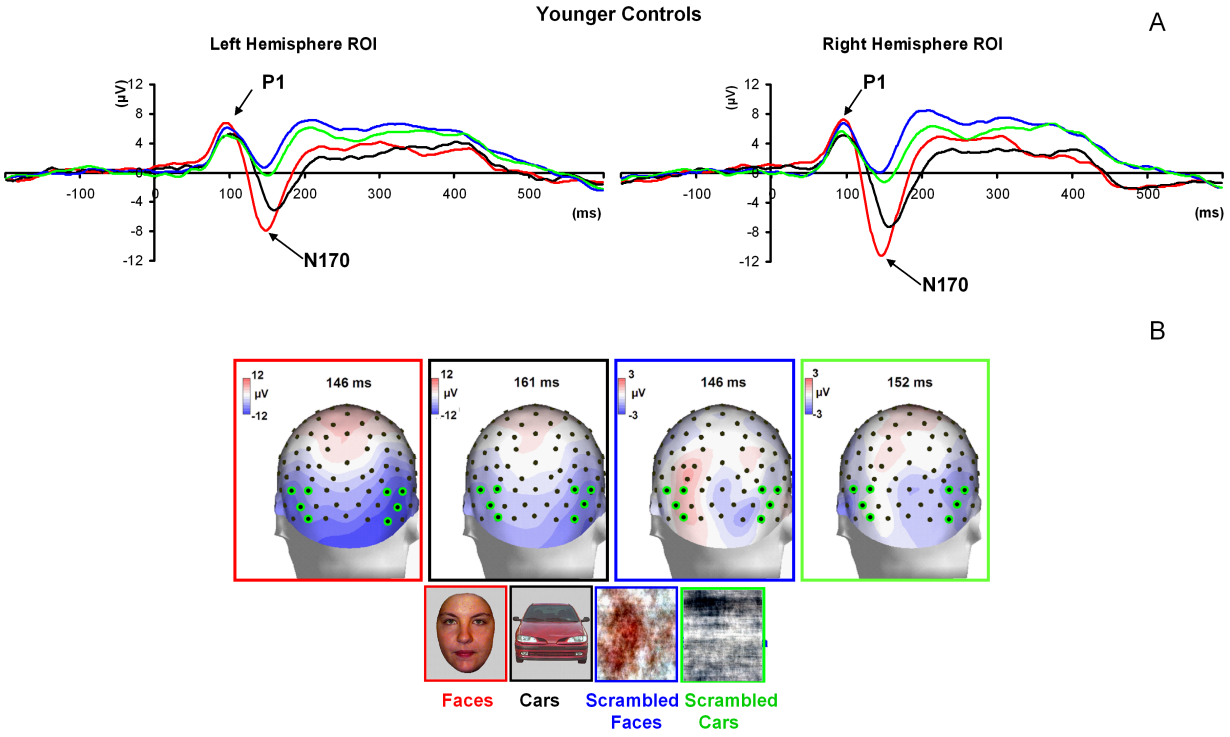


**Figure 2.11: Results obtained by healthy participants in experiment 1 (faces vs. objects), Study 1.** - (A). Visual ERPs elicited by all stimulus types in the group of younger controls, highlighting the sensitivity to faces of the P1 and N170 (the ROIs are based on 4 channels highlighted in green in the topographical maps). Note that P1 was larger in amplitude both to faces and phase-scrambled faces than to cars and phase-scrambled cars. In contrast, the N170 was small for meaningless (phase-scrambled) stimuli, and showed a larger response to faces than cars. (B). Topographical maps of the N170 for the group of younger controls tested in this study. The channels included in the ROIs are highlighted in green.

| Faces | | | | Cars | | | |
|---|---|---|---|---|---|---|---|
| Right Hemisphere | | Left Hemisphere | | Right Hemisphere | | Left Hemisphere | |
| Amp | Lat | Amp | Lat | Amp | Lat | Amp | Lat |
| 8.29 | 97.55 | 7.32 | 94.27 | 6.50 | 99.45 | 6.60 | 101.9 |
| ±1.84 | ±7.83 | ±2.94 | ±8.73 | ±3.75 | ±10.31 | ±2.41 | ±13.08 |
| Scrambled Faces | | | | Scrambled Cars | | | |
| Right Hemisphere | | Left Hemisphere | | Right Hemisphere | | Left Hemisphere | |
| Amp | Lat | Amp | Lat | Amp | Lat | Amp | Lat |
| 8.15 | 102.00 | 7.51 | 104.18 | 7.03 | 98.18 | 6.31 | 100.18 |
| ±2.60 | ±14.85 | ±3.07 | ±14.83 | ±2.67 | ±13.27 | ±2.34 | ±14.11 |

**Table 2.2: Mean amplitude and latency values of P1 component for younger participants.** - The channels where the component reached its highest amplitude (P8/7, PO8/O7, PPO10h/9h and PO10/9) were averaged together to form two regions of interest, one in the right and another one in the left hemisphere (Amplitude: $\mu$V, Latency: ms).

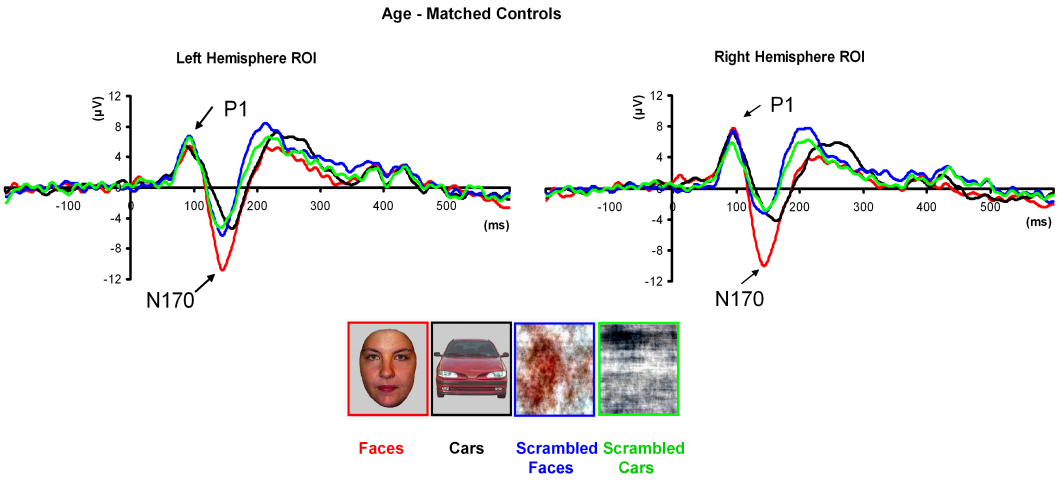


**Figure 2.12: Averaged waveforms of the age-matched participants in response to faces, cars and their scrambled counterparts.** - Age-matched controls also exhibited a P1 larger in amplitude both to faces and phase-scrambled faces than to cars and phase-scrambled cars. In contrast, the N170 was small for meaningless (phase-scrambled) stimuli and showed a larger response to faces than cars.

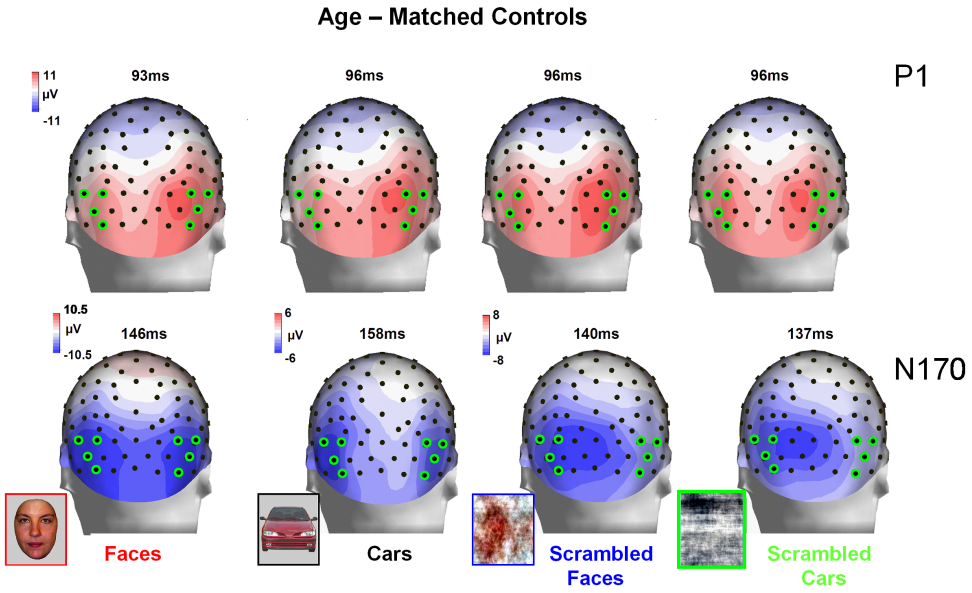


**Figure 2.13: Scalp voltage distribution of P1 and N170 components for age-matched participants.** - The latency value indicated corresponds to the time-point at which each component was maximal.

75 and 96 ms, there was also a negative component observed on the exact same electrodes (Figure 2.14) suggesting that, following stimulus onset, current flows alternate direction over the lesion site. This unusual time-locked visual component observed over the lesion site complicates the identification of the P1 for the patient PS. Nevertheless, the P1 could be measured adequately due to its lateral distribution and its peak falling in between the maxima of the unusual component.

The statistical analysis was carried out using the 8 repetitions performed by PS. To this end, latency and amplitude values were averaged over all 4 electrodes located away from the lesion where the P1 component was maximal before 120 ms (PO8/09, PPO10h/9h, PO6/5 and P8/7). For the P1 amplitude, there were main effects of Shape (ANOVA, $F\ (1,7) = 8.61, p < 0.05$; scrambled>intact) and Hemisphere (ANOVA, $F(1,7) = 19.57, p < 0.001$; right >left). All other effects were non-significant: $ps > 0.05$. Regarding P1 latency for PS, there was a main effect of Shape (ANOVA, $F\ (1,7) = 52.19, p < 0.001$) and Category (ANOVA, $F\ (1,7) = 9.80, p < 0.001$) which was qualified by an interaction between Shape and Category (ANOVA, $F\ (1,7) = 5.98, p < 0.05$). This interaction was due to an earlier P1 latency for faces compared to scrambled faces (t-test, $t(7) = 7.53, p < 0.001$), while the latency delay for scrambled cars as compared to cars was significant (t-test, $t(7) = 4.85, p = 0.002$) but smaller (Figure 2.15). There was also a main effect of Hemisphere (ANOVA,

$F(1,7) = 56.92, p < 0.001$) due to higher latency values in the right than in the left hemisphere.

*PS vs controls:* An index of P1 face-sensitivity in amplitude, which is due to low level visual cues, was computed for each participant (11 younger controls, 4 age-matched controls and PS) by comparing the averaged response obtained for faces and scrambled faces to the averaged response obtained for cars and scrambled cars over the right hemisphere only. For younger controls, the average and standard deviation of the difference was $1.00 \pm 1.51$ while for the age-matched controls it was $0.48 \pm 1.00$ and for PS it was $0.21 \pm 1.24$). Although, the positive difference on the P1 (face-sensitivity) is of small amplitude in patient PS, it was not out of range of the controls, and in fact, 2 age-matched controls and 3 younger controls did not present with any positive difference on the P1.

In summary, PS' first component in response to visual stimuli could be identified as the P1, with a lateral occipital topography. It was prominent on the same electrodes as normal participants, even though its late response, particularly on the more medial channels, appeared to be contaminated by the presence of unusual components over the lesion sites. There was no evidence of a sensitivity to low-level visual cues of faces for PS' P1 (i.e., larger amplitude to faces and scrambled faces than cars and scrambled cars), contrary to young controls taken as a group (Figure 2.11A). However, such effects were not found in all individual controls, so that it is impossible to conclude for any abnormality in PS' data at this level.

**Electrophysiological data: N170 component**

*Younger controls:* The N170 peaked at about 150 ms. It was most prominent over lateral occipital electrodes (P8/7, PO8/7, PO10/9, PPO10h/9), especially in the right hemisphere, and it reached its highest amplitude at P8 / P7. It was larger for the intact versions of the stimuli and slightly delayed for cars (Table 2.4, Figure 2.11). There was a significant main effect of Shape (ANOVA, $F(1, 10) = 51.72$, $p<0.001$), of Category (ANOVA, $F(1, 10) = 8.77$, $p<0.05$) and of Hemisphere (ANOVA, $F(1, 10) = 5.13$, $p<0.05$; right>left). The main effects of Shape and Category were qualified by a significant interaction between the two factors (ANOVA, $F(1, 10) = 10.71$, $p<0.05$). Post-hoc comparison showed that the N170 to faces was significantly larger than the N170 to cars (t-test, $t(10) = 3.95$, $p<0.05$) while there were no differences between scrambled faces and scrambled cars (t-test, $t(10) = 1.65$, $p>0.05$).

Regarding the N170 latency, statistical analysis showed a main effect of Shape (ANOVA, $F(1, 10) = 9.57$, $p<0.05$) and Category (ANOVA, $F(1, 10) = 59.171$, $p<0.001$). There was a significant interaction between the two factors (ANOVA, $F(1, 10) = 7.03$, $p<0.05$) since the N170 was delayed for cars compared to faces (t-test, $t(10) = 5.19$, $p<0.001$) and to a lesser extent for scrambled cars compared to scrambled faces (t-test, $t(10) = 4.18$, $p<0.001$) (Figure 2.11A).

| Faces | | | | Cars | | | |
|---|---|---|---|---|---|---|---|
| Right Hemisphere | | Left Hemisphere | | Right Hemisphere | | Left Hemisphere | |
| Amp | Lat | Amp | Lat | Amp | Lat | Amp | Lat |
| 6.93 | 110.88 | 3.19 | 94.75 | 7.06 | 105.50 | 3.87 | 85.63 |
| ±1.79 | ±6.42 | ±0.89 | ±5.70 | ±1.54 | ±0.18 | ±1.30 | ±3.15 |
| Scrambled Faces | | | | Scrambled Cars | | | |
| Right Hemisphere | | Left Hemisphere | | Right Hemisphere | | Left Hemisphere | |
| Amp | Lat | Amp | Lat | Amp | Lat | Amp | Lat |
| 8.11 | 121.88 | 4.07 | 95.13 | 7.32 | 117.50 | 4.44 | 99.38 |
| ±2.57 | ±5.57 | ±1.38 | ±4.22 | ±1.58 | ±6.46 | ±1.17 | ±5.83 |

**Table 2.3: Mean amplitude and latency values of P1 component for PS.** - The channels where the component reached its highest amplitude (P8/7, PO8/O7, PPO10h/9h and PO6/5) were averaged together to form two regions of interest, one in the right and another one in the left hemisphere (Amplitude: $\mu$V, Latency: ms).

| Faces | | | | Cars | | | |
|---|---|---|---|---|---|---|---|
| Right Hemisphere | | Left Hemisphere | | Right Hemisphere | | Left Hemisphere | |
| Amp | Lat | Amp | Lat | Amp | Lat | Amp | Lat |
| -11.74 | 146.18 | -7.99 | 147.82 | -7.61 | 157.46 | -5.22 | 159.18 |
| ±7.86 | ±1.65 | ±3.89 | ±10.51 | ±5.74 | ±10.59 | ±3.81 | ±11.84 |
| Scrambled Faces | | | | Scrambled Cars | | | |
| Right Hemisphere | | Left Hemisphere | | Right Hemisphere | | Left Hemisphere | |
| Amp | Lat | Amp | Lat | Amp | Lat | Amp | Lat |
| -1.65 | 142.91 | 0.14 | 145.09 | -2.76 | 147.37 | -1.11 | 148.82 |
| ±2.93 | ±14.52 | ±2.60 | ±13.69 | ±4.41 | ±5.17 | ±2.51 | ±4.15 |

**Table 2.4: Mean amplitude and latency values of N170 component for younger participants.**- The channels where the component reached its highest amplitude (P8/7, PO8/O7, PPO10h/9h and PO10/9) were averaged to form two regions of interest, one in the right and another one in the left hemisphere. (Amplitude: $\mu$V, Latency: ms).

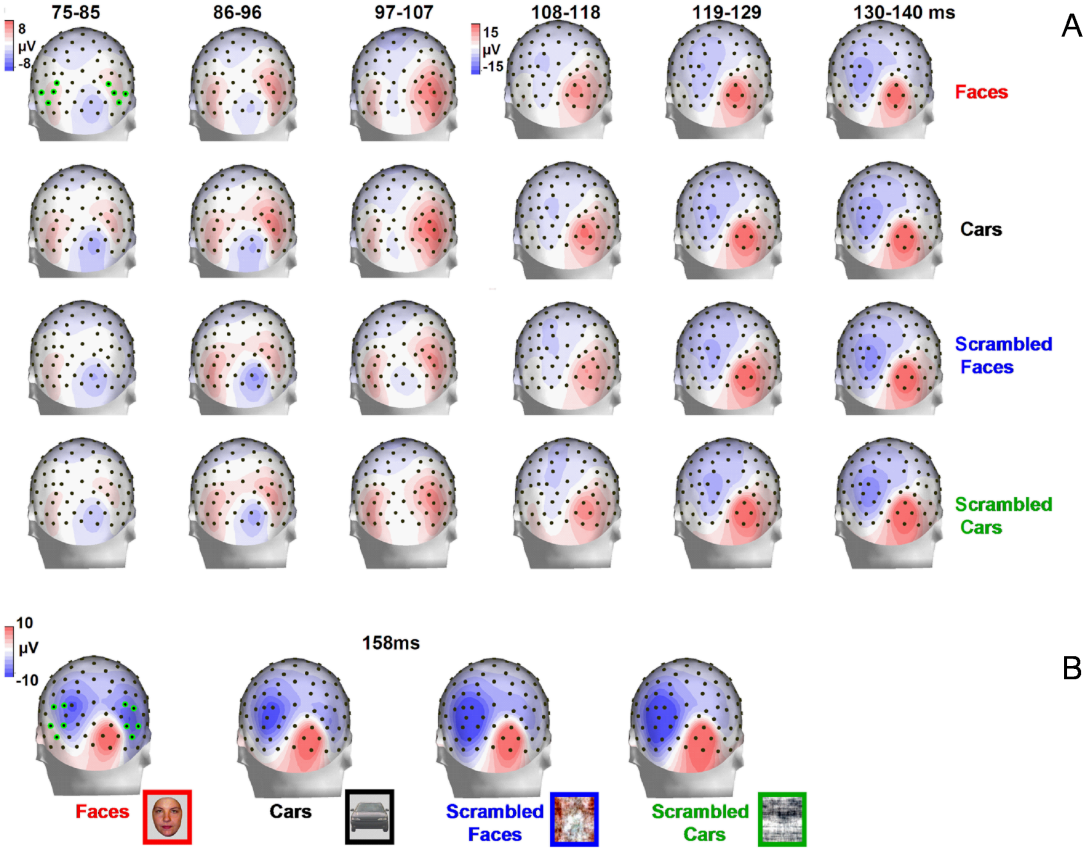


**Figure 2.14: Evolution of electrophysiological responses to visual stimulation at the back of the head of patient PS.** - Following visual stimulation, large evoked potentials were recorded on the right posterior medial sites, over PS' main lesion, with an alternation of negative and positive current flows out of the brain (negative at 75-85 ms, positive at 130-140 ms). These unusual components were most prominent before and after the lateral P1 component. It showed a large positive response during the N170 time-window (around 150 ms) which was contingent with a negative potential over left lateral occipital sites, an N170-like component (below). The display of topographies at the bottom of the figure corresponds to the peak of the N170 and shows that this component can only be identified in the right hemisphere, having the largest response to faces. The electrodes that have been used to form the ROIs for the P1 and N170 analysis, respectively, are highlighted in green.

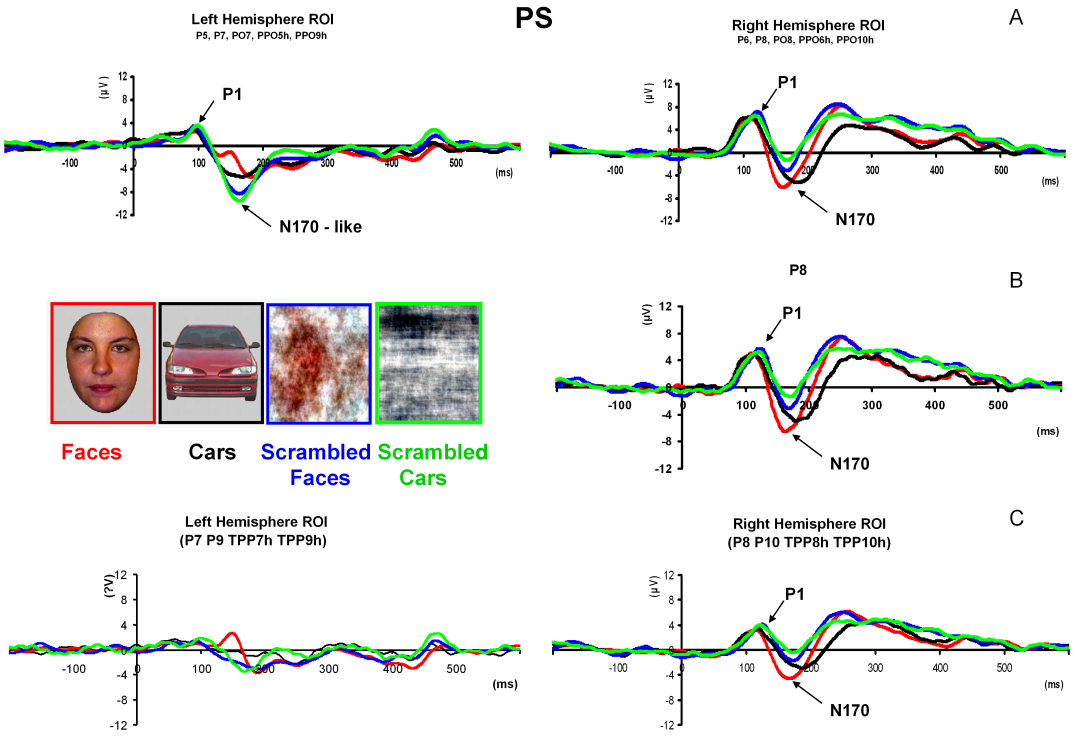


**Figure 2.15: Waveforms recorded over PS' scalp following visual stimulation in experiment 1 (faces vs. objects).** - The waveforms correspond to an average of 8 recording sessions (averages of each session are displayed in Figure 2.16) in which 86 trials were presented for each condition. The first response was identified as a P1, which did not differ much across conditions, but was slightly delayed and larger for scrambled stimuli. The second visual component showed a typical N170 response profile only in the right hemisphere (larger response to meaningful stimuli, larger and earlier response to faces than cars). Its topography (Figure 2.14) was slightly different than in normal controls due to the presence of a large unusual visual component recorded on the right posterior medial channels, over the main right hemisphere lesion. The 'N170-like' component, recorded on electrode sites over the left lateral occipital channels, did not show any of the characteristics associated with an N170. It presented the largest response to phase-scrambled stimuli and the lowest and most delayed response to faces. Different ROIs are presented because the larger response to faces than the other conditions was most pronounced on more anterior lateral channels (B, C) than on channels where all conditions elicited the largest N170 (A).

| Faces | | | | Cars | | | |
|---|---|---|---|---|---|---|---|
| Right Hemisphere | | Left Hemisphere | | Right Hemisphere | | Left Hemisphere | |
| Amp | Lat | Amp | Lat | Amp | Lat | Amp | Lat |
| -6.86 | 161.25 | -6.90 | 180.13 | -5.73 | 181.50 | -6.69 | 171.13 |
| ±1.66 | ±8.28 | ±3.99 | ±10.86 | ±0.83 | ±7.84 | ±4.10 | ±15.71 |
| Scrambled Faces | | | | Scrambled Cars | | | |
| Right Hemisphere | | Left Hemisphere | | Right Hemisphere | | Left Hemisphere | |
| Amp | Lat | Amp | Lat | Amp | Lat | Amp | Lat |
| -3.56 | 167.88 | -9.68 | 168.25 | -1.92 | 169.13 | -10.74 | 162.88 |
| ±2.57 | ±6.75 | ±3.23 | ±10.53 | ±1.24 | ±8.98 | ±2.62 | ±6.62 |

**Table 2.5: Mean amplitude and latency values of N170 component for PS.-** The channels where the component reached its highest amplitude for all conditions (P8/7, PO8/O7, PPO10h/9h, P6/5 and PPO6h/5h) were averaged together to form two regions of interest, one in the right and another one in the left hemisphere. (Amplitude: $\mu$V, Latency: ms).

*PS:* Following the P1, there was a clear bilateral negativity that resembled the N170 component exhibited by normal participants (Table 2.5; Figures 2.14B and 2.15). In the right hemisphere, it started at about 145 ms and reached its highest amplitude at about 160 ms on the lateral occipital electrodes, especially at P6, P8, PO8, PPO6h, and PPO10h. It was maximal for faces but it was also found for the other conditions albeit with a reduced amplitude, and with a latency delay for pictures of cars (Figure 2.15). It coexisted with the above-described positive unusual deflection that peaked in the right medial occipital electrodes around 140 ms (Figure 2.14A).

In the left hemisphere, there was also a large negative deflection that was maximal at lateral occipital electrodes but it differed in several aspects from the negativity observed in the right hemisphere. Specifically, it appeared around 15 ms earlier than in the right hemisphere and coexisted with the unusual positive deflection observed in the lowest, right medial occipital electrodes. Additionally, it reached its highest amplitude also later, at around 170 ms (Figures 2.14B and 2.15) and was located on slightly more parieto-occipital channels. Most importantly, it was much smaller for faces than for the remaining conditions (Figure 2.14A). These atypical characteristics clearly indicate that the left hemisphere negative peak did not correspond to the normal N170 component as observed both in healthy individuals and on right lateral occipital electrodes for PS. Consequently, analysis were performed for the right hemisphere only, using the averaged

latency and amplitude values over the 5 electrodes where the component was maximal, and only the factors of Shape (non-scrambled, scrambled) and Category (faces, cars) were used.

In the right hemisphere, there was a main effect of Shape (ANOVA, $F(1, 7) = 153.87$, $p<0.001$) on N170 amplitude. This was due to larger values for intact than scrambled stimuli. There was also a main effect of Category (ANOVA, $F(1, 7) = 10.92$, $p<0.05$) because of larger amplitude for faces/scrambled faces than for cars/scrambled cars. However, the interaction between these two factors failed to reach significance (ANOVA, $F(1, 7) = 0.37$, $p = 0.56$). The statistical analysis on the latency in the same hemisphere revealed that there was a main effect of Category (ANOVA, $F(1, 7) = 37.47$, $p<0.001$) but also an interaction involving the factors of Shape and Category (ANOVA, $F(1, 7) = 29.23$, $p<0.001$) due to a longer latency for cars compared to faces (t-test, $t(7) = 6.74$, $p<0.001$) and compared to scrambled cars (t-test, $t(7) = 3.68$, $p<0.05$), and for scrambled faces compared to faces (t-test, $t(7) = 3.99$, $p<0.05$).

In summary, the N170 resembled the component observed in normal participants only in the right hemisphere since it was larger for meaningful than scrambled stimuli, and larger for faces compared to cars. It was also significantly delayed for cars as compared to faces, as in normal controls of this study. The above-described pattern was observed in all 8 repetitions of the experiment (Figure 2.16) and also when the data was re-referenced to Fz, a procedure that was done because the data could have been potentially affected by an average-reference that incorporated electrodes where the unknown (large) component was present (Figure 2.17). Finally, it is also worth noting that the selection of electrodes for the ROI of the right hemisphere was based on the observation that the largest negative peak was found on the same channels for all conditions (Figure 2.15). However, the largest difference between faces and the other conditions was observed on the most anterior and lowest of the 5 channels (P8) (Figure 2.15), which is generally - or is among one of - the optimal channel(s) to disclose the N170 face effect (Rossion & Jacques, 2008). For patient PS, averaging conditions over P8 and the more anterior and lower neighboring channels over the right occipito-temporal lobe (P10, TPP8h, TPP10h) showed the clearest face effect on the N170 (Figure 2.15).

*PS vs. controls. Comparison of effects:* We first performed a PS-based analysis for which we used the electrode where the patient presented the highest N170 amplitude value to the presentation of faces in most of the 8 repetitions of the experiment (P8). Then, we also performed an individual-based analysis for which we used the electrode where every participant had the highest amplitude value for faces. In the case of PS, we took the electrode where she had the highest value for each application of the paradigm. Note that in all cases this analysis involved only the right hemisphere and was performed using the Crawford and Howell's method (Crawford *et al.*, 2009).

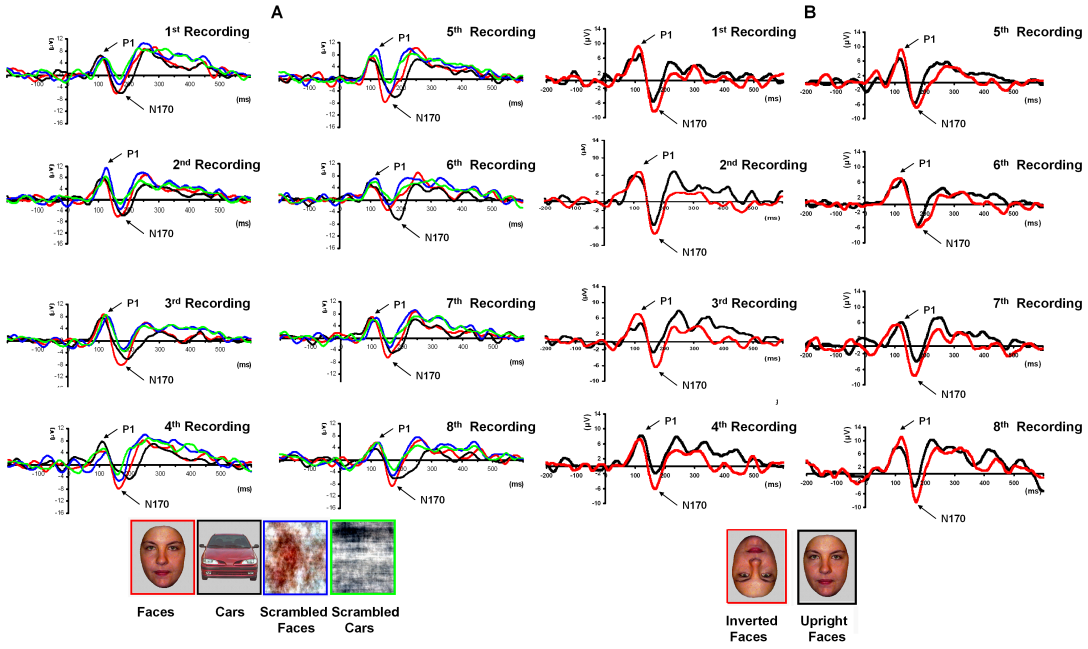


**Figure 2.16: PS' EEG waveforms for each of the experimental repetitions of experiment 1 (faces vs. objects) and 2 (face inversion).** - (A). PS' averaged waveforms on the lateral occipital channels that form the regions of interest in the right hemisphere (RH) for each of the 8 repetitions of experiment 1. Despite the relatively low signal-to-noise ratio observed in each of the sessions, most probably due to brain damage, the reliability of the results across sessions with respect to the presence of an N170 in the right hemisphere can be observed. (B). 8 recording sessions of experiment 2, showing the latency delay and amplitude increase for inverted as compared to upright faces. The latency delay was not present in one of the recording sessions only (7th), where the preceding component (P1) was substantially delayed for upright faces.

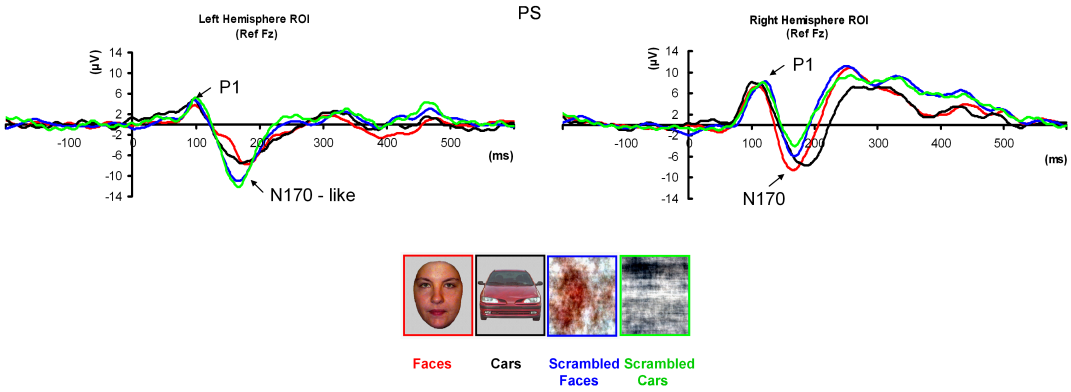


**Figure 2.17: PS' waveforms re-referenced to Fz.** - The grand averaged of all repetitions of experiment 1 performed by PS is displayed. The waveforms are re-referenced to Fz to demonstrate they are reference independent.

PS based analysis revealed that there were no differences regarding the amplitude ($t(14) = 0.55, p = 0.30$) and the latency ($t(14) = 1.5, p = 0.08$) of the N170 component in response to faces between PS and controls. There were no differences either in response to cars (amplitude: $t(14) = 0.33, p = 0.37$) (latency: $t(14) = 1.36, p = 0.10$). We also computed a Normalized Face Effect Index [NFEI = (faces-cars)/(faces+cars)] for which there was no difference between PS and controls (NFEI amplitude: $t(14) = 0.67, p = 0.26$) (NFEI latency: $t(14) = 0.00, p = 0.50$).

The individual based analysis confirmed that there were no significant differences between PS and controls in terms of the N170 amplitude ($t(14) = 0.70, p = 0.25$) nor in terms of the latency ($t(14) = 1.40, p = 0.09$). Similar results were obtained in response to cars (amplitude: $t(14) = 0.35, p = 0.36$) (latency: $t(14) = 2.21, p = 0.02$) as well as when the NFEI was used (NFEI amplitude: $t(14) = 0.33, p = 0.38$) (NFEI latency: $t(14) = 0.81, p = 0.22$) (Figure 2.18). Taken together, these results show that PS electrophysiological response to faces and objects did not differ significantly from that presented by normal participants.

Admittedly, there is quite a large variance among individual participants in the N170 response to faces and other stimuli, which may have masked abnormal latencies and amplitudes for PS. However, this variance is part of the phenomenon of interest, and we can safely conclude that there is no reason to believe that PS shows a different pattern of N170 response in the right hemisphere compared to normal observers. Experiment 2 aimed at reinforcing this conclusion by testing the effect of inversion, a manipulation that is known to affect the latency and amplitude of the N170 in response to faces.

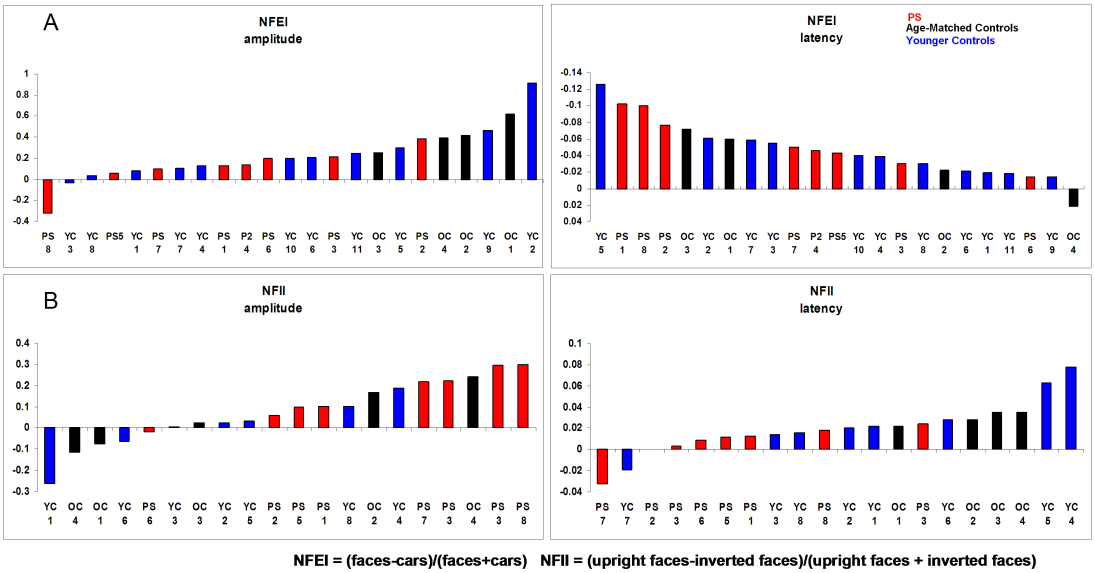


**Figure 2.18: Normalized Face Effect Index and Normalized Face Inversion Effect Index** - This figure shows both the mean NFEI (Normalized Face Effect Index = (faces-cars)/(faces+cars)) and the mean NFII (Normalized Face Inversion Index = (inverted faces - upright faces) / (inverted faces + upright faces)) of the individually based analysis for both PS and controls

#### 2.2.3.2 EEG data. Experiment 2: Face Inversion

**Behavioral data:**

Performance was above 93% for all conditions and PS accuracy was the highest (Table 2.6). Correct RTs were not significantly different than the controls (Upright Faces: t-test, t(14) = 0.95, p = 0.18; Inverted Faces: t-test, t(14) =1.71, p=0.05).

| | Accuracy (%) | | Reaction Time (ms) | |
|---|---|---|---|---|
| | Upright Faces | Inverted Faces | Upright Faces | Inverted Faces |
| Young Controls | 97.49 ± 2.97 | 96.496 ± 4.5 | 504.23 ± 80.38 | 505.96 ± 95.78 |
| Age matched Controls | 96.06 ± 3.54 | 93.81 ± 2.73 | 623.33 ± 60.51 | 591.70 ± 55.06 |
| PS | 99.46 ± 0.60 | 99.58 ± 0.57 | 701.96 ± 94.95 | 742.57 ± 88.73 |

**Table 2.6: Behavioral results experiment 2 (face inversion)** - Mean accuracy and response time achieved by each experimental group in experiment 2, upright vs. inverted faces.

**Electrophysiological data. N170 component**

*Normal controls:* For the sake of brevity, in the following we will concentrate on the N170 results since the P1 component did not exhibit any characteristic worth mentioning in addition to those already described for the previous experiment. For control participants, the N170 was delayed and larger for inverted faces compared to upright faces, although the effect was clearer on amplitude for age-matched controls (Figure 2.19) than in the group of younger controls. The reduce inversion effect observed in the group of younger controls was due to the fact that only 4 out of 8 participants presented a higher amplitude for inverted than upright faces (Figure 2.20). For the N170 amplitude, there were no main effects of Orientation (ANOVA, $F(1,7) = 0.51, p = 0.50$) or Hemisphere (ANOVA, $F(1,7) = 3.55, p = 0.10$), but there was a highly significant effect of Orientation (ANOVA, $F(1,7) = 18.11, p < 0.001$) due to longer latencies for inverted than upright faces.

*PS:* As in the previous experiment, here PS also presented with a negative peak between 140 ms and 190 ms on lateral occipital electrodes but it corresponded to an N170 only in the right hemisphere (Figure 2.19). There was a larger amplitude for inverted than upright faces (t-test, $t(7) = 5.42, p = 0.001$). Although there was a delay for inverted faces in 6 of the sessions at least (Figure 2.16), the opposite effect was

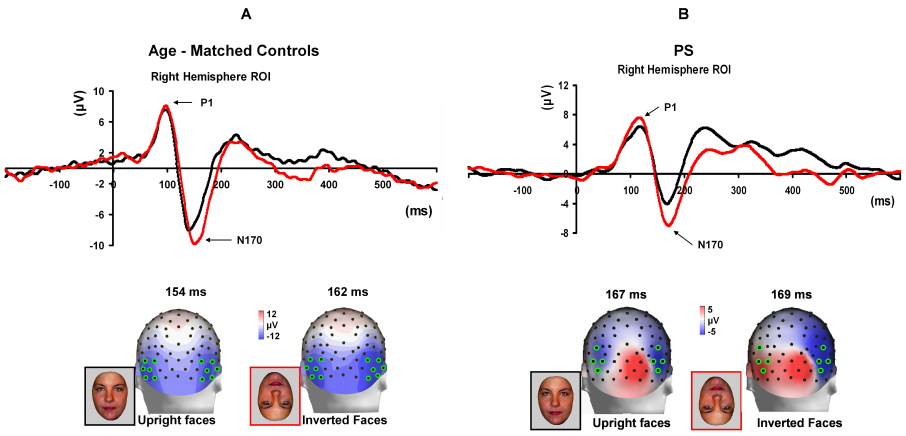


**Figure 2.19: Results obtained by PS and age-matched healthy participants in experiment 2 (face inversion).** - (A). The effect of face inversion on the right N170 for the 4 age-matched normal controls tested in experiment 2. The N170 was larger in amplitude and delayed to inverted faces, as previously shown in many studies. (B). The effect of face inversion (amplitude increase and latency delay, see text for further details) on the right N170 for PS.

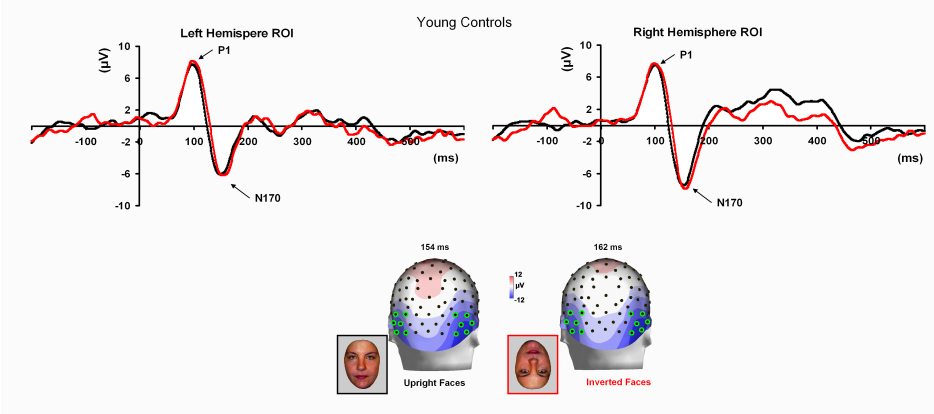


**Figure 2.20: Results obtained by the group of young participants in experiment 2 (face inversion).** - The waveforms and topographies of the N170 component of young participants in response to both upright and inverted faces are displayed.

found in session 7, so that overall there was no significant difference between conditions in terms of latency (t-test, $t(7) = 1.55, p = 0.17$). The opposite effect appeared to be related to a delayed P1 component for upright faces in that session (Figure 2.15). To take into account this pre-N170 difference, we selected the electrode where the N170 was highest and subtracted the P1 latency from the N170 latency. This peak-to-peak analysis revealed that the N170 (-P1) in response to inverted faces was significantly delayed compared to upright faces (t-test, $t(7) = 2.05, p = 0.04$).

*PS vs. controls. Comparison of effects:* As for the previous experiments PS' results were compared to controls' results using the Crawford and Howell's method (Crawford *et al.*, 2009). The PS based analysis revealed that there were no differences between PS and controls response regarding the amplitude ($t(14) = 0.17$, $p < 0.05$) and the latency ($t(14) = 1.63$, $p > 0.05$) of the (right) N170 component in response to upright faces. Similar observations were made for inverted faces (amplitude: $t(14) = 0.14, p > 0.05$) (latency: $t(14) = 1.85, p > 0.05$). Likewise, there were no differences regarding the Normalized Face Inversion Index (NFII = (inverted faces - upright faces) / (inverted faces + upright faces) (NFII amplitude: $t(14) = 0.92, p > 0.05$) (NFII latency: $t(14) = 0.23, p > 0.05$). This indicates that PS inversion effect on the N170 was at least as large as in normal controls.

The individual based analysis confirmed that there were no difference regarding PS response to upright faces (amplitude: $t(14) = 0.87, p > 0.05$) (latency: $t(14) = 1.65, p > 0.05$), inverted faces (amplitude: $t(14) = 0.51, p > 0.05$) (latency: $t(14) = 0.88, p > 0.05$). There were no differences for the NFII either (NFII amplitude: $t(14) = 0.95, p > 0.05$) (NFII latency: $t(14) = 1.15, p > 0.05$) (Figure 2.18).

#### 2.2.3.3 MEG data. Experiment 1: faces vs. objects

In all experimental conditions, the magnetometer MEG data from PS exhibited a first magnetic deflection (M100) between 80 and 120 ms, analogous to the P1 in her EEG data, with a dipolar field pattern (positive on right, negative on left; see Figure 2.21) suggestive of an occipital generator. This was followed by a second deflection, at least for faces, that again started at about 145 ms, and was associated with a more complex field pattern suggestive of at least two dipolar sources (with a more superior negative lobe plus a more inferior positive lobe on the right, reflected in the left; see Figure 2.22). Cars produced a similar field pattern of weaker amplitude, while scrambled images produced a simpler field pattern of similar magnitude. The corresponding topographic plots for the RMS of the planar gradiometers are shown in Figure 2.23.

In order to parallel the EEG analysis, pairs of homologous left and right hemisphere ROIs were defined on the basis of MEG channels showing maximal deflection for all conditions from 120-190ms versus baseline (though note that, for the magnetometer

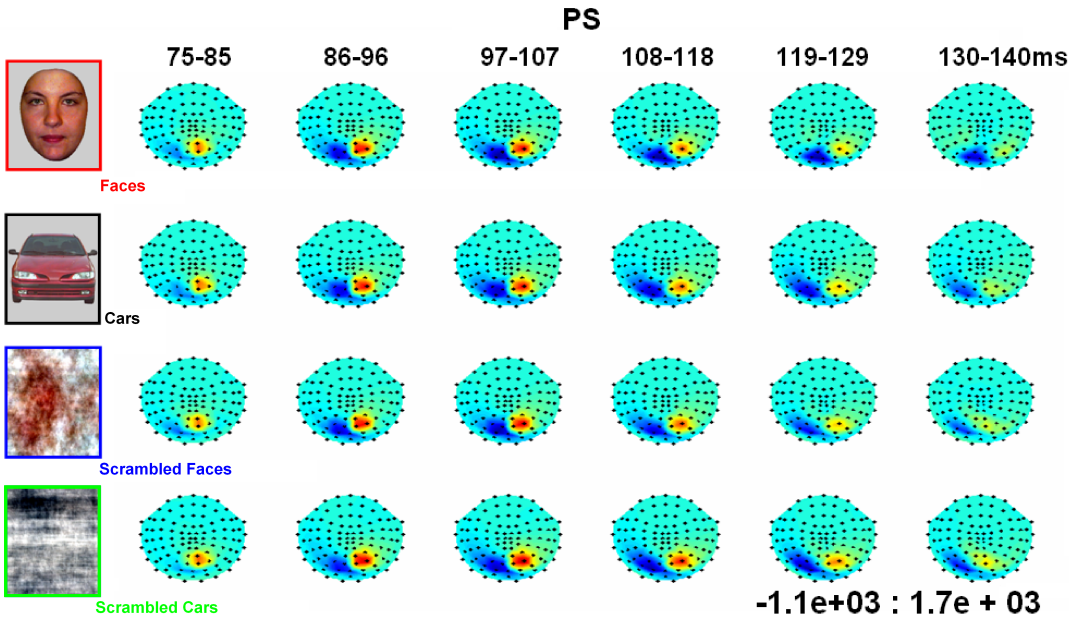


**Figure 2.21: M100 component for patient PS in experiment 1 (faces vs. objects) as recorded by MEG magnetometers.** - Evolution of magnetic fields evoked by visual stimulation as recorded by 102 magnetometers for patient PS averaged across time windows around the M100 component.

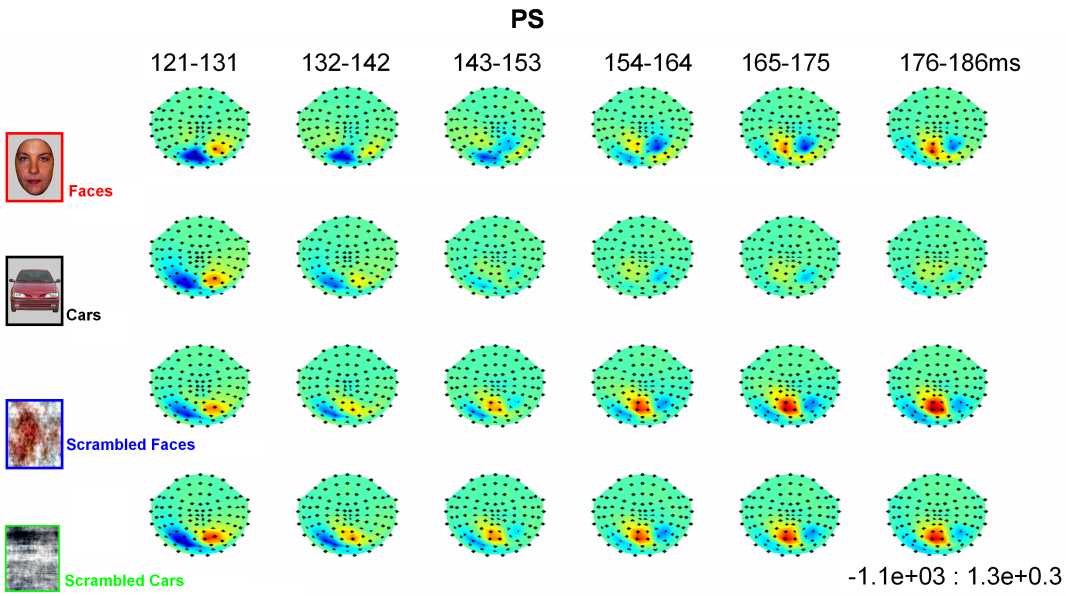


**Figure 2.22: M170 component for patient PS in experiment 1 (faces vs. objects) as recorded by MEG magnetometers.** - Evolution of magnetic fields evoked by visual stimulation as recorded by 102 magnetometers for patient PS averaged across 10ms time windows around the M170 component in Experiment 1 (viewed from above, nasion upward; data are interpolated linearly between sensors, indicated by black dots, after their spherical projection onto a 2D surface). Red and blue indicate outward and inward radial direction of magnetic flux through single flux coils within the helmet (in units of fT).

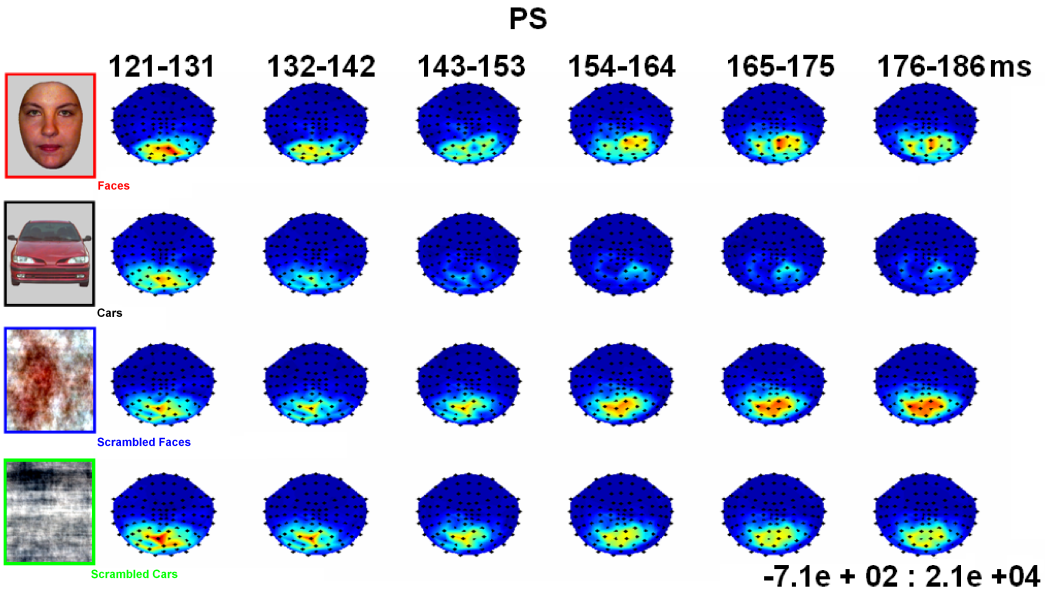


**Figure 2.23: M170 component for patient PS in experiment 1 (faces vs. objects) as recorded by MEG gradiometers.** - Evolution of magnetic fields evoked by visual stimulation as calculated from the root-mean-square (RMS) of signals recorded by each of the two orthogonal planar gradiometers at the 102 locations for patient PS averaged across 10ms time windows around the M170 component in Experiment 1 (viewed from above, nasion upward; data are interpolated linearly between sensors, indicated by black dots, after their spherical projection onto a 2D surface). Red indicates increased signal magnitude (RMS) relative to pre-stimulus baseline (in units of fT/m).

data, the sensors showing the maximal deflection will not be directly above the underlying current generator). Two such ROI pairs were defined, based on the three channels showing the maximal negative deflection in either the right hemisphere (the superior ROI pair in Figure 2.24), or in the left hemisphere (the inferior ROI pair in Figure 2.25). In both of these superior and inferior pairs, the right ROI, but not the left ROI, showed a greater deflection for Faces than the other three conditions, which peaked around 160ms (henceforth the M170). This pattern of face sensitivity in both of the right ROIs, but in neither of the left ROIs, is consistent with one dipolar generator in each hemisphere (rather than two midline generators), only the right of which was sensitive to faces.

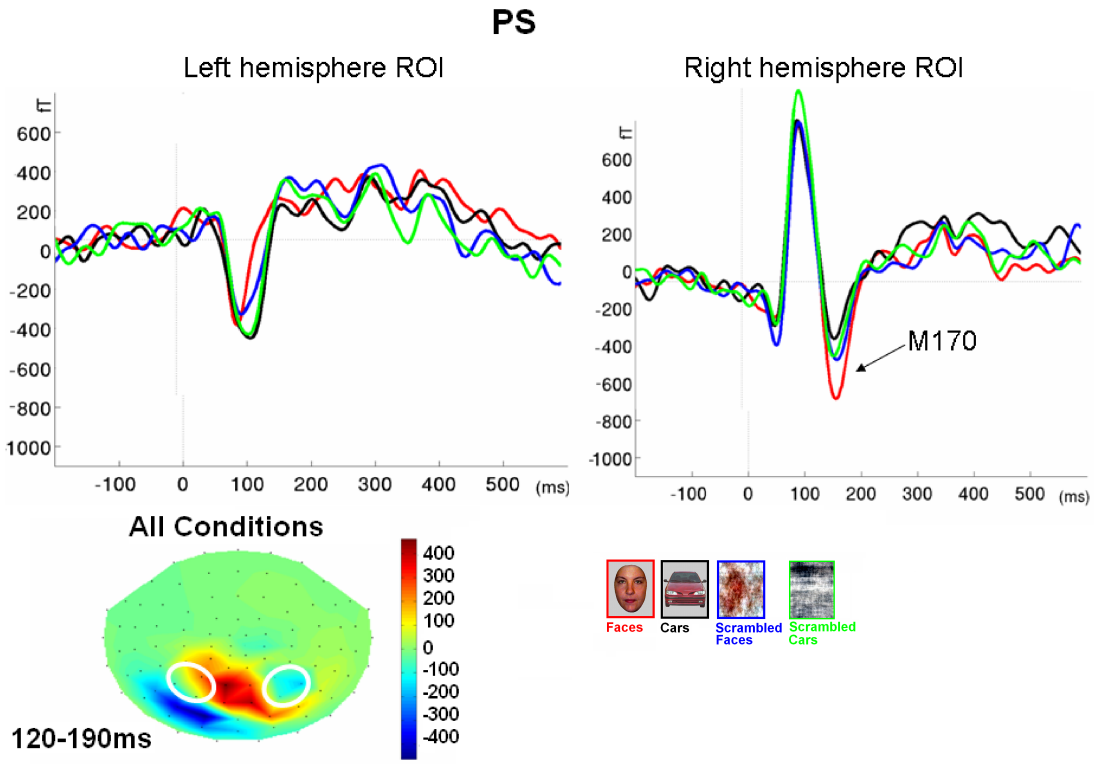


**Figure 2.24: MEG superior left and right ROIs in experiment 1 (faces vs. objects).** - Evoked responses averaged across three channels for the more superior left and right ROIs in Experiment 1 (see Figure 2.25 for more inferior ROIs). These channels were chosen as those with the maximal negative deflection versus baseline in the right hemisphere from 120-190ms, averaged across conditions, highlighted in white on topography below (these are Neuromag channels MEG2441, MEG2311 and MEG2231 for the right ROI, and MEG1841, MEG1631 and MEG1911 for the left ROI).

The median latency across trials of the maximal negative deflection in Figure 2.24

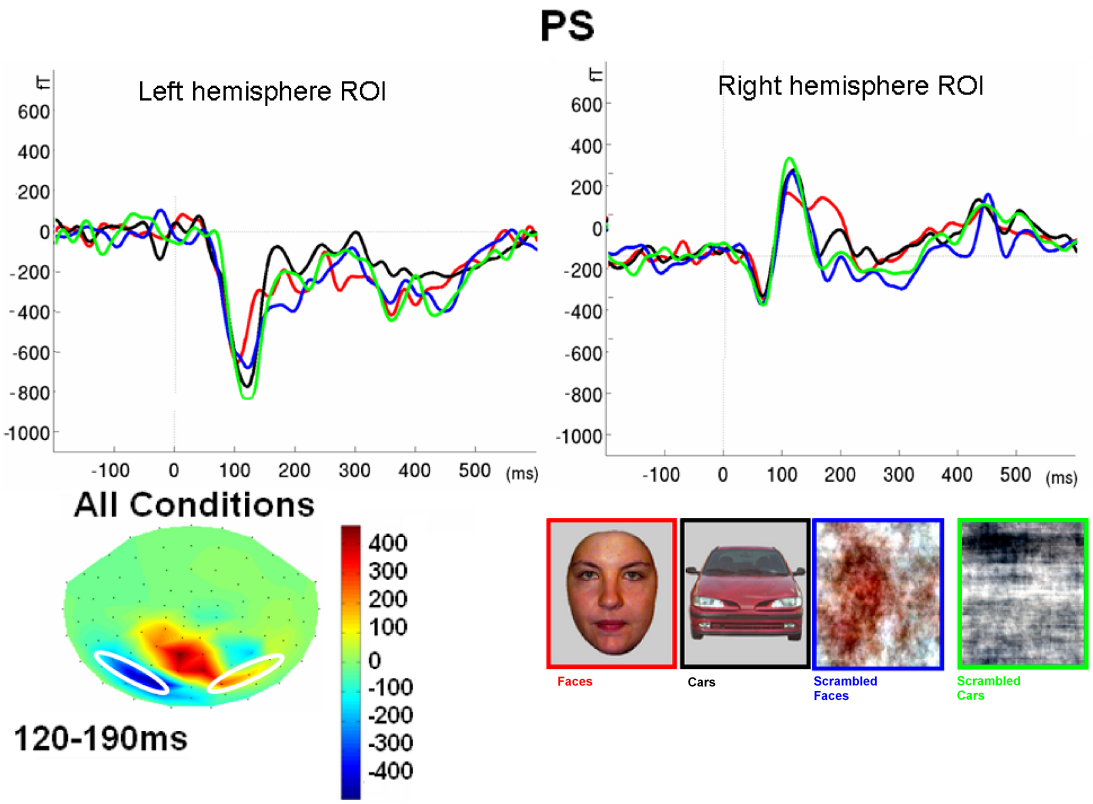


**Figure 2.25: Evoked responses averaged across three channels for the more inferior left and right ROIs in experiment 1 (faces vs. objects).** - The channels included in the ROIs were chosen as those with the maximal negative deflection versus baseline in the left hemisphere from 120-190ms, averaged across conditions, highlighted in white on topography below (these are Neuromag channels MEG2521, MEG2321 and MEG2341 for the right ROI, and MEG1641, MEG1941 and MEG1921 for the left ROI) (see Figure 2.24 for more superior ROIs).

was 164 ms for Faces, 160 ms for Cars and 164 ms for both scrambled images. A 2x2x2 mixed effects ANOVA on the mean amplitude during this time window within each ROI for each trial showed a reliable three-way interaction between Hemisphere, Category and Shape, (ANOVA, $F(1,614) = 5.52, p < 0.05$). Follow-on between-trial ANOVAs on each hemisphere separately showed a reliable interaction between Category and Shape in the right ROI, (ANOVA, $F(1,614) = 6.51, p < 0.05$), but not in the left ROI, (ANOVA, $F(1,614) < 1$). Post hoc pairwise comparisons across conditions in the right ROI showed that Faces produced more negative deflections than any other of the three conditions, (t-test, $ts > 2.28, ps < 0.05$), two-tailed (the only other significant pairwise difference was more negative deflection for Scrambled Faces than Cars, (t-test, $t(301) = 2.11, p < 0.05$). For the left ROI, the main effects of Category, (ANOVA, $F(1,614) = 3.17, p = 0.08$), and of Shape, (ANOVA, $F(1,614) = 3.602, p = 0.058$) approached significance, with trends for more positive responses for Scrambled vs. Intact stimuli, and for Face-derived than Car-derived stimuli. Only the pairwise difference between Scrambled Faces and Cars reached significance, (t-test, $t(301) = 2.68, p < 0.01$). The absence of a clear M170 component in the left hemisphere, coupled with the reliable interaction with Hemisphere, supports the EEG findings in suggesting the presence of a Face-related M170 in the right hemisphere only.

#### 2.2.3.4 MEG data. Experiment 2: Face Inversion

As in the previous experiment, the magnetometer MEG data from PS exhibited a first magnetic deflection (M100) between 80 and 120 ms, with a dipolar field pattern (positive on right, negative on left; see Figure 2.26) suggestive of an occipital generator. This was followed by a second deflection that was maximal around 160 ms, and was associated with a more complex field pattern for Faces, as in Experiment 1 (with a more superior negative lobe plus a more inferior positive lobe on the right, reflected in the left; see Figure 2.27). Inverted faces produced a simpler field pattern of similar magnitude, though with a less marked dipolar pattern over the left hemisphere. The corresponding topographic plots for the RMS of the planar gradiometers are shown in Figure 2.28.

As in the previous experiment, two pairs of ROIs were defined, based on the negative and positive lobes within each hemisphere. The three channels showing the maximal negative deflection versus baseline in the right hemisphere, and their left hemisphere homologues, were identical to those in Experiment 1 (Figure 2.29). The more inferior ROIs, defined by the maximal negative deflection in the left hemisphere, contained three channels close to those in Experiment 1, but slightly more inferior (see Figure 2.30).

The evoked fields from the more superior ROI pair showed a M100 in both hemispheres, but an additional positive deflection (at least for upright faces) in the left ROI, whose origin is unclear (and which was not seen in Experiment 1). Nonetheless, as in

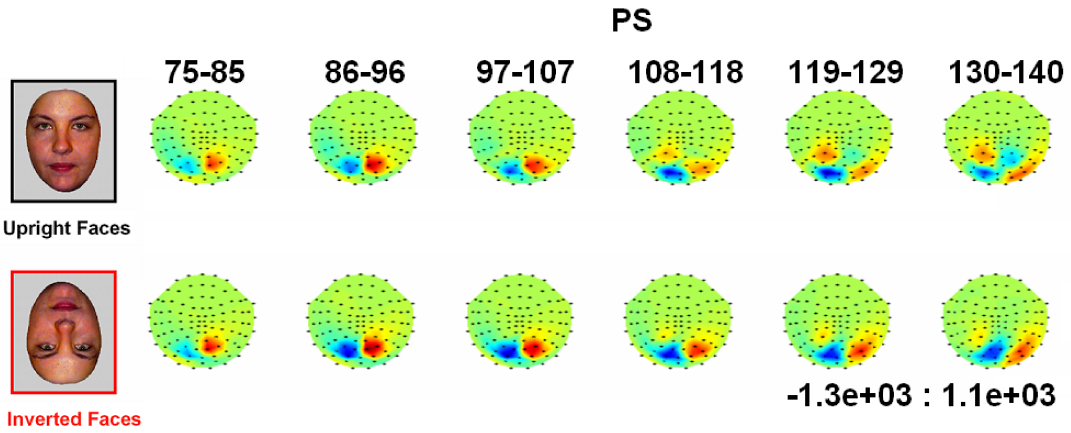


**Figure 2.26: M100 component for PS in experiment 2 (face inversion) as recorded by MEG magnetometers.** - Evolution of magnetic fields evoked by visual stimulation as recorded by 102 magnetometers for patient PS averaged across 10 ms time windows around the M100 component in Experiment 2 (viewed from above, nasion upward; data are interpolated linearly between sensors, indicated by black dots, after their spherical projection onto a 2D surface). Red and blue indicate outward and inward radial direction of magnetic flux through single flux coils within the helmet (in units of fT).

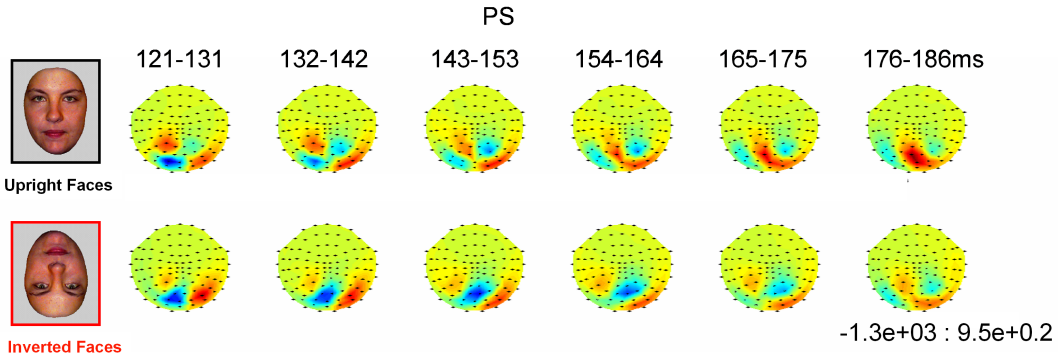


**Figure 2.27: M170 component for PS in Experiment 2 (face inversion) as recorded by MEG magnetometers.** - Evolution of magnetic fields evoked by visual stimulation as recorded by 102 magnetometers for patient PS averaged across 10ms time windows around the M170 component in Experiment 2 (viewed from above, nasion upward; data are interpolated linearly between sensors, indicated by black dots, after their spherical projection onto a 2D surface). Red and blue indicate outward and inward radial direction of magnetic flux through single flux coils within the helmet (in units of fT).

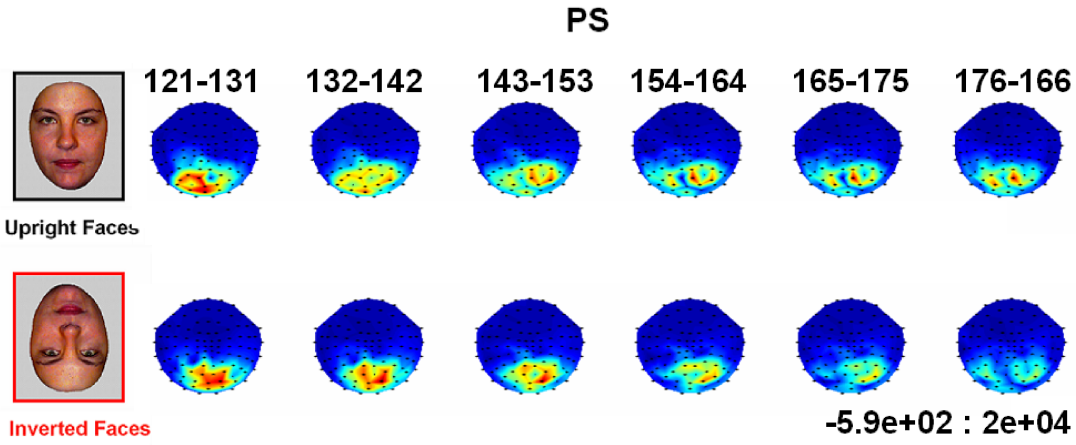


**Figure 2.28: M170 component for PS in experiment 2 (face inversion) as recorded by MEG gradiometers.** - Evolution of magnetic fields evoked by visual stimulation as calculated from the root-mean-square (RMS) of signals recorded by each of the two orthogonal planar gradiometers at the 102 locations for patient PS averaged across 10 ms time windows around the M170 component in Experiment 2 (viewed from above, nasion upward; data are interpolated linearly between sensors, indicated by black dots, after their spherical projection onto a 2D surface). Red indicates increased signal magnitude (RMS) relative to pre-stimulus baseline (in units of fT/m).

Experiment 1, a M170 component was only seen in the right ROI, which appeared delayed for Inverted relative to Upright Faces. Indeed, the median latency across trials of the maximal negative deflection in the right ROI in Figure 2.27 was 152 ms for Upright Faces and 168 ms for Inverted Faces, a difference that was reliable using a Mann-Whitney nonparametric test (U(167)=2333 (Z=3.69), p<0.001, two-tailed).

Using a 30 ms window centered on the median latency for each condition separately, a 2x2 mixed effects ANOVA on the mean amplitude during this time window within each ROI for each trial showed a reliable main effect of Hemisphere, (ANOVA, F(1,165)=177.82, p<0.001), but no main effect of Inversion or interaction, (ANOVA, Fs (1,165)<1.29, p=0.26). Follow-on pairwise comparisons did not show a reliable amplitude difference in either left, (t-test, $t(165) = 0.68, p = 0.50$), or right, (t-test, $t(165) = 0.94, p = 0.345$) ROIs. Thus, like with the EEG data, there is a clear component evoked by both upright and inverted faces around 160 ms in the right but not left ROI, though unlike the EEG data, this component had a greater latency, rather than greater amplitude, for inverted relative to upright faces. The more inferior pair of ROIs did not show the same pattern of results, possibly reflecting a different generator (Figure 2.30).

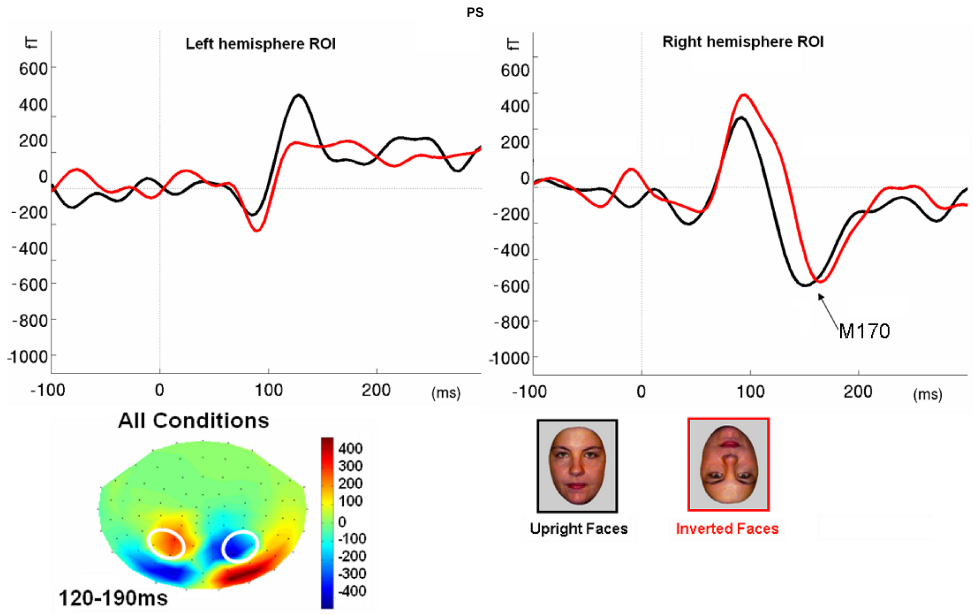


**Figure 2.29: Evoked responses averaged across three channels for the more superior left and right ROIs in experiment 2 (face inversion).** - The channels included in the ROIs were those with the maximal negative deflection versus baseline in the right hemisphere from 120-190ms, averaged across conditions, highlighted in white on topography below. These are Neuromag channels MEG2441, MEG2311 and MEG2231 for the right ROI; and MEG1841, MEG1631 and MEG1911 for the left ROI (see Figure 2.30 for more inferior ROIs).

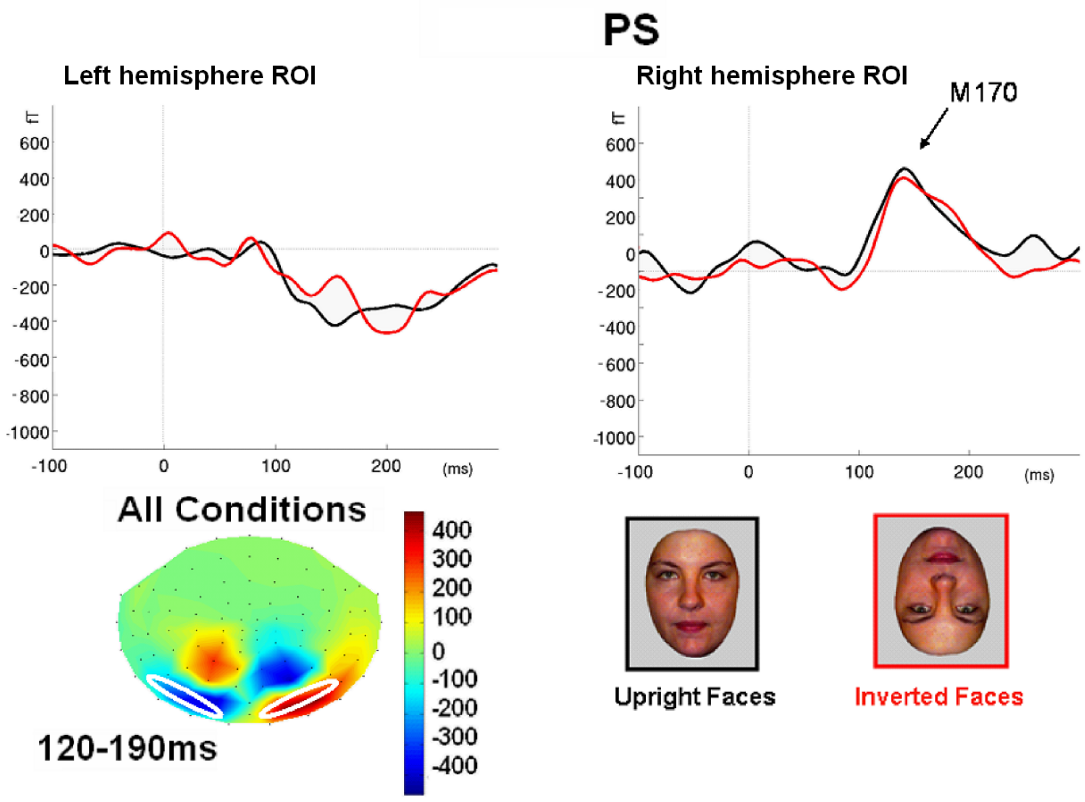


**Figure 2.30: Evoked responses averaged across three channels for the more inferior left and right ROIs in experiment 2 (face inversion).** - The channels included in the ROIs were those with the maximal negative deflection versus baseline in the left hemisphere from 120-190 ms, averaged across conditions, highlighted in white on topography below (these are Neuromag channels MEG2331, MEG2511 and MEG2521 for the right ROI, and MEG1931, MEG1731 and MEG1721 for the left ROI, see Figure 2.29 for the more superior ROIs).

### 2.2.4 Discussion

The present study was designed to determine the characteristics of the electrophysiological response to faces in a patient who suffers from pure prosopagnosia following brain damage. Our first and main goal was to determine whether the N170/M170 face effect can emerge on the scalp despite damage to the right inferior occipital cortex and no evidence for face preferential responses in this part of the cortex as tested in previous fMRI studies (Rossion, 2003; Rossion *et al.*, 2003b). The answer to this first question is positive: despite her well established prosopagnosia and her extensive brain damage, PS presented the traditional N170 amplitude increase in response to faces compared to non-face stimuli on the right occipito-temporal electrodes. Although the presence of unusual large components over the lesion sites disrupted the N170 scalp topography at right occipital medial sites, PS right N170 appeared to be of normal absolute amplitude for faces, and differential amplitude with respect to the N170 elicited by pictures of cars. In experiment 2, the N170 also exhibited an amplitude increase and delay for inverted faces compared to upright faces, as classically found in normal observers with an intact brain. These results were replicated across several EEG recording sessions. The early face preferential response over the right hemisphere was also found for the patient in an independent MEG recording session, showing remarkable similarities (timing, delay for inverted faces) between the M170 and N170, and suggesting that PS N170 was not overly distorted by the deformations in her skull/scalp or the lesions in her cortex (see Figure 2.8). These observations were complemented by the finding that PS' N170/M170 components could not be identified on the left hemisphere sensors in any recording session, either in EEG or MEG. The implications of these observations will be discussed in the next sections.

#### 2.2.4.1 Generic face sensitive processes as reflected in the N170/M170 face effect

Behaviorally, PS is able to categorize a visual stimulus as a face, being as good and fast as normal observers as previous studies have demonstrated (e.g., Rossion *et al.* (2011); Schiltz *et al.* (2006)). Neuroimaging studies have also shown a larger response to faces than objects in her right fusiform gyrus (FFA) and pSTS (Rossion, 2003; Rossion *et al.*, 2003b; Sorger *et al.*, 2007) and the magnitude of this higher response to faces in fMRI does not appear to differ between PS and normal controls in these studies. The present findings complement these observations by showing that PS' brain differentiates between faces and other categories as early as normal observers, that is well before 200 ms. More precisely, she exhibits an N170/M170 face effect in the right hemisphere. This result is in agreement with the view that the N170 face effect is related to the initial perception of a stimulus as a face or, in other words,

to the activation of a generic face representation in high-level visual cortex (Bentin *et al.*, 1996; Rossion & Jacques, 2010; Sagiv & Bentin, 2001). Moreover, the delay and amplitude increase of the N170/M170 to inverted faces is also in agreement with PS' behavioral performance: she is capable of telling an upright from an inverted face, and perceives a face as a face even when it requires configural/holistic processing (i.e., when facial parts are not visible or diagnostic, see Rossion *et al.* (2011)).

However, the patient's difficulties arise when faces have to be individualized, with several recent behavioral studies showing that the patient is no longer able to individualize faces using holistic processes (Busigny *et al.*, 2010; Ramon *et al.*, 2010a). Therefore, we would expect that when sensitivity to individual faces is tested, PS' electrophysiological response to faces would be different than that of normal observers. Testing this hypothesis could be done by recording the N170/M170 in the context of a face identity adaptation paradigm. That is, in normal subjects, the N170 is reduced in amplitude when the same face is immediately repeated compared to the presentation of a different face (Ewbank *et al.*, 2008; Heisz *et al.*, 2006; Jacques *et al.*, 2007) an effect that is absent for inverted faces (Jacques *et al.*, 2007) and thus cannot be merely accounted for by low-level stimulus repetition. In the same way that PS' FFA does not show sensitivity to individual faces in such adaptation paradigms (Schiltz *et al.*, 2006) we would predict that PS' N170, as identified in the present study, would be of equal amplitude to different and repeated faces, or at least present a significantly smaller release from adaptation than in normal observers.

#### 2.2.4.2 The right inferior occipital cortex is not necessary to generate the right N170 / M170 effect

An important issue raised by our findings relates to the anatomical structures that support the N170/M170 face effect, in particular over the right hemisphere, where the N170 is typically the largest (Bentin *et al.*, 1996; Rossion *et al.*, 2003a). To remind the reader, source localization studies have suggested that, in addition to the lateral occipito-temporal gyrus, the anterior/middle FG (mainly) as well as the posterior superior temporal sulcus (pSTS) are related to the N170/M170 face effect observed on the scalp (see introduction section). In fMRI, preferential activation to faces is generally observed concomitantly at least in the inferior occipital gyrus (OFA), middle fusiform gyrus (FFA), and the posterior section of the superior temporal sulcus (pSTS). Since PS presents a reliable N170/M170 amplitude modulation over the right hemisphere electrodes despite her well-defined lesion in the right inferior occipital gyrus, we can exclude this area as an indispensable structure for generating the N170/M170 increase to faces on the scalp. However, both the middle fusiform gyrus and the pSTS are intact in PS right hemisphere, and both areas show face-preferential responses as demonstrated in fMRI (Sorger *et al.*, 2007). Consequently, the present data suggest that face-preferential

responses in the middle fusiform gyrus (FFA), and probably the pSTS, may be sufficient for generating the amplitude increase of the N170/M170 component in response to faces. This observation is in agreement with and complements the findings of significant correlations between fMRI signal and N170 amplitude for faces in fusiform and superior temporal gyri, either using a parametric paradigm in which the amplitude of the N170 is modulated by varying the level of noise in a face stimulus (Horovitz *et al.*, 2004) or relying on the variance of signal across a large sample of participants (Sadeh & Yovel, 2010). They also provide new evidence supporting the claim of Dalrymple *et al.* (2011) that at least two of the three major functional areas must be functionally intact to generate the N170 face effect.

With respect to this last issue and the findings made here, they are at least three caveats that should be mentioned. First, our observation of an N170 face effect despite no right OFA does not eliminate the putative contribution of the (right) inferior occipital cortex to the generation of the right N170/M170 in the normal brain, and to its larger amplitude to faces. Indeed, the component recorded on the scalp reflects the combination of electromagnetic fields produced by multiple possible cortical current sources with overlapping time-courses. It is likely that in the normal brain, all of these populations of neurons showing a preferential response to faces contribute to the N170/M170 face effect, including the so-called OFA in the inferior occipital cortex (Henson *et al.*, 2009; Rossion & Jacques, 2008). Moreover, fields produced by current flows in opposite orientations may partially cancel out each other. Given this, the removal of one of the sources following brain damage might also paradoxically increase the amplitude of signals recorded on the scalp. Note that such an increase was not observed here for the patient PS, who showed a reliable enhanced N170/M170 to faces, but which nevertheless corresponded to one of the smallest effects observed in the controls. Moreover, the N170 maxima were recorded over the same electrodes as in normal controls, suggesting that the orientation of the equivalent dipole generating the component remained largely intact without any putative contribution from face-preferential clusters of neurons in the inferior occipital cortex. A second caveat worth mentioning is that there is a huge amount of variability in the amplitude of the N170/M170 component, and its larger amplitude to faces, in the normal brain: these components and effects can be up to 10 times larger in one individual's brain as compared to another's. Hence, one cannot exclude that PS N170/M170 face effect would have been much larger without the brain damage affecting her right inferior occipital gyrus. Finally, the N170 (but not the M170) recorded on PS scalp was not only significantly larger to faces than cars, but was also larger for scrambled faces than scrambled cars, unlike what was found in normal controls. This observation suggests that the early face-preferential response over PS right hemisphere appears to be partially driven by low-level visual cues (e.g., color and spatial frequency spectrum, see Rossion & Caharel (2011)).

Interestingly, there is evidence that low-level visual cues, in particular color and spatial frequency spectrum as shown with the stimuli used here, play a small role in driving face preferential responses in the middle fusiform gyrus (i.e., in generating the FFA, Andrews *et al.* (2010); Yue *et al.* (2011)). Therefore, it may be that the enhanced sensitivity to low level visual cues at the level of the N170 for PS is related to an increase of the contribution from face-preferential responses in the middle fusiform gyrus, given the absence of any possible contribution from sources in the inferior occipital cortex in the patient's brain. In this context, the lack of sensitivity to low-level visual cues from MEG data recorded in the same patient might reflect a larger contribution from sources localized in the upper or lower banks of the pSTS, which would be tangential to the recording electrodes on the scalp (e.g., Watanabe *et al.* (2003)).

Despite these warnings, the present claim that the (right) OFA is not a necessary component for generating the early N170/M170 electrophysiological response on the scalp remains entirely valid and it is in agreement with the lack of correlation between the N170 amplitude and OFA signal across normal individuals (Sadeh & Yovel, 2010). Therefore, one may wonder what would be the neuro-functional pathway responsible of generating face preferential activation in the middle fusiform gyrus, which likely contributes heavily to the response recorded here on the scalp at around 150 ms. In other words: if there is no OFA input, what would be the anatomical route that could convey early face-related information to the FFA? A study using Diffusion Tensor Imaging (DTI) has shown that there are direct connections between early visual areas such as V3 and V3A and the FFA in humans (Kim *et al.*, 2006) so that the OFA is not a necessary intermediate stage. More specifically, recent DTI measurements and tractography analysis performed in the patient PS appear to show direct fibre connections (inferior longitudinalis fasciculus, FLI, see Catani *et al.* (2003)) between early visual areas such as V1 and the right FFA (unpublished data obtained in our lab) extending into the right anterior lobe. Hence, such connections might subtend the emergence of face preferential responses in the right fusiform gyrus, leading to the effect recorded on the scalp in the present study.

#### 2.2.4.3 The absence of left N170 following the left middle fusiform lesion

The N170 shown by normal controls in response to faces was smaller in the left than in the right hemisphere. The larger amplitude for faces as compared to non-face objects is also typically smaller in the left than in the right hemisphere, although it was not the case here (see Rossion *et al.* (2003a) for evidence and discussion of this issue). Interestingly, we did not observe any N170/M170 or any other early face preferential response for PS over left electrode sites. At first glance, this observation is surprising because PS' posterior lesion in the left hemisphere is much smaller than in the right hemisphere (Sorger *et al.*, 2007). Moreover, it encompasses only the middle section

of the fusiform gyrus on the ventral surface of the occipito-temporal cortex, further away from the scalp recording sites than the right hemisphere lesion. Hence, this observation is quite interesting because it supports the view that the left middle fusiform gyrus is not only sufficient but perhaps is a necessary component to generate a left N170/M170. Moreover, a left OFA, which is a small face preferential activation not systematically found in PS' brain (Sorger *et al.*, 2007) appears to be insufficient to generate the N170. Thus, considering the contrast between the findings at right (N170) and left sensors (no N170), our observations point to both a sufficient and necessary role of the middle fusiform gyrus in generating early face preferential responses on the scalp. Interestingly, the ERP data of two brain-damaged patients (R-IOT1; B-OT/AT1) tested by Dalrymple *et al.* (2011) support this view. Having said this, we should acknowledge that the conclusions drawn from the present left hemisphere data on patient PS should be qualified, for two reasons. First, we cannot exclude that damage in the right hemisphere can influence what is observed over the left hemisphere, in a patient with bilateral damage. Therefore loss of the left N170 could reflect loss of the left middle fusiform gyrus combined with remote effects of loss of the right inferior occipital cortex in patient PS. More generally, even if it appears that loss of the left middle fusiform gyrus leads to loss of the left N170 for the patient PS, this does not logically mean that loss of the right middle fusiform gyrus would always lead to loss of the right N170. Second, there are observations from other studies that qualify the claim that an FFA would be necessary to generate the N170. For instance, Bobes *et al.* (2003) reported a left N170 face effect in their prosopagnosic patient FE despite an extensive lesion of the left fusiform gyrus. Without functional activations, the integrity of the FFA and especially the OFA in the left hemisphere of their patient remains unknown, but the patient lesions appeared to be much larger than PS and concerned a very large part of the middle fusiform gyrus. Most importantly, in the study of Dalrymple *et al.* (2011) one patient had middle fusiform damage (and no FFA) in the right hemisphere and nevertheless presents with an N170 face effect on the scalp. Taken together, these observations highlight the important role of the right FFA in generating an early N170 face effect. However, they also indicate that integrity of the right middle fusiform gyrus is not always necessary to generate such an effect over the right hemisphere, providing that two other components of the face network (inferior occipital cortex and STS potentially) are intact.

#### 2.2.4.4 The effect of face inversion on the N170 and M170 without right inferior occipital cortex

PS' N170 and M170 over the right hemisphere electrodes was delayed in response to inverted faces, as in normal observers of the present study and in numerous previous studies, reinforcing the identification of the component as being the N/M170. In MEG,

PS' M170 was not increased in response to inverted faces, and this observation is in agreement with the literature: face inversion does not normally affect the M170 amplitude (e.g., Linkenkaer-Hansen *et al.* (1998); Liu *et al.* (2002); Watanabe *et al.* (2003)). Here, the traditional N170 increase of amplitude for inverted faces was found in many controls but not for all of them, and could reflect a difference in the respective contribution of the multiple sources generating the N170, depending on how the cortex is folded and thus how the sources are oriented with respect to the recording sites on the scalp. That is, sources in the inferior occipital cortex, where larger responses to inverted faces can be observed in intracranial recordings might contribute more to the scalp potential for some participants than sources in the middle fusiform gyrus, where responses to upright and inverted faces appear to be of equal magnitude (Rosburg *et al.*, 2010).

However, this reasoning is at odds with the effect of inversion on PS' N170, since there was a large and significant increase of amplitude to inverted faces despite damage to her right inferior occipital cortex. There are at least two ways to account for these observations. First, PS N170 increase to inverted faces might be due to other face-related sources, for instance in her pSTS, in which face-selective responses have been observed with fMRI. Second, and more likely, the increased N170 to face inversion may originate from non-face-selective cortical sources that are preserved in her right inferior occipital cortex, such as the ventral section of the lateral occipital cortex (Sorger *et al.*, 2007) and in which larger responses to inverted faces have been observed in fMRI studies (Haxby *et al.*, 1999).

### 2.2.5 Conclusions

We observed early characteristic face preferential response over the right but not left hemisphere in a patient presenting prosopagnosia following damage to the right inferior occipital cortex and left middle fusiform gyrus. These observations indicate that a right inferior occipital cortex is not necessary to produce early face-preferential responses in the human brain and suggest that face-preferential responses in the right middle fusiform gyrus (FFA) is an important component of such early N170 face-preferential responses associated with the activation of generic face representations.

**Acknowledgments:**

We thank Elias Mouchlianitis for assistance collecting the MEG data. Most of all, we thank PS for her time and patience. Bruno Rossion is supported by the Belgian National Fund for Scientific Research (Fonds de la Recherche Scientifique - FNRS); Richard Henson is supported by the UK Medical Research Council. This work was supported by an ARC (Actions de Recherche Concertes) grant 07/12-007, Communauté

Francaise de Belgique and a mandat d'impulsion scientifique FNRS to BR and by UK Medical Research Council grant WBSE U.1055.05.012.00001.01.

# Chapter 3

# Characterization of the SSVEP sensitivity to facial identity in healthy humans

In Chapter 1, the main characteristics of the steady state potentials were reviewed. It was also explained that this technique presents several advantages over ERP procedure, especially for the study of face perception processes in brain lesion patients. Motivated by these advantages, this chapter will introduce two studies aimed at determining the stimulus properties that are optimal for the use of steady state potentials in the field of face perception research in healthy humans. Before doing so, the evidence demonstrating how the stimulus characteristics can influence, in general, the visual steady state brain response will be introduced.

## 3.1 Relation between stimulus characteristics and the steady state brain response

The amplitude, apparent latency, topography and anatomical substrate of the steady state response can vary in a complex manner according to several features of the visual stimuli such as color, depth, spatial and temporal frequencies (Herrmann, 2001; Regan, 1989; Van der Tweel & Lunel, 1965). The earliest studies aimed at determining the curve of response amplitude versus stimulus modulation frequency of the visual system demonstrated that the response to sinusoidally modulated flickering light is maximal near 9-10 Hz (Van der Tweel & Lunel, 1965), 16-18 Hz (Regan, 1968b) and 40-50 Hz (Regan, 1968b; Van der Tweel & Lunel, 1965). Based on this observation, three frequency regions or subsystems were defined: the low, medium and high

frequency subsystems (Mcgeorge, 1978; Regan, 1972).

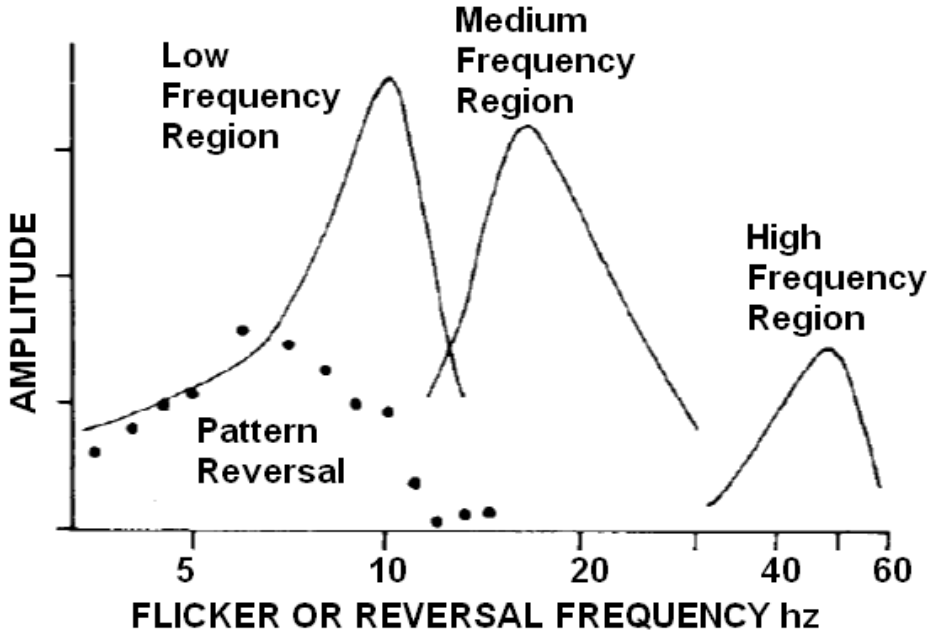


**Figure 3.1: Frequency subsystems.** - The response to a flickering unpatterned stimulus showing the low, medium and high frequency subsystems. Each of them has different sensitivities to low level aspects of the visual stimuli. Reproduced from Regan (2009).

The high frequency subsystem has a spectral sensitivity close to the observer's psychophysical luminosity function and is influenced by the size of the stimuli, but not its color (Mcgeorge, 1978; Regan, 1968b, 1989). Such response properties closely resemble the properties of the monkey magnocellular neurons, which suggested that the high frequency steady state response is originated along the magnocellular projections to the lateral geniculate nucleus (Regan, 2009; Regan & Lee, 1993).

The medium frequency subsystem is sensitive to the color of the stimuli. For example, a red flicker on a red background evokes a response similar to the response evoked by a white light but a red flicker on a blue background evokes almost no response (Milner *et al.*, 1974; Regan, 1989). These color effects depends upon whether the response is observed at the stimulation frequency or at the second harmonic. For instance, a yellow adapting light enhances the 16 Hz response to a 16 Hz flicker and reduces the 16 Hz response to an 8 Hz flicker. The properties of the 16 - 18 Hz response are closely similar to the properties of the parvocellular pathway neurons in the monkey (Regan, 1989).

Finally, the response within the low frequency subsystem can be recorded over widespread scalp regions in response to various stimulus types (Mcgeorge, 1978; Regan,

1989). Usually, it has considerable harmonic content to the point that the second harmonic can be greater than the fundamental response (Mcgeorge, 1978; Regan, 1972, 1989; Van der Tweel & Lunel, 1965).

These observations have been corroborated by later studies using various types of visual stimulus. Herrmann (2001) have observed that the amplitude of the steady state increases for a flickering light presented at 10, 20, 40 and 80 Hz. In response to large black and white checkerboard reversals, both the EEG and MEG signals have been found to be maximal between 4-8 Hz and 10-14 Hz as well as between 15-20 Hz (Thorpe *et al.*, 2007). Green concentric rings and dense random dot pattern stimuli have been seen to produce a maximal steady state response at 8 Hz (Ding *et al.*, 2006) and at 8 and 12 Hz, respectively (Srinivasan *et al.*, 2006).

The influence of stimulation frequency on the steady state brain response has also been demonstrated by intracranial recordings in the visual cortex of anesthetized cats (Rager & Singer, 1998). By inserting electrodes in visual areas 17 and 18 it has been shown that the brain response to flickering light is highest between 6-8 Hz and 16-30 Hz and decays between 12-14 Hz (Rager & Singer, 1998). Additionally, the authors observed that it takes about 300 ms for the brain response to show a stable, regular oscillatory pattern, which is present during the whole stimulation and ends abruptly with the last flash (Rager & Singer, 1998).

Using Positron Emission Tomography (PET) or fMRI, some authors have aimed at determining the brain areas associated to the steady state response increments observed for particular frequencies. The majority of studies have reported significant increases in the PET/fMRI signal in the visual cortex for stimulation frequencies between 8 and 10 Hz (Bayram *et al.*, 2011; Fox & Raichle, 1984, 1985; Kaufmann *et al.*, 2001; Mentis *et al.*, 1997; Singh *et al.*, 2003; Wang *et al.*, 2006). By performing a whole brain analysis, Mentis *et al.* (1997) have further demonstrated that the PET response curve increases at extrastriate visual areas and decreases at the frontal lobe, cingulate gyrus and superior temporal gyrus.

Studies that have recorded EEG and fMRI under the same experimental conditions in order to provide more direct evidence of the correspondence between the pattern of responses observed using each technique exhibit contradictory results. Some authors have reported that the increase in the fMRI response between 8 -10 Hz correlates strongly with the steady state response as recorded with EEG (Singh *et al.*, 2003) but others have observed a strong correlation between 14-26 Hz and 30-46 Hz and no correlation between 6 and 12 Hz (Bayram *et al.*, 2011). In partial agreement with this last result, some authors have reported that whereas the maximal EEG response appears for 15 Hz at occipital electrodes and for 25 Hz at frontal electrodes, the maximal PET response is obtained at 5 Hz in the primary visual cortex (Pastor *et al.*, 2003).

Methodological aspects may explain the disparities in the results. For example, while Singh *et al.* (2003) performed the fMRI and EEG recordings in different sessions and used checkerboards patterns illuminated with flashes whose mean light intensity was not corrected; Bayram *et al.* (2011) performed simultaneous EEG/fMRI recordings, took into account the influence of intra-subject and stimulus variability in the correlation analysis and used flashing light as a stimulus. Differences in the results may also arise due to a poor sampling of the frequency ranges used for the stimulation (see, e.g., Pastor *et al.* (2003)).

However, despite discrepancies in the exact frequency values found to elicit the highest brain response, the accumulated evidence undoubtedly demonstrates that the magnitude of the neural activity is highest for certain stimulation frequencies.

This phenomenon has been interpreted by some authors in analogy with classical oscillatory systems, i.e., spring-mass, electromagnetic oscillations. Specifically, they have proposed that it evidences the brain 'resonance' properties (Başar, 1972; Basar, 1980; Schuermann & Basar, 1994). Resonance refers to *"the ability of brain networks to facilitate (or activate) electrical transmission within determined frequency bands, when an external sensory stimulation signal is applied."* (Schuermann & Basar, 1994), p161.

For this phenomenon to occur, the external stimulation signal must match -or be 'tuned' to- the natural frequency of the brain network. In the case of the steady state technique, resonance may appear when the cyclic external stimulation forces the brain neural assemblies to respond at a rate similar to their natural frequency. After a certain time period, responses that occur at frequencies different to the stimulation frequency attenuate -or damp- and only those which have the frequency of the signal remain (Başar, 1972; Basar, 1980; Schuermann & Basar, 1994). Given the relatively broad spectrum of frequencies that elicit the highest brain response and that such response stops once the stimulation is interrupted, some authors have further hypothesized that neuronal assemblies may behave as broadly tuned and strongly damped oscillators (Rager & Singer, 1998).

Evidence suggesting the existence of self-sustained broadly tuned pacemaker mechanisms in the brain, which predispose the neuronal groups to engage in oscillatory activity at certain frequencies and eventually establish resonance, have been gathered at the level of the retinal ganglion cells (Neuenschwander & Singer, 1996), the thalamus (Amzica *et al.*, 1992; Hutcheon *et al.*, 1996; Nuñez *et al.*, 1992; Steriade *et al.*, 1991, 1993) and the cortex (Eckhorn *et al.*, 1988; Gray *et al.*, 1989; Gutfreund *et al.*, 1995; Hutcheon *et al.*, 1996; Steriade & Amzica, 1996). Central core projection systems could also modulate the oscillatory behavior of neuronal groups. For example, it has been shown that the thalamic activity shifted from low to high frequencies due to the modulatory influence of the mesencephalic reticular formation (McCormick & Bal, 1994; Singer, 1977; Steriade *et al.*, 1990).

Other authors have interpreted the increase in the brain response for certain frequencies according to the temporal properties of the activation cycle of the neuronal system specialized in the analysis of the external input (Fox & Raichle, 1984, 1985; Mentis *et al.*, 1997).

As already explained in Chapter 1, section 1.1, neurons use action potentials to transmit information. These action potentials are generated when the membrane potential of a neuron reaches a threshold value. They travel down the axon toward synapses terminating at postsynaptic neurons, where they initiate postsynaptic currents that summate to trigger or inhibit new action potentials. This cycle of activation occurs at a given rate determined by the neurons biochemical properties (Buzsaki, 2006). If the periodic input arrives to the target neuronal assemblies at a rate faster than the temporal activation cycle of the network, then it may interfere with the processing of the precedent stimuli decreasing the strength of the brain response. If the rate is slower, then the relatively long interval between stimuli may give rise to a dead time in the response cycle and a consequent decrease in the signal strength. But if the temporal rate of the stimulus coincides with the activation cycle of the neuron, its excitability may increase and so the amplitude of its response. This increase in the neuronal excitability may be propagated to the remaining cells of the assembly (Fox & Raichle, 1984, 1985; Mentis *et al.*, 1997).

The two interpretations presented above are not mutually exclusive: the resonance properties of particular neuronal groups may be best manifested when they are forced to respond at a temporal rate that coincides with their temporal activation cycle.

Irrespective of the nature of the physiological mechanisms underlying the increase in the brain response for particular frequencies or for particular physical characteristics of the stimuli, it is clear that the absolute magnitude of the steady state response can vary as a function of several stimulus parameters, a fact that can influence the experimental results. For instance, observing that the magnitude of the EEG signal remains unaltered after the presentation of a given stimulus can be interpreted as a lack of brain sensitivity to the stimulus when it may be due to a poor choice of the stimulation frequency. Hence, it is of capital importance to know how a certain stimulus property affects the steady state response before using this technique to study a given brain process.

The next two sections will present two studies aimed at clarifying this issue with regard to facial images. Specifically, the first study will determine whether the sensitivity of the steady state response to facial identity varies as a function of particular features of the face image such as gender and presence of skin color and hair. The second study will determine whether such sensitivity changes according to the presentation rate of the stimulus.

## 3.2 Study 2: SSVEP sensitivity to facial identity across variations in face appearance

*Esther Alonso Prieto*[1] *and Bruno Rossion*[1]

[1] Université catholique de Louvain, Louvain-la-Neuve, Belgium

(This article is in preparation)

**Abstract**

A recent study showed that EEG power at a constant frequency of stimulation (3.5 Hz) was much larger when different individual faces were presented compared to when the same face was presented repeatedly (Rossion & Boremanse, 2011). This result demonstrated the reliability of the SSVEP technique for the study of the brain processes underlying face perception and individualization. Here, we aimed at determining whether this phenomenon can be extrapolated to facial images that diverge in certain features such as gender and presence vs. absence of skin color and hair. This issue is of importance for the introduction of the SSVEP technique in the field of face perception research because (a) the SSVEP response can vary in a complex manner as a function of stimulus parameters and (b) manipulations to the gender or appearance of the facial stimuli are common in face perception studies. Going a step further, the present study also aims to characterize the temporal evolution of the SSVEP response to individual faces in order to deepen our comprehension of the SSVEP phenomenon. Eight observers were confronted with sequences of faces presented at 4.00 and 5.88 Hz (or faces/second) while high-density EEG (128 channels) was recorded. Four types of faces traditionally employed in face perception studies that diverge in gender, presence of skin color and hair were presented. Fast-Fourier Transform (FFT) of EEG and computation of signal-to-noise ratio (SNR) showed that the brain steady state response was larger for different than identical faces for all stimulus types. At 5.88 Hz, the difference in the strength of the response between different and identical faces was highest for different faces that presented all internal and external features. Additionally, our results demonstrated that the SSVEP to faces of varying identity is characterized by an initial transient response corresponding to the ERPs P1 and N170 followed by a steady response at the stimulation frequency. This steady response increases exactly when changes in the identity of the faces are introduced. These observations corroborate the reliability of the SSVEP to study face perception processes.

**keywords: Face perception, SSVEP, identity adaptation, EEG, skin color, external facial features**

### 3.2.1 Introduction

The presentation of rhythmic stimuli generates a quasi-sinusoidal brain electrical signal whose fundamental frequency is identical to that of the rhythmic stimuli and whose discrete frequency components remain constant in amplitude and phase during the stimulation period (Regan, 1966, 1972, 1989, 2009; Regan & Regan, 1988). This phenomenon was first described by Regan et al. in the visual domain and coined steady state visual evoked potential (SSVEP) (Regan, 1966, 1989).

The SSVEP technique has been successfully used to study different aspects of cognition such as visual attention (Chen *et al.*, 2003; Hillyard *et al.*, 1998), binocular rivalry (Srinivasan, 2004; Srinivasan *et al.*, 1999), working memory (Silberstein *et al.*, 2001) and figure - ground segregation (e.g., Appelbaum *et al.* (2006, 2008)). In this type of experiments, a sinusoidal contrast or luminance modulation is superimposed on images -or aspects of the images- that are task relevant. Measures of the cognitive process under study are then derived from modulations of the steady state response amplitude or phase (Regan, 1972, 1989; Regan & Regan, 1988).

Recently, Rossion & Boremanse (2011) demonstrated the reliability and usefulness of the SSVEP technique to the study of the brain processes underlying face individualization. To this end, the authors designed an experiment in which subjects were presented with sequences of either identical or different faces at a temporal rate of 3.5 Hz expecting to observe a reduction in the brain response for identical faces compared to different faces. Such experimental design relied on the well-known phenomenon of neural adaptation, also called repetition suppression, habituation or repetition effect (note that the use of this last term is preferred throughout this document).

The repetition effect refers to the reduction of neural activity following recurrence of the same stimulus (Grill-Spector & Malach, 2001; Grill-Spector *et al.*, 2006; Henson & Rugg, 2003; Kovács *et al.*, 2006); (for earlier studies of stimulus repetition suppression effects in single neurons in monkeys' infero-temporal cortex, see Baylis & Rolls (1987); Brown & Norcia (1997); Li *et al.* (1993); Ringo (1996)) and it is traditionally used for studying the sensitivity of particular structures or specific time windows to a property of a stimulus that is changed vs. kept constant (e.g., face selective structures that are sensitive to differences between individual faces should show a smaller response when the same individual face stimulus is repeated compared to the presentation of different face stimuli).

In line with their hypothesis, Rossion & Boremanse (2011) observed that the SSVEP response to faces exhibited a main frequency component that corresponded to the stimulation frequency (3.5 Hz) and that the magnitude of such response was higher

when different faces were presented compared to when identical faces were presented. It was concluded that SSVEPs are an appropriate marker of the sensitivity of the face perception network to changes in face identity and can be used to study how the brain codes individual faces (Rossion & Boremanse, 2011).

However, in their study, the authors used a very limited set of facial stimuli: all faces were cropped (the hair and facial shape line were removed), presented an homogenous skin color and represented male individuals. These face images were not representative of the variety of facial stimuli that can be used in face perception studies, an aspect that can be seen as a limitation for the definitive introduction of the SSVEP technique as a standard method to investigate face individualization and recognition in humans. The present study aims to overcome this limitation by determining whether the sensitivity of the SSVEP response to face identity can be equally observed for female and male faces, which, for example, may or may not present skin color and external features (hair and ears). In addition and taking advantage of the large number of data recorded in each participant we also aim at attaining a better characterization of the SSFRE phenomenon previously observed in the study of Rossion & Boremanse (2011).

These specific facial features (gender, skin color and hair) were chosen because of their diagnostic role in face individualization processes. For instance, when skin color (also termed surface reflectance, texture, albedo, or pigmentation) is exaggerated relative to its veridical version, recognition performance is enhanced (Lee & Perrett, 1997). Similarly, a more efficient view generalization is attained after including texture maps on the face while keeping identical the skin color across faces (Troje & Buelthoff, 1996). Skin color also seems to be especially diagnostic to recognize familiar faces (Russell *et al.*, 2007), which suggests that our prior experiences influences the degree to which we rely on the surface properties of a face (Vuong *et al.*, 2005). Some authors have proposed that the importance of skin color lays on allowing a better segmentation of facial features, especially when shape cues are degraded (Sinha & Poggio, 2002).

Regarding face external features (e.g., hair and face shape line), behavioral studies have shown that although recognition is better when the internal features of the face are present, it is still possible to identity faces based solely on the presence of external features (Ellis *et al.*, 1979). The combination of external features and internal features (eye, mouth, nose and their arrangements) may aid the creation of a holistic face representation that helps the identification of unfamiliar faces (Ellis *et al.*, 1979; O'Donnell & Bruce, 2001; Sinha & Poggio, 1996, 2002; Young *et al.*, 1985, 1987).

Face selective regions are also sensitive to the presence of external features as demonstrated by intracranial recordings in the macaque temporal lobe (Freiwald *et al.*, 2009) and fMRI studies in humans (Andrews *et al.*, 2010). Specifically, in humans the FFA and OFA but not the STS are sensitive to the repeated presentation of images of internal or external face features (Andrews *et al.*, 2010).

Here an experiment is presented which, following the study of Rossion & Boremanse (2011), confronted healthy subjects with either identical or different faces while their brain electrical activity was recorded. Four types of facial stimuli often employed in face perception studies were used: real faces that depicted all internal and external features, synthesized faces that did not present hair, real faces that were cropped around the external face line but presented skin color and the same cropped faces depicted in gray scale. The stimulation was sinusoidally modulated at 4.00 Hz (one stimulation cycle was completed after 250 ms) and 5.88 Hz (one stimulation cycle was completed after 170 ms). This selection was motivated by a recent study which demonstrated that skin color seems to be processed by the face perception system around 250 ms after the presentation of the stimuli while the face shape seems to be processed around 170 ms (Caharel *et al.*, 2009b). This conclusion was drawn from the observation that the amplitude of the N170 component is modulated by differences in face shape while the amplitude of the N250 component is modulated by differences in both face shape and skin color (Caharel *et al.*, 2009b). Both components are considered temporal markers of face perception processes: while the N170 is the earliest and most reliable face selective response that can be recorded from the human scalp (Jacques & Rossion, 2009; Rossion & Caharel, 2011; Rossion & Jacques, 2008; Rossion *et al.*, 2000b, 2003a), the N250 is sensitive to the repetition of individual faces (e.g. Begleiter *et al.* (1995); Schweinberger *et al.* (1995); Tanaka *et al.* (2006)). We hypothesized that the sensitivity of the SSVEP to individual faces should appear for all stimulus types and frequencies. However, given that both external and internal facial features help to individualize faces, we also hypothesized that the SSVEP sensitivity to individual faces may be enhanced by the combined appearance of both properties.

### 3.2.2 Materials and methods

#### 3.2.2.1 Participants

Seven right handed healthy participants (5 males, mean age 28 $\pm$ 5 years) with normal or corrected-to-normal vision took part in the experiment. They all provided written informed consent prior to the experiment.

#### 3.2.2.2 Stimuli

Four types of faces were used:

- The Real Cropped (RC) set of faces consisted of 18 female and 18 male facial photographs with neutral expressions. All photographs were cropped around the face external line shape and equalized in luminance. The eyes were also aligned on a horizontal plane.

- The Real Cropped Gray (RCG) set of faces consisted of the same RC faces but with the color information removed so that they were depicted in a gray scale.

- Karolinska Directed Emotional Faces (KDEF): The KDEF is a set of 4900 pictures of human facial expressions developed in 1998 by Daniel Lundqvist, Anders Flykt and Professor Arne Oehman of the Karolinska Institutet, Stockholm, Sweden (Figure 3.2). For the purpose of this experiment, only 18 male and female faces with neutral expressions were selected. None of the faces presented beards, mustaches, earrings, eyeglasses or visible make-up. All subjects wore special gray T-shirts.

- The Max Planck (MP) database contains images of 7 views of 200 laser-scanned (Cyberware TM) (Blanz & Vetter, 1999) heads without hair (Figure 3.2). The 200 head models were synthesized by morphing real scans to avoid close resemblances to real individuals (Troje & Buelthoff, 1996). Among these 200 head models, 18 male and 18 female were randomly selected to be used in this experiment. Note that in contrast to the MP faces used in the study of Rossion & Boremanse (2011) they were not cropped in the current study.

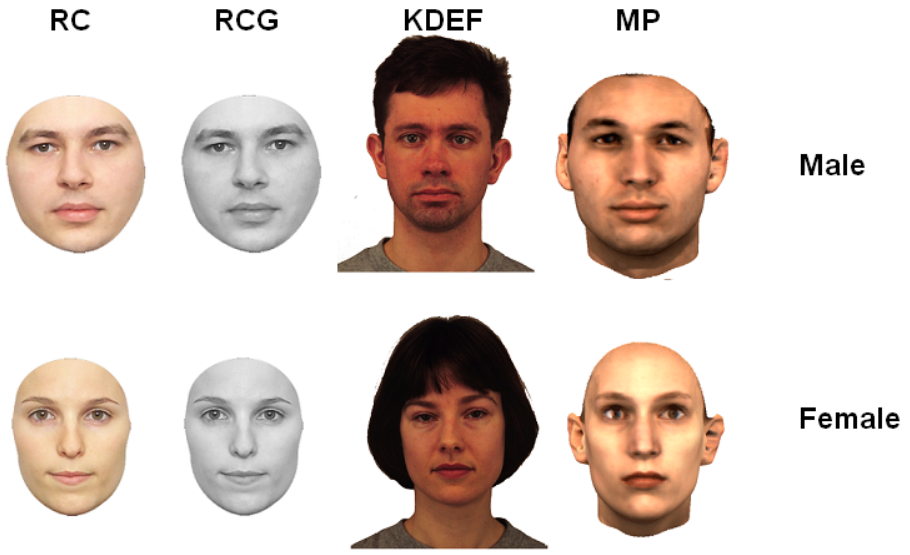


**Figure 3.2: Facial stimuli employed in the experiment** - Subjects were presented four types of stimulus: Real Cropped (RC), Real Cropped Gray (RCG) faces, Karolinska Directed Emotional Faces (KDEF) and Max Planck faces (MP).

#### 3.2.2.3 Procedure

The base stimuli subtended 4° by 5.73° of visual angle at a viewing distance of 100 cm. A small, black dot was located centrally on the top part of the face nose, slightly below the line of the eyes, corresponding roughly to the optimal fixation point for fast face identification (Hsiao & Cottrell, 2008; Orban de Xivry *et al.*, 2008) (Figure 3.3). These stimuli were displayed on a computer screen (100 Hz vertical refreshing rate) using a custom-made application (SinStim) running on Matlab. To modulate the rate of stimuli appearance on the screen, SinStim used a temporal raised-sinusoidal waveform. Thus, the stimulation sequence begun with a gray background and the first face of the sequence reached full luminance after half a cycle. This implies that for a stimulation frequency of 4.00 Hz, the first face of the sequence reached full luminance at 125 ms whereas for a stimulation frequency of 5.88 Hz, the first face of the sequence reached full luminance at 85 ms. At the beginning of the stimulation sequence and at each minimal level of visual stimulation (gray background maxima) a trigger was sent from the parallel port of the stimulation computer to the EEG recording computer. The whole sequence lasted 84 s. It began with 15 s during which the same face was presented followed by 69 s during which the face either remained identical (identical face condition) or changed identity (different face condition). In the last case, the 18 individual faces were presented in random order in the sequence with the only constraint that the same face identity could not appear immediately after having been presented. To minimize low-level (i.e., pixel-wise) adaptation, the base face stimulus changed size at every single presentation (random size between 82% and 112% of base face size) in all conditions (Figure 3.3).

The experimental session included two stimulation blocks. One block consisted of two runs for each frequency, one run for the identical faces condition and another run for the different faces condition. They were always applied consecutively but their order, whether the identical or the different faces condition was presented first, was counterbalanced across sessions and subjects. The order of the stimulation frequency to use was determined randomly. In the second block, the order used was exactly the opposite to the one used in the first block.

Subjects were instructed to fixate the black dot and to press the space bar every time they detected the dot changed from black to red. Every color change lasted for 400 ms and occurred between 11 and 16 times during a stimulation run. This orthogonal task was used to maintain participants level of attention constant during all conditions of stimulation while maintaining fixation.

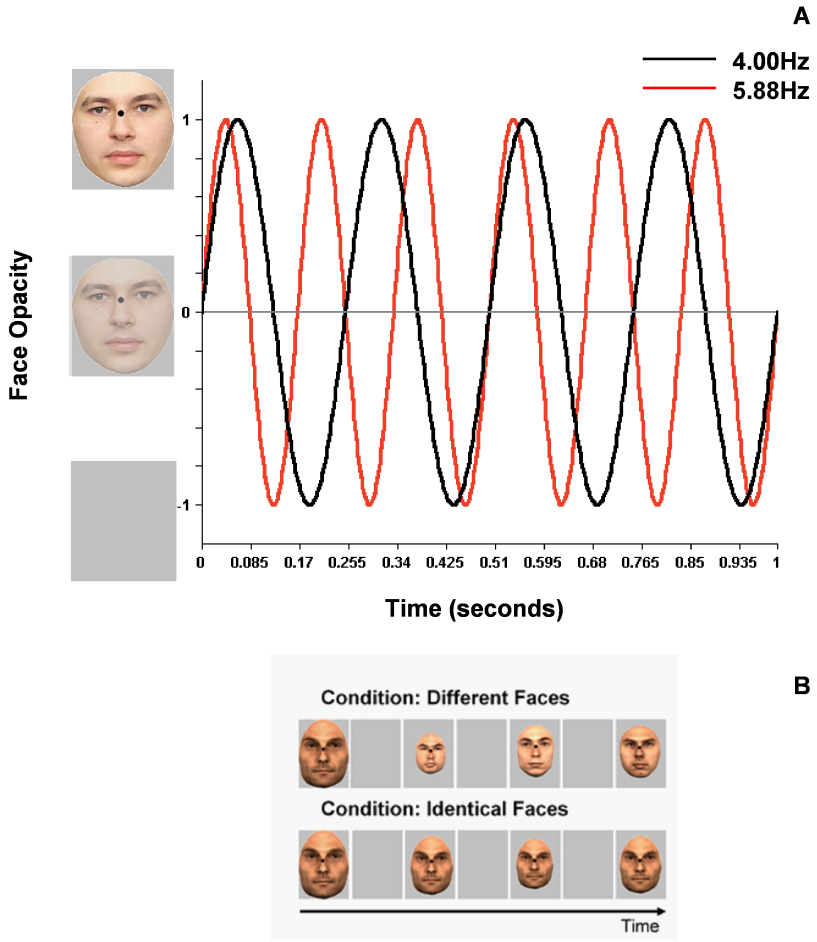


**Figure 3.3: Schematic view of the experiment used in Study 2** - (A) Stimuli generation: Full front pictures of faces were presented using a sinusoidal modulation. The beginning of the 90 s sequence was always the gray background. The lower contrast face stimulus in the midline, in between the background and the full face stimulus, represents an intermediary stage of stimulation at the onset of the face stimulus. (B) The two experimental conditions used in the study, different face condition and identical face condition. Note that there were large changes of size between each face picture to minimize low-level adaptation effects.

#### 3.2.2.4 EEG recording

After electrode-cap placement, subjects were seated in light- and sound-attenuated room. EEG was recorded from 128 Ag/AgCl electrodes mounted in an electrode cap (Waveguard, ANT; for a 2D mapping of electrode labels and positions, see `http://www.ant-neuro.com/products/caps/waveguard/layouts/128/` and also Figure 3.4). Electrode positions included the standard 10-20 system locations and additional intermediate sites. Vertical and horizontal eye movements were monitored using four additional electrodes placed on the outer canthus of each eye and in the inferior and superior areas of the right orbit. During EEG recording, all electrodes were referenced to the left mastoid reference, and electrode impedances were kept below 10 kΩ. EEG was digitalized at a 1000 Hz sampling rate and a digital anti-aliasing filter of 0.27 * sampling rate was applied at recording (at 1000 Hz sampling rate, the usable bandwidth is 0 to 270 Hz).

#### 3.2.2.5 EEG analysis

**Frequency domain analysis using Fast Fourier Transform (FFT):**

After recording, the data was first band-pass filtered between 0.5 Hz-100 Hz and then re-referenced to a common average reference. Electrodes with artifacts other than eye blinks were pooled using neighboring channels.

Afterwards, Fast Fourier Transform algorithm (FFT) was applied to a 64 s window of stimulation starting 17 s after the beginning of the stimulation to avoid the possible influence of transient responses triggered by the onset of the stimulation train, and to allow the system to get entrained by the stimulation (Chen *et al.*, 2003; Srinivasan *et al.*, 1999). For a 64 s analysis window, the resulting frequency resolution is 0.015625 Hz, which allowed to distinguish clearly two closely spaced frequency components or frequency bins (e.g., a frequency bin at 4.00 Hz is followed by a frequency bin at 4.015625 Hz).

At each electrode and frequency bin (from 0 to 100 Hz), the FFT amplitude spectrum ($\mu V$) was extracted for each run and each condition separately in every participant. On this data, the signal-to-noise ratio (SNR) index was calculated. This index was defined as the ratio of the amplitude at the frequency of interest to the average amplitude of the 10 neighboring bins skipping the three nearest bins. These bins were excluded because they may have contained residual EEG activity due to either spectral leakage produced by signal processing algorithms or slight inaccuracies in the visual stimulation (missing frames) (Srinivasan *et al.*, 1999). This SNR measure has been successfully used to enhance SSVEP peaks (Wang *et al.*, 2006). All computations were done using Matlab.

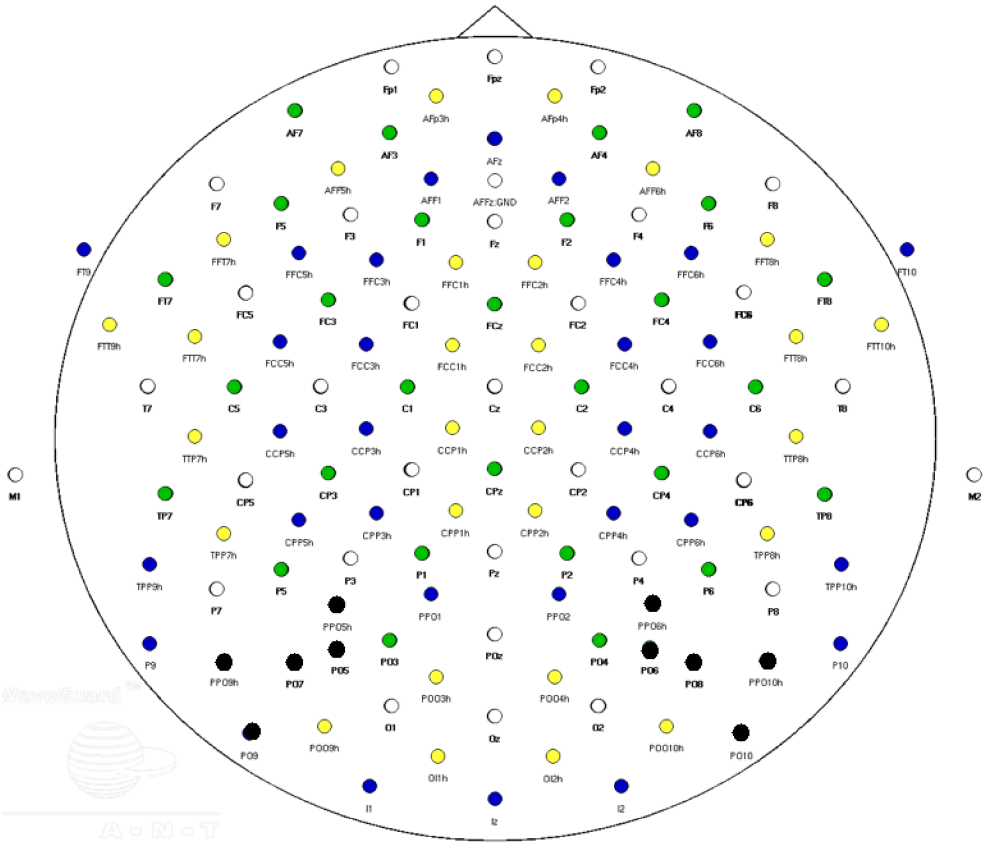


**Figure 3.4: 128 electrodes layout used for EEG recording** - Electrodes that were selected to form the regions of interest are highlighted in black (see text for further details on this point).

In order to determine how the stimulus manipulations influence the process of detecting changes in its identity, the SNR based FFT amplitude values were averaged across all subjects and then both conditions were subtracted (different face condition − identical face condition) for each electrode, separately. In this way, positive values would indicate that the SNR was highest for the different face condition. This index was called *Steady State Face Repetition Effect* or SSFRE.

After calculating the SSFRE, it was plotted on the scalp for each stimulation frequency using a SSFRE by frequency scale adjusted according to the electrode that exhibited the highest SSFRE at that particular stimulation frequency.

Based on these maps, regions of interest (ROIs) were determined including clusters of electrodes that showed the highest SSFRE. The SSFRE values averaged over these ROIs were submitted to ANOVA analysis using stimulus gender (female vs. male),

hemisphere (right vs. left) and stimulus type (MP, KDEF, RC, RCG) as factors ($p < 0.05$). Given that there is an inverse relation between EEG amplitude and frequency (Buzsaki, 2006), the ANOVA analysis was done for each frequency separately to avoid biasing the results in favor of the slowest stimulation frequency. Multiple comparison error rate was controlled using the Greenhouse-Geisser correction.

**Time domain analysis using EEG narrow band filtering:**

For each participant, time-domain EEG data was averaged separately for each of the two conditions (same face, different faces). Afterwards, the data was band-pass filtered around the fundamental frequency of interest (e.g. for stimulation frequency of 4.00 Hz the data was band pass filtered between 3.00 and 5.00 Hz). The resulting bandpass filtered files were then grand-averaged by condition. Since similar results were obtained for both stimulation frequencies, here only the results obtained for 4.00 Hz will be illustrated.

**Time-frequency analysis using Morlet wavelets:**

In the time-frequency analysis, each individual data file (from 2 s before the beginning of the experimental sequence to 83 s after) was time-frequency (TF) transformed using a Morlet wavelet algorithm (implemented in a custom-made software for EEG data analysis 'Letswave') between 0 and 30 Hz with parameters of 100 lines, $\sigma = 10$ and $\omega = 0.15$. TF matrices were averaged within each condition and stimulation frequency, separately for each participant, and then grand-averaged across different types of faces to increase power.

### 3.2.3 Results

#### 3.2.3.1 Behavior

Participants detected accurately the color changes (95-100% correct responses), without differences in amount of correct responses and reaction times between conditions.

#### 3.2.3.2 Frequency domain analysis: entrainment and SSFRE at the stimulation frequency

In order to verify that all types of facial stimulus provoked an increase in the SNR at the frequency component that corresponded to the stimulation frequency, the SNR signal was averaged over all subjects and electrodes for each condition separately and the obtained values were plotted as a function of stimulation frequency. As it is shown

in Figure 3.5, all face pictures, regardless of their characteristics, elicited an increase in the SNR value at the frequency bin corresponding to the stimulation.

In a second step, the SSFRE was calculated for each electrode and stimuli separately, averaged across subjects and finally plotted on the scalp (Figures 3.6 and 3.7). For all stimuli and stimulation frequencies, the highest effect was observed over occipito-temporal electrodes of both hemispheres especially PO6/5, PO8/7, PO10/9, PPO6h/5h, PPO10h/9h (Figure 3.6 and Figure 3.7; see Figure 3.4 for the location of these electrodes).

The level of entrainment exhibited by these electrodes when either identical or different faces were presented at a temporal rate of 4.00 Hz is illustrated in Figures 3.8, 3.9, 3.10 and 3.11. Figures 3.12, 3.13, 3.14 and 3.15 present the level of entrainment for faces presented at a temporal rate of 5.88 Hz. Note how in all cases the signal averaged across these set of electrodes increased at the stimulation frequencies compared to the neighboring frequency bins.

The SSFRE values at these electrodes were averaged for each hemisphere, stimuli and frequency separately to form ROIs that were latter submitted to ANOVA analysis with factors of *stimuli type*(KDEF, MP, RC, RCG), *hemisphere* (right and left) and *stimuli gender* (female and male faces).

The ANOVA analysis demonstrated that at 4.00 Hz there were no significant differences in the SSFRE caused by each stimulus (Figure 3.16) while at 5.88 Hz there was a main effect of *stimulus type* (ANOVA, $F(3, 18) = 7.1, p = 0.002$) (Figure 3.17 and an interaction between *gender* and *hemisphere* (ANOVA, $F\ (1, 6) = 7.23, p = 0.036$) (Figure 3.18). Collapsing across factors of gender and stimuli revealed that the main effect of stimulus type was due to the fact that the SSFRE obtained in response to the KDEF stimuli was significantly higher than the SSFRE obtained for the RC (t-test, $t(6) = 3.14, p = 0.01$), RCG (t-test, $t(6) = 4.15, p = 0.00$) and MP (t-test, $t(6) = 3.43, p = 0.00$) stimuli. Collapsing across the stimulus type revealed that the interaction between gender and hemisphere was due to the fact that the SSFRE obtained for the left hemisphere ROI was significantly smaller for female than for male faces (t-test, $t(6) = 5.96, p = 0.00$). It was also significantly smaller than the SSFRE obtained for the right hemisphere ROI when female faces were presented (t-test, $t(6) = 2.1, p = 0.04$) (Figure 3.18).

#### 3.2.3.3 Time-frequency analysis

The results of the time-frequency analysis are presented in Figure 3.19, Figure 3.20, Figure 3.21, which display the frequency content of the EEG signal as a function of time for all experimental conditions.

Figure 3.19 clearly shows that the presentation of different faces elicited a continuous response at 4.00 Hz. This response started at about 2 seconds after the onset of

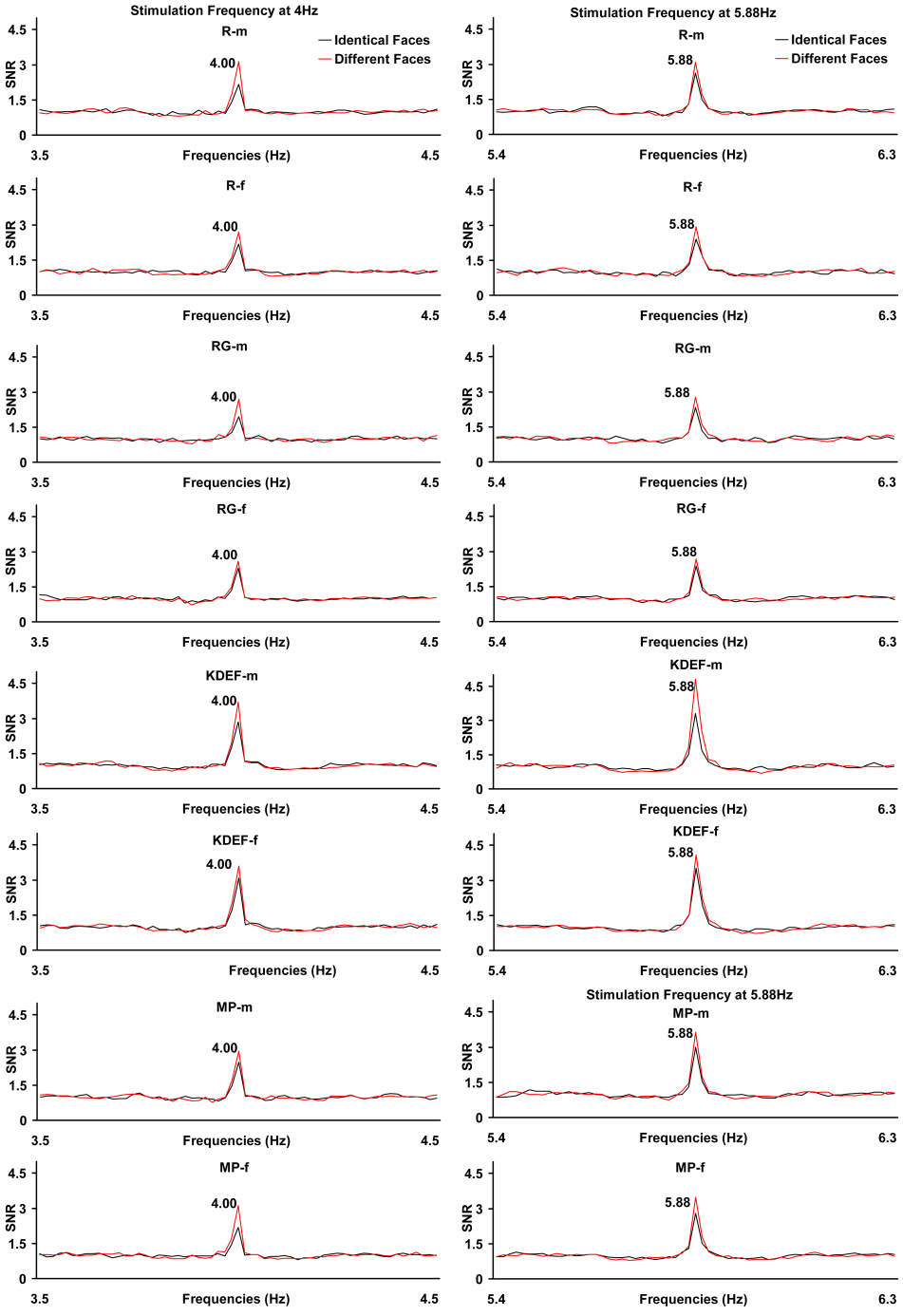


**Figure 3.5: SNR for all stimuli employed in Study 2** - For each facial stimuli used in this experiment, the SNR values averaged across subjects, sessions and electrodes are displayed for 30 frequency bins centered around the value that corresponded to the stimulation frequency. Note how the SNR increases for the stimulation frequency. (R: real cropped, RG: real cropped gray, MP: Max Planck and KDEF: Karolinska Directed Emotional Faces; m: male faces, f: female faces).

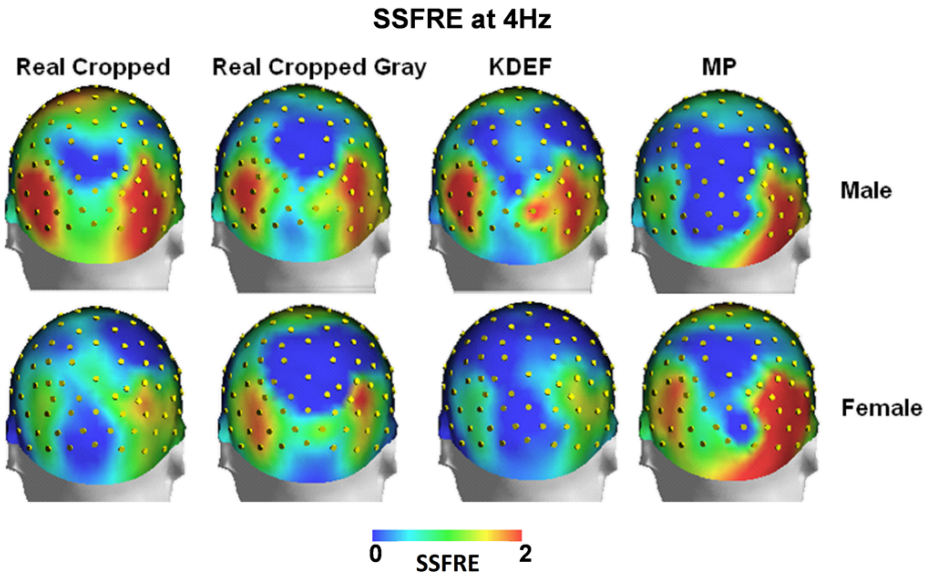


**Figure 3.6: SSFRE scalp distribution for each stimulus type presented at 4Hz** - The SSFRE was averaged across subjects for each stimulus separately. Note the characteristic SSFRE topographic distribution (focused over occipito-temporal electrodes with a right hemisphere dominance), which is present for all stimuli.

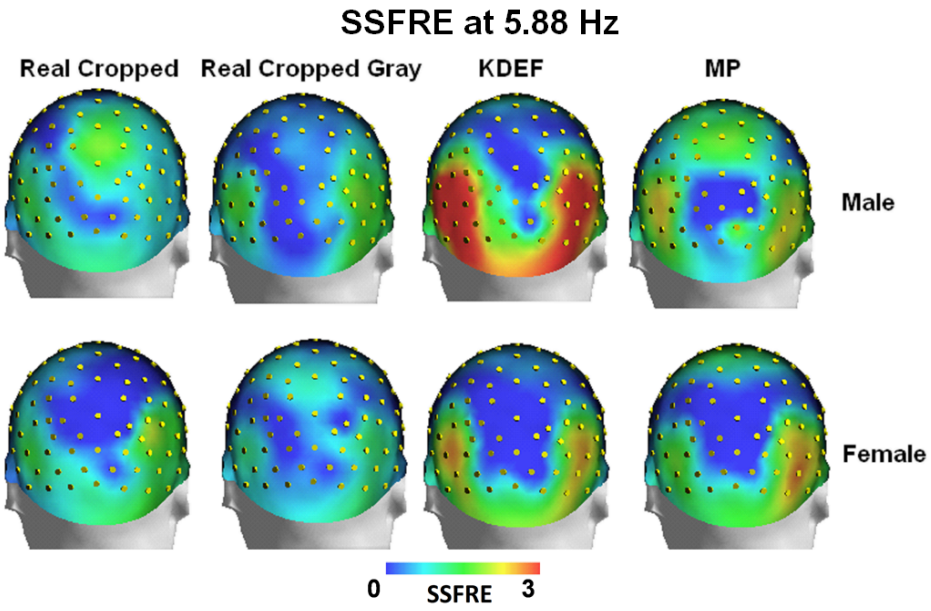


**Figure 3.7: SSFRE scalp distribution for each stimulus type presented at 5.88 Hz** - The SSFRE was averaged across subjects for each stimulus separately and plotted on the scalp. It is evident that SSFRE topographic distribution is focused over occipito-temporal electrodes with a right hemisphere dominance for all stimuli.

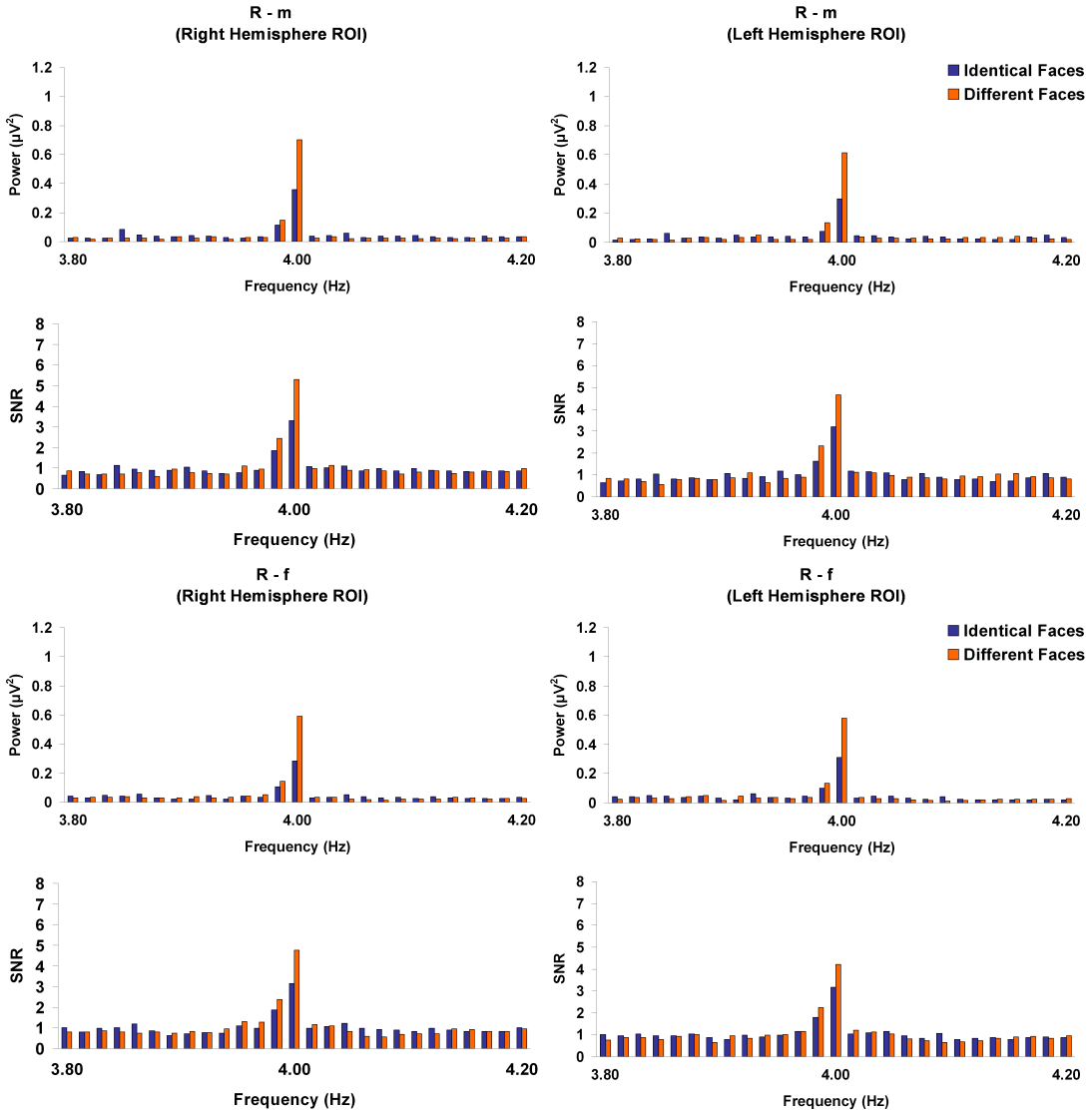


**Figure 3.8: Entrainment to the stimulation frequency (male and female real cropped faces, R - m and R - f, presented at 4.00 Hz).**

FFT power spectrum and SNR values averaged across subjects, sessions and electrodes PO6/5, PO8/7, PO10/9, PPO6h/5h, PPO10h/9h are displayed only for 26 frequency bins centered on the corresponding stimulation frequencies. Figures 3.9, 3.10 and 3.11 present the data corresponding to the remaining facial stimuli employed in this experiment.

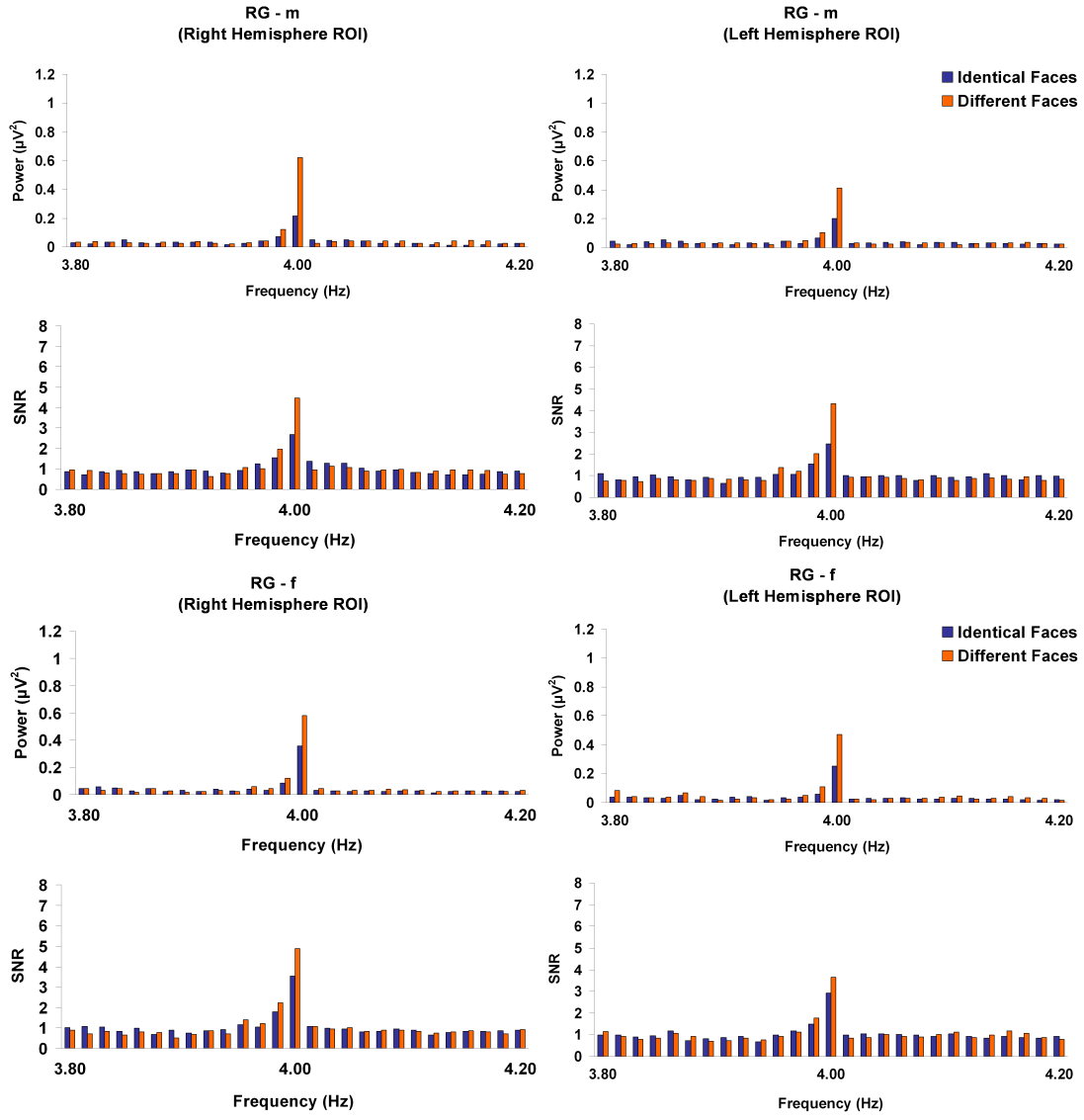


**Figure 3.9: Entrainment to the stimulation frequency (male and female real, gray, cropped faces, RG - m and RG - f, presented at 4.00 Hz).**

FFT power spectrum and SNR values averaged across subjects, sessions and electrodes PO6/5, PO8/7, PO10/9, PPO6h/5h, PPO10h/9h are displayed only for 26 frequency bins centered on the corresponding stimulation frequencies. Figures 3.8, 3.10 and 3.11 present the data corresponding to the remaining facial stimuli employed in this experiment.

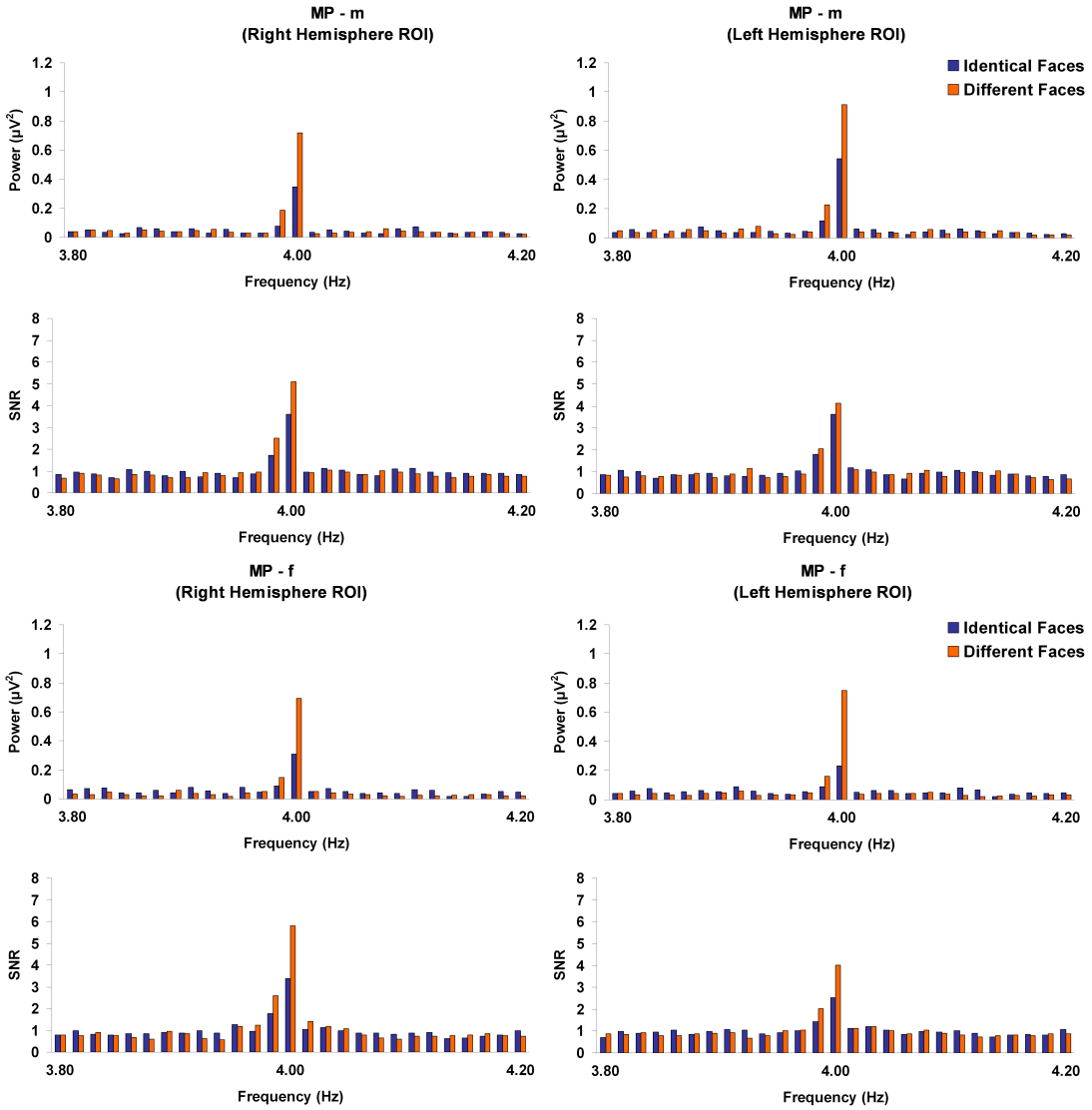


**Figure 3.10: Entrainment to the stimulation frequency (male and female Max Planck faces, MP - m and MP - f, presented at 4.00 Hz).**

FFT power spectrum and SNR values averaged across subjects, sessions and electrodes PO6/5, PO8/7, PO10/9, PPO6h/5h, PPO10h/9h are displayed only for 26 frequency bins centered on the corresponding stimulation frequencies. Figures 3.8, 3.9 and 3.11 present the data corresponding to the remaining facial stimuli employed in this experiment.

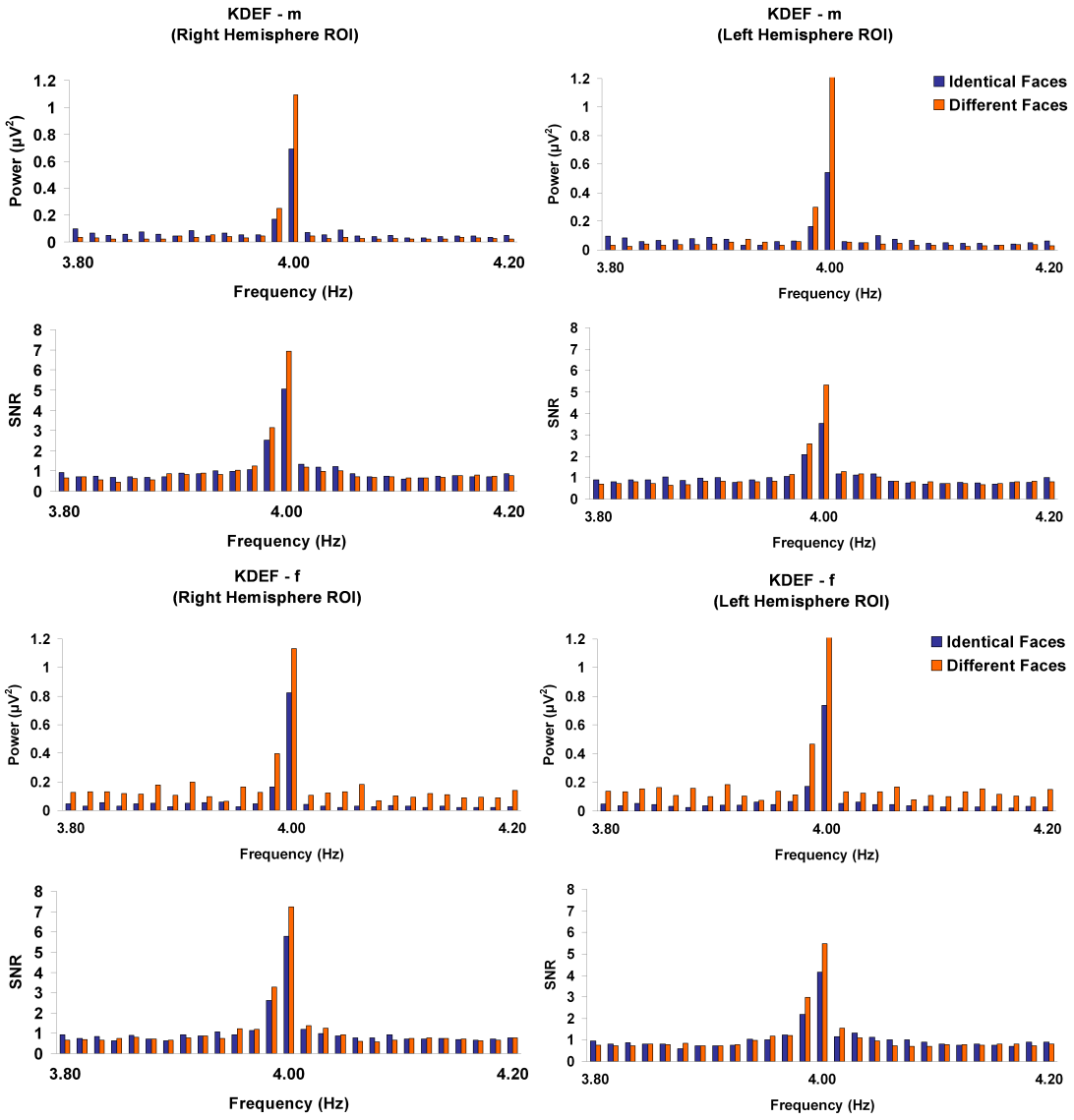


**Figure 3.11: Entrainment to the stimulation frequency (male and female KDEF faces, KDEF - m and KDEF - f, presented at 4.00 Hz).**

FFT power spectrum and SNR values averaged across subjects, sessions and electrodes PO6/5, PO8/7, PO10/9, PPO6h/5h, PPO10h/9h are displayed only for 26 frequency bins centered on the corresponding stimulation frequencies. Figures 3.8, 3.9 and 3.10 present the data corresponding to the remaining facial stimuli employed in this experiment.

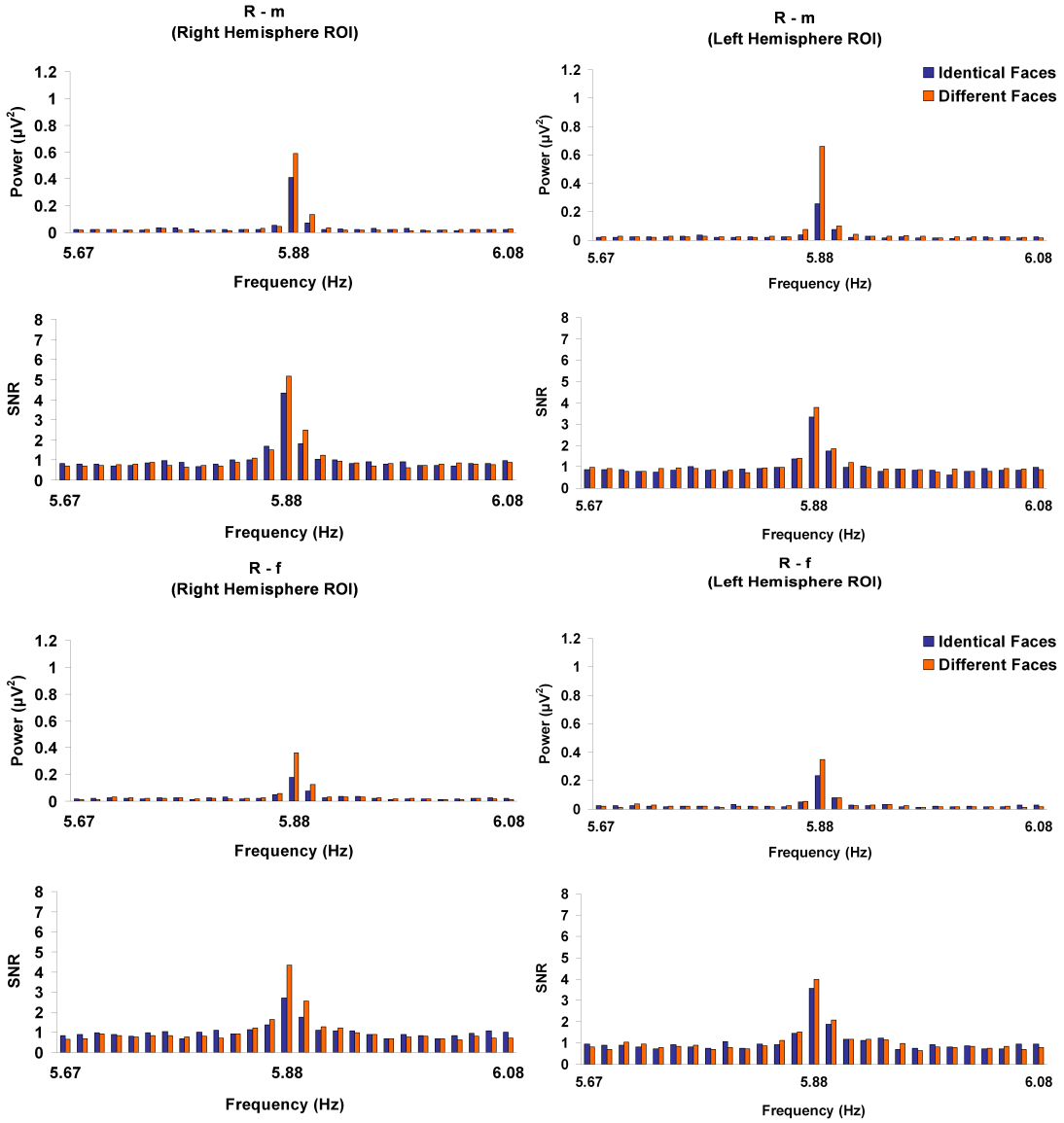


**Figure 3.12: Entrainment to the stimulation frequency (male and female real cropped faces, R - m and R - f, presented at 5.88 Hz).**

FFT power spectrum and SNR values averaged across subjects, sessions and electrodes PO6/5, PO8/7, PO10/9, PPO6h/5h, PPO10h/9h are displayed only for 26 frequency bins centered on the corresponding stimulation frequencies. Figures 3.13, 3.14 and 3.15 present the data corresponding to the remaining facial stimuli employed in this experiment.

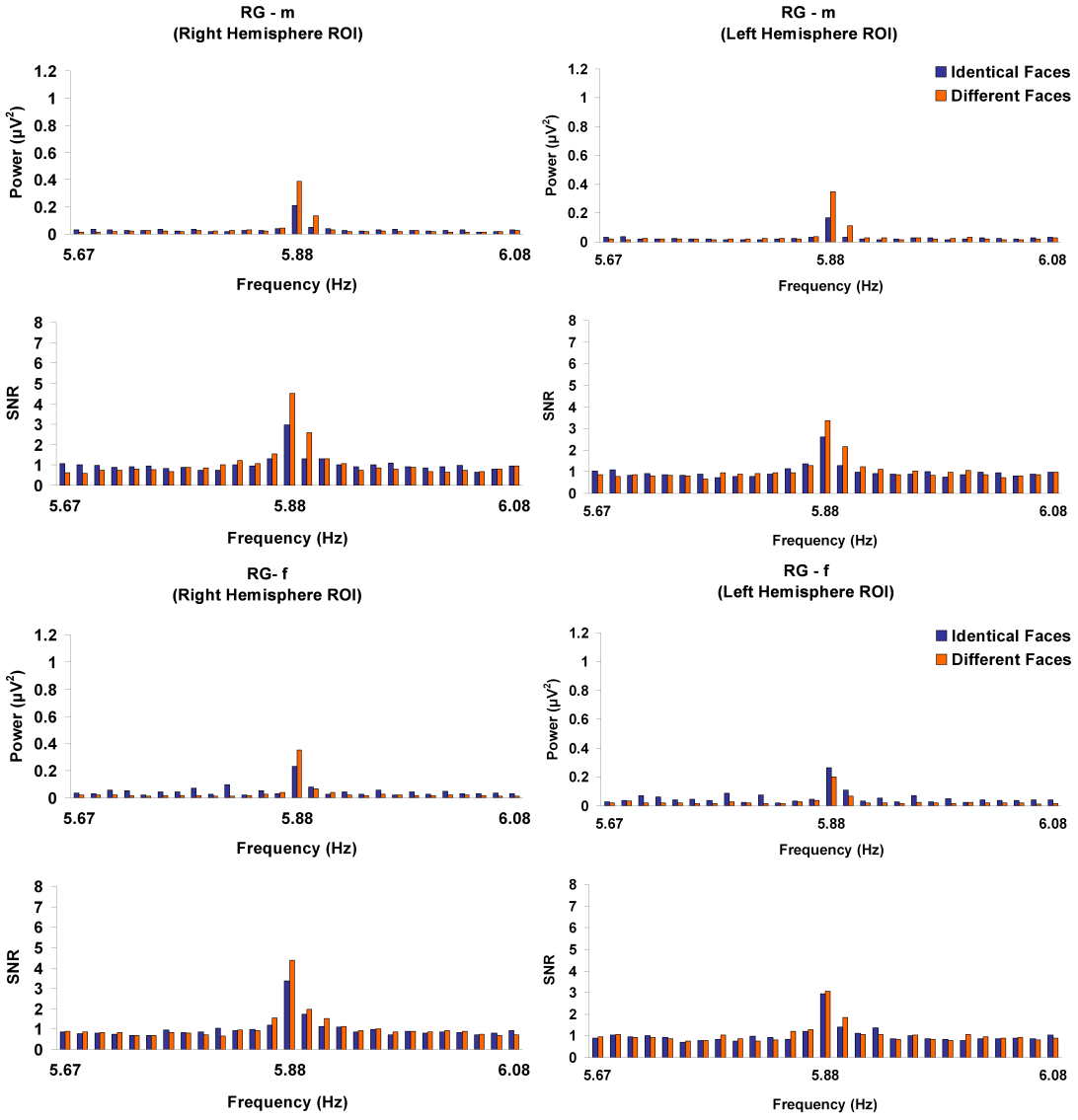


**Figure 3.13: Entrainment to the stimulation frequency (male and female real cropped faces, RG - m and RG - f presented at 5.88 Hz).**

FFT power spectrum and SNR values averaged across subjects, sessions and electrodes PO6/5, PO8/7, PO10/9, PPO6h/5h, PPO10h/9h are displayed only for 26 frequency bins centered on the corresponding stimulation frequencies. Figures 3.12, 3.14 and 3.15 present the data corresponding to the remaining facial stimuli employed in this experiment.

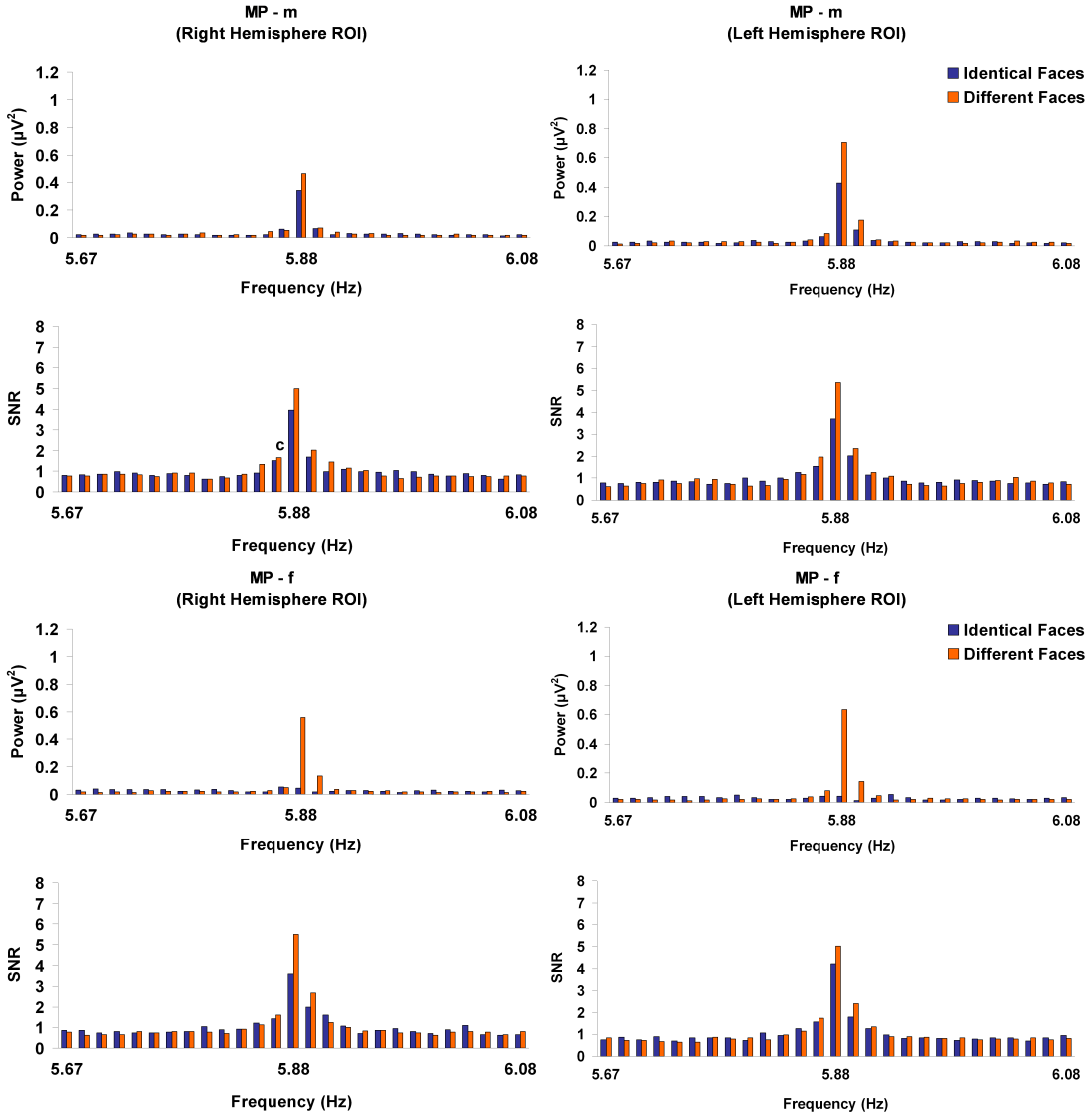


**Figure 3.14: Entrainment to the stimulation frequency (male and female Max Planck faces, MP - m and MP - f presented at 5.88 Hz).**

FFT power spectrum and SNR values averaged across subjects, sessions and electrodes PO6/5, PO8/7, PO10/9, PPO6h/5h, PPO10h/9h are displayed only for 26 frequency bins centered on the corresponding stimulation frequencies. Figures 3.12, 3.13 and 3.15 present the data corresponding to the remaining facial stimuli employed in this experiment.

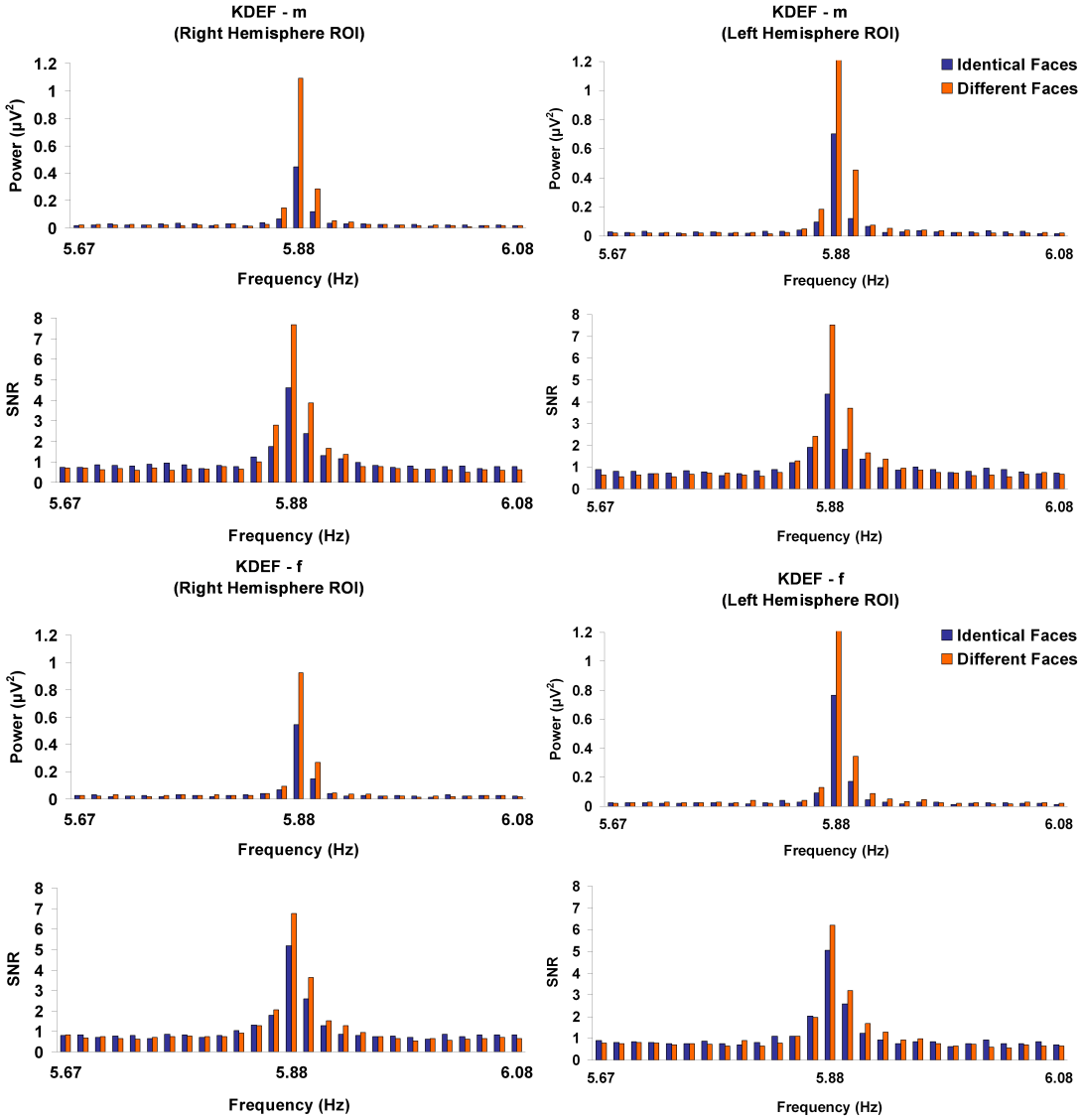


**Figure 3.15: Entrainment to the stimulation frequency (male and female real cropped faces, KDEF - m and KDEF - f presented at 5.88 Hz).**

FFT power spectrum and SNR values averaged across subjects, sessions and electrodes PO6/5, PO8/7, PO10/9, PPO6h/5h, PPO10h/9h are displayed only for 26 frequency bins centered on the corresponding stimulation frequencies. Figures 3.12, 3.13 and 3.14 present the data corresponding to the remaining facial stimuli employed in this experiment.

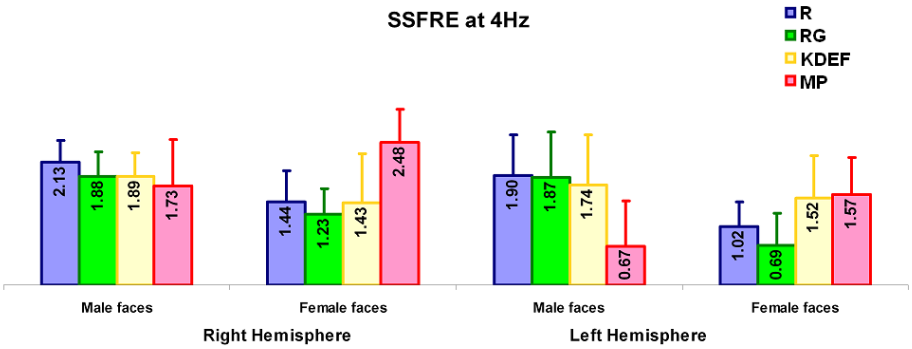


**Figure 3.16: Mean (box) and standard deviation (whisker) of the SSFRE for each stimulus type presented at 4Hz** - For each stimulus the mean SSFRE value and its corresponding standard deviation is indicated. The ANOVA analysis did not show significant differences between these values (ANOVA: $p > 0.05$).

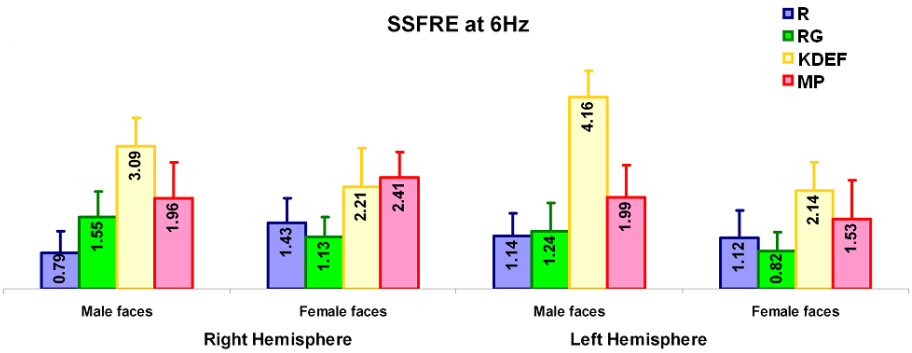


**Figure 3.17: Mean (box) and standard deviation (whisker) of the SSFRE for each stimulus type presented at 5.88Hz** - For each stimulus, the mean SSFRE value and its corresponding standard deviation is indicated. The ANOVA analysis revealed a main effect of stimulus type and an interaction between gender and hemisphere (see text for further details).

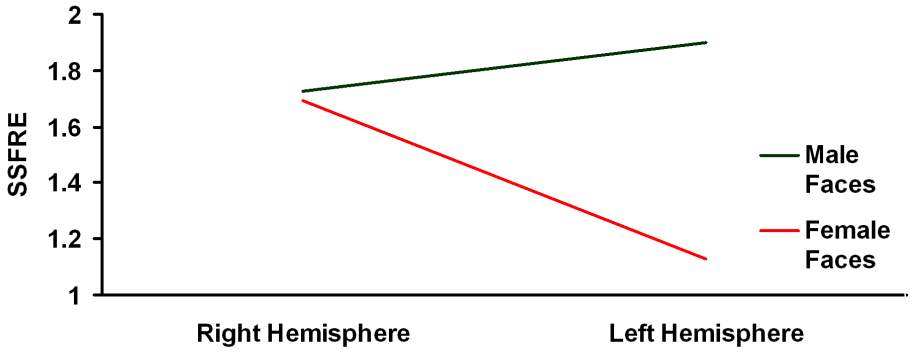


**Figure 3.18: SSFRE obtained after collapsing across stimulus type** - In order to test the ANOVA interaction between factors of gender and hemisphere the SSFRE was collapsed across levels of the factor stimulus type. Comparing the obtained values revealed that the ANOVA interaction was due to the fact that the SSFRE obtained for the left hemisphere ROI was significantly smaller for female than for male faces and also significantly smaller than the SSFRE obtained for the right hemisphere ROI when female faces were presented (see text for further details).

stimulation and lasted throughout the entire stimulation period. A continuous response was also visible in the alpha band (8 - 12 Hz), preventing assessment of the 8.00 Hz (second harmonic) and 12.00 Hz (third harmonic) responses.

A large increase of activity between 3.00 and 14.00 Hz was also visible right after stimulus onset. Interestingly, a second activation increase in the response appeared exactly when the identity of the faces began to vary in the different faces condition (15 s after the beginning of the stimulation) but the frequency range of this response was less specific, spreading over lower frequency ranges, which suggested that it corresponded partly to a transient evoked potential (perhaps a P300 to the first different face identity, a 'rare event' after a succession of 60 identical face identities during the initial 15 seconds of stimulation) (Figure 3.19).

Figure 3.20 shows the exact same analysis performed for identical faces. The activity increase at the beginning of the steady-state response at 4.00 Hz was also clearly visible, as well as the sustained response in the alpha range. However, the 4.00 Hz response decreased progressively along the recording window, and was clearly of smaller amplitude than when different faces were presented.

Subtraction between both conditions showed very clearly that the difference between conditions started immediately after the introduction of the change of stimulation and lasted throughout the entire duration of the stimulation (Figure 3.21).

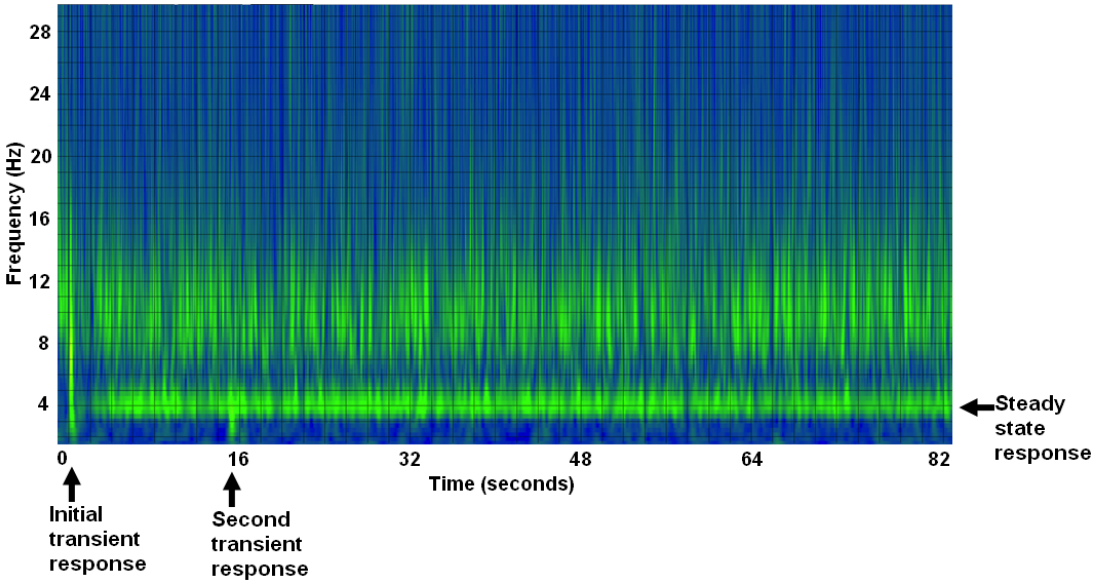


**Figure 3.19: Time frequency analysis of the EEG signal recorded in response to different faces presented at 4.00 Hz for electrode P8** - The figure presents the frequency decomposition of the EEG signal as a function of time (green color, in opposition to blue, represents an increase in the magnitude of the brain response at a particular frequency and time point). Note the presence of a continuous response at 4.00 Hz, which started shortly after the appearance of the first facial stimulus and lasted throughout the entire stimulation. Note also the continuous although more diffuse response in the alpha range (8 - 12 Hz) as well as the large but transient activity increase between 3.00 and 14.00 Hz at the beginning of the stimulation and between 1 and 4 Hz at 15 s.

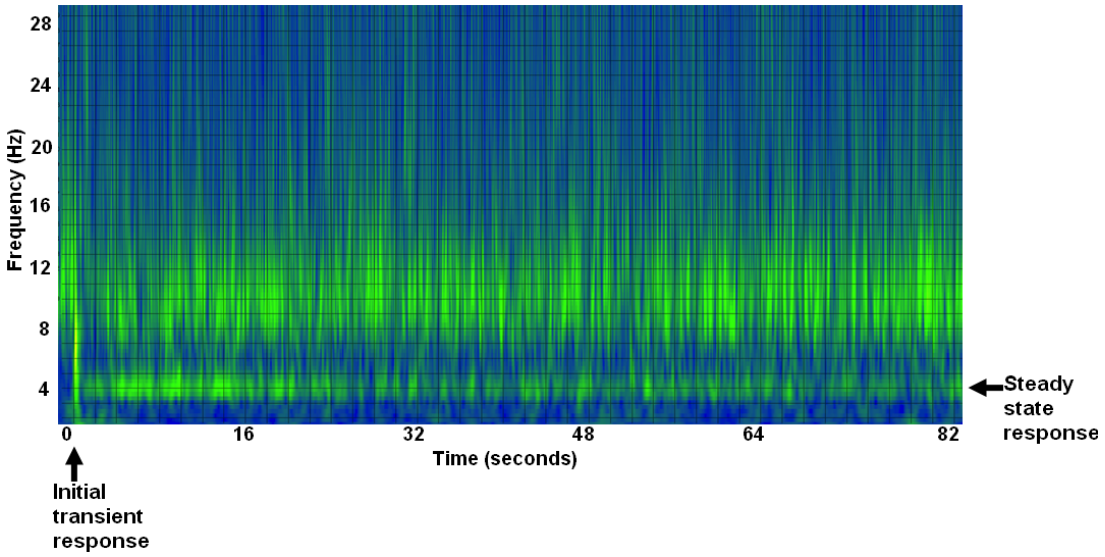


**Figure 3.20: Time frequency analysis of the EEG signal recorded in response to identical faces presented at 4.00 Hz for electrode P8** - The figure presents the frequency decomposition of the EEG signal as a function of time (green color, in opposition to blue, represents an increase in the magnitude of the brain response at a particular frequency and time point). As in the case of the presentation of different faces, identical faces elicited a continuous response at 4.00 Hz which started shortly after the appearance of the first facial stimulus and lasted throughout the entire stimulation. A continuous although more diffuse response in the alpha range (8 - 12 Hz) was also present during the whole stimulation. At the beginning of the stimulation there was a transient activity increase between 3.00 and 14.00 Hz. However, there was no evoked potential observed after 15 s of stimulation.

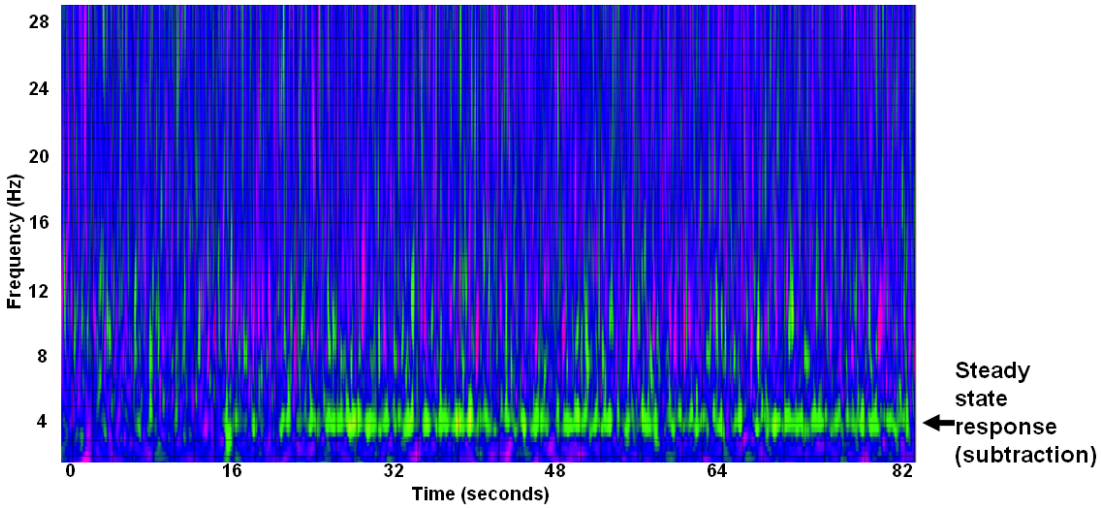


**Figure 3.21: Subtraction of the time frequency decomposition of the EEG signal recorded in response to different - identical faces presented at 4.00 Hz for electrode P8** - The figure clearly demonstrates that the difference between different and identical faces appeared around 15 s, when the first different face was presented and lasted throughout the stimulation. (Green color, in opposition to blue, represents an increase in the magnitude of the brain response at a particular frequency and time point).

#### 3.2.3.4 Narrow-band filtering

Figure 3.22 shows the EEG signal band pass filtered around the stimulation frequency for the entire period of stimulation. In terms of amplitude, the signal corresponding to the different faces condition clearly dominated over the signal corresponding to the identical faces condition especially after 15 s of stimulation.

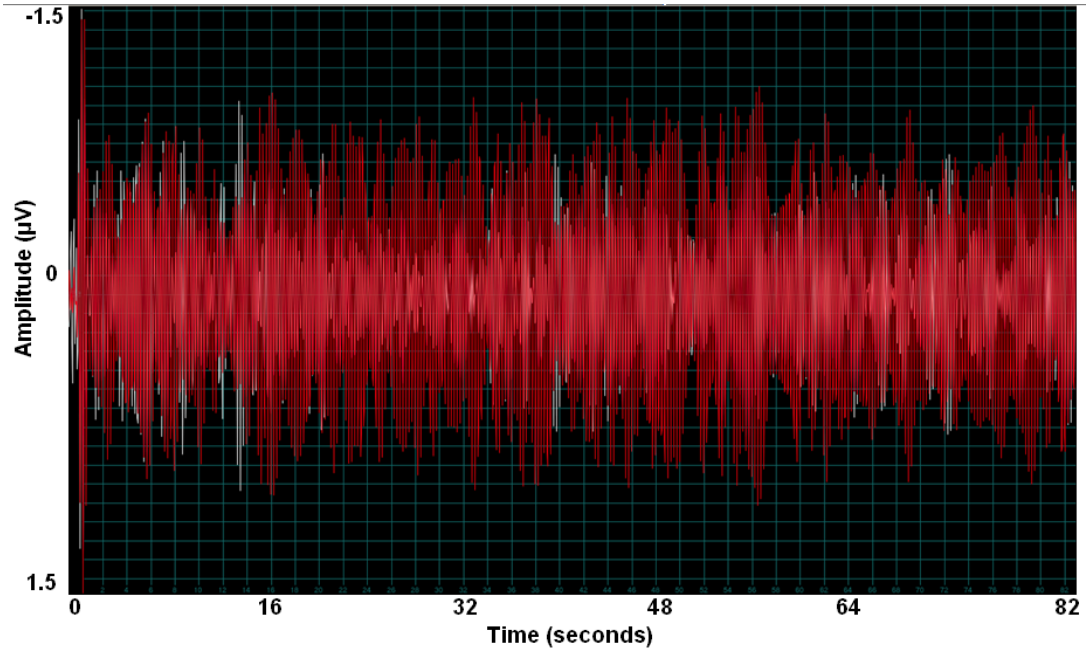


**Figure 3.22: The amplitude of the EEG signal is displayed as a function of time for both conditions** - The figure shows the EEG signal band pass filtered around the stimulation frequency for both conditions. Note how the signal registered in response to different faces (red) dominates over the signal registered in response to identical faces (white).

To illustrate the predominance of the EEG response to different faces over the response to identical faces, Figure 3.23 shows the recording window between 10 and 20 s. One can clearly see that the increase of amplitude was time-locked to the introduction of variations in the identity of the face (15 s after the beginning of the stimulation).

As previously mentioned, the time frequency analysis showed that right after the beginning of the stimulation there was a diffuse increase in the signal strength between 3.00 and 14.00 Hz for both conditions (Figure 3.19 and Figure 3.20). This was also observed when the amplitude of the EEG signal was plotted as a function of time (Figure 3.24). This initial amplitude increase in the response was followed by the

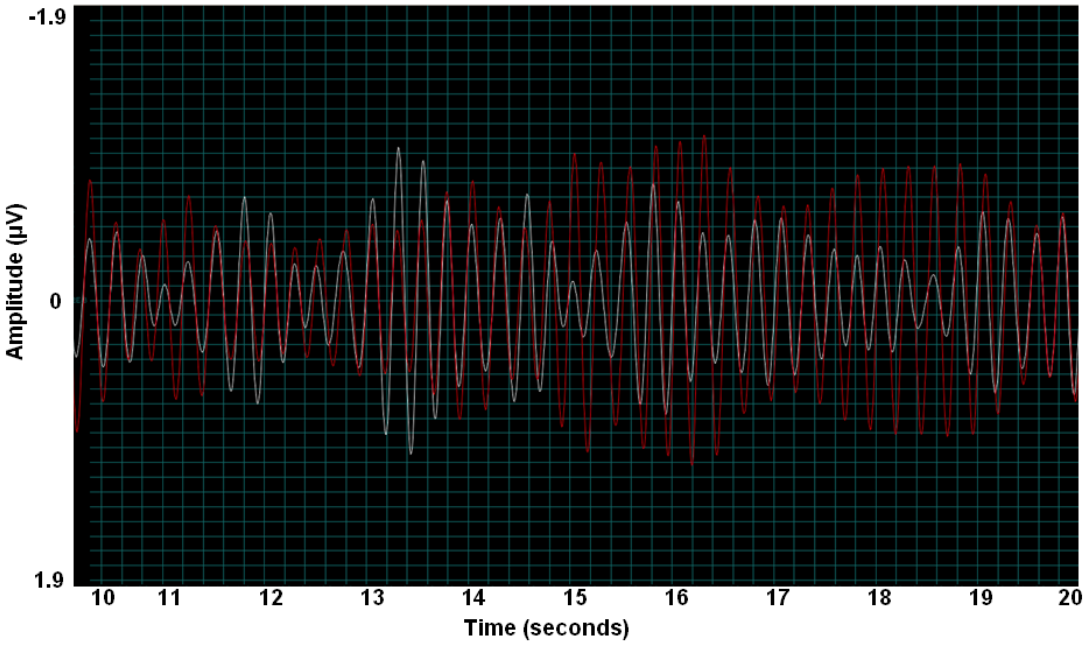


**Figure 3.23: The EEG signal is displayed between 10 and 20 s post-stimulus for both conditions** - Note how the signal registered in response to different faces (red) is of much higher amplitude that the signal registered in response to identical faces (white) especially after 15 s of stimulation exactly when the face identity began to vary in the different faces condition.

steady-state mode, which lasted during the whole stimulation period, with no obvious difference between the 2 conditions.

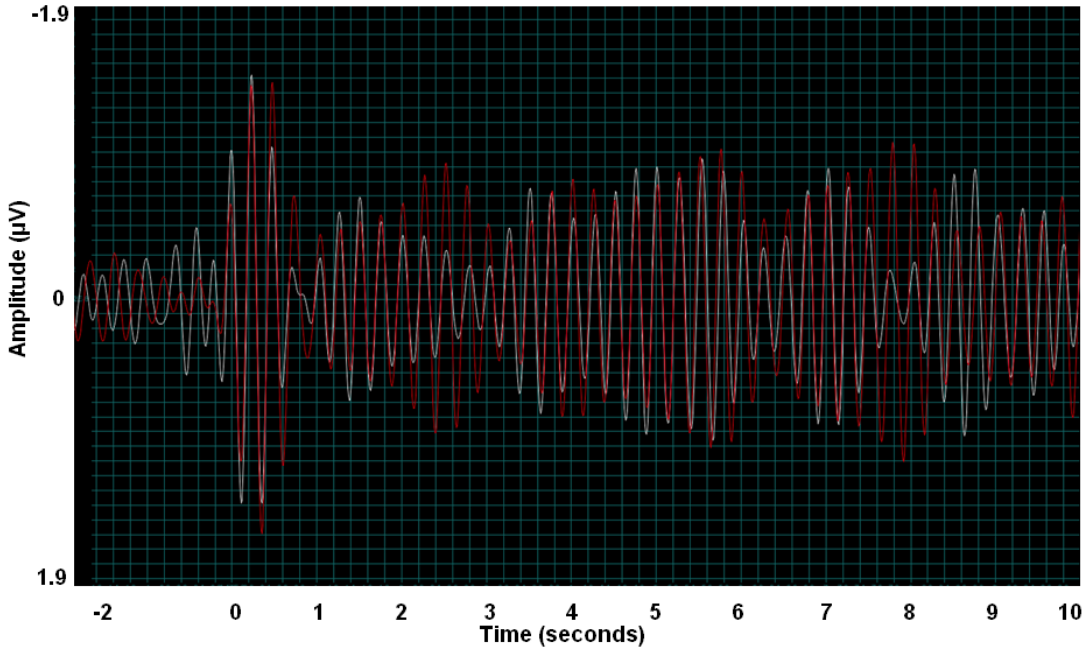


**Figure 3.24: The EEG signal is displayed between 2 s before the stimulation and 10 s after for both conditions in electrode P8** - Note how right after the beginning of the stimulation there is an amplitude increase for both conditions.

In order to determine whether the observed initial amplitude increase corresponded to the N170 transient component, the narrow band filtered data was plotted from 1 s before the stimulation to 1 s after for the electrode where such voltage change was maximal in the different faces condition, PPO10h. Figure 3.25 clearly shows that a positive deflection around 150 ms is followed by a negative deflection around 200 s which closely resembled the P1-N170 ERPs. Note that compared to the traditional latencies of these components, both responses are delayed by about 60 ms. This is not surprising because for a facial stimuli whose presentation is modulated sinusoidally at 4 Hz, it takes about 125 ms to be fully displayed on the screen.

### 3.2.4 Discussion

Our results confirmed that faces in general are able to elicit a brain response at a frequency identical to the stimulus presentation rate and that the magnitude of that response is highest when the identity of the face is varied compared to when it remains

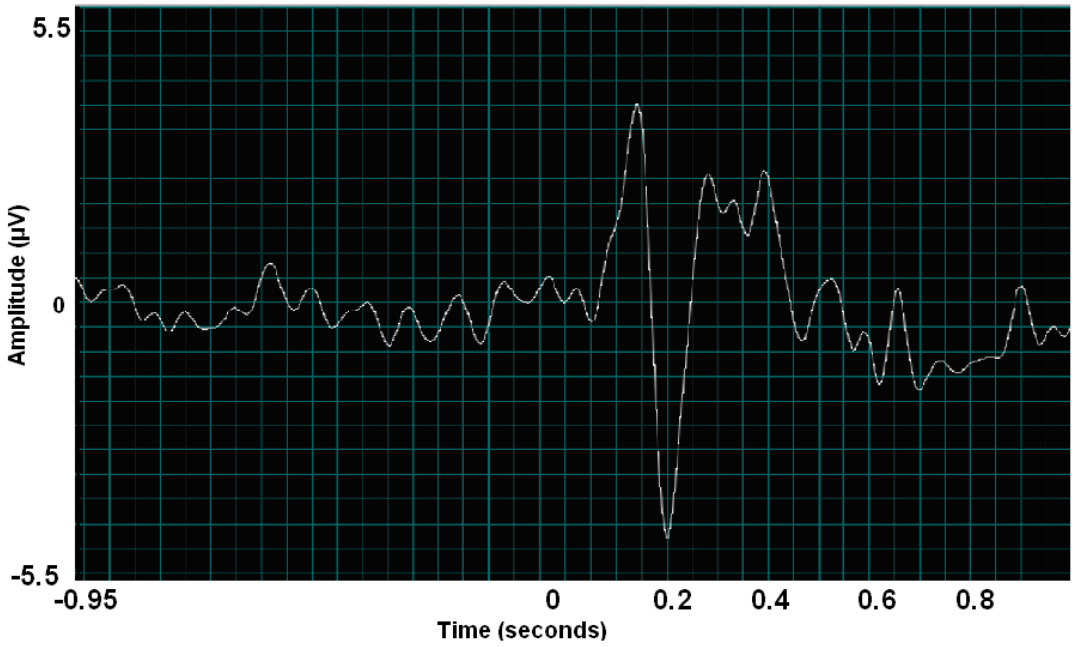


**Figure 3.25: Changes in the EEG signal across time in response to different faces** - The EEG signal is displayed between 1 s before the stimulation and 1 s after for the different faces condition in electrode PPO10h. Note the positive and negative deflections that appeared right after the beginning of the stimulation.

unchanged. Our results extended previous studies in two aspects: by characterizing this phenomenon in the time domain and showing that it appears for faces that diverge in several dimensions such as gender, presence of skin color and hair.

Regarding the first aspect, the characterization of the SSVEP sensitivity to facial identity in the time domain, our results showed that shortly after the beginning of the stimulation a transient response was elicited. This transient response included two of the strongest and earliest visual ERPs, the P1 and the N170, which appeared with a latency delay caused by the time it took for the sinusoidally modulated visual stimuli to be fully displayed on the screen (around 125 ms for a frequency stimulation of 4.00 Hz). The frequency content of these transient responses was diffusely distributed between 3.00 and 14.00 Hz. A few seconds after the appearance of the P1-N170 complex, a steady state response, characterized by an increase in the magnitude of the signal exactly at the stimulation frequency, was evident. This steady state response lasted during the whole stimulation period and its magnitude began to diverge between both experimental conditions when the first face that conveyed a different identity appeared. Taken together, these observations strongly support the sensitivity of the SSVEP to face identity.

Regarding the second aspect, the influence of certain facial features on the SSVEP response to face identity, our results showed that such sensitivity did not depend on particular features of the face image. On the contrary, it appears for faces that diverge in gender, skin color or presence of hair. However, two particular observations need further discussion.

First, it was observed that the SSFRE elicited by KDEF faces at 5.88 Hz was higher than the SSFRE elicited by the remaining stimuli. The KDEF faces were the only ones that included all face features, the internal ones and the external ones, even hair arranged according to each face bearer personal style. Our results suggest that the presence of these additional features aided identity discrimination leading to an increase in the magnitude of the SSVEP for different faces. This suggestion is in line with previous behavioral (Ellis *et al.*, 1979; O'Donnell & Bruce, 2001; Sinha & Poggio, 1996, 2002; Young *et al.*, 1985) and fMRI studies (Andrews *et al.*, 2010; Axelrod & Yovel, 2010; Betts & Wilson, 2010) showing that both internal and external features are used by the perceiver to identify unfamiliar faces. fMRI studies have further demonstrated that the fusiform face area (FFA), a structure that is part of the face perception anatomical network (Haxby *et al.*, 2000), is sensitive not only to the internal and external face features separately but also to their reciprocal influence suggesting that both types of cues are used to build up a holistic face representation that finally tributes to the discrimination of the face identity (Axelrod & Yovel, 2010).

Second, it was observed that the SSFRE elicited by female faces was significantly smaller for the left hemisphere ROI. This result is difficult to interpret not only consid-

ering the present study, which was not designed to detect inter-hemispheric differences in the identification of female and male faces, but also considering the state of the literature. There are few studies that have reported a slight bias in favor of the female face in the right hemisphere compared to the left hemisphere. For example, one study reported a slight advantage for classifying female faces presented tachistoscopically in the left visual field, and thus preferentially processed in the brain right hemisphere (Rhodes, 1985). Another study using chimeric faces composed by one male and one female halves reported that face halves presented in the left visual hemifield are preferred when subjects have to determine the gender of female faces (Parente & Tommasi, 2008). However, the evidence is not conclusive and it is not clear why there would be an inter-hemispheric difference in brain activation when confronting faces of different gender. Future studies need to be designed to clarify this issue.

Summarizing, by showing the sensitivity of the SSVEP to facial identity and demonstrating that it can be extrapolated to different types of faces, our results confirmed the usefulness of the SSVEP as a tool to investigate the neural coding of individual faces and high-level visual representations in general.

## 3.3 Study 3: Defining the fundamental stimulation frequency for individual face perception

*Esther Alonso Prieto*[1] *and Bruno Rossion*[1]
[1] Université catholique de Louvain, Louvain-la-Neuve, Belgium
(This article is in preparation)

**Abstract**

Recent studies have shown that EEG power at a constant frequency of stimulation (3.5 Hz) is much larger when different individual faces are presented compared to when the same face is presented repeatedly (Rossion & Boremanse, 2011) and that this effect can be extrapolated to different types of faces (see Study 2 in this thesis). Here, we defined the stimulation frequency ranges that are optimal to provoke this effect. Four observers were submitted to 84 s sequences of faces presented at different rates (1 Hz to 16 Hz or faces/second) while high-density EEG (128 channels) was recorded. Fast-Fourier Transform (FFT) of EEG and computation of signal-to-noise ratio (SNR) showed a larger response to different faces than identical faces between 4.00 and 9.09 Hz on occipito-temporal sites. In three observers, this difference increased gradually from 3.03 to 5.88 Hz, peaked at 5.88 Hz and decreased from 5.88 to 9.09 Hz. In one observer the peak of maximal difference was at 4.00 Hz although it was at 5.88 Hz over the left hemisphere. These observations indicate that individual faces are best discriminated

perceptually when the face is presented at 5.88 Hz. Such a fundamental frequency rate should be used by future studies that aim at tagging the sensitivity to individual faces in the human brain. Interestingly, at 5.88 Hz it takes 160 ms for the sinusoidal stimulation to complete a full cycle, and this time value coincides with the latency of the earliest face identity adaptation effect as found on the face-sensitive N170 component after flash stimulation. Hence, while the exact nature of the relation between the N170 and the phenomenon reported here in the frequency domain is still to be determined, our results support the view that the human brain requires about 160 ms to process individual facial information efficiently.

**keywords: Face perception, SSVEP, N170, identity adaptation, EEG**

### 3.3.1 Introduction

The presentation of a rhythmic stimulus elicits a brain response that remains constant in amplitude and phase throughout all the stimulation period and can be decomposed into sinusoids at the stimulation frequency and its multiple, harmonic frequencies. When obtained in response to a visual stimulation, this response is called steady state visual evoked potential (SSVEP) (Regan, 1966, 1989, 2009).

SSVEPs have distinct advantages for the study of brain processes as response magnitudes, and signal-to-noise ratios (SNRs) can be measured objectively (Regan, 1989). As a result, they have proven to be useful to investigate brain mechanisms involved in the analysis of low level properties of the visual stimuli (Ales & Norcia, 2009; Braddick *et al.*, 1986; Campbell & Maffei, 1970; Heinrich & Bach, 2003; Tyler & Kaitz, 1977), spatial and selective attention (Andersen *et al.*, 2009; Morgan *et al.*, 1996), and figure−ground segregation (Appelbaum *et al.*, 2006, 2008).

They have also been used to demonstrate how the brain response is influenced by variations in the affective content of pictures (Keil *et al.*, 2003), object familiarity (Kaspar *et al.*, 2010), and facial expression (Mayes *et al.*, 2009).

Recently, it has been proposed that SSVEP technique can also be useful to investigate how individual faces are coded in the human brain. To support such suggestion, the SSVEP sensitivity to facial identity was demonstrated ((Rossion & Boremanse, 2011), and see also Study 2 in this thesis).

However, the steady state response does not change monotonously with changing stimulus frequency but exhibits clear peaks around 10 Hz and local maxima around 20, 40 and 80 Hz, (Herrmann, 2001; Regan, 1968a, 1989; Van der Tweel & Lunel, 1965). That is why researchers who use SSVEP to study cognition usually try to employ these frequencies for the stimulation in order to guarantee the largest responses. Given that the previous studies which have demonstrated the reliability of the SSVEP technique to study face individualization processes used a few stimulation frequencies (3.5 Hz in

the case of Rossion & Boremanse (2011), 4.00 and 5.88 Hz in the case of Study 2 in this thesis) the question of whether the brain steady state response to individual faces varies as a function of stimulation frequency remains undetermined. Answering this question is one of the goals of the current study.

We hypothesize that the steady state response to individual faces will differ as a function of the stimulus presentation temporal rate. The highest steady state response will be obtained for frequencies that prevent the temporal scatter or the interference between neuronal discharges in response to consecutive stimuli leading to better synchronization of afferent volleys, better summation of postsynaptic potentials and, therefore, higher amplitude of the signal detected by the scalp EEG.

The frequencies that have better chances to cause such a temporal organization of cellular discharges might be those that coincide with the temporal activation cycle of the neuronal assembly specialized in processing the rhythmic visual input and, specifically, the experimental manipulations implemented to such input, i.e., changes to face identity. Evidence suggests that the temporal activation cycle of the face processing system, from the retina to the temporal cortex, ranges between 100 and 250 ms (corresponding to frequencies between 4 and 10 Hz). Thus, face selective responses can be recorded intracranially from the monkey brain as early as 80-100 ms after stimulus onset (Perrett *et al.*, 1982) and from the human brain around 200 ms (Allison *et al.*, 1999; McCarthy *et al.*, 1999; Puce *et al.*, 1999). Scalp recordings in humans have demonstrated that the first and most reliable face selective response occurs at the time of the N170 event related potential, between 120 and 190 ms (Bentin *et al.*, 1996; Boetzel *et al.*, 1995; Jacques *et al.*, 2007; Rossion & Caharel, 2011). Following the N170, a second face sensitive response can be registered also on the scalp, the N250, which has been associated with the extraction of information about facial shape and skin color to process further the identity of the face bearer (Caharel *et al.*, 2009b).

To fulfill the goals of this study, an experiment was designed in which the electroencephalographic activity of healthy participants was recorded while they viewed faces that were flickering at different frequencies (between 1 and 16.66 Hz). In one condition, the same face was presented during the whole trial while in the other condition different faces were presented. We expected to observe a consistent reduction in the magnitude of the brain response for the identical faces condition compared to different faces condition. This could be interpreted as an index of the sensitivity of the system to face identity changes. We also expected this difference to be highest for stimulation frequencies ranging between 4 and 10 Hz.

## 3.3.2 Materials and methods

### 3.3.2.1 Participants

Four healthy adult participants (age 28, 30, 35, 36 years), all males, right handed with normal or corrected-to-normal vision took part in the experiment after providing their written informed consent.

### 3.3.2.2 Stimuli

Eighteen full front pictures of male faces selected from a large database of laser-scanned faces (Max Planck Institute), widely used in many previous studies of face processing (e.g., Leopold *et al.* (2005); O'Toole *et al.* (1999)), (Figure 3.26). They were equalized in luminance and superimposed on a light grey background.

### 3.3.2.3 Experimental procedure, EEG recording and analysis

The procedure employed in this study to implement the experiment and record the EEG data was identical to that used in Study 2. The reader is remitted to Section 3.2.2.3.

In contrast to Study 2, here the facial stimuli were presented at fundamental frequencies (f): 1.00, 2.00, 3.03, 4.00, 5.00, 5.88, 7.14, 8.33, 9.09, 10.00, 11.11, 12.48, 14.28 and 16.66Hz. Those rates were chosen from frequencies between 1 and 17 Hz that could be accurately displayed by the stimulation display, which had 100 Hz refresh rate. Additionally, subjects were tested four times at different days.

Regarding the analysis of the EEG data, here only the FFT analysis was performed using an analysis window of 64 s (temporal resolution = 0.015625 Hz). On this data, the signal-to-noise ratio (SNR) index was calculated and in order to determine how the stimulus manipulations influence the process of detecting changes in its identity, the SNR based FFT amplitude values were averaged across all subjects and then both conditions were subtracted (different face condition − identical face condition) for each electrode separately to obtain the *Steady State Face Repetition Effect* or SSFRE index. To remind the reader, a positive SSFRE indicates that the SNR was highest for the different face condition. This index was plotted on the scalp for each stimulation frequency using a SSFRE by frequency scale adjusted according to the electrode that exhibited the highest SSFRE at that particular stimulation frequency. Based on these maps, regions of interest (ROIs) were determined. Such ROIs included neighboring electrodes that showed the highest SSFRE. The SSFRE for each of these ROIs was calculated for each participant and plotted as a function of frequency together with standard errors, which were calculated across repetitions of the experiment. In this way, the SSVEP frequency tuning curve was characterized for each individual participant.

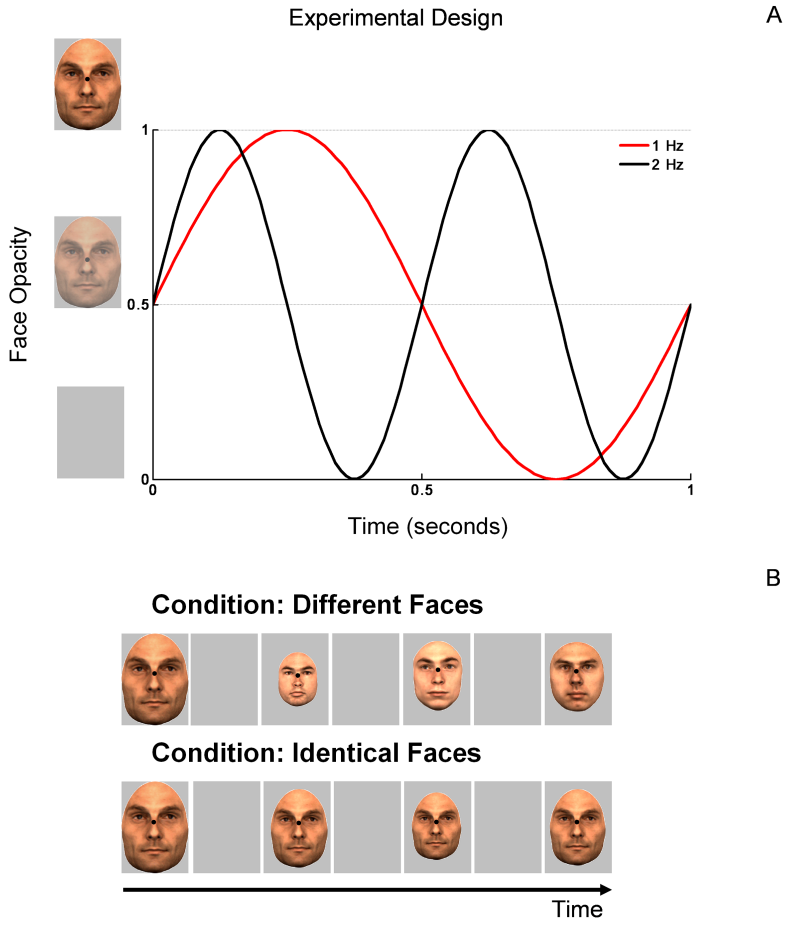


**Figure 3.26: Schematic view of the experiment applied in Study 3** - (A) Stimulus generation: Full front pictures of faces were presented using a sinusoidal modulation. The beginning of the 90 s sequence was always the gray background. The lower contrast face stimulus in the midline, in between the background and the full face stimulus, represents an intermediary stage of stimulation at the onset of the face stimulus. (B) The two experimental conditions used in the study, different face condition and identical face condition. Note that there were large changes of size between each face picture to minimize low-level adaptation effects.

### 3.3.3 Results

#### 3.3.3.1 Behavior

As in Study 2, participants detected accurately the color changes (95-100% correct responses), without differences in amount of correct responses and reaction times between conditions.

#### 3.3.3.2 Entrainment of the scalp signal to the stimulation frequency

As it can be seen in Figures 3.27, 3.28, 3.29, 3.30 and 3.31 the data averaged over all subjects showed that repetitive presentation of either identical or different faces, provoked an FFT power increase at each of the fundamental stimulus frequencies (f) compared to the neighboring frequency components or bins. This result evidences that the brain signal was driven by the stimulus presentation rate irrespective of the particular stimulation frequency or experimental condition.

Similar results were obtained for the SNR calculated using the FFT amplitude values instead of power (Figures 3.32, 3.33, 3.34, 3.35 and 3.36). Note that the use of the SNR index instead of FFT power counteracted the influence of noise in the data and stood out the signal increase at the stimulation frequencies.

Figures 3.32, 3.33, 3.34, 3.35 and 3.36 also show that for both conditions there were additional peaks which occurred at frequencies multiple of the stimulation or fundamental frequency f (e.g., 2f, 3f ... nf). For a fundamental frequency f = 1.00 Hz, these additional peaks were observed for harmonics 2f to 10f. For f = 2.00 Hz, they were observed for 2f to 6f. For f = 3.03 Hz and f = 4.00 Hz they were present at 2f, 3f and 4f. For all remaining frequencies except f = 5.88 Hz and f = 10.00 Hz additional SNR peaks appeared only at 2f. For f = 5.88 Hz and f = 10.00 Hz they appeared at 2f and 3f although the 3f peak was of small magnitude.

#### 3.3.3.3 SSFRE at the fundamental frequency

The grand averaged SSFRE calculated using the SNR values was plotted on the scalp and scaled to a minimum value of SNR = 0 to determine the frequencies and scalp regions where the different face condition caused a brain signal increase compared to the identical face condition. As it is evident in Figure 3.37, at 1.00 and 2.00 Hz the SSFRE was negative at all electrodes, except for isolated central electrodes at 2.00 Hz. At 3.03 Hz, the topographical distribution of the SSFRE focused over particular right hemisphere electrodes in the occipito-temporal region and over central electrodes. At 4.00 Hz, additional electrodes in the occipito-temporal region of the left hemisphere also showed a positive effect. This topographical distribution, positive values over bilateral occipito-temporal electrodes with a right hemisphere dominance together with smaller

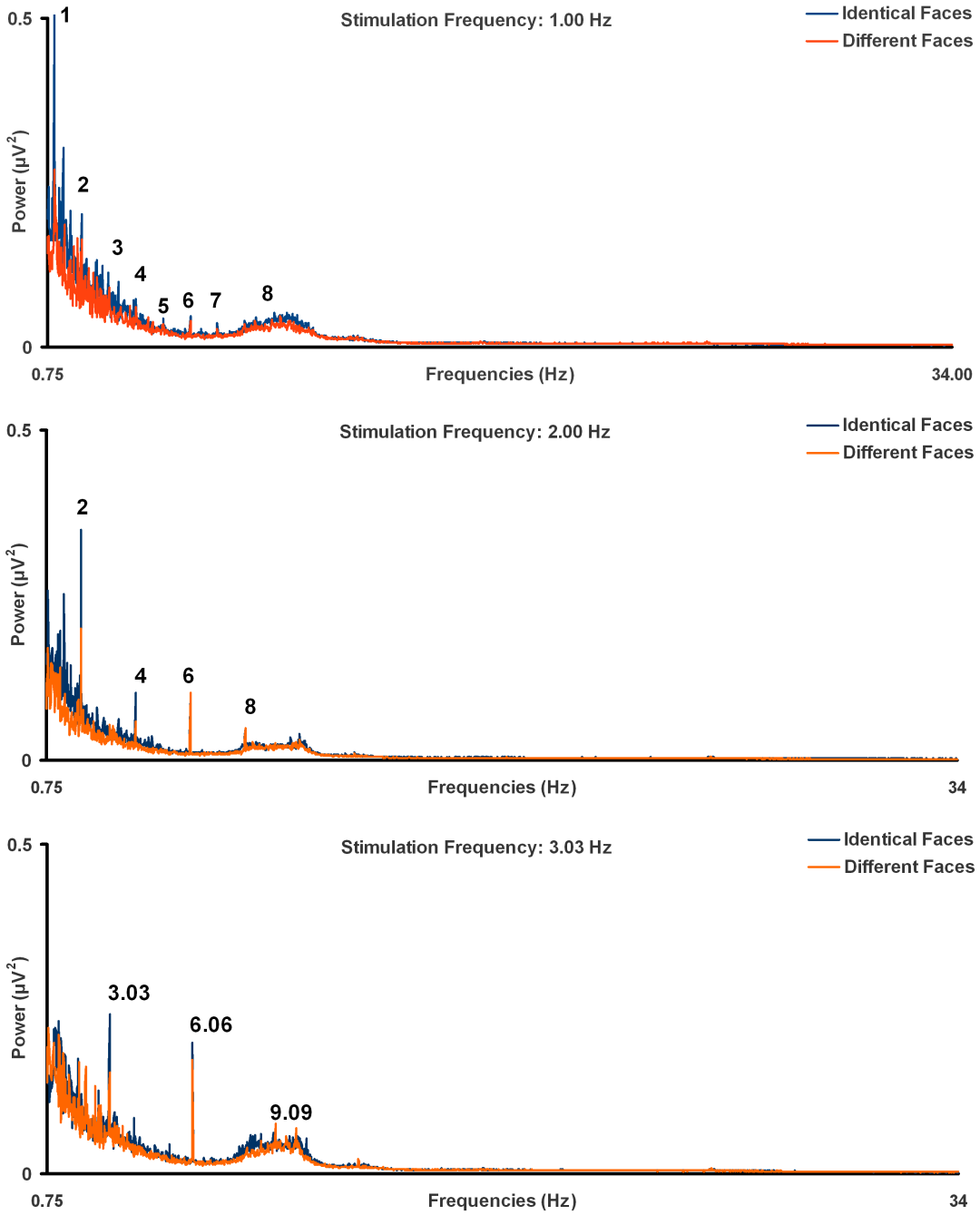


**Figure 3.27:** FFT power spectrum: 1.00 to 3.03 Hz

For stimulation frequencies 1.00, 2.00 and 3.03 Hz, the FFT power spectrum averaged across subjects, sessions and electrodes is displayed for all frequency bins until 34 Hz. Both experimental conditions, identical and different faces, are represented. Figures 3.28, 3.29, 3.30 and 3.31 present the power spectrum corresponding to the remaining stimulation frequencies.

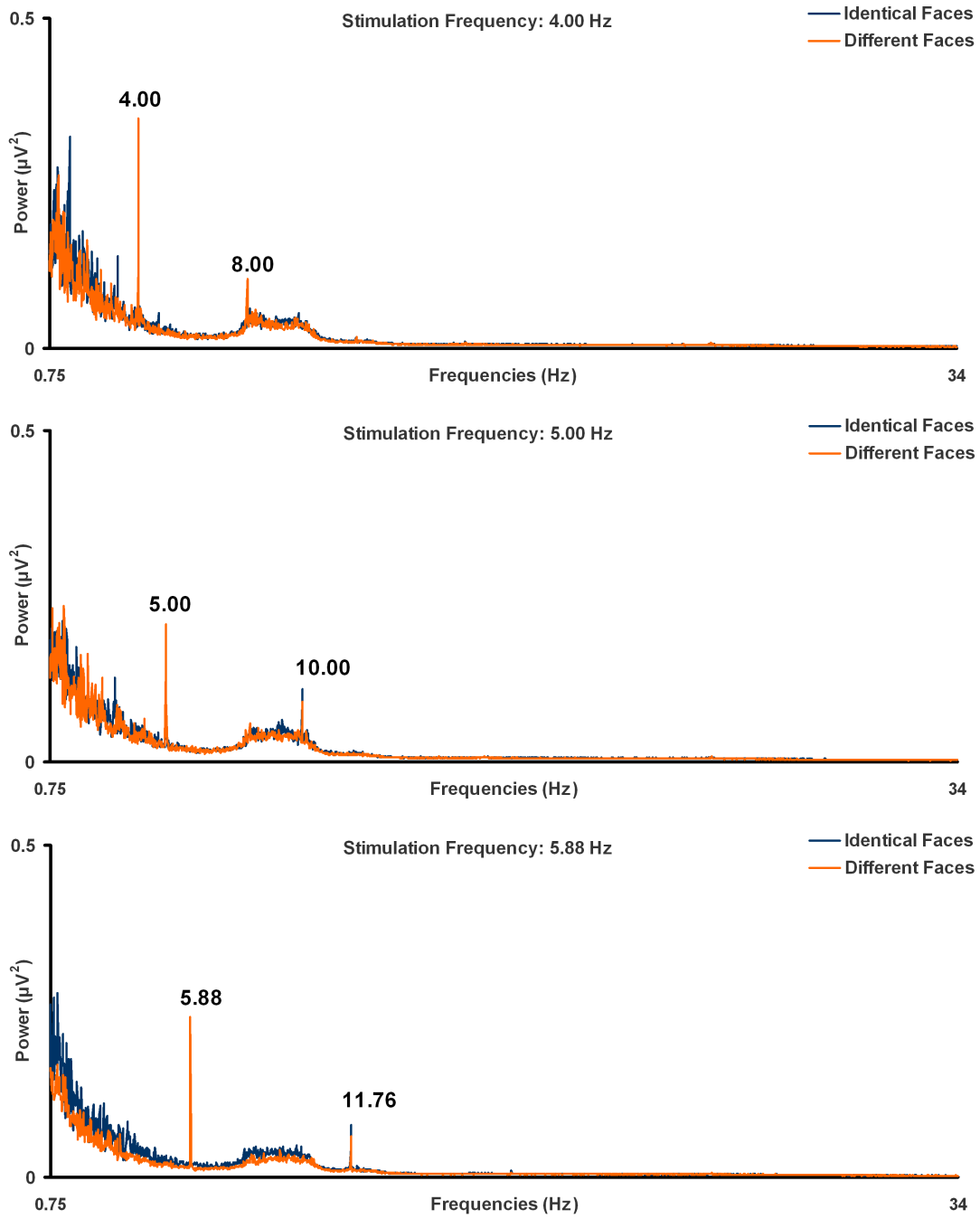


**Figure 3.28:** FFT power spectrum: 4.00 to 5.88 Hz

For stimulation frequencies 4.00, 5.00 and 5.88 Hz, the FFT power spectrum averaged across subjects, sessions and electrodes is displayed for all frequency bins until 34 Hz. Both experimental conditions, identical and different faces, are represented. Figures 3.27, 3.29, 3.30 and 3.31 present the power spectrum corresponding to the remaining stimulation frequencies.

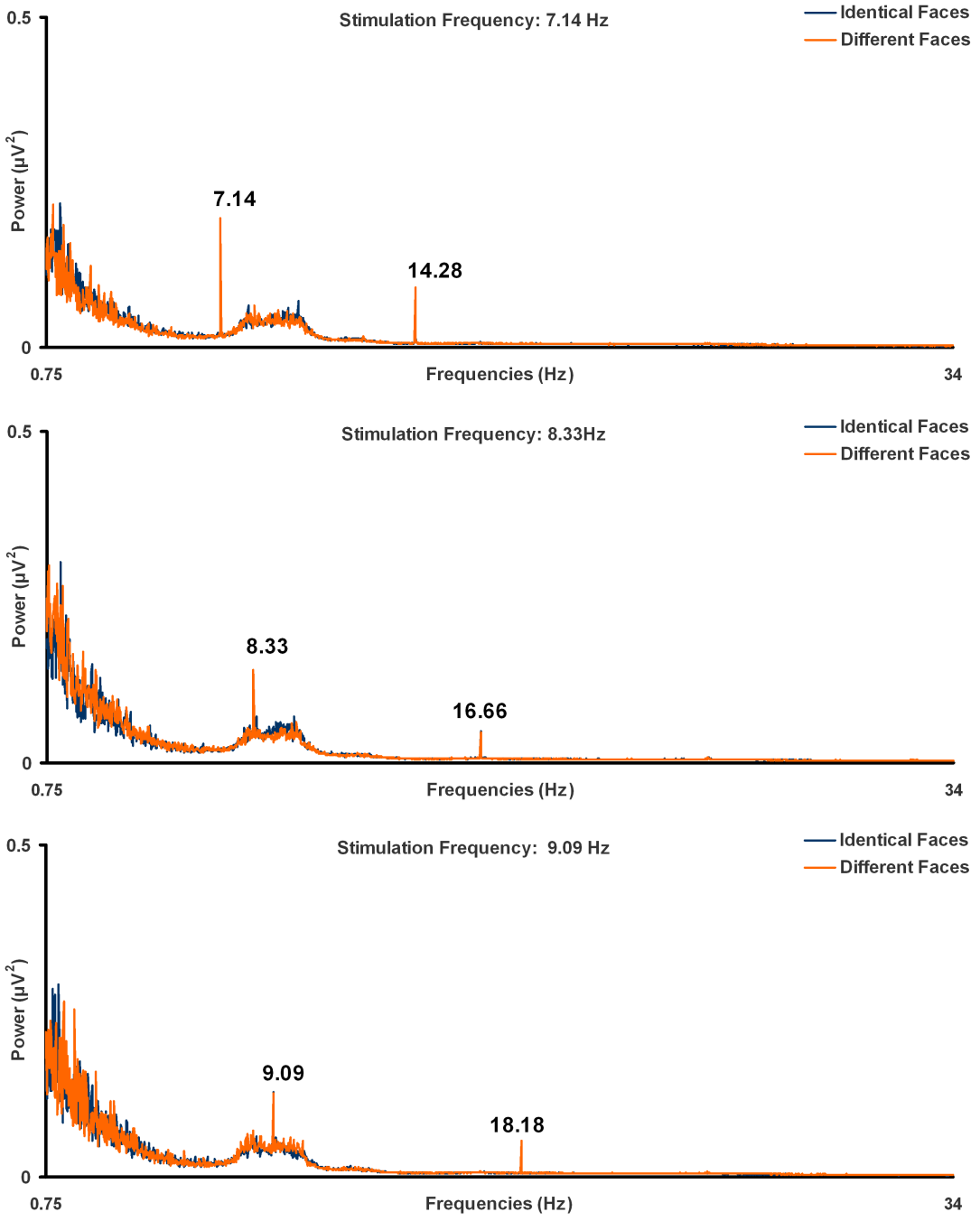


**Figure 3.29:** FFT power spectrum: 7.14 to 9.09 Hz

For stimulation frequencies 7.14, 8.32 and 9.09 Hz, the FFT power spectrum averaged across subjects, sessions and electrodes is displayed for all frequency bins until 34 Hz. Both experimental conditions, identical and different faces, are represented. Figures 3.27, 3.28, 3.30 and 3.31 present the power spectrum corresponding to the remaining stimulation frequencies.

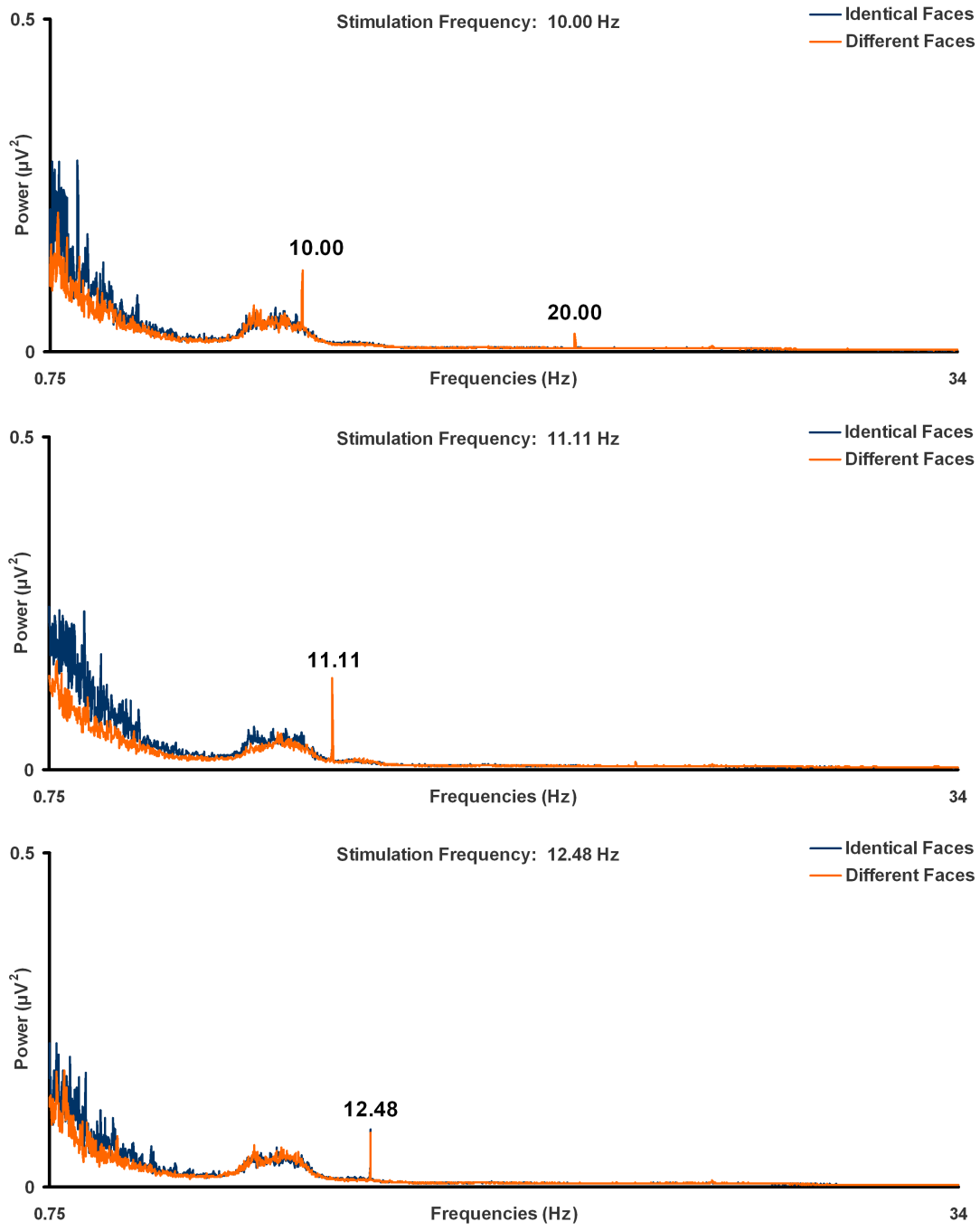


**Figure 3.30:** FFT power spectrum: 10.00 to 12.48 Hz

For stimulation frequencies 10.00, 11.11 and 12.48 Hz, the FFT power spectrum averaged across subjects, sessions and electrodes is displayed for all frequency bins until 34 Hz. Both experimental conditions, identical and different faces, are represented. Figures 3.27, 3.28, 3.29 and 3.31 present the power spectrum corresponding to the remaining stimulation frequencies.

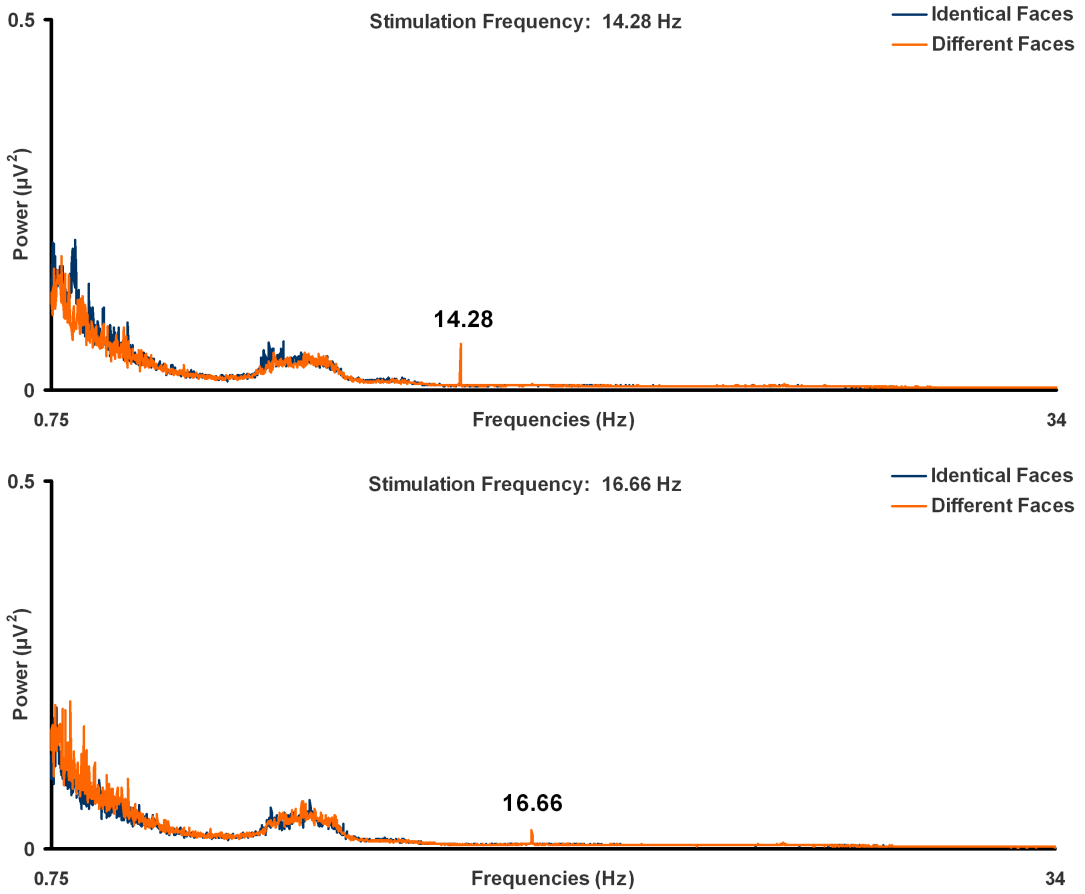


**Figure 3.31:** FFT power spectrum: 14.28 to 16.66 Hz

For stimulation frequencies 14.28 and 16.66 Hz, the FFT power spectrum averaged across subjects, sessions and electrodes is displayed for all frequency bins until 34 Hz. Both experimental conditions, identical and different faces, are represented. Figures 3.27, 3.28, 3.29 and 3.30 present the power spectrum corresponding to the remaining stimulation frequencies.

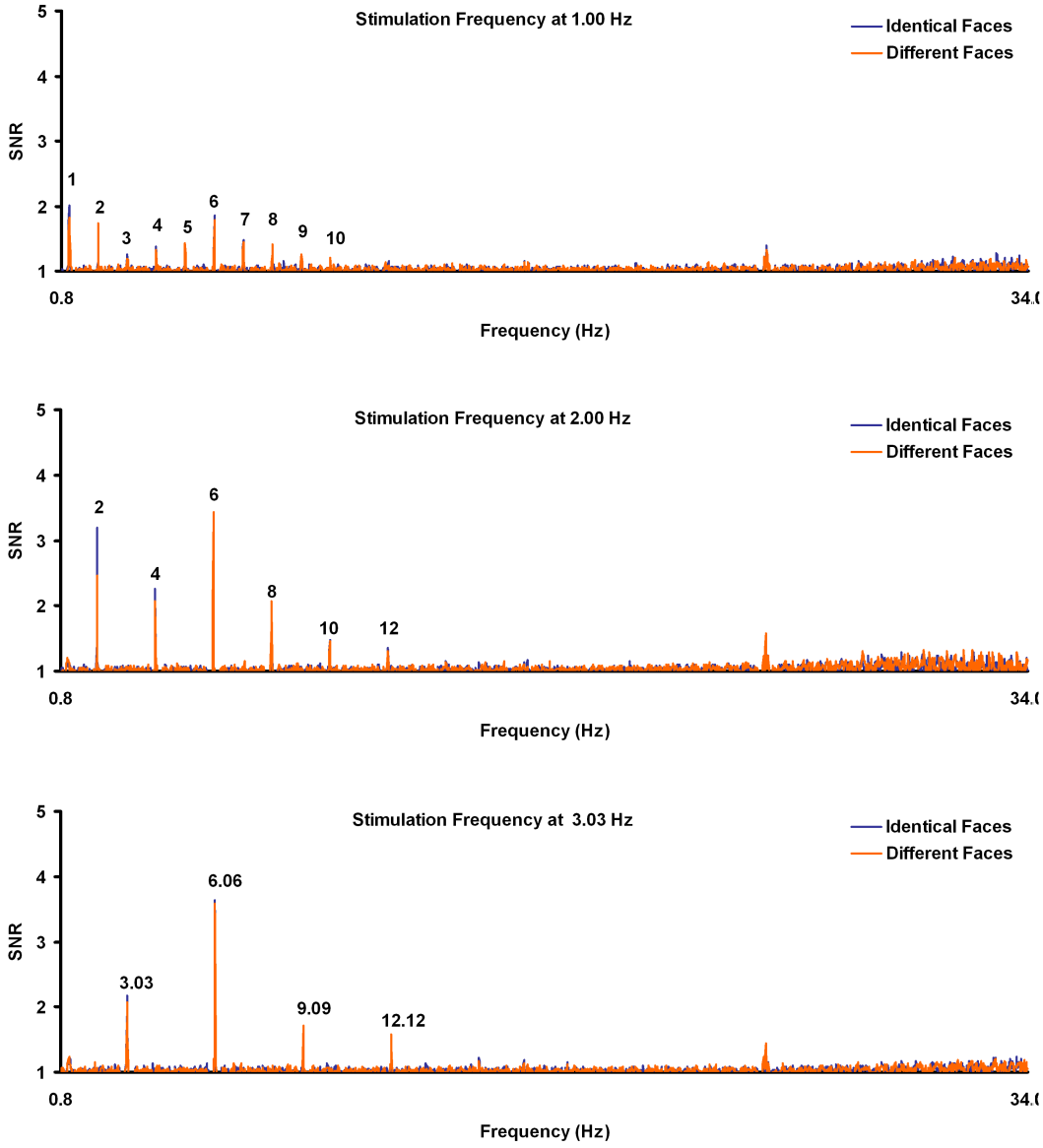


**Figure 3.32:** SNR for stimulation frequencies 1.00 to 3.03 Hz.

The SNR was calculated using the FFT amplitude values instead of power, averaged across subjects, sessions and electrodes and finally displayed for all frequency bins until 34 Hz. Both experimental conditions, identical and different faces, are represented. Figures 3.33, 3.34, 3.35 and 3.36 present the SNR corresponding to the remaining stimulation frequencies.

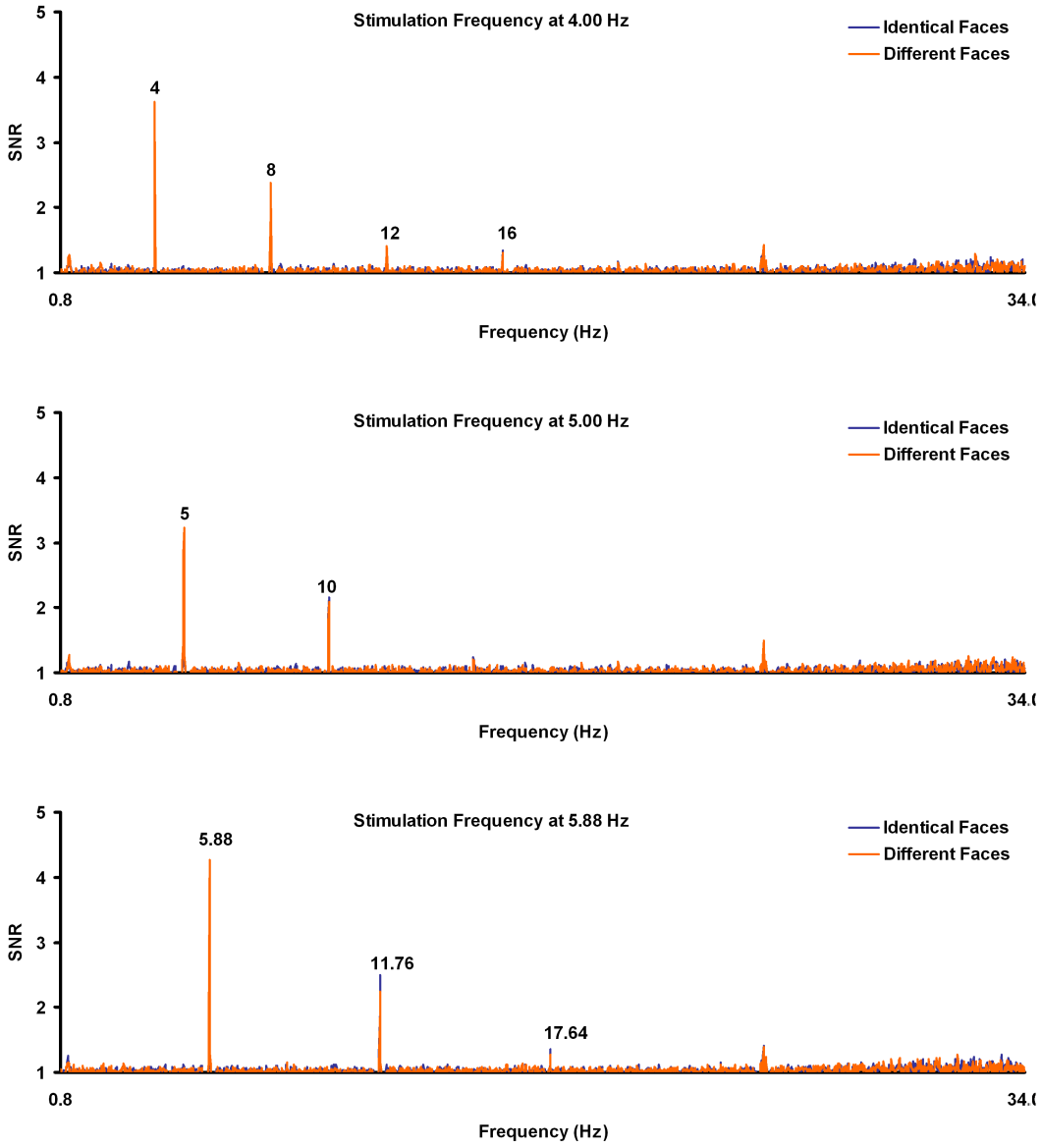


**Figure 3.33:** SNR for stimulation frequencies 4.00 to 5.88 Hz.

The SNR was calculated using the FFT amplitude values instead of power, averaged across subjects, sessions and electrodes and finally displayed for all frequency bins until 34 Hz. Both experimental conditions, identical and different faces, are represented. Figures 3.32, 3.34, 3.35 and 3.36 present the SNR corresponding to the remaining stimulation frequencies.

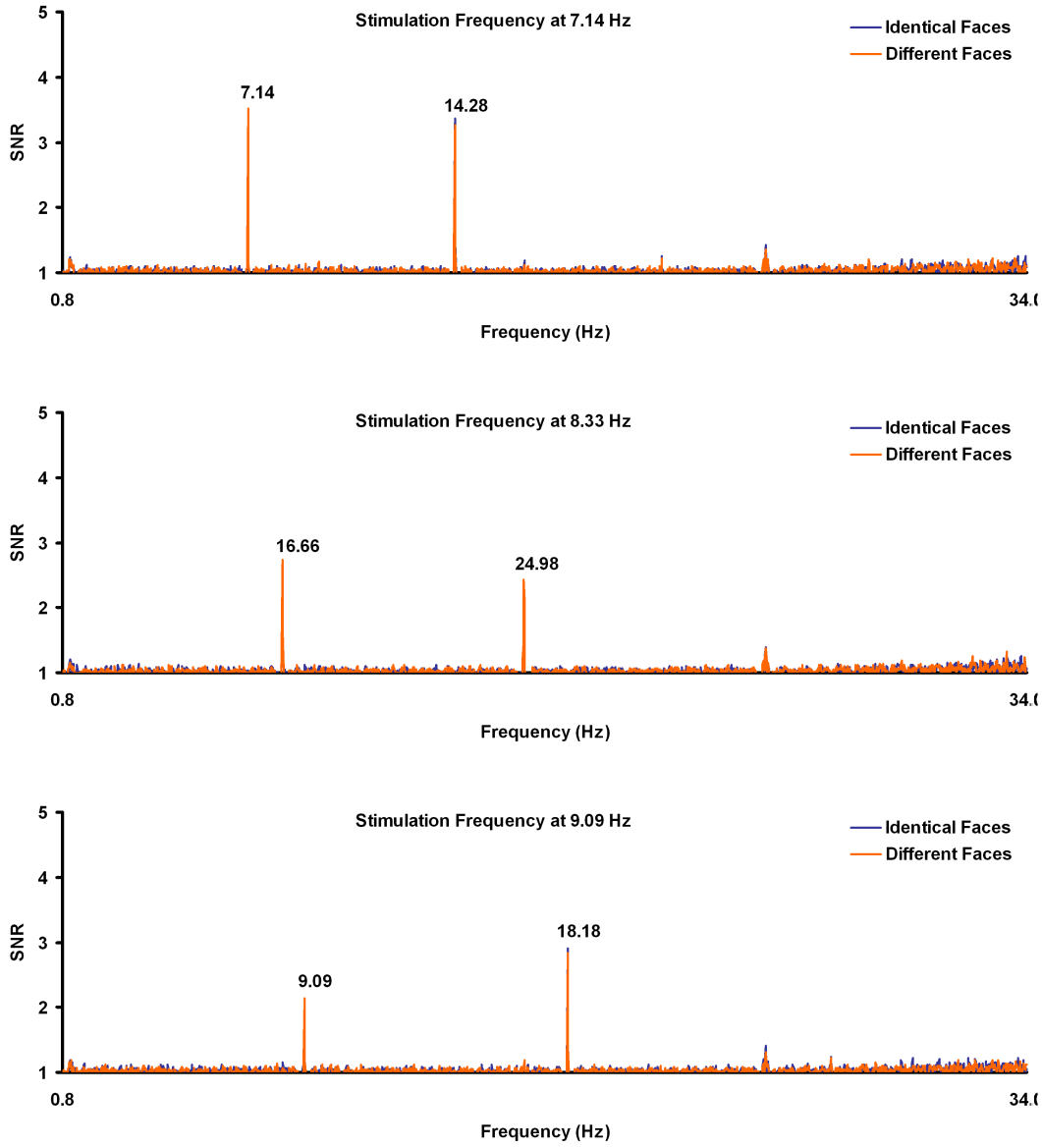


**Figure 3.34:** SNR for stimulation frequencies 7.14 to 9.09 Hz.

The SNR was calculated using the FFT amplitude values instead of power, averaged across subjects, sessions and electrodes and finally displayed for all frequency bins until 34 Hz. Both experimental conditions, identical and different faces, are represented. Figures 3.32, 3.33, 3.35 and 3.36 present the SNR corresponding to the remaining stimulation frequencies.

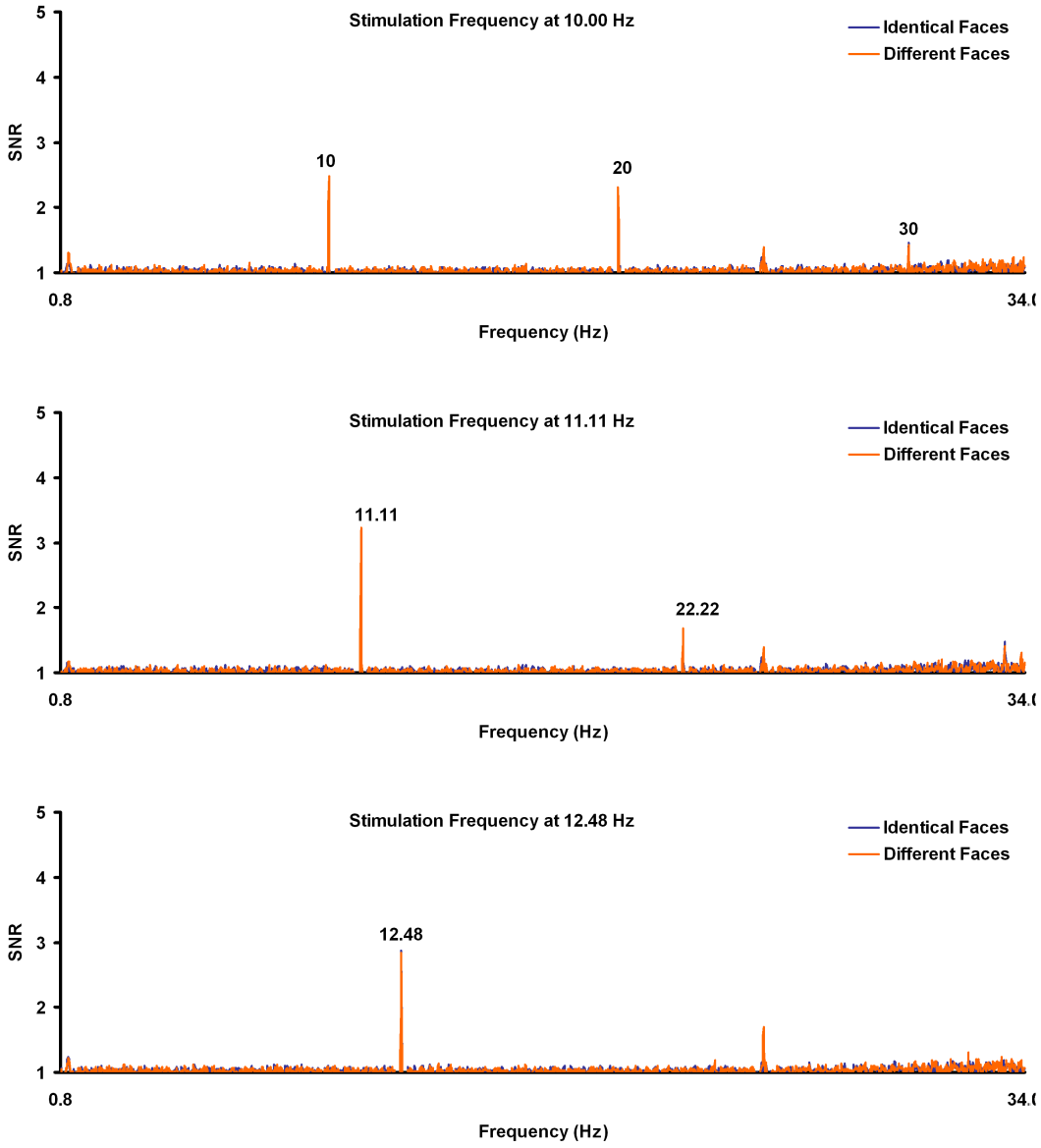


**Figure 3.35:** SNR for stimulation frequencies 10.00 to 12.48 Hz.

The SNR was calculated using the FFT amplitude values instead of power, averaged across subjects, sessions and electrodes and finally displayed for all frequency bins until 34 Hz. Both experimental conditions, identical and different faces, are represented. Figures 3.32, 3.33, 3.34 and 3.36 present the SNR corresponding to the remaining stimulation frequencies.

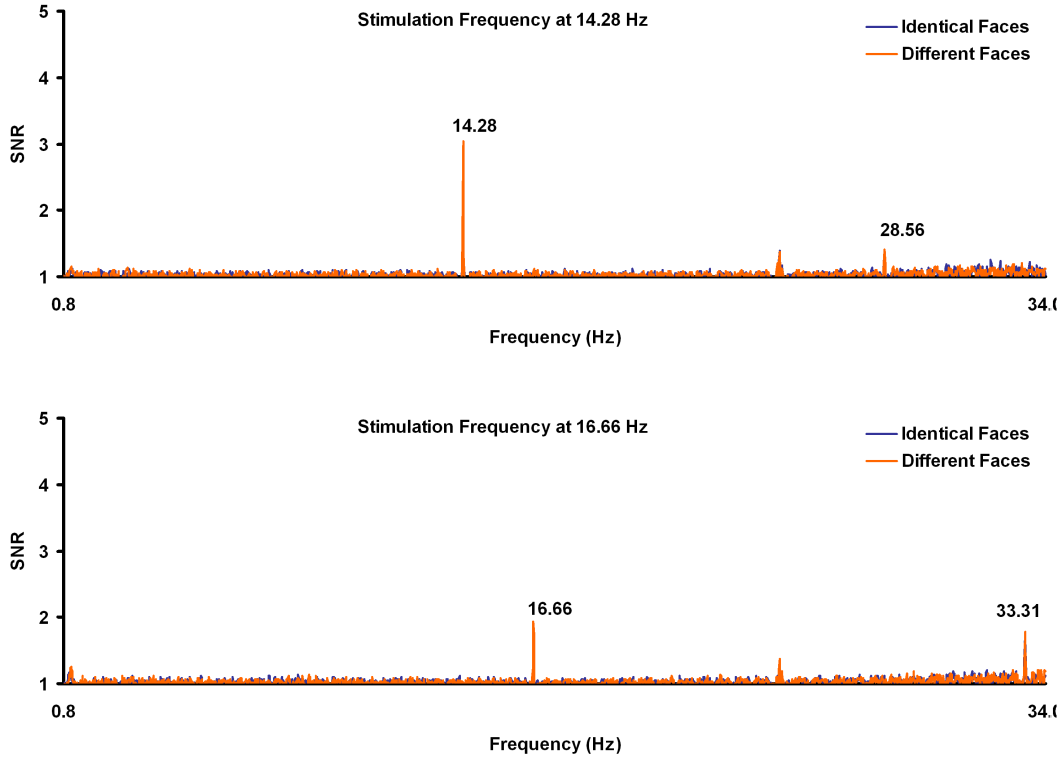


**Figure 3.36:** SNR for stimulation frequencies 14.28 to 16.66 Hz.

The SNR was calculated using the FFT amplitude values instead of power, averaged across subjects, sessions and electrodes and finally displayed for all frequency bins until 34 Hz. Both experimental conditions, identical and different faces, are represented. Figures 3.32, 3.33, 3.34 and 3.35 present the SNR corresponding to the remaining stimulation frequencies.

but still positive values in central electrodes characterized the SSFRE from 4.00 to 11.11 Hz. At 12.48 and 14.28 Hz, the SSFRE topograhical distribution changed and the highest SSFRE was observed over occipito-temporal electrodes of the left hemisphere. At 16.66 Hz, it was observed over the central occipital area.

Figure 3.37 also shows that the highest absolute SSFRE was obtained between 4.00 and 11.11 Hz. To give further support to this observation, all topographical maps were re-scaled to the highest SSFRE value obtained across frequencies, which was observed at 5.88 Hz (Figure 3.38). By doing so, it became evident that the characteristic topographic distribution, i.e., highest SSFRE over occipito-temporal electrodes with a right hemisphere dominance and over central electrodes, characterized the SSFRE at stimulation frequencies between 4.00 Hz and 11.11 Hz.

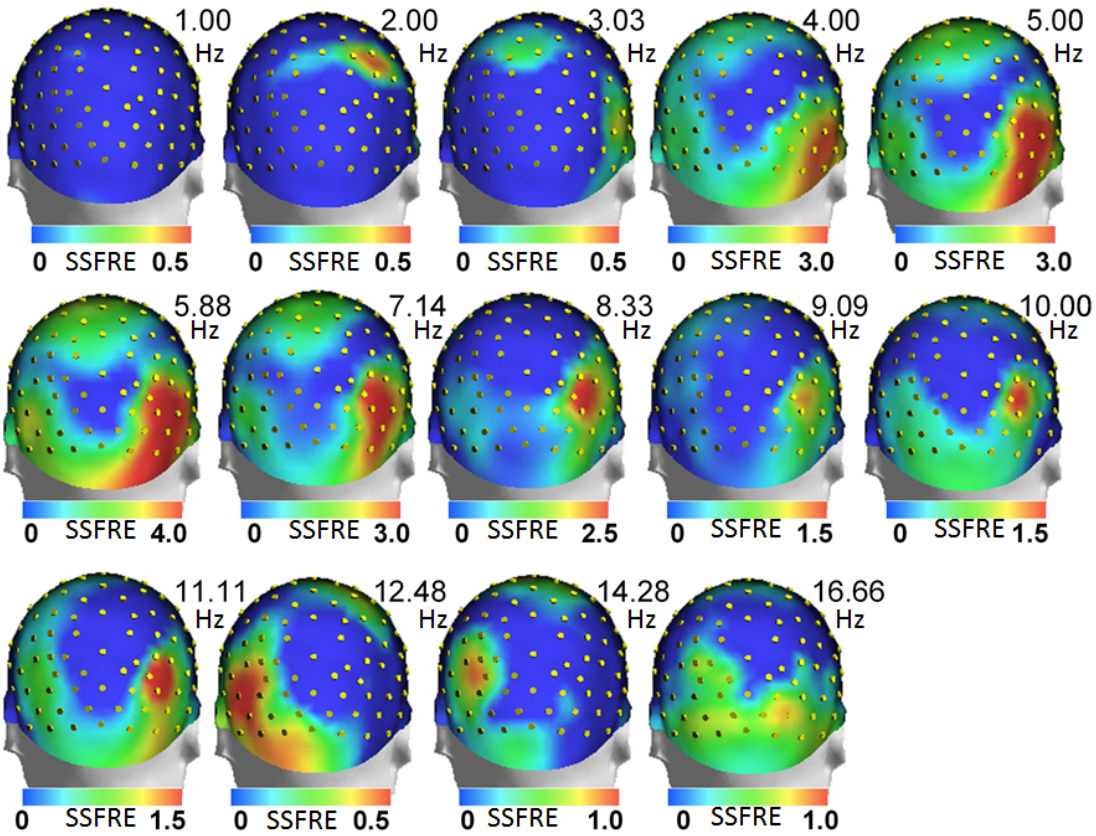


**Figure 3.37: SSFRE topographical distribution scaled for each frequency independently.** - For all stimulation frequencies, the SSFRE values were displayed on the scalp. Note that all maps are scaled according to the highest SSFRE value exhibited at that particular stimulation frequency.

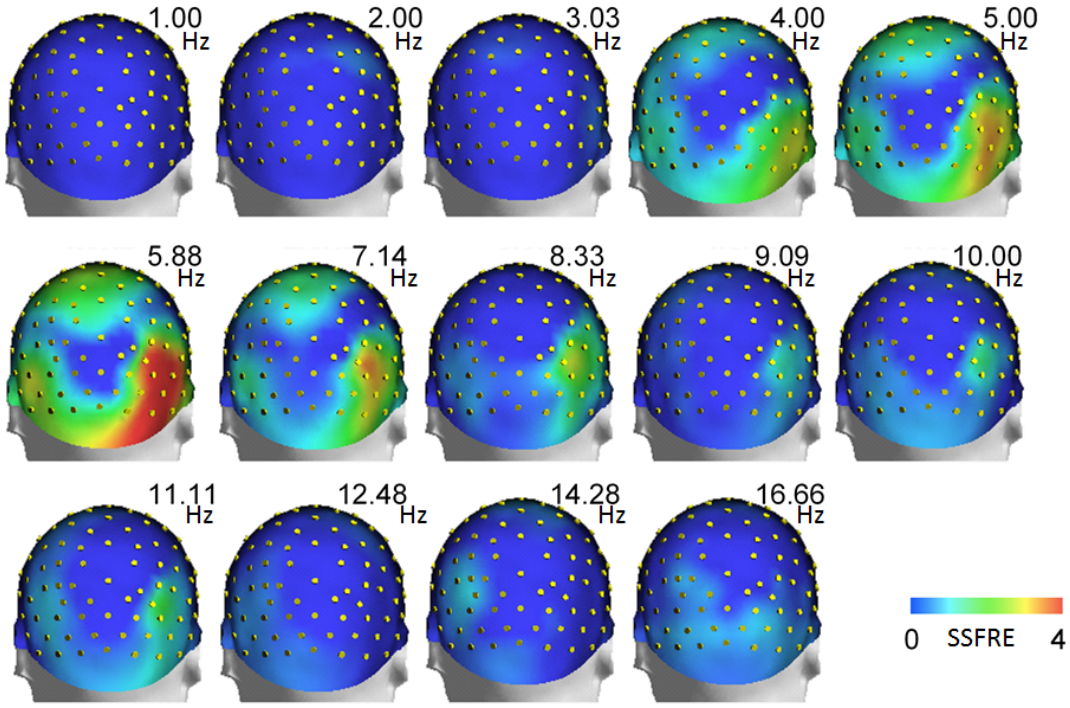


**Figure 3.38: SSFRE topographical distribution scaled according to the stimulation frequency that provoked the highest effect.** - For all stimulation frequencies, the SSFRE values were displayed on the scalp. Note that the scale corresponds to the stimulation frequency (5.88 Hz) that provoked the highest effect.

It also became evident that the magnitude of the effect increased steadily from 4.00 to 5.88 Hz, peaked at 5.88 Hz and decreased steadily from 7.14 to 11.11 Hz. The smallest and predominantly negative SSFRE appeared at 1.00 and 2.00 Hz while the smallest but positive SSFRE appeared between 12.48 and 16.66 Hz. In the last case, the SSFRE topographical distribution changed. Thus, a left hemisphere predominance was observed only at 12.48 and 14.28 Hz while the occipito-central distribution was observed only at 16.66Hz (Figure 3.38).

The occipito-temporal electrodes that exhibited the highest SSFRE values between 4.00 and 11.11 Hz were P8/P7, PO8/O7, PO10/O9 and PPO10h/9h (Figure 3.39).

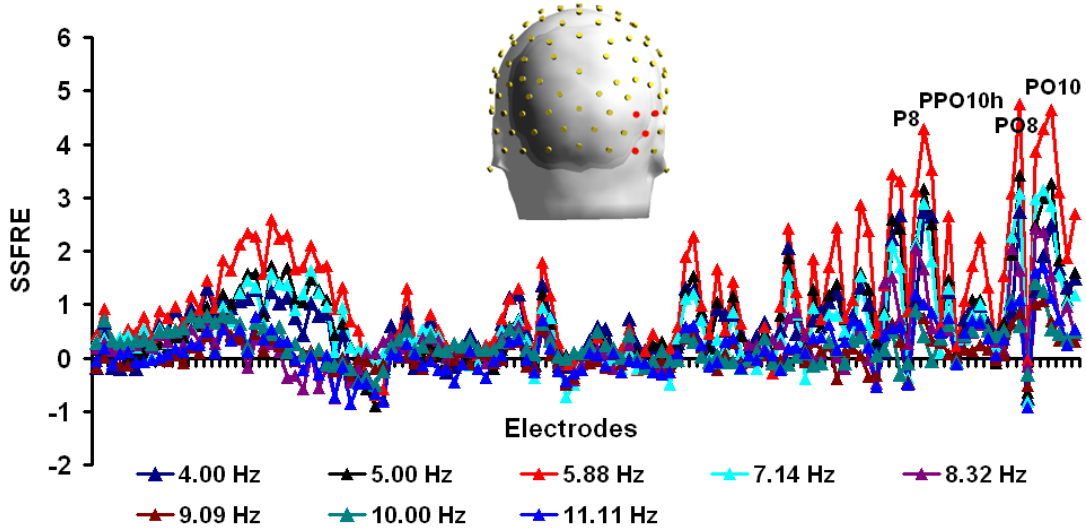


**Figure 3.39: SSFRE between 4 and 11.11 Hz for each electrode** - The SSFRE obtained between 4 and 11.11 Hz was plotted for each electrode separately. The electrodes that exhibited the highest effect are indicated and highlighted in red in a 3-D model of the electrodes distribution.

The level of entrainment to the stimulation frequency exhibited by these electrodes for both conditions separately is illustrated in Figures 3.40, 3.41, 3.42, 3.43 and 3.44. Note how in all cases the signal increased at the stimulation frequencies compared to the neighboring frequency bins.

The electrodes that exhibited the highest SSFRE were averaged for each hemisphere separately to form regions of interest (ROIs). Afterwards, the obtained ROI based SSFRE values were plotted as a function of stimulation frequency to illustrate the frequency sensitivity curve of the SSFRE. As it can be seen in Figure 3.47 the SSFRE frequency sensitivity curve is bell shaped around 5.88 Hz.

In order to demonstrate that the above described frequency sensitivity curve of the SSFRE was reproducible across, as well as, intra subjects, the ROIs were calculated for

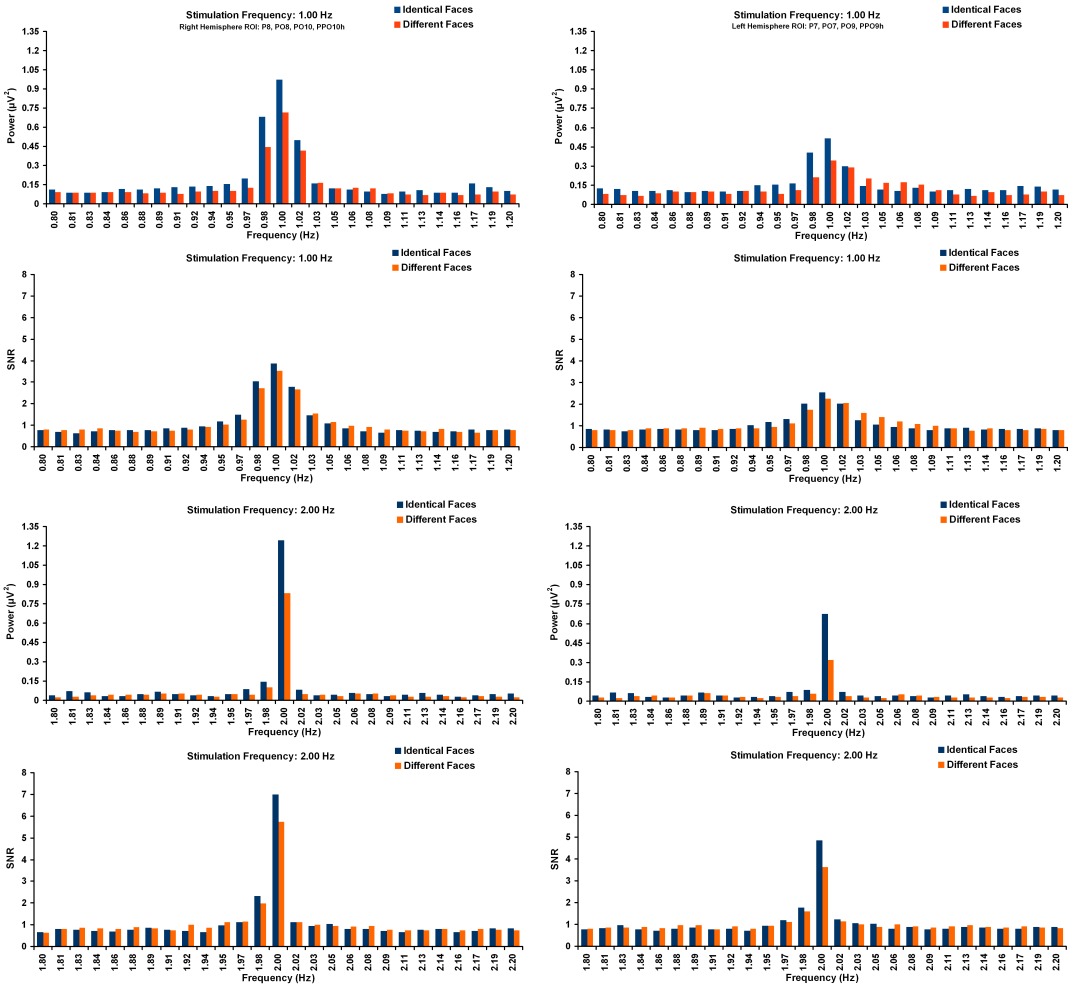


**Figure 3.40:** Entrainment to the stimulation frequency (1.00 and 2.00 Hz).

For stimulation frequencies 1.00 and 2.00 Hz the FFT power spectrum and SNR values averaged across subjects, sessions and electrodes P8/P7, PO8/O7, PO10/O9 and PPO10h/9h is displayed only for 26 frequency bins centered on the corresponding stimulation frequencies. Both experimental conditions, identical and different faces are represented. Figures 3.41, 3.42, 3.43, 3.44, 3.45, 3.46 present the data corresponding to the remaining stimulation frequencies.

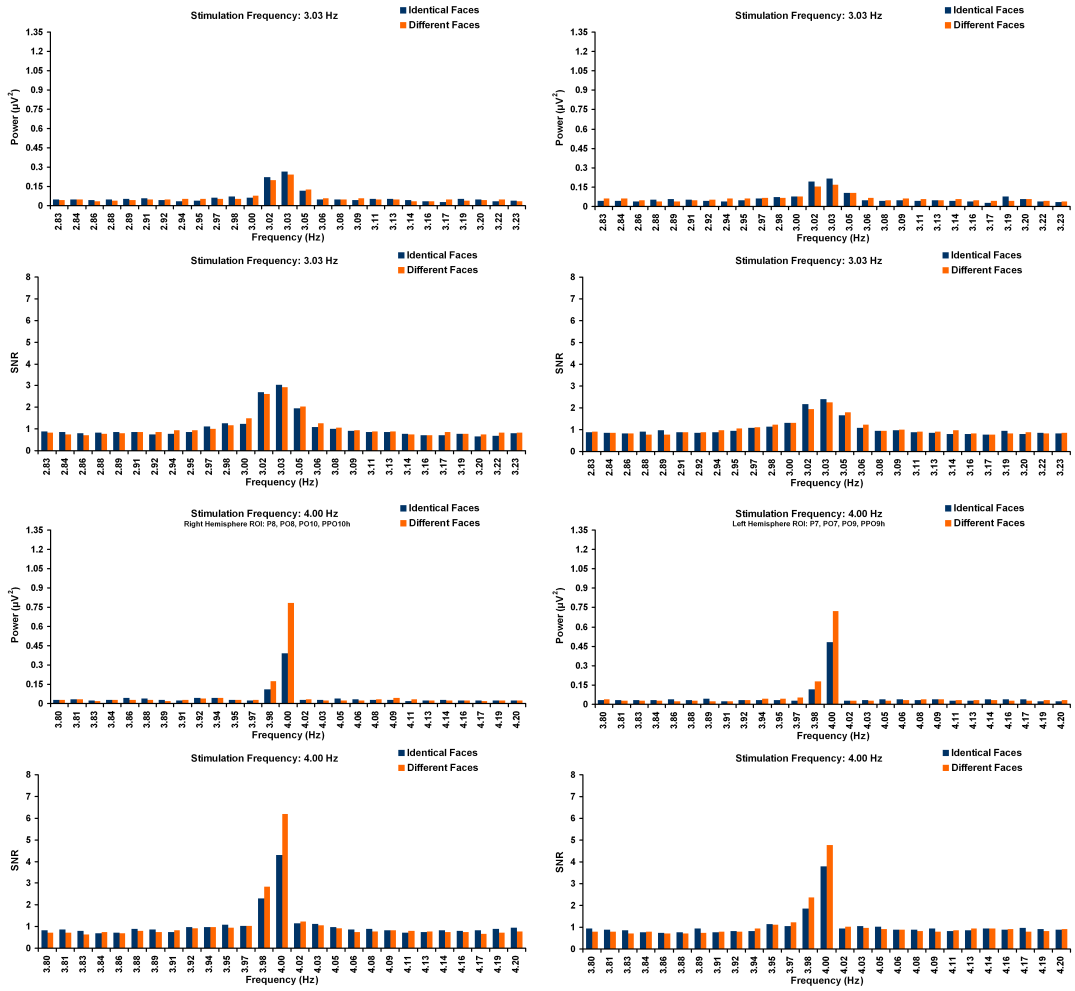


**Figure 3.41:** Entrainment to the stimulation frequency (3.00 and 4.00 Hz).

For stimulation frequencies 3.00 and 4.00 Hz, the FFT power spectrum and SNR values averaged across subjects, sessions and electrodes P8/P7, PO8/O7, PO10/O9 and PPO10h/9h is displayed only for 26 frequency bins centered on the corresponding stimulation frequencies. Both experimental conditions, identical and different faces are represented. Figures 3.40, 3.42, 3.43, 3.44, 3.45 and 3.46 present the data corresponding to the remaining stimulation frequencies.

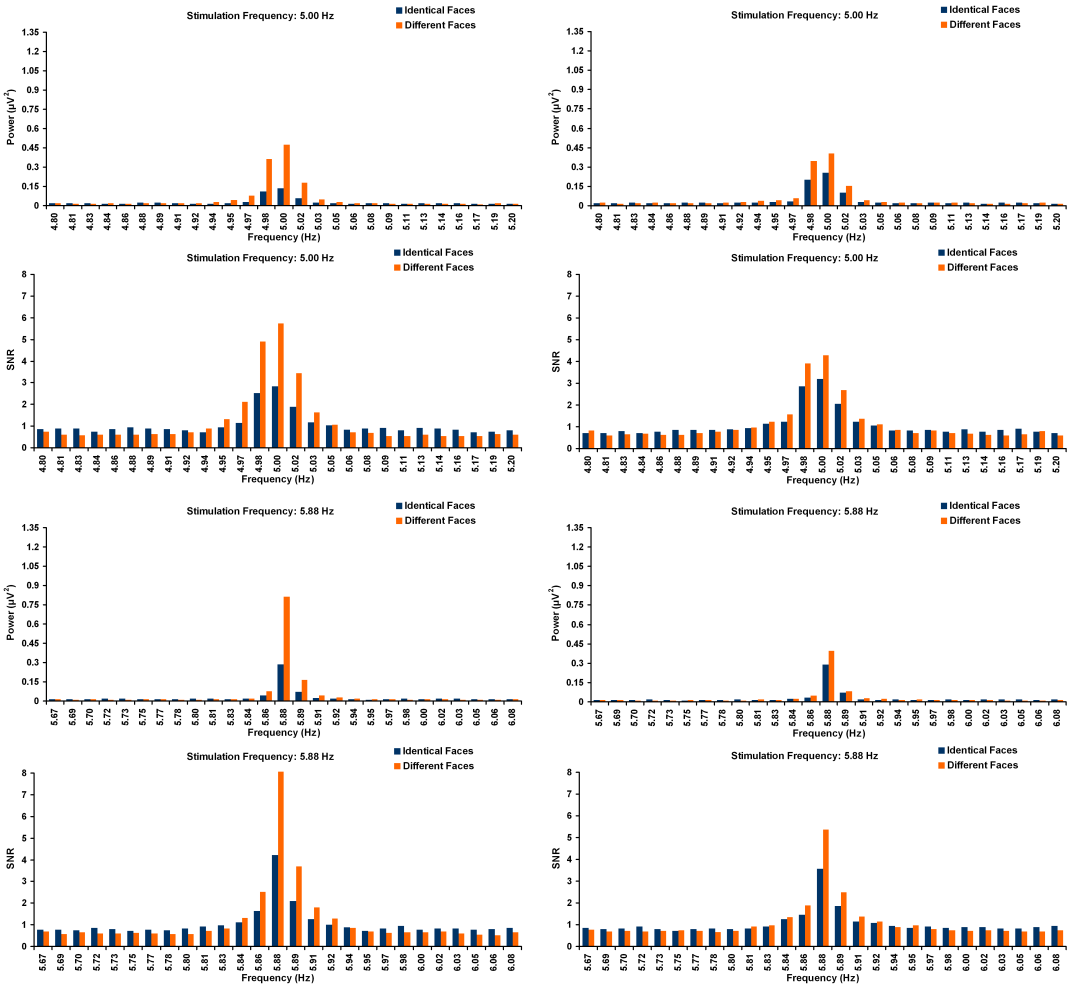


**Figure 3.42:** Entrainment to the stimulation frequency (5.00 and 5.88 Hz).

For stimulation frequencies 5.00 and 5.88 Hz, the FFT power spectrum and SNR values averaged across subjects, sessions and electrodes P8/P7, PO8/O7, PO10/O9 and PPO10h/9h is displayed only for 26 frequency bins centered on the corresponding stimulation frequencies. Both experimental conditions, identical and different faces are represented. Figures 3.40, 3.41, 3.43, 3.44, 3.45 and 3.46 present the data corresponding to the remaining stimulation frequencies.

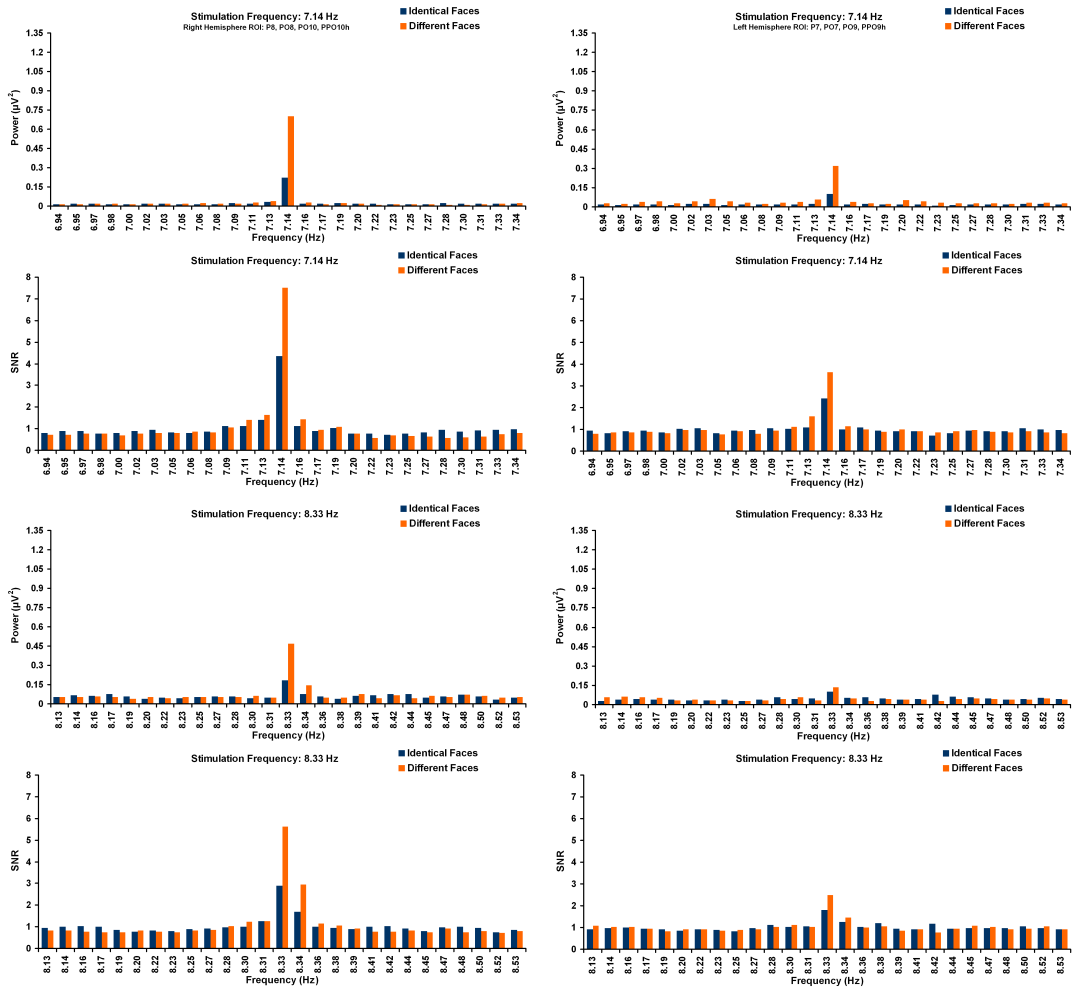


**Figure 3.43:** Entrainment to the stimulation frequency (7.14 and 8.33 Hz).

For stimulation frequencies 7.14 and 8.33 Hz, the FFT power spectrum and SNR values averaged across subjects, sessions and electrodes P8/P7, PO8/O7, PO10/O9 and PPO10h/9h is displayed only for 26 frequency bins centered on the corresponding stimulation frequencies. Both experimental conditions, identical and different faces are represented. Figures 3.40, 3.41, 3.42, 3.44, 3.45 and 3.46 present the data corresponding to the remaining stimulation frequencies.

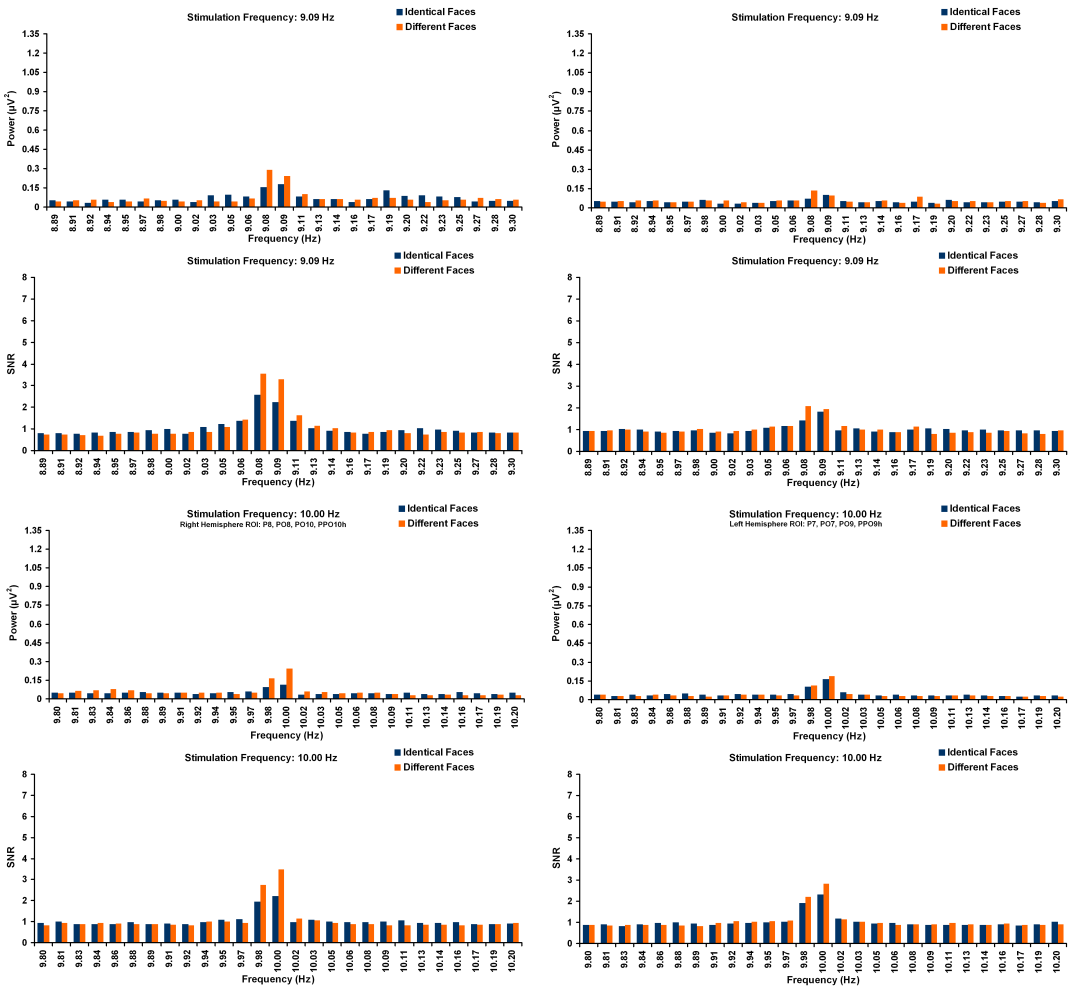


**Figure 3.44:** Entrainment to the stimulation frequency (9.09 and 10.00 Hz).

For stimulation frequencies 9.09 and 10.00 Hz, the FFT power spectrum and SNR values averaged across subjects, sessions and electrodes P8/P7, PO8/O7, PO10/O9 and PPO10h/9h is displayed only for 26 frequency bins centered on the corresponding stimulation frequencies. Both experimental conditions, identical and different faces are represented. Figures 3.40, 3.41, 3.42, 3.43, 3.45 and 3.46 present the data corresponding to the remaining stimulation frequencies.

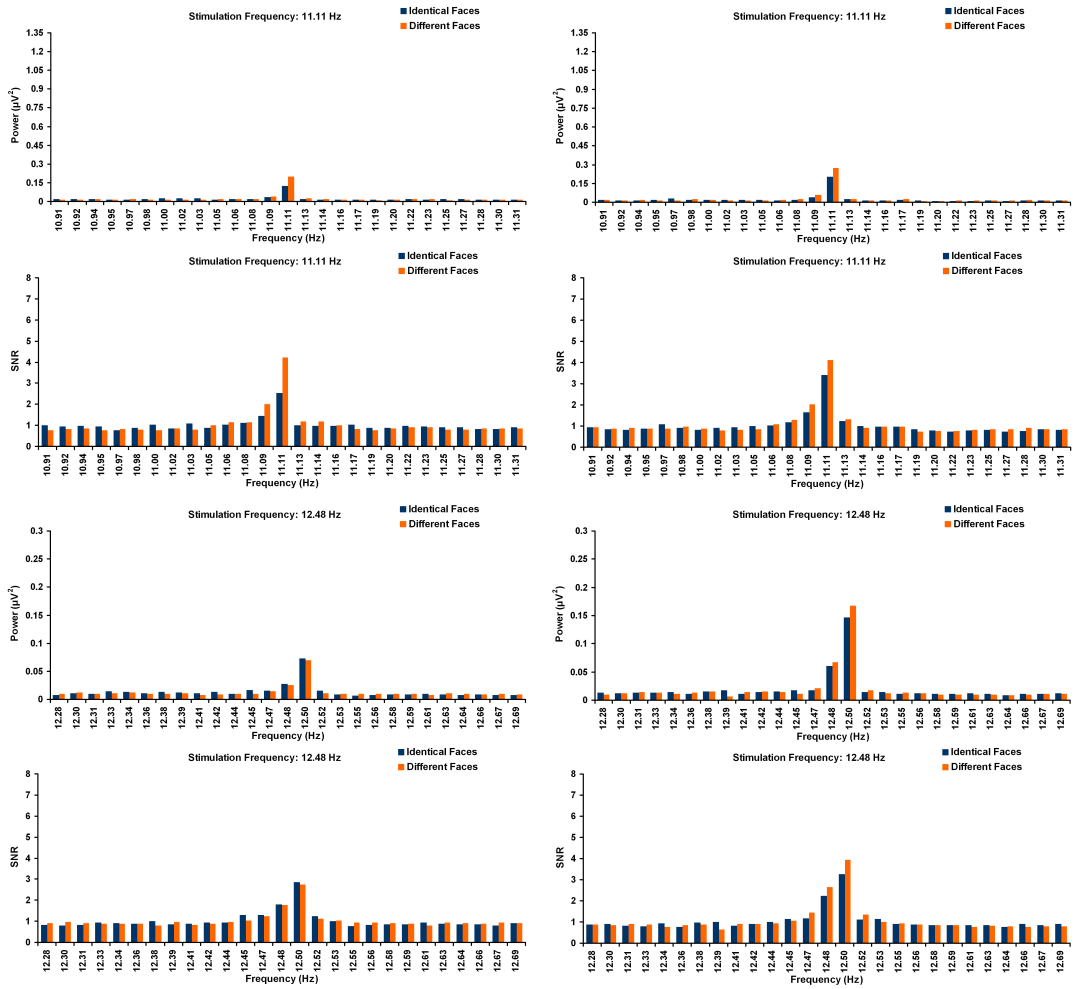


**Figure 3.45:** Entrainment to the stimulation frequency (11.11 and 12.48 Hz).

For stimulation frequencies 11.11 and 12.48 Hz, the FFT power spectrum and SNR values averaged across subjects, sessions and electrodes P8/P7, PO8/O7, PO10/O9 and PPO10h/9h is displayed only for 26 frequency bins centered on the corresponding stimulation frequencies. Both experimental conditions, identical and different faces are represented. Figures 3.40, 3.41, 3.42, 3.43, 3.44 and 3.46 present the data corresponding to the remaining stimulation frequencies.

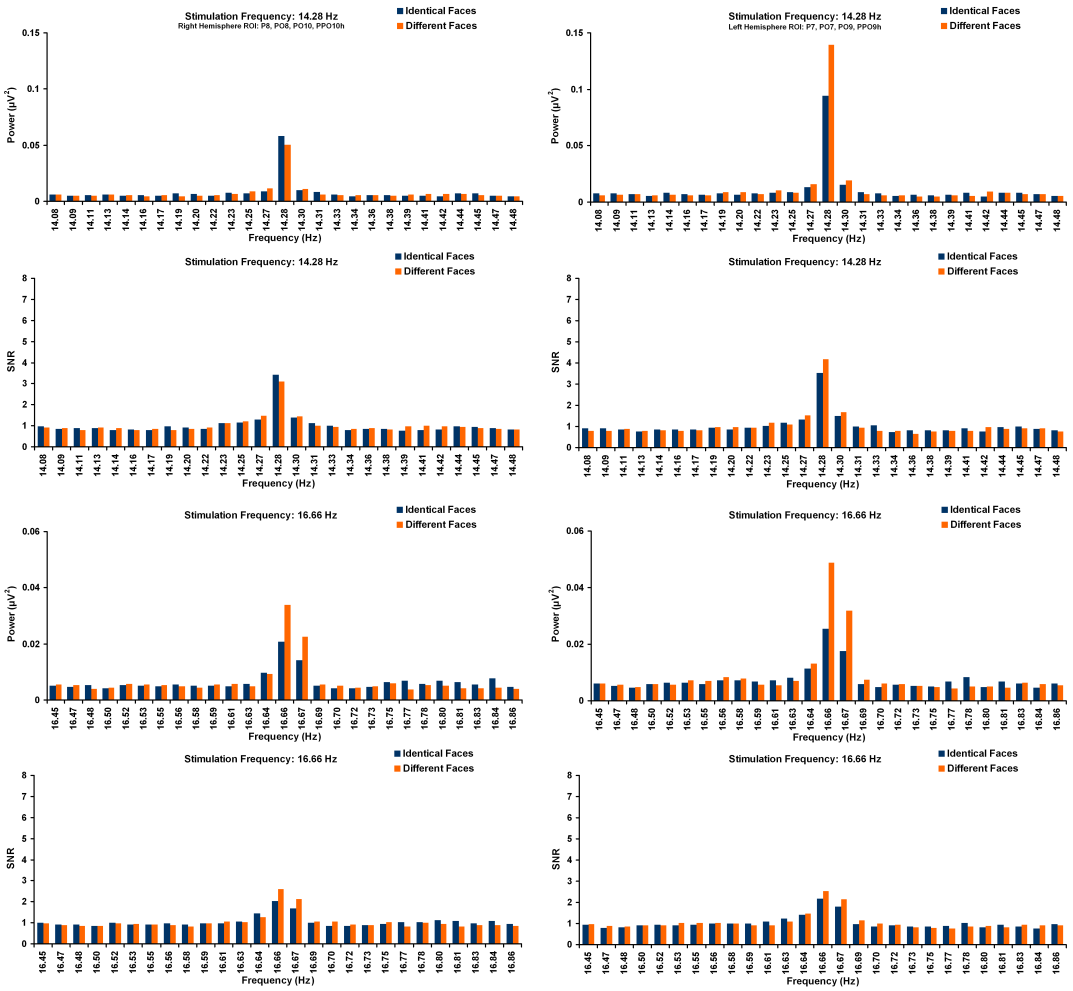


**Figure 3.46:** Entrainment to the stimulation frequency (14.28 to 16.66 Hz).

For stimulation frequencies 14.28 and 16.66 Hz, the FFT power spectrum and SNR values averaged across subjects, sessions and electrodes P8/P7, PO8/O7, PO10/O9 and PPO10h/9h is displayed only for 26 frequency bins centered on the corresponding stimulation frequencies. Both experimental conditions, identical and different faces are represented. Figures 3.40, 3.41, 3.42, 3.43, 3.44 and 3.45 present the data corresponding to the remaining stimulation frequencies.

each participant and experimental repetition independently. Then, they were averaged across repetitions and the standard errors were calculated as follows:

$$SE = \frac{\sqrt{\sum_i^N (x_i - \mu)^2}}{(N-1)\sqrt{N}} \tag{3.1}$$

where $N$ is the amount of repetitions for a particular experimental condition, $x$ is the observed value at a particular repetition and $\mu$ is the mean over all sample items.

As it can be observed in Figure 3.48, the general SSFRE pattern was clearly present for subjects 1, 2 and 3. S3 presented a slight SSFRE decrease at 5.00 Hz but still the highest effect was found at 5.88 Hz and it decreased for the surrounding frequencies from 3.03 to 10.00 Hz (Figure 3.48). S4 exhibited the highest effect at 4.00 and 5.00 Hz while at 5.88 Hz it was slightly smaller (Figure 3.48). The general SSFRE pattern was also observed in the left hemisphere although the magnitude of the effect was smaller than in the right hemisphere. Note that S4, who presented the highest SSFRE at 4.00 and 5.00 Hz in the right hemisphere, presented the highest value at 5.88 Hz in the left hemisphere (Figure 3.48).

#### 3.3.3.4 SSFRE at harmonics of the fundamental frequency

As it was previously mentioned, both the FFT amplitude spectrum and the derived SNR values exhibited noticeable peaks for both conditions at frequency bins multiple of the fundamental frequency evidencing that the stimuli drove the brain signal also at those harmonics. However, the magnitude and spatial distribution of the SSFRE varied across harmonics. Consequently, we set two criteria in order to determine the harmonics that increased the brain signal within areas of the face processing network when the identity of the facial stimulus was varied. First, the SSFRE should be equal to or even higher than the 50 % SSFRE obtained at the corresponding fundamental frequency. Second, it had to reach that 50 % threshold over at least 3 contiguous electrodes over a focal scalp region.

These two criteria were fulfilled by harmonic 2f of f = 1.00 Hz, f = 3.03 Hz, f = 4.00 Hz and f = 10.00 Hz as well as by harmonic 3f of f = 2.00 Hz and f = 3.03 Hz (Figure 3.49 and Figure 3.50). Note that the SSFRE value at harmonic 2f of f = 8.32 Hz and f = 11.11 Hz is close to the 50 % of the SSFRE value reached at the corresponding fundamental frequency. Also, the SSFRE distribution of 2f harmonics of f = 14.28 Hz and f = 16.66 Hz, although near 50 % of the SSFRE reached at the fundamental frequency, was not focused on particular, neighboring electrodes but it was diffused over the entire scalp (Figure 3.51).

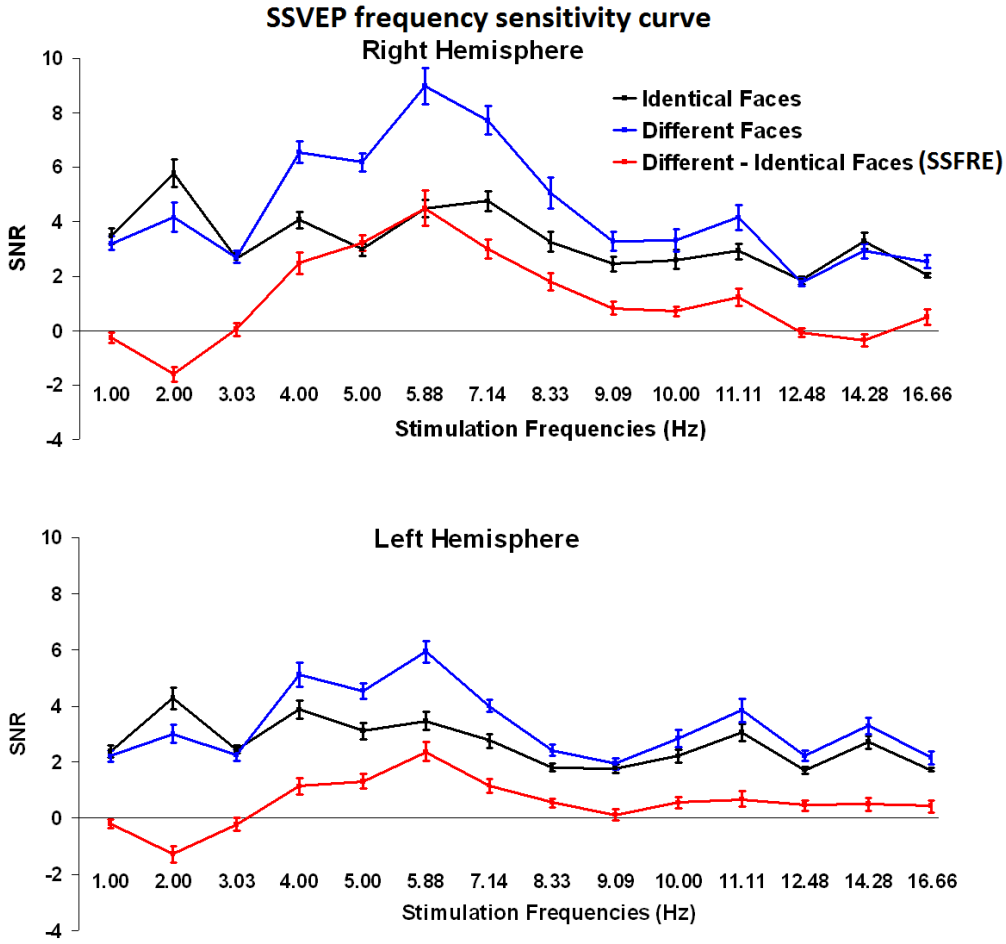


**Figure 3.47: SSFRE frequency sensitivity curve** - SNR values were averaged over face sensitive electrodes P8/P7, PO8/O7, PO10/O9 and PPO10h/O9h for each experimental condition as well as for the difference between those conditions (SSFRE) and plotted as a function of stimulation frequency. Note that the highest SSFRE values are obtained between 4.00 and 11.11 Hz peaking at 5.88 Hz. Note also that this result is on account of an SNR increase when different faces were presented whereas SNR values when identical faces where presented remained relatively stable across frequencies.

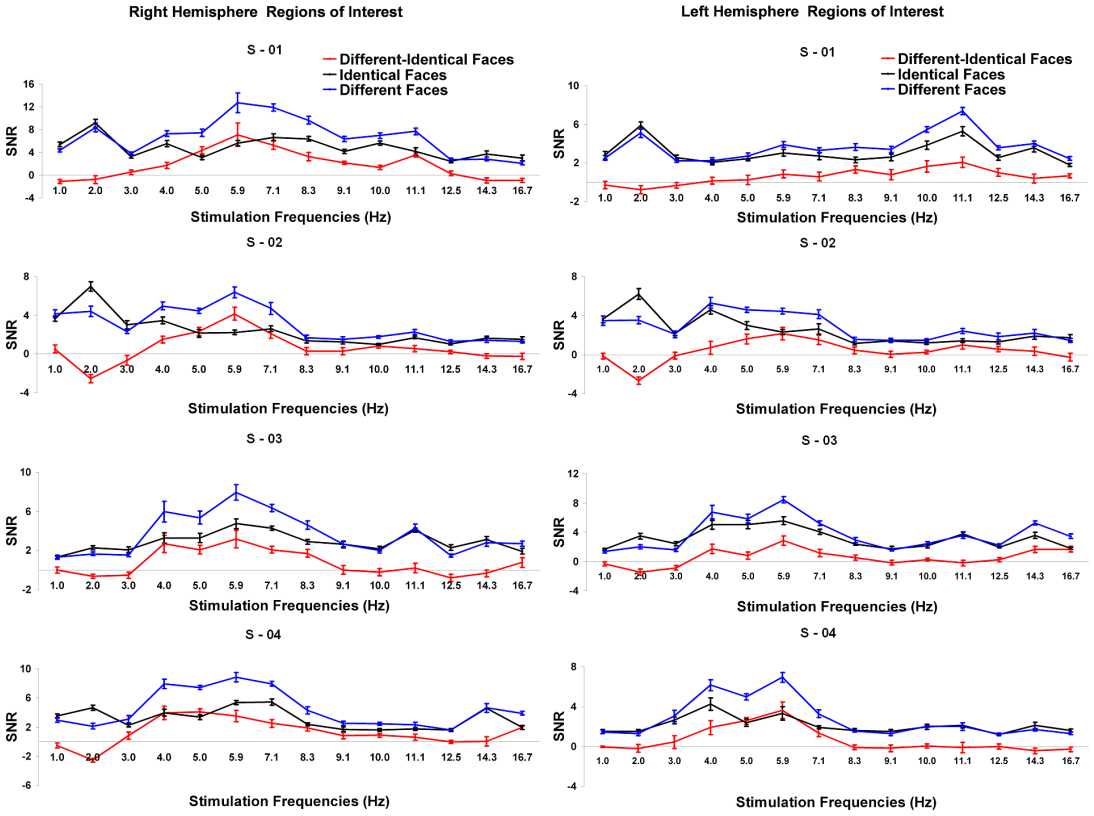


**Figure 3.48: SSFRE frequency sensitivity curve for each participant** - The general SSFRE pattern as a function of stimulation frequencies was reproduced across subjects. Note the right hemisphere dominance of this effect.

Within the harmonics that fulfilled both criteria, two distinctive SSFRE topographic patterns were observed. The first pattern corresponded to harmonics 2f of f = 1.00 Hz, f = 3.03 Hz and f = 4.00 Hz as well as to harmonics 3f of f = 2.00 Hz and f = 3.03 Hz. It was narrowly focused on occipito-temporal electrodes mainly in the right hemisphere. For f = 3.03 Hz and f = 4.00 Hz it also involved posterior central regions (Figure 3.49). This distribution resembled that obtained for a fundamental stimulation frequency of f = 5.88 Hz. The second pattern corresponded to harmonics 2f of f = 8.32 Hz, f = 10.10 Hz and f = 11.11 Hz and it was focused on posterior central electrodes (Figure 3.50 and Figure 3.51).

### 3.3.4 Discussion

The periodic presentation of a facial stimulus at rates between 1.0 and 16.66 Hz provoked a brain response characterized by sharp FFT amplitude increases at the fundamental frequencies used for stimulation. The magnitude of the difference between the response obtained for different and identical faces, the SSFRE, varied as a function of this fundamental frequency. Thus, the SSFRE was highest for stimulation frequencies between 4.00 and 9.09 Hz. Within this range, the SSFRE peaked at 5.88 Hz and decreased steadily from 5.88 to 4.00 Hz and from 5.88 to 9.09 Hz. The highest values appeared over occipito-temporal scalp regions, especially in the right hemisphere, and also over central regions. Below 3.03 Hz, the SSFRE was negative. In other words, the highest brain response was observed for the condition in which the face identity remained unchanged. At 12.48 and 14.28 Hz, the SSFRE was positive but its topography involved occipito-temporal electrodes with a left hemisphere dominance. At 16.66 Hz, the SSFRE was still positive but exhibited an occipito-central distribution.

#### 3.3.4.1 Optimal stimulus presentation rate to process individual face information in the human brain

The brain response is highest for external simple inputs, e.g., a sinusoidally - modulated light, between 9 - 10 Hz, 16 - 18 Hz and 40 - 50 Hz; (Herrmann, 2001; Rager & Singer, 1998; Regan, 1966, 1968a,b, 1989, 2009), as reported by EEG studies; or between 6 and 8 Hz, as reported by fMRI studies (Fox & Raichle, 1984, 1985; Mentis *et al.*, 1997). Here, we showed that also for high level stimuli, such as faces of varying identity, certain frequency ranges (4.00 - 9.09 Hz) are preferred.

The exact physiological mechanism that explains this brain preference for certain stimulation frequencies is not yet fully understood. Some authors have proposed that this phenomenon is caused by an increase in the neuronal response synchronization as a result of the presentation of a repetitive external input whose temporal presentation rate is such that it prevents the temporal dispersion of the response or interference

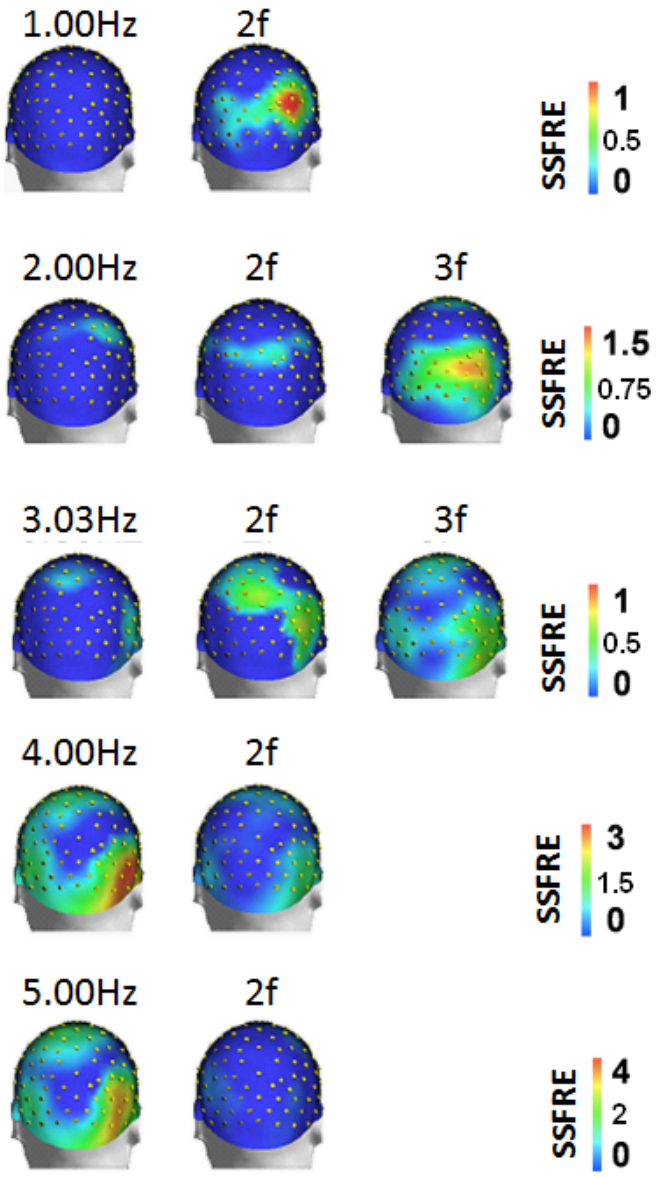


**Figure 3.49: The SSFRE scalp distribution for each stimulation frequency and corresponding harmonics for fundamental frequencies 1.00 to 5.00 Hz**- The SSFRE topographic maps are displayed for fundamental stimulation frequencies 1.00 - 5.00 Hz and relevant harmonics (see text for details). To allow comparing the magnitude of the SSFRE at the fundamental and at the corresponding harmonics, all maps are scaled according to the highest SSFRE value exhibited at the fundamental stimulation frequency. Note that not for all harmonics the SSFRE was equal to or even higher than the 50 % SSFRE obtained at the corresponding fundamental frequency over at least 3 contiguous electrodes indicating that varying the identity of the face did not influence the brain signal at that frequency component.

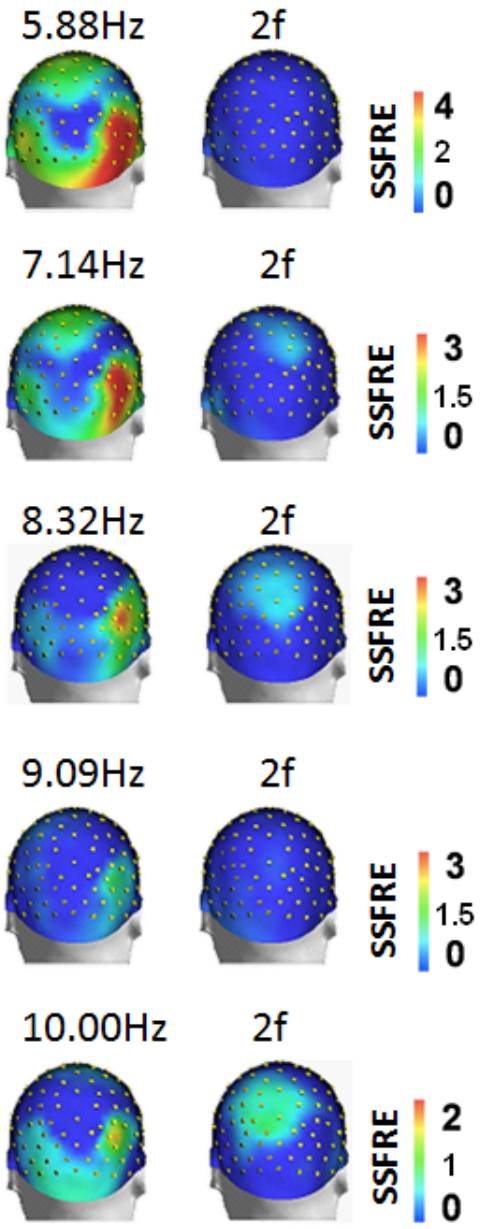


**Figure 3.50: The SSFRE scalp distribution for each stimulation frequency and corresponding harmonics for fundamental frequencies 5.88 to 10.00Hz-** The SSFRE topographic maps are displayed for fundamental stimulation frequencies 5.88 - 10.00 Hz and relevant harmonics (see text for details). Maps are scaled as explained in Figure 3.49.

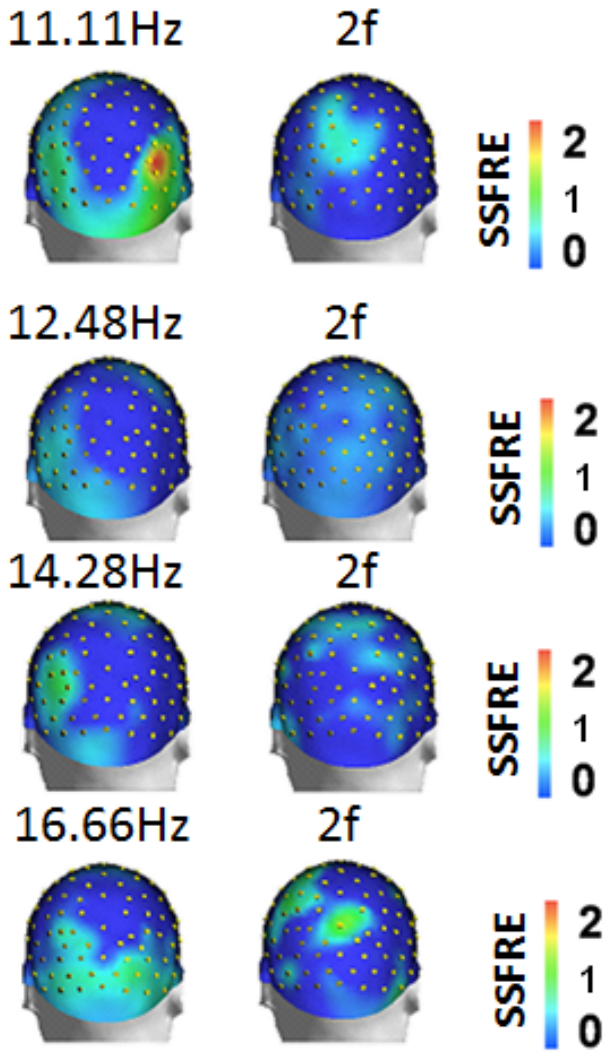


**Figure 3.51: The SSFRE scalp distribution for each stimulation frequency and corresponding harmonics for fundamental frequencies 11.11 to 16.66Hz**- The SSFRE topographic maps are displayed for fundamental stimulation frequencies 11.11 - 16.66 Hz and relevant harmonics (see text for details). Maps are scaled as explained in Figure 3.49.

between the after-discharge to the first stimuli and the onset-response to the following one (Fox & Raichle, 1984, 1985; Macknik, 2006; Mentis *et al.*, 1997). As we found the highest SSFRE for frequency ranges that matched the temporal activation cycle of the face processing network, we can suggest that the stimulus temporal presentation rate that best guarantees the synchronization of neuronal responses is the one that coincides with the temporal activation cycle of the neuronal assembly specialized in processing the particular stimuli. The temporal activation cycle of a neuronal group determines its availability to respond to a given stimulus, but when the latter is repeated at fixed time intervals, it forces the neurons to respond at a certain rate biasing the open time probability of ion channels and the propagation of excitatory and inhibitory postsynaptic potentials. If the inter-stimulus interval coincides with the neuronal activation cycle, then a higher amount of neurons are available to respond to the input and can synchronize their responses, which will result in an amplification of the output along the targeted neuronal network causing a noticeable augment in the amplitude of the signal registered on the scalp (Basar, 1998; Buzsaki, 2006; Nunez & Srinivasan, 2005).

This suggestion is additionally supported by the observation that when the facial stimuli are presented at a rate that does not coincide with the temporal activation cycle of the face processing network, the magnitude of the SSFRE diminishes and its topographic distribution changes. At the slowest stimulus presentation rate (1.00 and 2.00 Hz), cognitive processes unrelated to the stimulation might have taken place, which contributed to the temporal scatter of neuronal responses. At the fastest stimulus presentation rate (12.48 - 16.66 Hz), the offset response of the first stimulus could have overlapped with the onset response to the second stimulus interfering with each other's proper encoding. Single units recordings in the primary visual cortex of primates have already demonstrated the existence of this interference phenomenon for stimuli simpler than the one employed here (Macknik, 2006). Thus, when two brief flashes are presented in close succession (inter stimuli intervals of 30 ms or less that correspond to a stimulus presentation rate of 17 Hz) the onset-response to the second flash is absent (Macknik, 2006). Both mechanisms, temporal scatter and interference of responses, lead to a noticeable decrease of the amplitude of the scalp signal. However, they do not imply that the identity changes were not detected as confirmed by the verbal reports of the participants in the experiment.

Changes in the SSFRE topographic distribution for the fastest stimulus presentation rates used here also suggest that at these frequencies, brain structures outside the core face processing network were predominantly influenced by the stimulation. At 12.48 and 14.28 Hz, the SSFRE was higher over the left than the right occipito - temporal electrodes. Considering that some studies have shown that face selective activity can be even greater in the left than in the right fusiform gyrus if subjects focus their attention on particular features of the face, which suggests that the left hemisphere may process

a feature-based representation of the face (Rossion *et al.*, 2000a) it can be hypothesized that for this high frequencies (12.48 and 14.28 Hz) a feature based processing may have occurred.

At 16.66 Hz, the SSFRE was highest over central occipital electrodes, which resembles the topographic distribution of early ERP components that respond strongly to basic stimulus properties such as luminance and contrast between 70 and 90 ms after stimulus onset (Clark & Hillyard, 1996; Di Russo *et al.*, 2002; Heinze *et al.*, 1994; Jeffreys & Axford, 1972; Khoe *et al.*, 2004). This distribution is also suggestive of generators in primary visual cortex. Therefore, we might speculate that at such a high stimulus presentation rate, mainly the neurons in early visual structures of the retino - thalamo - cortical system were responding synchronously to the stimulation. These neuronal groups might not be capable of discriminating between faces of different identities, which could explain also why there is a decrease in the overall magnitude of the SSFRE. Further studies need to be conducted to corroborate this suggestion.

As previously mentioned, flash patterned stimulus also elicits the highest response when it is presented at a temporal rate of 6 - 7 Hz. This observation would suggest that our results are related to the analysis of low level properties of the stimulus. Nonetheless, several arguments support their face specificity. First, we manipulated the size of the stimuli, which avoided retinal adaptation to basic image properties. Second, a very specific topography emerged clearly for those frequencies where the SSFRE was highest: a maximum at lateral occipital electrodes in both hemispheres but with right hemisphere dominance, with a second activation in central electrodes. Electrodes located in those regions have traditionally shown the highest face selectivity in studies of the N170 component (Bentin *et al.*, 1996; Eimer, 2000a; Rossion & Caharel, 2011; Rossion *et al.*, 2000b, 2003a) and its positive counterpart, the VPP (Jeffreys, 1996).

#### 3.3.4.2 SSFRE as a function of harmonic frequencies

Our results also showed that the periodic presentation of facial stimuli provoked additional FFT amplitude components corresponding to harmonic frequencies. The SSFRE at these harmonics varied as a function of frequency. For the harmonics of 1.00, 2.00, 3.03 and 4.00 Hz, the SSFRE focused also on right occipito-temporal electrodes while for the harmonics of 7.14, 8.32, 10.00 and 11.11 Hz, besides being of smaller magnitude compared to the above mentioned frequencies, it focused on central occipital regions. For harmonics of 12.24, 14.28 and 16.66 Hz, the SSFRE was diffuse over the entire scalp.

The SSVEP at harmonic frequencies might represent the activation of neuronal groups different to those activated by the fundamental frequency as suggested by previous studies (Pastor *et al.*, 2007; Podvigin *et al.*, 2004) and supported by our own

observations of differences in the topographic distribution of the SSFRE at each harmonic.

For harmonics 2f of f = 1.00 Hz and f = 3.03 Hz as well as 3f of f = 2.00 Hz the SSFRE was even higher than that observed at the corresponding fundamental frequency and was distributed over right occipito-temporal electrodes. Interesting enough, these range of harmonic frequencies coincided with the range of fundamental frequencies that also showed this pattern. This observation was especially true for the second harmonic of fundamental frequencies 3.03 and 4.00 Hz (corresponding to frequency values of 6.06 and 8.00 Hz) and gives further support to our proposal that the optimal frequency range to activate the face processing network lies between 4.00 and 9.09 Hz with the highest response obtained around 5.88 Hz. Harmonics corresponding to higher fundamental frequencies did not seem to tag the face processing network since the SSFRE was of small magnitude (note that it not even reached the 50% of the SSFRE observed at the corresponding fundamental frequency) and focused over high centro-occipital electrodes.

### 3.3.5 Conclusions

Here we confirmed the adequacy of the experimental design as well as the suitability of the SSVEP technique in general to study face perception processes. Even further, our study optimizes the testing conditions to be used by demonstrating that the optimal stimulus presentation rate to investigate face identification processes using the SSVEP technique ranges between 4.00 and 9.09 Hz. Within this range, the highest brain responses are obtained at 5.88 Hz. Given that this frequency range coincides with the latency of the face selective responses as found in human and animals studies, it can be concluded that the human brain is best prepared to individualize a facial stimulus when it arrives to the visual cortex at a temporal rate that matches the activity cycle of the face processing network. Consequently, future studies that aim at studying face perception processes using the steady state technique should select stimulus presentation rates that coincide with the temporal activation cycles of the neuronal groups involved in the face perception process under study.

# Chapter 4

# Characterization of the SSVEP sensitivity to facial identity in prosopagnosic patient PS

## 4.1 Study 4: Steady State Visual Potentials to individual faces in acquired prosopagnosia

*Esther Alonso Prieto*[1] *and Bruno Rossion*[1]
[1] Université catholique de Louvain, Louvain-la-Neuve, Belgium
(This article is in preparation)

**Abstract**

Event related potential (ERP) studies of brain lesion patients have to deal with two important issues: the need to use a high amount of trials to overcome the influence of noise in the data and possible distortions in the morphology of ERP components. Both issues are related to changes in the volume conductive properties of the damaged tissues and their surroundings and can limit the applicability of such studies. The use of the Steady State Visual Evoked Potential (SSVEP) technique can help to overcome these problems because it has a high signal to noise ratio and offers the possibility of quantifying the experimental variables easily and objectively. Recently, it has been demonstrated the applicability of this technique to the study of face perception and the optimal testing conditions to be used have been defined (see Study 2 and 3 in this thesis). The current study aims to determine whether such conditions apply also to prosopagnosic patient PS. In a first experiment, patient PS and four healthy age matched controls, were confronted with sequences of faces presented at different rates

(1 to 16.66 Hz or faces/second) while high-density EEG (128 channels) was recorded. As in a previous study of healthy, young individuals (see Study 2 and 3 in this thesis), Fast-Fourier Transform (FFT) of EEG and computation of signal-to-noise ratio (SNR) showed a larger response to different faces than identical faces between 4.00 and 9.09 Hz on occipito-temporal electrodes. For both, PS and the controls, this difference peaked at 5.88 Hz. However, this effect was noticeably decreased for PS and exhibited a different topographical distribution. In a second experiment, PS was studied using only one stimulation frequency (5.88 Hz) but 4 different types of facial stimulus, which varied according to gender and presence of skin color and hair. In general, none of these manipulations prevent the SSVEP amplitude increase for different faces as found in experiment 1. However, the effect decreased as the amount of external facial information decreased being minimal for gray, cropped faces. These observations indicate that the testing conditions that guarantee optimal results in SSVEP studies of face perception are similar in PS and healthy individuals. They also demonstrate that the SSVEP technique is sensitive to face identification deficits providing further support for its use in the study of prosopagnosic individuals.

**keywords: prosopagnosia, SSVEP, identity adaptation, EEG**

### 4.1.1 Introduction

Patient PS is probably one of the most extensively studied prosopagnosic individuals worldwide. This high scientific interest has been raised because of two aspects of her neuropsychological and lesional profiles that differentiate her from other brain lesions patients. First, she is a pure case of prosopagnosia, in other words, she has lost the ability to recognize familiar faces but has preserved all other cognitive functions (Busigny *et al.*, 2010; Rossion, 2003; Rossion *et al.*, 2011; Schiltz *et al.*, 2006; Sorger *et al.*, 2007). Second, her brain lesion encompasses the right occipital face area (OFA) while sparing the right fusiform face area (FFA). The opposite pattern is present in the left hemisphere (Rossion *et al.*, 2003a; Schiltz *et al.*, 2006; Sorger *et al.*, 2007). As a result of this profile, she can be studied to answer specific theoretical questions about the functional roles of two of the core regions of the face processing network (the OFA and the FFA) avoiding the influence of confounding variables such as the presence of difficulties in other cognitive domains or the presence of lesions in other brain regions.

Most of the studies that involve patient PS have used behavioral techniques or fMRI (e.g., Busigny *et al.* (2010); Rossion (2003); Rossion *et al.* (2011); Schiltz *et al.* (2006); Sorger *et al.* (2007)). Recently, an event related study was designed to demonstrate that the face selective activation of the FFA found with fMRI takes place within 170 ms after stimulus onset and that the OFA is not a necessary generator of the N170 face

effect (the amplitude increase in response to faces compared to other object categories) (Alonso *et al.*, 2011).

This study was not only important because of the theoretical points that helped to elucidate but also because it demonstrated two limitations of the use of the ERP technique in studying patient PS. These limitations were concerned with: (a) the presence of noise in the data, which obliged the authors to repeat the experiment several times to ensure reliability of results and (b) the peculiarities observed in the scalp expression of the ERPs of interest, possibly due to changes in the conductivity properties of the brain tissue. It is known that brain lesions can create an eccentric conductive inhomogeneity in the volume conductor affecting the shape and magnitude of the EEG and MEG signals (van den Broek *et al.*, 1998).

Trying to find a way to overcome these limitations, two experiments that studied the SSVEP to faces of varying identity were performed in order to demonstrate the usefulness of this technique in the field of face perception research. In these previous studies, the stimulation frequencies that guarantee optimal results in the healthy brain were determined (Study 2 in this thesis). It was also demonstrated the SSVEP sensitivity to face identity for various types of facial stimuli as well as the robustness of this response to changes in the amount of facial features present in the face pictures (Study 3 in this thesis). In the current study, identical procedure is employed to determine whether these optimal testing conditions can be extrapolated to patient PS. This is important because it will allow studying this patient in the future using the same experimental conditions that are optimal for healthy controls avoiding the influence of confounding variables related to the methodological procedure.

### 4.1.2 Materials and methods

#### 4.1.2.1 Participants

**Patient PS**

The lesional and neuropsychological profiles of patient PS have been characterized fully in Chapter 1, section 1.2.2.

**Normal controls:**

Four age-matched female controls (mean age = 59.33 ± 2.52 years, all right handed) were also tested. They had normal or corrected-to-normal vision and gave their informed consent after detailed information about the experiment was provided. The study was approved by the ethical committee of the Université catholique de Louvain and was in agreement with the Declaration of Helsinki.

#### 4.1.2.2 Experimental procedure and EEG recording

The experimental procedure employed here was identical to that employed in Studies 2 and 3 presented in this thesis. Similarly, the EEG data was recorded under identical conditions.

In brief, in experiment 1, faces were presented flickering at different frequencies between 1 and 16.66 Hz during the same recording session. Two experimental conditions, which manipulated the identity of the facial stimuli, were applied: identical faces and different faces. The order of these two conditions was counterbalanced across repetitions of the experiment for the same subject as well as intra-subjects. The order of the stimulation frequencies to use was randomized within the experimental session. Each condition was applied 2 times. In the case of PS, 4 recording sessions were performed whereas only one session was performed for the controls.

Experiment 2 was only applied to patient PS. It consisted of the presentation of different facial stimuli at a fixed temporal rate of 5.88 Hz. These stimuli were the KDEF set of faces, full color, cropped faces and gray, cropped faces (see section 3.3.2.2 for a full description of the stimuli). To remind the reader, the KDEF faces presented all external features including hair. The remaining faces were cropped and one set was presented in full color and the other set in gray scale (see Figure 3.2 for an example of the stimuli). Considering that previous studies have shown that PS is moderately impaired at discriminating face gender (Caldara *et al.*, 2005; Rossion, 2003) this variable was not considered in the analysis (female and male faces were analyzed together).

#### 4.1.2.3 EEG recording

The EEG data was analyzed following the procedure employed in Study 2. In brief, the FFT analysis was performed using an analysis window of 64 s (temporal resolution = 0.015625 Hz) and then the signal-to-noise ratio (SNR) index was calculated. In order to determine how the stimulus manipulations influence the process of detecting changes in its identity, the SNR based FFT amplitude values were averaged across all repetitions of the experiment in the case of PS and across all subjects in the case of healthy participants. Afterwards, both conditions were subtracted (different face condition − identical face condition) for each electrode separately to obtain the *Steady State Face Repetition Effect* or SSFRE index. To remind the reader, a positive SSFRE indicates that the SNR was highest for the different face condition. This index was plotted on the scalp for each stimulation frequency using a SSFRE by frequency scale adjusted according to the electrode that exhibited the highest SSFRE at that particular stimulation frequency. Based on these maps, regions of interest (ROIs) were determined including neighboring electrodes that showed the highest SSFRE. The ROI

values as a function of stimulation frequency were characterized for PS and for the group of healthy controls.

### 4.1.3 Results

#### 4.1.3.1 Experiment 1

As it can be seen in Figures 4.1, 4.2, 4.3, 4.4 and 4.5 , the brain signal of patient PS exhibited a noticeable frequency increase that reflected the frequency of the inducing stimuli (fundamental frequency, f).

When the SSFRE was calculated, it was observed that, in the case of PS, this index was positive for most of the stimulation frequencies used. However, not for all stimulation frequencies a positive SSFRE was observed in well localized group of neighboring electrodes but over widespread regions. The fundamental frequencies at which the SSFRE was highest and focused on particular scalp areas ranged between 2.00 and 10.00 Hz (Figure 4.6). Within this range, three main regions of interest (ROIs) could be distinguished:

- inferior occipital ROI involved electrodes POO10h, Ol1h, Ol2h, O2, I2, Oz and Iz and it appeared for frequencies 2.00, 3.03, 5.88, 7.14 and 10.00 Hz.

- right and left hemispheres parieto-occipital ROIs involved electrodes P2/1, P4/3, P6/5, PO4/5, PO8/7, PPO2/1, PPO6h/5h.

In order to determine the frequency sensitivity curve of the SSFRE for PS, the electrodes that formed these 3 ROIs were averaged together for each stimulation frequency, condition and session separately and the resulting SSFRE was plotted as a function of stimulation frequency. The obtained values indicated that her SSFRE was near zero for fundamental frequencies below 4.00 Hz and above 8.32 Hz. At 4.00 Hz the SSFRE began to rise gradually, peaked at 5.88 Hz and decreased again from 5.88 Hz to 8.32 Hz. Interesting enough, the parieto-occipital ROI in the left hemisphere was the only exception to this pattern since it did not exhibit the characteristic SSFRE peak at 5.88 Hz. On the contrary, it remained stable between 4.00 and 7.14 Hz (Figure 4.7).

PS frequency sensitivity SSFRE curve was compared to that of the age and sex - matched healthy participants tested in this study. To this end, for the controls the SSFRE was also calculated and regions of interest were determined. As in the case of the healthy young male subjects tested in Study 3, the female subjects tested here presented the highest SSFRE between 4.00 and 9.09 Hz especially over occipito-temporal electrodes in the right hemisphere. Specifically, the electrodes that exhibited the highest effect were P6/5, P10/9, PO6/5, PO8/7, PPO10h/9h and, consequently, they were selected to form the ROIs of this group (Figure 4.8).

Figure 4.9 shows the frequency sensitivity curve of the SSFRE obtained for both, PS and the healthy controls; at the right parieto-occipital ROI together with confidence

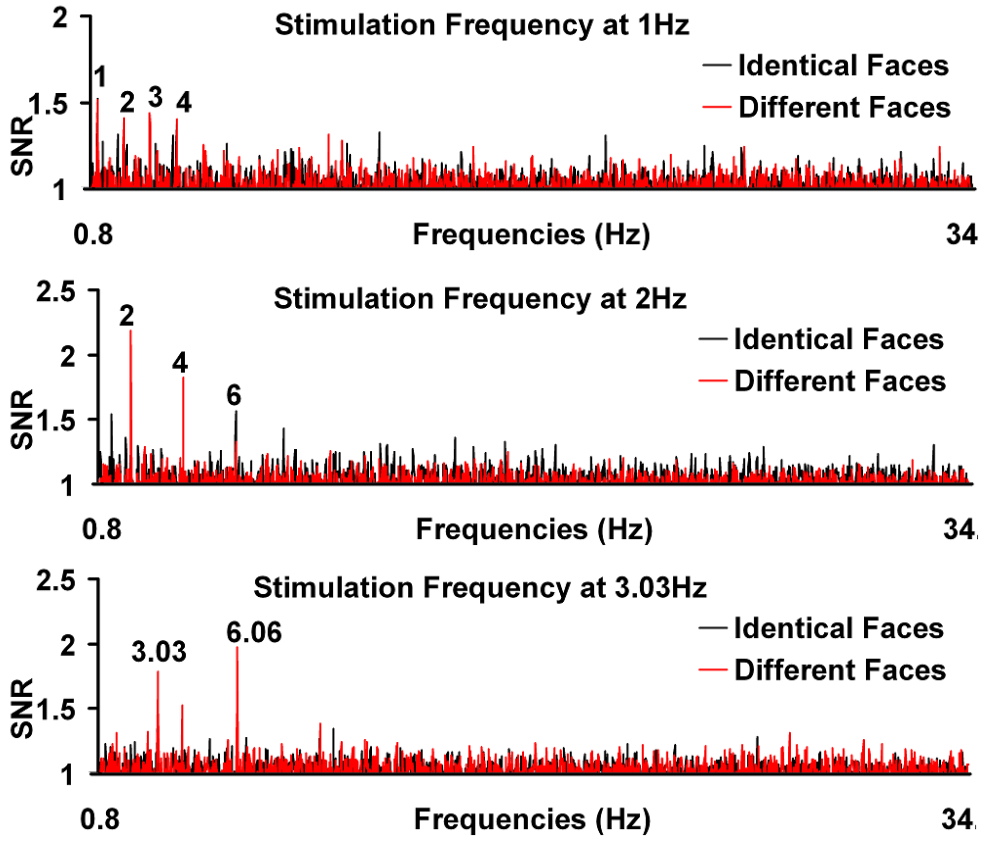


**Figure 4.1: SNR values obtained for patient PS: 1.00 to 3.03 Hz** - For stimulation frequencies 1.00, 2.00 and 3.03 Hz, the SNR values obtained for patient PS in each experimental condition are displayed. Note that the values were averaged across all experiment repetitions and electrodes. Only 68 frequency bins, centered around the stimulation frequency are shown. Figures 4.2, 4.3, 4.4 and 4.5 present the data corresponding to the remaining stimulation frequencies.

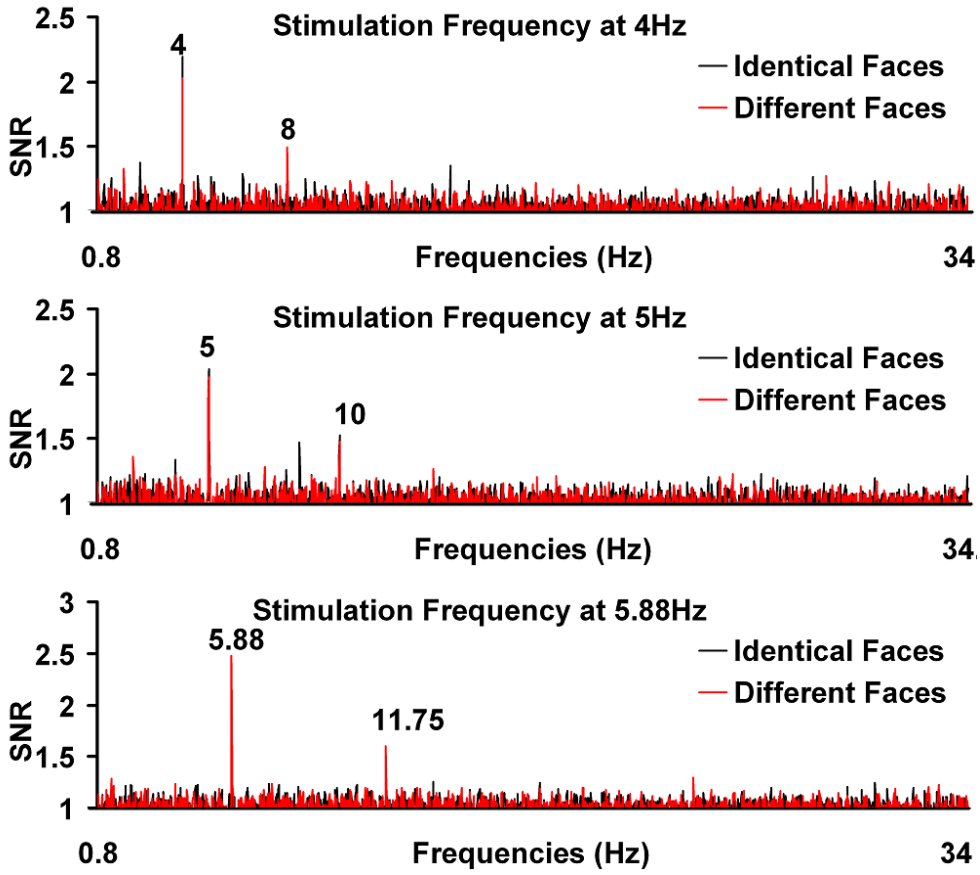


**Figure 4.2: SNR values obtained for patient PS: 4.00 to 5.88 Hz** - For stimulation frequencies 4.00, 5.00 and 5.88 Hz, the SNR values obtained for patient PS in each experimental condition are displayed. Note that the values were averaged across all experiment repetitions and electrodes. Only 68 frequency bins, centered around the stimulation frequency are shown. Figures 4.1, 4.3, 4.4 and 4.5 present the data corresponding to the remaining stimulation frequencies.

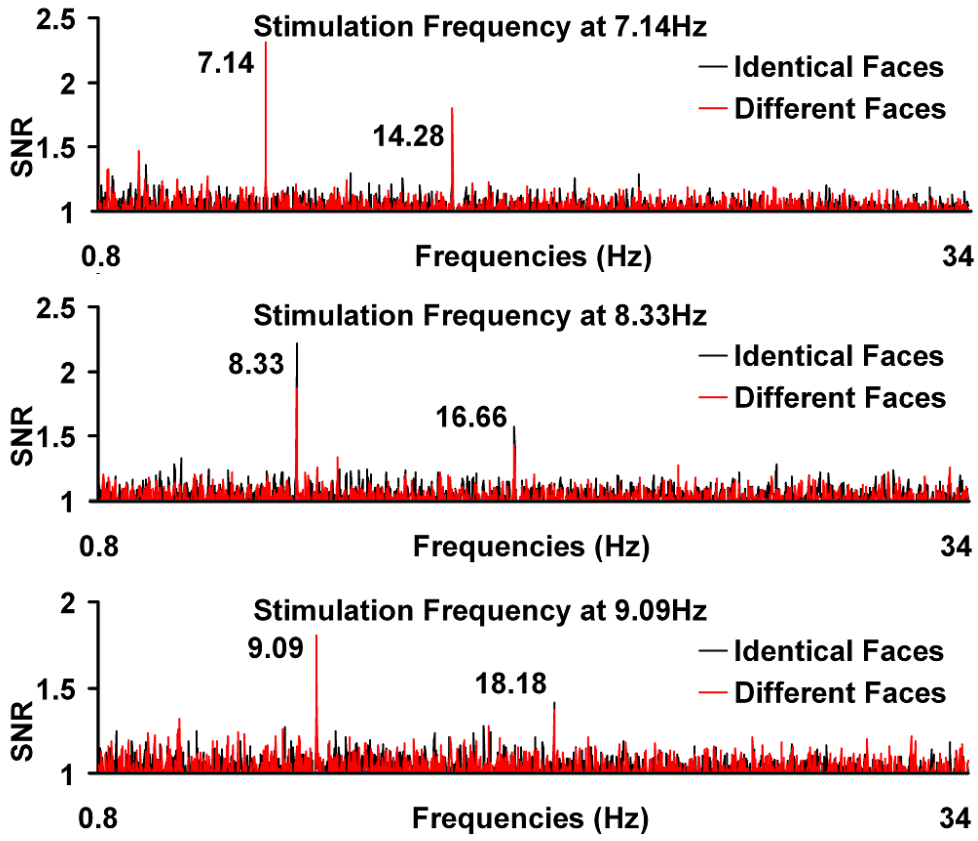


**Figure 4.3: SNR values obtained for patient PS: 7.14 to 9.09 Hz** - For stimulation frequencies 7.14, 8.32 and 9.09 Hz, the SNR values obtained for patient PS in each experimental condition are displayed. Note that the values were averaged across all experiment repetitions and electrodes. Only 68 frequency bins, centered around the stimulation frequency are shown. Figures 4.1, 4.2, 4.4 and 4.5 present the data corresponding to the remaining stimulation frequencies.

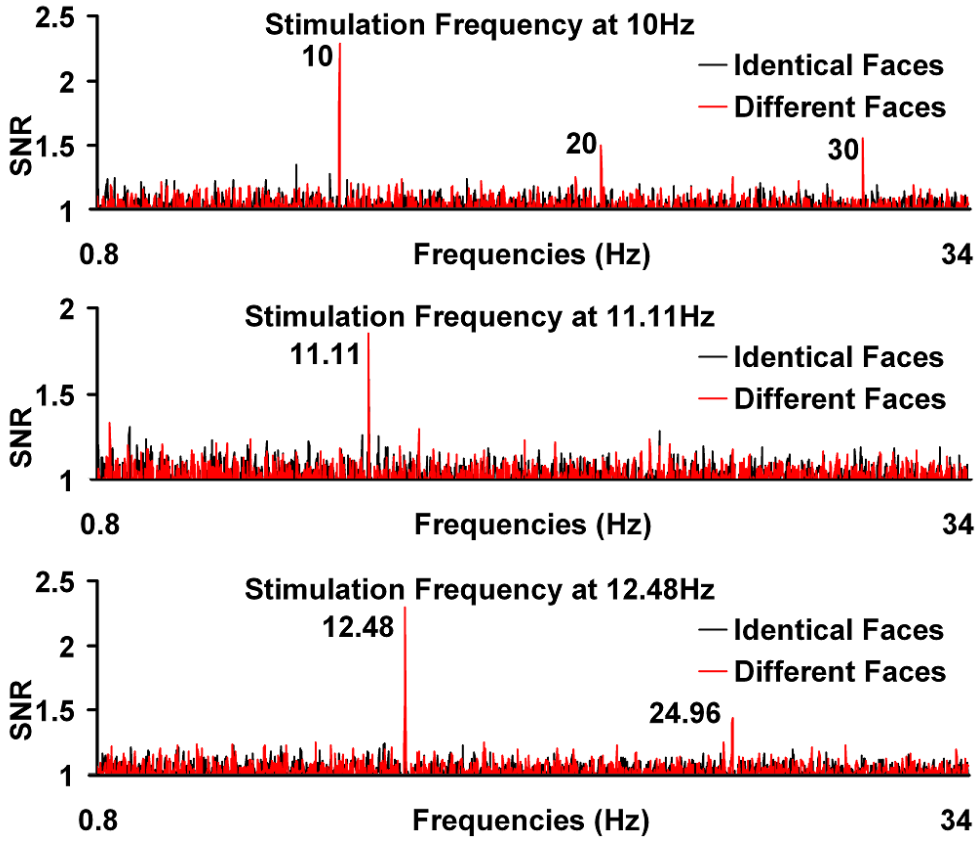


**Figure 4.4: SNR values obtained for patient PS: 10.00 to 12.48 Hz** - For stimulation frequencies 10.00, 11.11 and 12.48 Hz, the SNR values obtained for patient PS in each experimental condition are displayed. Note that the values were averaged across all experiment repetitions and electrodes. Only 68 frequency bins, centered around the stimulation frequency are shown. Figures 4.1, 4.2, 4.3 and 4.5 present the data corresponding to the remaining stimulation frequencies.

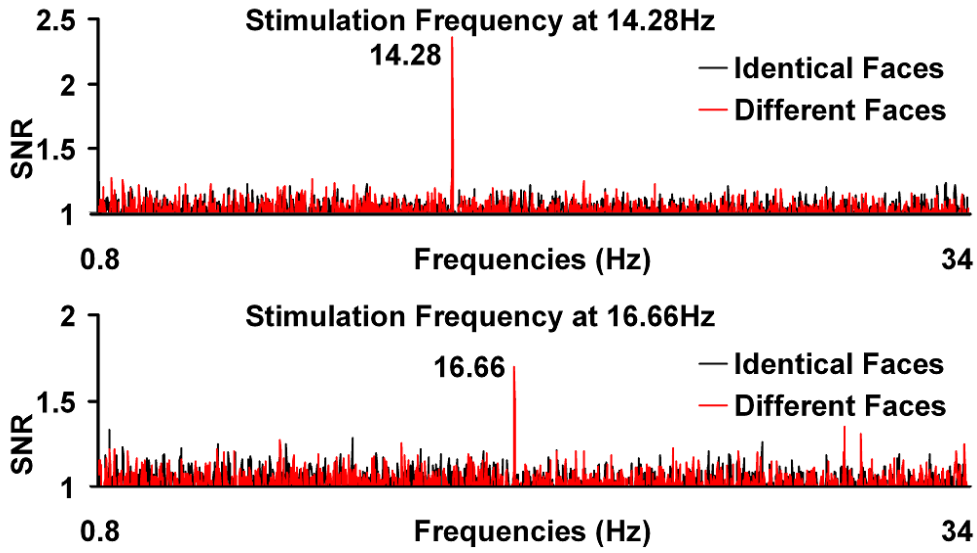


**Figure 4.5: SNR values obtained for patient PS: 14.28 to 16.66 Hz** - For stimulation frequencies 14.28 and 16.66 Hz, the SNR values obtained for patient PS in each experimental condition are displayed. Note that the values were averaged across all experiment repetitions and electrodes. Only 68 frequency bins, centered around the stimulation frequency are shown. Figures 4.1, 4.2, 4.3 and 4.4 present the data corresponding to the remaining stimulation frequencies.

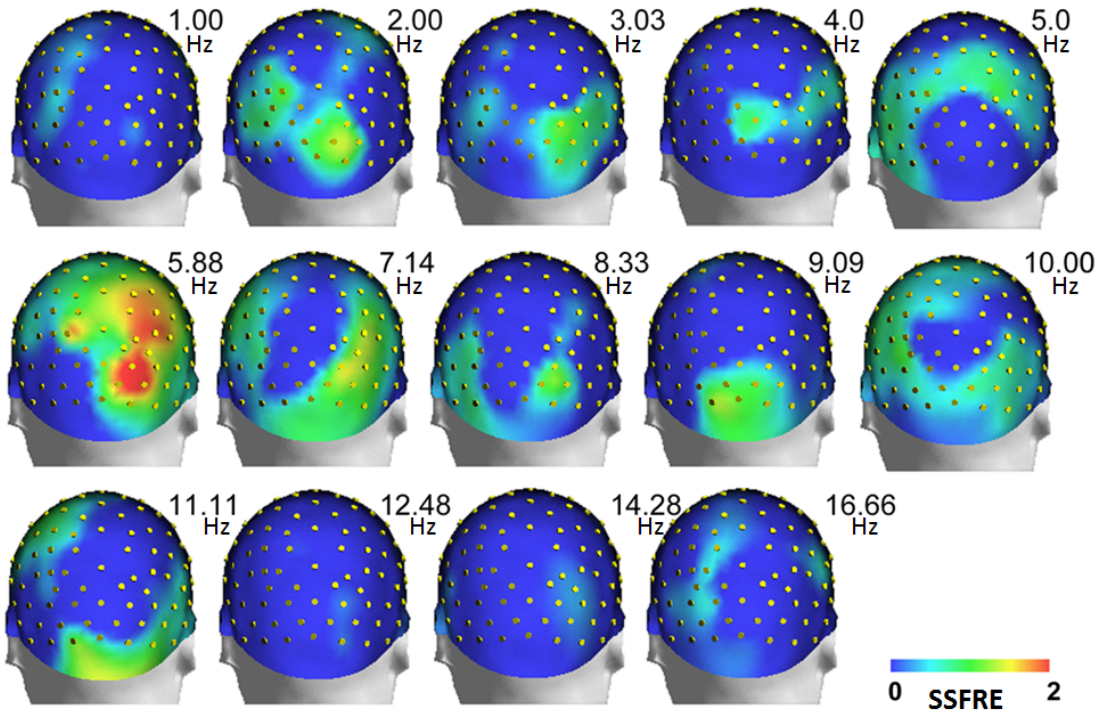


**Figure 4.6: SSFRE topographic distribution for patient PS** - The SSFRE was calculated and then averaged across all experimental repetitions performed by PS and plotted on the scalp. All maps are scaled according to the frequency that showed the highest effect

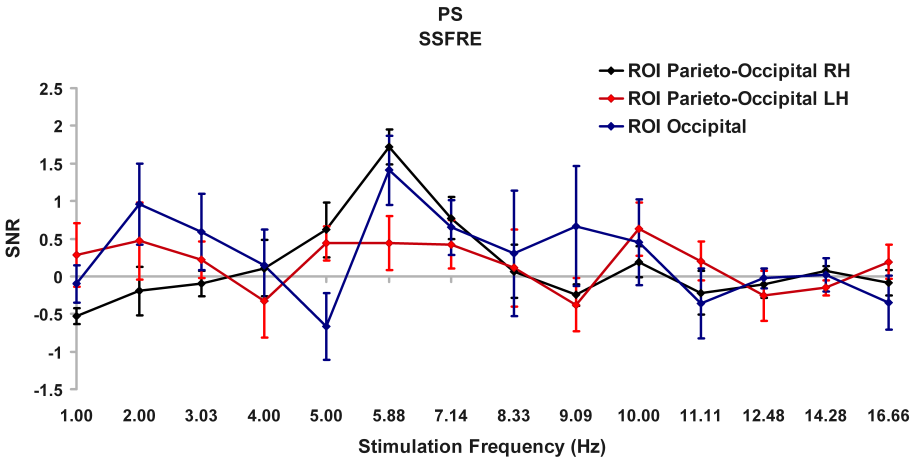


**Figure 4.7: PS SSFRE frequency sensitivity curve** - The SNR values were averaged across a group of neighboring electrodes that exhibited the highest SSFRE across stimulation frequencies to define ROIs. The resulting values were plotted as a function of stimulation frequency.

intervals (CI). This ROI was selected to calculate the CI because it exhibited the highest SSFRE in both groups. CI were calculated according to the following formula:

$$\begin{aligned} \text{upper } 95\% &= \mu + (SD * 1.96) \\ \text{lower } 95\% &= \mu - (SD * 1.96) \end{aligned}$$

where 1.96 is the approximate value of the 97.5 percentile point of the normal distribution (95% of the area under a normal curve lies within roughly 1.96 standard deviations of the mean), which is usually used to approximate 95% confidence intervals.

SD is the standard deviation, calculated over the amount of repetitions for a particular experimental condition, in the case of PS; and the amount of subjects in the case of healthy controls.

In general, the SSFRE of PS was lower than that of controls since for most of the stimulation frequencies PS values lied along the lower CI of the age - matched participants. For stimulation frequencies of 5.00, 9.09 and 10.00 Hz; the SSFRE of PS fell completely out of the CI defined by the controls (Figure 4.9).

#### 4.1.3.2 Experiment 2

Given that experiment 1 showed that the magnitude of PS brain signal increased at the frequency value that corresponded to the stimulation frequency and for the sake

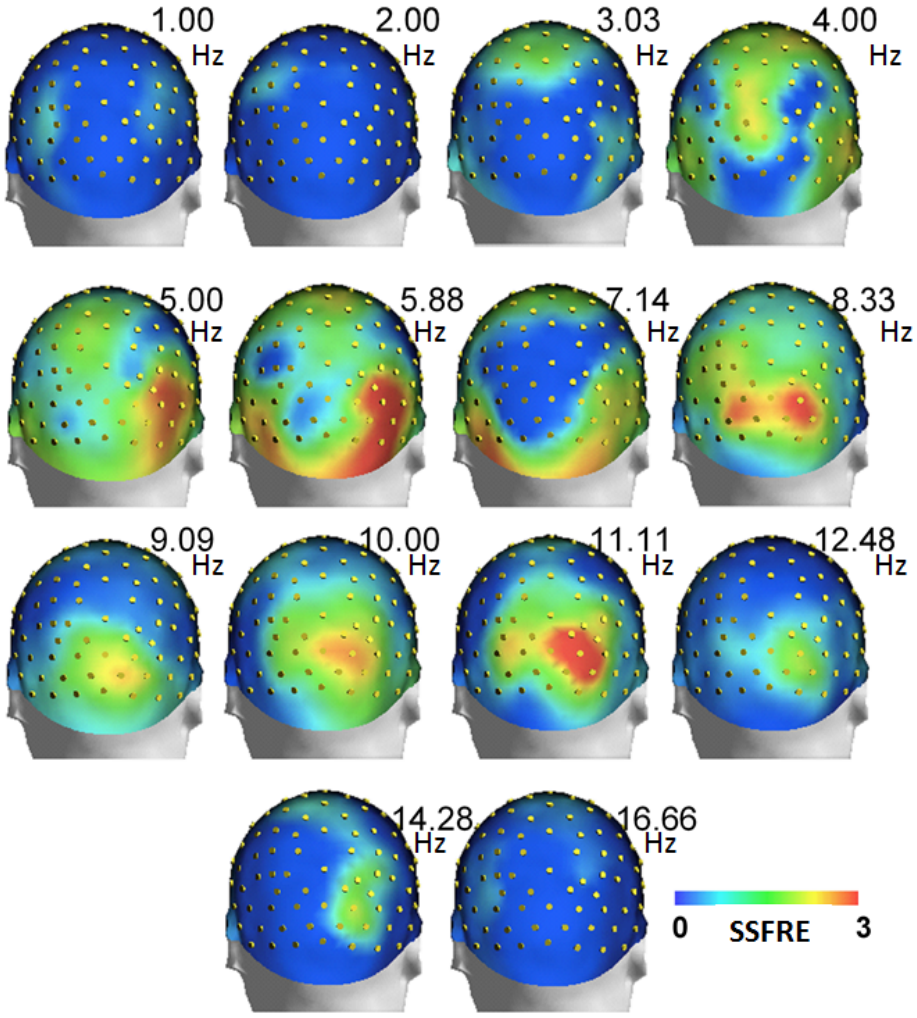


**Figure 4.8: SSFRE topographic distribution for healthy controls, sex and age matched with PS.** - The SSFRE corresponding to healthy participants is displayed. Note that the SSFRE is highest over occipito-temporal electrodes in the right hemisphere especially at 5.88 Hz.

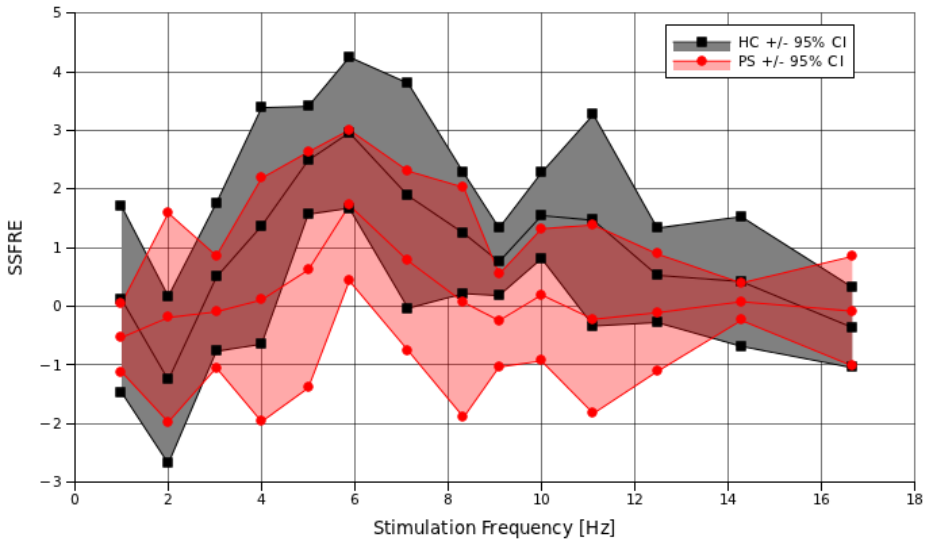


**Figure 4.9: SSFRE frequency sensitivity curve of PS and age matched controls together with confidence intervals.** - The SSFRE corresponding to PS and healthy controls is displayed together with 95% confidence intervals. Note that although the SSFRE of PS described the same bell shaped distribution characteristic of controls, her values lied along the lowest confidence interval for most of the stimulation frequencies.

of brevity, only the results concerned with her SSFRE in response to different types of faces will be presented.

Figure 4.10 shows that KDEF stimuli elicited the highest SSFRE. Its topographic distribution is noticeably similar to the topographic distribution of the SSFRE elicited by the MP faces at 5.88 Hz in experiment 1: it is maximal in the right hemisphere over parieto-temporal and occipital electrodes forming two well defined scalp regions. The RC faces elicit also a high SSFRE although smaller when compared to the effect provoked by KDEF stimuli. As in the case of the KDEF, its right hemisphere distribution encompasses parieto-temporal and occipital electrodes but, in contrast to the KDEF faces, it is present also in the left hemisphere. Interesting enough, the SSFRE is observable only in the left hemisphere for the RCG faces.

### 4.1.4 Discussion

The results obtained in experiment 1 demonstrated that, as in the case of healthy individuals, PS brain signal can be driven by the presentation of either identical or different faces at temporal rates between 1.00 and 16.66 Hz. The overall magnitude of her EEG signal increases when different faces are presented. This increase is specially accentuated for presentation rates between 2.00 and 11.11 Hz and its maximal

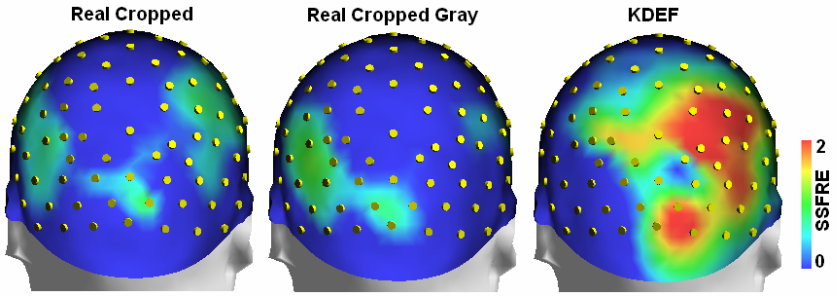


**Figure 4.10: SSFRE topographic distribution for PS in response to the different types of facial stimuli used in this study.** -

at 5.88 Hz. These results demonstrate that the SSVEP technique can also be used to study patient PS and that the optimal testing conditions in her case coincide with those found for healthy controls. This is important because it allows future studies to homogenize the experimental conditions between PS and controls and, consequently, perform direct intergroup comparisons.

However, her SSFRE diverge qualitatively and quantitatively from that observed in controls. Qualitatively, its topographic distribution encompasses parieto-occipital electrodes, which also exhibit face sensitivity in ERP studies of faces but are located slightly higher than the electrodes with the highest SSFRE in the controls tested here. Additionally and in contrast to controls, it also encompasses occipito-temporal electrodes located in the lower part of the back side of the head. This topographic distribution resembles the topography previously observed in an N170 study of the same patient (Study 1 in this thesis). It may be the result of brain volume conductivity changes due to the OFA lesion but it may also be due to the activation of the lateral occipital complex (LOC). This area, which responds more strongly when pictures of object shapes are presented preserving low level visual information such as texture, visual noise or scrambled objects (Grill-Spector *et al.*, 1999; Vinberg & Grill-Spector, 2008) supports PS residual ability to discriminate individual faces as recently demonstrated in an fMRI adaptation study of this patient (Dricot *et al.*, 2008a).

Quantitatively, the magnitude of the SSFRE in PS is in general lower than that of controls. This finding is in line with the idea that her ability to discriminate individual face exemplars is supported by an area not specialized for faces, the LOC, and that behaviorally her performance is deficient although above chance level (Rossion, 2003).

In the second experiment, it was shown that, in general, the SSFRE of patient PS is present for different types of faces. Especially, the response evoked by the KDEF faces is highly similar in magnitude and scalp distribution to that obtained for the MP faces in the first experiment. In contrast, the magnitude of the SSFRE obtained in response to RC and RCG faces decreased compared to the SSFRE obtained for KDEF

and MP faces. Even further, it completely disappeared from the right hemisphere in the case of RCG faces. It is well known that prosopagnosic patients use facial cues such as hair, skin color or face shape line to discriminate faces (Damasio *et al.*, 1982; Hecaen & Angelergues, 1962; Rossion, 2003). When these cues are removed their performance is impoverished (Damasio *et al.*, 1982; Hecaen & Angelergues, 1962; Meadows, 1974). Consequently, it is not surprising to see that a decrease in the amount of information that can indicate face identity changes provoke a decrease in the SSFRE of patient PS. This finding also straightens the sensitivity of the technique in general to detect even subtle changes in the efficiency of face perception processes.

### 4.1.5 Conclusions

Here we confirmed that the SSVEP technique can be used to study prosopagnosic patients since it is sensitive to the activation of the face perception system even when damaged. It was also shown that the experimental conditions that elicit the optimal response in healthy individuals can be applied to PS, an observation that can be used by future studies of this patient.

# Chapter 5

# General discussion and future perspectives

The last decades have experienced an increasing scientific interest in the neurophysiological mechanisms underlying face perception. Just introducing these two very generic keywords, "face perception", in Pubmed search engine retrieves 25 papers published between 1990 and 1995, 47 papers published between 1996 and 2000, 117 published between 2001 and 2005 and 275 published between 2005 and 2010.

The gathered evidence strongly supports the face selectivity of specific brain regions. It has also helped to elucidate the nature of the facial information these anatomical structures encode and process. However, debate still exists regarding the functional organization and timing of the activations of these distributed group of areas. This issue has remained elusive mainly because its solution demands obtaining combined information about where in the brain and when a given process takes place. One way to obtain such information is studying prosopagnosic patients, who have lost the ability to recognize people's identity based on their facial appearance after lesions to specific brain areas, by means of the EEG/MEG. This way, anatomical information is provided by the lesional profile of the patients and time information is given by the EEG/MEG. This approach has been adopted in this thesis to address several open questions about face perception and also to characterize the electrophysiological profile of a pure case of prosopagnosia.

In the second chapter of this thesis the focus of interest relied on the following issues:

1. Timing of the face selective activation of area FFA.

   Does the FFA exhibit face selective activations during the first stages of face processing even in the absence of inputs from the lower visual area OFA?

2. Neural generators of the face selective ERP, N170.

   Is the OFA an indispensable neural source of the N170?

3. Characterization of the electrophysiological profile of prosopagnosic patient PS.

Study 1 demonstrated that prosopagnosic patient PS, who has damage to the right OFA, exhibited both the face selective ERP named N170 and the face selective ERF named M170. Given that these components are the first and most reliable responses that can be recorded on the human scalp and that the FFA is one of their possible neural sources, the study suggested that the FFA is active within early stages of face perception even in absence of feedforward inputs from the OFA. This observation provided further support to a non-hierarchical model of face perception. Such model, introduced by Rossion and colleagues, proposes that the OFA is not a necessary entry point to the face processing network and that face selectivity in lower visual areas may arise as a result of feedback inputs from higher areas.

Study 1 also showed that the OFA was not an indispensable neural source of the component N170 shedding light on a debate that has prevailed in the N170 literature for a long time.

In addition, Study 1 characterized the electrophysiological profile of patient PS. This is important because PS is a case of pure prosopagnosia whose study had proven to be very useful to respond specific theoretical questions about face perception. She has been extensively studied with fMRI but not with EEG or MEG, loosing the possibility of obtaining valuable information on the temporal activation course of face selective areas. Study 1 showed that analyzing PS' EEG recordings is complicated because changes in the volume conductivity properties of the brain tissue after the lesion may affect her scalp signal by increasing the noise and modifying the morphology of the ERP waveforms. The characterization attained here will help to interpret the results of future EEG studies of this patient.

But this last result also demonstrated the need to find EEG measures more suitable for the study of prosopagnosic patients. The SSVEP could be such measure considering that it has a high signal-to-noise ratio, can be acquired reliably in brief periods of time and can be easily quantified in the frequency domain independently of the morphology of the waveform.

Motivated by these observations, Studies 2 and 3 focused on the following issues:

1. Defining the optimal experimental conditions to be used in SSVEP studies of face perception.

   Is the SSVEP sensitive to changes in the identity of different types of faces, which diverge in gender, skin color and presence of hair?

At which stimulus presentation rate the SSVEP sensitivity to facial identity is highest?

Regarding the first question, Study 2 demonstrated that the SSVEP sensitivity to facial identity appeared despite modifications of the stimulus characteristics such as gender, presence of skin color or hair. Given that such sensitivity increased for faces that presented more cues that are diagnostic for face individualization, the results indicated that the SSVEP can capture even subtle changes in the activation of the face perception brain network. Finally, Study 2 characterized the time evolution of the SSVEP to faces of varying identity showing that the transient components P1 and N170 appeared soon after the beginning of the stimulation and were followed by a steady state response which increased its magnitude exactly when changes in the identity of the face were introduced.

Regarding the second question, Study 3 showed that the strength of the SSVEP sensitivity to facial identity varied as a function of stimulation frequency. Thus, it is highest between 4.00 and 9.09 Hz and especially pronounced at 5.88 Hz. This range of frequencies coincide with the temporal activation course of the face perception system, as determined by electrophysiological recordings in humans and animals. Consequently, the results of Study 3 suggested that the neuronal response, which is forced to be produced at a certain rate by the rhythmic stimulation, will be highest when the pace of the stimulation guarantees that a large amount of neurons summate their responses. An increase in the synchronization of the neuronal response will result in an amplification of the output along the targeted neuronal network and will cause a noticeable augment in the amplitude of the signal registered on the scalp.

Study 3 also demonstrated that the SSVEP to faces is composed of additional components multiple of the stimulation frequency. The influence of variations in the identity of the face was higher for some of the harmonics of the lowest stimulation frequencies, suggesting that when such low stimulation frequencies are employed, the effect of experimental manipulations should be also studied at the higher harmonics. Harmonics of the highest stimulation frequencies exhibited changes in the topographical distribution of the SSVEP to identity variations. This result suggested that these harmonics may have been sensitive to variations in the cognitive strategies used to process the stimuli and also to variations in the neuronal substrates of the scalp signal.

As the main motivation of the above reviewed experiments was to use the SSVEP technique to study prosopagnosic patients as an alternative to ERP, a fourth study was performed to demonstrate that the experimental parameters that were able to elicit the highest SSVEP sensitivity to facial identity in healthy individuals could be extrapolated to patient PS. Experiment 1 of Study 4 showed that indeed, PS presented the same frequency sensitivity curve as healthy individuals although the magnitude of her response was decreased. Experiment 2 of the same study demonstrated that

her SSVEP to different faces appeared despite changes in the characteristics of the stimulus. However, it decreased when diagnostic cues were removed. It is well known that prosopagnosic patients use various cues to discriminate between different faces. Removing those cues significantly impair these patients at face discrimination tasks. Consequently, the obtained results give further support to the observation that the SSVEP is suitable to study face perception processes.

In pursuing this line of research, several questions were answered but also several questions remained open. For example, it is still not known whether the optimal testing conditions identified here can be extrapolated to other prosopagnosic patients with lesional profiles different to that of PS. Preliminary studies not reported here suggest that this does not need to be the case. In fact, prosopagnosic patient LR, who has extensive brain damage to the right temporal lobe, does not exhibit the highest SSVEP to faces of varying identity at 5.88 Hz but at 2.00 Hz. If this result is confirmed, it will indicate that future SSVEP studies of prosopagnosic patients have to choose carefully the stimulation frequency to use. The role of the response harmonics in prosopagnosic patients also needs further study. It was demonstrated here that, in healthy individuals, face identity variations can influence the magnitude and topographic distribution of the SSVEP at frequencies multiple of the stimulation frequency. This results suggested that harmonics can reflect the involvement of additional face selective areas and the adoption of different face processing strategies.

Further exploration of these possibilities will help neuroscientists not only to gain more detailed knowledge about the neural signature of face perception but also to learn more about key organizational principles of the human brain.

# References


Adolphs, R., Tranel, D., Damasio, H. & Damasio, A.R. (1995). Fear and the human amygdala. *The Journal of Neuroscience: The Official Journal of the Society for Neuroscience*, **15**, 5879–5891, PMID: 7666173. 22

Ales, J.M. & Norcia, A.M. (2009). Assessing direction-specific adaptation using the steady-state visual evoked potential: results from EEG source imaging. *Journal of Vision*, **9**, 8, PMID: 19761323. 129

Ales, J.M., Yates, J.L. & Norcia, A.M. (2010). V1 is not uniquely identified by polarity reversals of responses to upper and lower visual field stimuli. *NeuroImage*, **52**, 1401–1409, PMID: 20488247. 11

Allison, T., Ginter, H., McCarthy, G., Nobre, A.C., Puce, A., Luby, M. & Spencer, D.D. (1994). Face recognition in human extrastriate cortex. *Journal of Neurophysiology*, **71**, 821 –825. 47, 53

Allison, T., Puce, A., Spencer, D.D. & McCarthy, G. (1999). Electrophysiological studies of human face perception. i: Potentials generated in occipitotemporal cortex by face and non-face stimuli. *Cerebral Cortex (New York, N.Y.: 1991)*, **9**, 415–430, PMID: 10450888. 2, 30, 31, 47, 130

Alonso, E., Caharel, S., Henson, R. & Rossion, B. (2011). Early (N170) face-sensitivity despite right lateral occipital brain damage in acquired prosopagnosia. *Fronteers of Neuroscience (in revision)*. 167

Amzica, F., Nuñez, A. & Steriade, M. (1992). Delta frequency (1-4 hz) oscillations of perigeniculate thalamic neurons and their modulation by light. *Neuroscience*, **51**, 285–294, PMID: 1465193. 94

Andersen, S.K., Müller, M.M. & Hillyard, S.A. (2009). Color-selective attention need not be mediated by spatial attention. *Journal of Vision*, **9**, 2.1–7, PMID: 19761293. 129

Andrews, T.J., Davies-Thompson, J., Kingstone, A. & Young, A.W. (2010). Internal and external features of the face are represented holistically in Face-Selective regions of visual cortex. *The Journal of Neuroscience*, **30**, 3544 –3552. 87, 98, 127

Appelbaum, L.G., Wade, A.R., Vildavski, V.Y., Pettet, M.W. & Norcia, A.M. (2006). Cue-invariant networks for figure and background processing in human visual cortex. *The Journal of Neuroscience: The Official Journal of the Society for Neuroscience*, **26**, 11695–11708, PMID: 17093091. 97, 129

Appelbaum, L.G., Wade, A.R., Pettet, M.W., Vildavski, V.Y. & Norcia, A.M. (2008). Figure-ground interaction in the human visual cortex. *Journal of Vision*, **8**, 8.1–19, PMID: 18831644. 97, 129

Atkinson, A.P. & Adolphs, R. (2011). The neuropsychology of face perception: beyond simple dissociations and functional selectivity. *Philosophical Transactions of the Royal Society B: Biological Sciences*, **366**, 1726 –1738. 1, 48

Axelrod, V. & Yovel, G. (2010). External facial features modify the representation of internal facial features in the fusiform face area. *NeuroImage*, **52**, 720–725. 127

Azzena, G.B., Conti, G., Santarelli, R., Ottaviani, F., Paludetti, G. & Maurizi, M. (1995). Generation of human auditory steady-state responses (SSRs). i: Stimulus rate effects. *Hearing Research*, **83**, 1–8, PMID: 7607975. 17, 19

Baker, T.J., Norcia, A.M. & Rowan Candy, T. (2011). Orientation tuning in the visual cortex of 3-month-old human infants. *Vision Research*, **51**, 470–478, PMID: 21236289. 12

Barbeau, E.J., Taylor, M.J., Regis, J., Marquis, P., Chauvel, P. & Liégeois-Chauvel, C. (2008). Spatio temporal dynamics of face recognition. *Cerebral Cortex*, **18**, 997 –1009. 2

Barton, J.J.S. (2008a). Prosopagnosia associated with a left occipitotemporal lesion. *Neuropsychologia*, **46**, 2214–2224, PMID: 18374372. 24, 25

Barton, J.J.S. (2008b). Structure and function in acquired prosopagnosia: lessons from a series of 10 patients with brain damage. *Journal of Neuropsychology*, **2**, 197–225, PMID: 19334311. 24

Barton, J.J.S., Press, D.Z., Keenan, J.P. & O'Connor, M. (2002). Lesions of the fusiform face area impair perception of facial configuration in prosopagnosia. *Neurology*, **58**, 71–78, PMID: 11781408. 24, 33, 47

Başar, E. (1972). A study of the time and frequency characteristics of the potentials evoked in the acoustical cortex. *Kybernetik*, **10**, 61–64, PMID: 5028692. 94

Basar, E. (1980). *EEG-brain dynamics : relation between EEG and Brain evoked potentials*. Elsevier/North-Holland Biomedical Press ,sole distributors for the U.S.A. and Canada Elsevier North-Holland, Amsterdam ;;New York ;New York N.Y. 20, 94

Basar, E. (1998). *Brain Function and Oscillations: Volume II: Integrative Brain Function. Neurophysiology and Cognitive Processes*. Springer, 1st edn. 20, 161

Baylis, G.C. & Rolls, E.T. (1987). Responses of neurons in the inferior temporal cortex in short term and serial recognition memory tasks. *Experimental Brain Research. Experimentelle Hirnforschung. Expérimentation Cérébrale*, **65**, 614–622, PMID: 3556488. 97

Bayram, A., Bayraktaroglu, Z., Karahan, E., Erdogan, B., Bilgic, B., Ozker, M., Kasikci, I., Duru, A.D., Ademoglu, A., Oztürk, C., Arikan, K., Tarhan, N. & Demiralp, T. (2011). Simultaneous EEG/fMRI analysis of the resonance phenomena in steady-state visual evoked responses. *Clinical EEG and Neuroscience: Official Journal of the EEG and Clinical Neuroscience Society (ENCS)*, **42**, 98–106, PMID: 21675599. 93, 94

# REFERENCES


Begleiter, H., Porjesz, B. & Wang, W. (1995). Event-related brain potentials differentiate priming and recognition to familiar and unfamiliar faces. *Electroencephalography and Clinical Neurophysiology*, **94**, 41–49, PMID: 7530638. 99

Behrmann, M., Avidan, G., Marotta, J.J. & Kimchi, R. (2005). Detailed exploration of face-related processing in congenital prosopagnosia: 1. behavioral findings. *Journal of Cognitive Neuroscience*, **17**, 1130–1149, PMID: 16102241. 23

Bentin, S. & Golland, Y. (2002). Meaningful processing of meaningless stimuli: the influence of perceptual experience on early visual processing of faces. *Cognition*, **86**, B1–14, PMID: 12208653. 40

Bentin, S., Allison, T., Puce, A., Perez, E. & McCarthy, G. (1996). Electrophysiological studies of face perception in humans. *Journal of Cognitive Neuroscience*, **8**, 551–565, PMID: 20740065. 2, 12, 38, 40, 48, 53, 85, 130, 162

Bentin, S., Deouell, L.Y. & Soroker, N. (1999). Selective visual streaming in face recognition: evidence from developmental prosopagnosia. *Neuroreport*, **10**, 823–827, PMID: 10208555. 49

Bentin, S., Degutis, J.M., D'Esposito, M. & Robertson, L.C. (2007). Too many trees to see the forest: performance, event-related potential, and functional magnetic resonance imaging manifestations of integrative congenital prosopagnosia. *Journal of Cognitive Neuroscience*, **19**, 132–146, PMID: 17214570. 49

Benton, A.L. (1980). The neuropsychology of facial recognition. *The American Psychologist*, **35**, 176–186, PMID: 7369623. 24

Benton, A.L., Sivan, A.B., Hamsher, K.d., Varney, N.R. & Spreen, O. (1994). *Contributions to Neuropsychological Assessment: A Clinical Manual*. Oxford University Press, USA, 2nd edn. 26

Betts, L.R. & Wilson, H.R. (2010). Heterogeneous structure in face-selective human occipito-temporal cortex. *Journal of Cognitive Neuroscience*, **22**, 2276–2288, PMID: 19803682. 127

Blanz, V. & Vetter, T. (1999). A morphable model for the synthesis of 3D faces. In *Proceedings of the 26th annual conference on Computer graphics and interactive techniques*, SIGGRAPH '99, 187–194, ACM Press/Addison-Wesley Publishing Co., ACM ID: 311556. 100

Bobes, M.A., Lopera, F., Garcia, M., Díaz-Comas, L., Galan, L. & Valdes-Sosa, M. (2003). Covert matching of unfamiliar faces in a case of prosopagnosia: an ERP study. *Cortex; a Journal Devoted to the Study of the Nervous System and Behavior*, **39**, 41–56, PMID: 12627752. 49, 88

Bodamer, J. (1947). Die prosop-agnosie. *Archive fuer Psychiatrie und Nervenkrankheiten*, **179**, 6–54. 2, 22, 23, 30, 47

Boetzel, K. & Gruesser, O.J. (1989). Electric brain potentials evoked by pictures of faces and non-faces: a search for "face-specific" EEG-potentials. *Experimental Brain Research*, **77**, 349–360, PMID: 2792281. 12, 38

Boetzel, K., Schulze, S. & Stodieck, S.R. (1995). Scalp topography and analysis of intracranial sources of face-evoked potentials. *Experimental Brain Research*, **104**, 135–143, PMID: 7621932. 2, 38, 45, 48, 49, 130

Bohorquez, J. & Ozdamar, O. (2008). Generation of the 40-Hz auditory steady-state response (ASSR) explained using convolution. *Clinical Neurophysiology: Official Journal of the International Federation of Clinical Neurophysiology*, **119**, 2598–2607, PMID: 18818122. 17, 19

Bouvier, S.E. & Engel, S.A. (2006). Behavioral deficits and cortical damage loci in cerebral achromatopsia. *Cerebral Cortex (New York, N.Y.: 1991)*, **16**, 183–191, PMID: 15858161. 24, 33, 47

Braddick, O.J., Wattam-Bell, J. & Atkinson, J. (1986). Orientation-specific cortical responses develop in early infancy. *Nature*, **320**, 617–619. 129

Breiter, H.C., Etcoff, N.L., Whalen, P.J., Kennedy, W.A., Rauch, S.L., Buckner, R.L., Strauss, M.M., Hyman, S.E. & Rosen, B.R. (1996). Response and habituation of the human amygdala during visual processing of facial expression. *Neuron*, **17**, 875–887, PMID: 8938120. 36

Broca (1865). Sur le siege de la faculte du langage articule. *Bulletins de la Societe d'anthropologie de Paris*, **6**, 377–393. 22

Brown, R.J. & Norcia, A.M. (1997). A method for investigating binocular rivalry in real-time with the steady-state VEP. *Vision Research*, **37**, 2401–2408, PMID: 9381675. 12, 97

Bukach, C.M., Bub, D.N., Gauthier, I. & Tarr, M.J. (2006). Perceptual expertise effects are not all or none: spatially limited perceptual expertise for faces in a case of prosopagnosia. *Journal of Cognitive Neuroscience*, **18**, 48–63, PMID: 16417682. 30

Busigny, T., Joubert, S., Felician, O., Ceccaldi, M. & Rossion, B. (2010). Holistic perception of the individual face is specific and necessary: evidence from an extensive case study of acquired prosopagnosia. *Neuropsychologia*, **48**, 4057–4092, PMID: 20875437. 25, 50, 51, 85, 166

Buzsaki, G. (2006). *Rhythms of the Brain*. Oxford University Press, USA, 1st edn. 6, 8, 95, 105, 161, 189

Caharel, S., d'Arripe, O., Ramon, M., Jacques, C. & Rossion, B. (2009a). Early adaptation to repeated unfamiliar faces across viewpoint changes in the right hemisphere: evidence from the n170 ERP component. *Neuropsychologia*, **47**, 639–643, PMID: 19084547. 2

Caharel, S., Jiang, F., Blanz, V. & Rossion, B. (2009b). The human brain recognizes individual faces faster from shape than surface reflectance diagnostic information. *Journal of Vision*, **9**, 548. 99, 130

Caldara, R., Schyns, P., Mayer, E., Smith, M.L., Gosselin, F. & Rossion, B. (2005). Does prosopagnosia take the eyes out of face representations? evidence for a defect in representing diagnostic facial information following brain damage. *Journal of Cognitive Neuroscience*, **17**, 1652–1666, PMID: 16269103. 25, 26, 168

Calder, A.J., Keane, J., Manes, F., Antoun, N. & Young, A.W. (2000). Impaired recognition and experience of disgust following brain injury. *Nature Neuroscience*, **3**, 1077–1078, PMID: 11036262. 22

Calder, A.J., Beaver, J.D., Winston, J., Dolan, R.J., Jenkins, R., Eger, E. & Henson, R.N. (2007). Separate coding of different gaze directions in the superior temporal sulcus. http://eprints.gla.ac.uk/32838/. 31

Campbell, F.W. & Maffei, L. (1970). Electrophysiological evidence for the existence of orientation and size detectors in the human visual system. *The Journal of Physiology*, **207**, 635–652, PMID: 54997405499740 PMCID: 1348732. 129

Capilla, A., Pazo-Alvarez, P., Darriba, A., Campo, P. & Gross, J. (2011). Steady-state visual evoked potentials can be explained by temporal superposition of transient event-related responses. *PloS One*, **6**, e14543, PMID: 21267081. 17, 19

Catani, M., Jones, D.K., Donato, R. & Ffytche, D.H. (2003). Occipito-temporal connections in the human brain. *Brain: A Journal of Neurology*, **126**, 2093–2107, PMID: 12821517. 87

Chen, Y., Seth, A.K., Gally, J.A. & Edelman, G.M. (2003). The power of human brain magnetoencephalographic signals can be modulated up or down by changes in an attentive visual task. *Proceedings of the National Academy of Sciences of the United States of America*, **100**, 3501–3506, PMID: 12626756. 97, 103

Clark, V.P. & Hillyard, S.A. (1996). Spatial selective attention affects early extrastriate but not striate components of the visual evoked potential. *J. Cognitive Neuroscience*, **8**, 387–402, ACM ID: 1596849. 162

Conti, G., Santarelli, R., Grassi, C., Ottaviani, F. & Azzena, G.B. (1999). Auditory steady-state responses to click trains from the rat temporal cortex. *Clinical Neurophysiology*, **110**, 62–70. 19

Crawford, J.R., Garthwaite, P.H. & Howell, D.C. (2009). On comparing a single case with a control sample: an alternative perspective. *Neuropsychologia*, **47**, 2690–2695, PMID: 19383506. 57, 67, 73

Dalrymple, K.A., Oruc, I., Duchaine, B., Pancaroglu, R., Fox, C.J., Iaria, G., Handy, T.C. & Barton, J.J.S. (2011). The anatomic basis of the right face-selective n170 IN acquired prosopagnosia: A combined ERP/fMRI study. *Neuropsychologia*, **49**, 2553–2563, PMID: 21601585. 49, 86, 88

Damasio, A.R., Damasio, H. & Van Hoesen, G.W. (1982). Prosopagnosia: anatomic basis and behavioral mechanisms. *Neurology*, **32**, 331–341, PMID: 7199655. 24, 30, 33, 47, 180

Dawson, G.D. (1954). A summation technique for the detection of small evoked potentials. *Electroencephalography and Clinical Neurophysiology*, **6**, 65–84, PMID: 13141922. 10, 11

De Haan, E.H. (1999). A familial factor in the development of face recognition deficits. *Journal of Clinical and Experimental Neuropsychology*, **21**, 312–315, PMID: 10474170. 23

De Renzi, E., Perani, D., Carlesimo, G.A., Silveri, M.C. & Fazio, F. (1994). Prosopagnosia can be associated with damage confined to the right hemisphere–an MRI and PET study and a review of the literature. *Neuropsychologia*, **32**, 893–902, PMID: 7969865. 24

Deffke, I., Sander, T., Heidenreich, J., Sommer, W., Curio, G., Trahms, L. & Lueschow, A. (2007). MEG/EEG sources of the 170-ms response to faces are co-localized in the fusiform gyrus. *NeuroImage*, **35**, 1495–1501, PMID: 17363282. 45, 49

Desimone, R. (2011). Face-Selective cells in the temporal cortex of monkeys. *Journal of Cognitive Neuroscience*, **3**, 1–8. 30

Desimone, R., Albright, T.D., Gross, C.G. & Bruce, C. (1984). Stimulus-selective properties of inferior temporal neurons in the macaque. *The Journal of Neuroscience: The Official Journal of the Society for Neuroscience*, **4**, 2051–2062, PMID: 6470767. 30

Di Russo, F., Martinez, A., Sereno, M.I., Pitzalis, S. & Hillyard, S.A. (2002). Cortical sources of the early components of the visual evoked potential. *Human Brain Mapping*, **15**, 95–111. 11, 162

Di Russo, F., Martinez, A. & Hillyard, S.A. (2003). Source analysis of event-related cortical activity during visuo-spatial attention. *Cerebral Cortex*, **13**, 486 –499. 11

Ding, J., Sperling, G. & Srinivasan, R. (2006). Attentional modulation of SSVEP power depends on the network tagged by the flicker frequency. *Cerebral Cortex (New York, N.Y.: 1991)*, **16**, 1016–1029, PMID: 16221931. 93

Dricot, L., Sorger, B., Schiltz, C., Goebel, R. & Rossion, B. (2008a). Evidence for individual face discrimination in non-face selective areas of the visual cortex in acquired prosopagnosia. *Behavioural Neurology*, **19**, 75–79, PMID: 18413922. 25, 179

Dricot, L., Sorger, B., Schiltz, C., Goebel, R. & Rossion, B. (2008b). The roles of "face" and "non-face" areas during individual face perception: evidence by fMRI adaptation in a brain-damaged prosopagnosic patient. *NeuroImage*, **40**, 318–332, PMID: 18164628. 25, 26, 33

Duchaine, B.C., Nieminen-von Wendt, T., New, J. & Kulomäki, T. (2003). Dissociations of visual recognition in a developmental agnosic: evidence for separate developmental processes. *Neurocase*, **9**, 380–389, PMID: 14972753. 23

Eckhorn, R., Bauer, R., Jordan, W., Brosch, M., Kruse, W., Munk, M. & Reitboeck, H.J. (1988). Coherent oscillations: a mechanism of feature linking in the visual cortex? multiple electrode and correlation analyses in the cat. *Biological Cybernetics*, **60**, 121–130, PMID: 3228555. 94

Eimer, M. (1998). Does the face-specific n170 component reflect the activity of a specialized eye processor? *Neuroreport*, **9**, 2945–2948, PMID: 9804295. 43

Eimer, M. (2000a). Event-related brain potentials distinguish processing stages involved in face perception and recognition. *Clinical Neurophysiology: Official Journal of the International Federation of Clinical Neurophysiology*, **111**, 694–705, PMID: 10727921. 2, 43, 162

Eimer, M. (2000b). The face-specific n170 component reflects late stages in the structural encoding of faces. *Neuroreport*, **11**, 2319–2324, PMID: 10923693. 2

Eimer, M. & McCarthy, R.A. (1999). Prosopagnosia and structural encoding of faces: evidence from event-related potentials. *Neuroreport*, **10**, 255–259, PMID: 10203318. 24, 25, 49

Ellis, A.W. (1992). Cognitive mechanisms of face processing. *Philosophical Transactions of the Royal Society of London. Series B, Biological Sciences*, **335**, 113–119, PMID: 1348131. 36

# REFERENCES


Ellis, H.D., Shepherd, J.W. & Davies, G.M. (1979). Identification of familiar and unfamiliar faces from internal and external features: some implications for theories of face recognition. *Perception*, **8**, 431–439, PMID: 503774. 98, 127

Enslein, K. & etc (1977). *Statistical Methods for Digital Computers: Vol.3*. John Wiley & Sons Inc. 13

Evans, J.J., Heggs, A.J., Antoun, N. & Hodges, J.R. (1995). Progressive prosopagnosia associated with selective right temporal lobe atrophy. a new syndrome? *Brain: A Journal of Neurology*, **118 ( Pt 1)**, 1–13, PMID: 7894996. 23

Ewbank, M.P., Smith, W.A.P., Hancock, E.R. & Andrews, T.J. (2008). The m170 reflects a viewpoint-dependent representation for both familiar and unfamiliar faces. *Cerebral Cortex (New York, N.Y.: 1991)*, **18**, 364–370, PMID: 17507454. 2, 85

Fairhall, S.L. & Ishai, A. (2007). Effective connectivity within the distributed cortical network for face perception. *Cerebral Cortex (New York, N.Y.: 1991)*, **17**, 2400–2406, PMID: 17190969. 48

Fawcett, I.P., Barnes, G.R., Hillebrand, A. & Singh, K.D. (2004). The temporal frequency tuning of human visual cortex investigated using synthetic aperture magnetometry. *NeuroImage*, **21**, 1542–1553, PMID: 15050578. 12

Foeldiak, P., Xiao, D., Keysers, C., Edwards, R. & Perrett, D.I. (2004). Rapid serial visual presentation for the determination of neural selectivity in area STSa. *Progress in Brain Research*, **144**, 107–116, PMID: 14650843. 30

Fox, C.J., Moon, S.Y., Iaria, G. & Barton, J.J.S. (2009). The correlates of subjective perception of identity and expression in the face network: an fMRI adaptation study. *NeuroImage*, **44**, 569–580, PMID: 18852053. 31, 34, 40

Fox, P.T. & Raichle, M.E. (1984). Stimulus rate dependence of regional cerebral blood flow in human striate cortex, demonstrated by positron emission tomography. *Journal of Neurophysiology*, **51**, 1109–1120, PMID: 6610024. 93, 95, 157, 161

Fox, P.T. & Raichle, M.E. (1985). Stimulus rate determines regional brain blood flow in striate cortex. *Annals of Neurology*, **17**, 303–305, PMID: 3873210. 93, 95, 157, 161

Freire, A., Lee, K. & Symons, L.A. (2000). The face-inversion effect as a deficit in the encoding of configural information: direct evidence. *Perception*, **29**, 159–170, PMID: 10820599. 43

Freiwald, W.A., Tsao, D.Y. & Livingstone, M.S. (2009). A face feature space in the macaque temporal lobe. *Nat Neurosci*, **12**, 1187–1196. 98

Fuentemilla, L., Marco-Pallarés, J. & Grau, C. (2006). Modulation of spectral power and of phase resetting of EEG contributes differentially to the generation of auditory event-related potentials. *NeuroImage*, **30**, 909–916, PMID: 16376575. 20

Galambos, R. (1982). Tactile and auditory stimuli repeated at high rates (30-50 per sec) produce similar event related potentials. *Annals of the New York Academy of Sciences*, **388**, 722–726. 12, 20

Galambos, R., Makeig, S. & Talmachoff, P.J. (1981). A 40-Hz auditory potential recorded from the human scalp. *Proceedings of the National Academy of Sciences of the United States of America*, **78**, 2643–2647, PMID: 6941317. 12, 17

Gauthier, I., Tarr, M.J., Moylan, J., Skudlarski, P., Gore, J.C. & Anderson, A.W. (2000). The fusiform "face area" is part of a network that processes faces at the individual level. *Journal of Cognitive Neuroscience*, **12**, 495–504, PMID: 10931774. 1, 31, 47

George, A. & Jose, J. (2009). Prosopagnosia: a rare presenting manifestation of frontotemporal lobar degeneration. *Neurology India*, **57**, 58–60, PMID: 19305079. 23

George, N., Evans, J., Fiori, N., Davidoff, J. & Renault, B. (1996). Brain events related to normal and moderately scrambled faces. *Brain Research. Cognitive Brain Research*, **4**, 65–76, PMID: 8883920. 2, 38, 53

George, N., Dolan, R.J., Fink, G.R., Baylis, G.C., Russell, C. & Driver, J. (1999). Contrast polarity and face recognition in the human fusiform gyrus. *Nat Neurosci*, **2**, 574–580. 35

George, N., Jemel, B., Fiori, N., Chaby, L. & Renault, B. (2005). Electrophysiological correlates of facial decision: insights from upright and upside-down mooney-face perception. *Brain Research. Cognitive Brain Research*, **24**, 663–673, PMID: 15890502. 40

Godefroy, O. & Bogousslavsky, J. (2007). *The Behavioral and Cognitive Neurology of Stroke*. Cambridge University Press, 1st edn. 23, 26

Goffaux, V., Gauthier, I. & Rossion, B. (2003). Spatial scale contribution to early visual differences between face and object processing. *Brain Research. Cognitive Brain Research*, **16**, 416–424, PMID: 12706221. 2, 43

Goffaux, V., Peters, J., Haubrechts, J., Schiltz, C., Jansma, B. & Goebel, R. (2011). From coarse to fine? spatial and temporal dynamics of cortical face processing. *Cerebral Cortex (New York, N.Y.: 1991)*, **21**, 467–476, PMID: 20576927. 48

Goldsmith, Z.G. & Liu, G.T. (2001). Facial recognition and prosopagnosia: past and present concepts. *Neuro-Ophthalmology*. 23

Grave de Peralta Menendez, R., Gonzalez Andino, S., Lantz, G., Michel, C.M. & Landis, T. (2001). Noninvasive localization of electromagnetic epileptic activity. i. method descriptions and simulations. *Brain Topography*, **14**, 131–137, PMID: 11797811. 45

Gray, C.M., Koenig, P., Engel, A.K. & Singer, W. (1989). Oscillatory responses in cat visual cortex exhibit intercolumnar synchronization which reflects global stimulus properties. *Nature*, **338**, 334–337, PMID: 2922061. 94

Grill-Spector, K. & Malach, R. (2001). fMR-adaptation: a tool for studying the functional properties of human cortical neurons. *Acta Psychologica*, **107**, 293–321, PMID: 11388140. 40, 97

Grill-Spector, K., Kushnir, T., Edelman, S., Avidan, G., Itzchak, Y. & Malach, R. (1999). Differential processing of objects under various viewing conditions in the human lateral occipital complex. *Neuron*, **24**, 187–203, PMID: 10677037. 179

Grill-Spector, K., Knouf, N. & Kanwisher, N. (2004). The fusiform face area subserves face perception, not generic within-category identification. *Nature Neuroscience*, **7**, 555–562, PMID: 15077112. 1, 31

Grill-Spector, K., Henson, R. & Martin, A. (2006). Repetition and the brain: neural models of stimulus-specific effects. *Trends in Cognitive Sciences*, **10**, 14–23, PMID: 16321563. 97

Gross, C.G., Rocha-Miranda, C.E. & Bender, D.B. (1972). Visual properties of neurons in inferotemporal cortex of the macaque. *Journal of Neurophysiology*, **35**, 96 –111. 30

Gutfreund, Y., yarom, Y. & Segev, I. (1995). Subthreshold oscillations and resonant frequency in guinea-pig cortical neurons: physiology and modelling. *The Journal of Physiology*, **483 ( Pt 3)**, 621–640, PMID: 7776248. 94

Halgren, E., Dale, A.M., Sereno, M.I., Tootell, R.B., Marinkovic, K. & Rosen, B.R. (1999). Location of human face-selective cortex with respect to retinotopic areas. *Human Brain Mapping*, **7**, 29–37, PMID: 9882088. 1, 31

Halgren, E., Raij, T., Marinkovic, K., Jousmaeki, V. & Hari, R. (2000). Cognitive response profile of the human fusiform face area as determined by MEG. *Cerebral Cortex (New York, N.Y.: 1991)*, **10**, 69–81, PMID: 10639397. 44, 45, 48

Hanslmayr, S., Klimesch, W., Sauseng, P., Gruber, W., Doppelmayr, M., Freunberger, R., Pecherstorfer, T. & Birbaumer, N. (2007). Alpha phase reset contributes to the generation of ERPs. *Cerebral Cortex (New York, N.Y.: 1991)*, **17**, 1–8, PMID: 16452640. 20

Hari, R., Haemaelaeinen, M. & Joutsiniemi, S.L. (1989). Neuromagnetic steady-state responses to auditory stimuli. *The Journal of the Acoustical Society of America*, **86**, 1033–1039, PMID: 2794240. 19

Harris, A. & Aguirre, G.K. (2010). Neural tuning for face wholes and parts in human fusiform gyrus revealed by FMRI adaptation. *Journal of Neurophysiology*, **104**, 336–345, PMID: 20505126. 33

Hasselmo, M.E., Rolls, E.T. & Baylis, G.C. (1989). The role of expression and identity in the face-selective responses of neurons in the temporal visual cortex of the monkey. *Behavioural Brain Research*, **32**, 203–218, PMID: 2713076. 2, 31

Haxby, Hoffman & Gobbini (2000). The distributed human neural system for face perception. *Trends in Cognitive Sciences*, **4**, 223–233, PMID: 10827445. 1, 2, 22, 31, 33, 35, 36, 47, 48, 127

Haxby, J.V., Ungerleider, L.G., Clark, V.P., Schouten, J.L., Hoffman, E.A. & Martin, A. (1999). The effect of face inversion on activity in human neural systems for face and object perception. *Neuron*, **22**, 189–199, PMID: 10027301. 31, 35, 89

Hecaen, H. & Angelergues, R. (1962). Agnosia for faces (prosopagnosia). *Archives of Neurology*, **7**, 92–100, PMID: 13905818. 180

Heinrich, S.P. (2010). Some thoughts on the interpretation of steady-state evoked potentials. *Documenta Ophthalmologica. Advances in Ophthalmology*, **120**, 205–214, PMID: 20101435. 17

Heinrich, S.P. & Bach, M. (2003). Adaptation characteristics of steady-state motion visual evoked potentials. *Clinical Neurophysiology: Official Journal of the International Federation of Clinical Neurophysiology*, **114**, 1359–1366, PMID: 12842735. 129

Heinze, H.J., Mangun, G.R., Burchert, W., Hinrichs, H., Scholz, M., Münte, T.F., Gös, A., Scherg, M., Johannes, S. & Hundeshagen, H. (1994). Combined spatial and temporal imaging of brain activity during visual selective attention in humans. *Nature*, **372**, 543–546, PMID: 7990926. 162

Heisz, J.J., Watter, S. & Shedden, J.M. (2006). Automatic face identity encoding at the n170. *Vision Research*, **46**, 4604–4614, PMID: 17097126. 2, 85

Henson, R.N., Mattout, J., Singh, K.D., Barnes, G.R., Hillebrand, A. & Friston, K. (2007). Population-level inferences for distributed MEG source localization under multiple constraints: application to face-evoked fields. *NeuroImage*, **38**, 422–438, PMID: 17888687. 45

Henson, R.N., Mouchlianitis, E. & Friston, K.J. (2009). MEG and EEG data fusion: simultaneous localisation of face-evoked responses. *NeuroImage*, **47**, 581–589, PMID: 19398023. 49, 86

Henson, R.N.A. & Rugg, M.D. (2003). Neural response suppression, haemodynamic repetition effects, and behavioural priming. *Neuropsychologia*, **41**, 263–270. 97

Herrmann, C.S. (2001). Human EEG responses to 1-100 hz flicker: resonance phenomena in visual cortex and their potential correlation to cognitive phenomena. *Experimental Brain Research. Experimentelle Hirnforschung. Expérimentation Cérébrale*, **137**, 346–353, PMID: 11355381. 12, 20, 91, 93, 129, 157

Herrmann, M.J., Ehlis, A., Ellgring, H. & Fallgatter, A.J. (2005a). Early stages (P100) of face perception in humans as measured with event-related potentials (ERPs). *Journal of Neural Transmission (Vienna, Austria: 1996)*, **112**, 1073–1081, PMID: 15583954. 43

Herrmann, M.J., Ehlis, A., Muehlberger, A. & Fallgatter, A.J. (2005b). Source localization of early stages of face processing. *Brain Topography*, **18**, 77–85, PMID: 16341576. 43, 45

Hillyard, S.A. & Anllo-Vento, L. (1998). Event-related brain potentials in the study of visual selectiveattention. *Proceedings of the National Academy of Sciences*, **95**, 781 –787. 11

Hillyard, S.A., Teder-Saelejaervi, W.A. & Muente, T.F. (1998). Temporal dynamics of early perceptual processing. *Current Opinion in Neurobiology*, **8**, 202–210, PMID: 9635203. 12, 97

Hoffman, E.A. & Haxby, J.V. (2000). Distinct representations of eye gaze and identity in the distributed human neural system for face perception. *Nature Neuroscience*, **3**, 80–84, PMID: 10607399. 2, 31, 35, 36

Hopf, J., Vogel, E., Woodman, G., Heinze, H. & Luck(Buzsaki, 2006; Nunez & Srinivasan, 2005)., S.J. (2002). Localizing visual discrimination processes in time and space. *Journal of Neurophysiology*, **88**, 2088–2095, PMID: 12364530. 12

# REFERENCES


Horovitz, S.G., Rossion, B., Skudlarski, P. & Gore, J.C. (2004). Parametric design and correlational analyses help integrating fMRI and electrophysiological data during face processing. *NeuroImage*, **22**, 1587–1595, PMID: 15275915. 86

Hsiao, J.H.w. & Cottrell, G. (2008). Two fixations suffice in face recognition. *Psychological Science*, **19**, 998–1006, PMID: 19000210. 101

Hubel, D.H. & Wiesel, T.N. (1962). Receptive fields, binocular interaction and functional architecture in the cat's visual cortex. *The Journal of Physiology*, **160**, 106–154.2, PMID: 14449617 PMCID: 1359523. 36

Hutcheon, B., Miura, R.M. & Puil, E. (1996). Subthreshold membrane resonance in neocortical neurons. *Journal of Neurophysiology*, **76**, 683–697, PMID: 8871191. 94

Illingworth, V. (1991). *The Penguin dictionary of physics / editor Valerie Illingworth*. London : Penguin. 17

Ishai, A. (2008). Let's face it: it's a cortical network. *NeuroImage*, **40**, 415–419, PMID: 18063389. 48

Ishai, A., Ungerleider, L.G., Martin, A., Schouten, J.L. & Haxby, J.V. (1999). Distributed representation of objects in the human ventral visual pathway. *Proceedings of the National Academy of Sciences of the United States of America*, **96**, 9379–9384, PMID: 10430951. 1

Ishai, A., Pessoa, L., Bikle, P.C. & Ungerleider, L.G. (2004). Repetition suppression of faces is modulated by emotion. *Proceedings of the National Academy of Sciences of the United States of America*, **101**, 9827 –9832. 36

Itier, R.J. & Taylor, M.J. (2002). Inversion and contrast polarity reversal affect both encoding and recognition processes of unfamiliar faces: a repetition study using ERPs. *NeuroImage*, **15**, 353–372, PMID: 11798271. 2, 38, 44

Itier, R.J. & Taylor, M.J. (2004). N170 or n1? spatiotemporal differences between object and face processing using ERPs. *Cerebral Cortex (New York, N.Y.: 1991)*, **14**, 132–142, PMID: 14704210. 12, 43, 45, 49

Jacques, C. & Rossion, B. (2006). The speed of individual face categorization. *Psychological Science*, **17**, 485–492, PMID: 16771798. 40, 49

Jacques, C. & Rossion, B. (2009). The initial representation of individual faces in the right occipito-temporal cortex is holistic: electrophysiological evidence from the composite face illusion. *Journal of Vision*, **9**, 8.1–16, PMID: 19761299. 43, 99

Jacques, C., d'Arripe, O. & Rossion, B. (2007). The time course of the inversion effect during individual face discrimination. *Journal of Vision*, **7**, 3, PMID: 17685810. 2, 40, 42, 85, 130

Jansen, B.H., Agarwal, G., Hegde, A. & Boutros, N.N. (2003). Phase synchronization of the ongoing EEG and auditory EP generation. *Clinical Neurophysiology: Official Journal of the International Federation of Clinical Neurophysiology*, **114**, 79–85, PMID: 12495767. 20

Jeffreys, D.A. (1989). A face-responsive potential recorded from the human scalp. *Experimental Brain Research. Experimentelle Hirnforschung. Expérimentation Cérébrale*, **78**, 193–202, PMID: 2591512. 12, 38, 48

Jeffreys, D.A. (1993). The influence of stimulus orientation on the vertex positive scalp potential evoked by faces. *Experimental Brain Research. Experimentelle Hirnforschung. Expérimentation Cérébrale*, **96**, 163–172, PMID: 8243578. 2, 38, 40

Jeffreys, D.A. (1996). Evoked potential studies of face and object processing. *Visual Cognition*, **3**, 1–38. 2, 38, 162

Jeffreys, D.A. & Axford, J.G. (1972). Source locations of pattern-specific components of human visual evoked potentials. i. component of striate cortical origin. *Experimental Brain Research. Experimentelle Hirnforschung. Expérimentation Cérébrale*, **16**, 1–21, PMID: 4646539. 162

Jiang, F., Dricot, L., Blanz, V., Goebel, R. & Rossion, B. (2009). Neural correlates of shape and surface reflectance information in individual faces. *Neuroscience*, **163**, 1078–1091, PMID: 19660529. 34

Kanwisher, N. & Yovel, G. (2006). The fusiform face area: a cortical region specialized for the perception of faces. *Philosophical Transactions of the Royal Society of London. Series B, Biological Sciences*, **361**, 2109–2128, PMID: 17118927. 1, 31, 32, 48

Kanwisher, N., McDermott, J. & Chun, M.M. (1997). The fusiform face area: A module in human extrastriate cortex specialized for face perception. *The Journal of Neuroscience*, **17**, 4302 –4311. 1, 31, 47, 48

Kaspar, K., Hassler, U., Martens, U., Trujillo-Barreto, N. & Gruber, T. (2010). Steady-state visually evoked potential correlates of object recognition. *Brain Research*, **1343**, 112–121, PMID: 20450897. 129

Kaufmann, C., Elbel, G.K., Goessl, C., Puetz, B. & Auer, D.P. (2001). Frequency dependence and gender effects in visual cortical regions involved in temporal frequency dependent pattern processing. *Human Brain Mapping*, **14**, 28–38, PMID: 11500988. 93

Keil, A., Gruber, T., Müller, M.M., Moratti, S., Stolarova, M., Bradley, M.M. & Lang, P.J. (2003). Early modulation of visual perception by emotional arousal: evidence from steady-state visual evoked brain potentials. *Cognitive, Affective & Behavioral Neuroscience*, **3**, 195–206, PMID: 14672156. 129

Kennerknecht, I., Grueter, T., Welling, B., Wentzek, S., Horst, J., Edwards, S. & Grueter, M. (2006). First report of prevalence of non-syndromic hereditary prosopagnosia (HPA). *American Journal of Medical Genetics. Part A*, **140**, 1617–1622, PMID: 16817175. 23

Khoe, W., Freeman, E., Woldorff, M.G. & Mangun, G.R. (2004). Electrophysiological correlates of lateral interactions in human visual cortex. *Vision Research*, **44**, 1659–1673, PMID: 15136002. 162

Kim, M., Ducros, M., Carlson, T., Ronen, I., He, S., Ugurbil, K. & Kim, D. (2006). Anatomical correlates of the functional organization in the human occipitotemporal cortex. *Magnetic Resonance Imaging*, **24**, 583–590, PMID: 16735179. 87

Kleinschmidt, A. & Cohen, L. (2006). The neural bases of prosopagnosia and pure alexia: recent insights from functional neuroimaging. *Current Opinion in Neurology*, **19**, 386–391, PMID: 16914978. 50

# REFERENCES


Klimesch, W., Schack, B., Schabus, M., Doppelmayr, M., Gruber, W. & Sauseng, P. (2004). Phase-locked alpha and theta oscillations generate the P1-N1 complex and are related to memory performance. *Brain Research. Cognitive Brain Research*, **19**, 302–316, PMID: 15062867. 20

Kovács, G., Zimmer, M., Bankó, É., Harza, I., Antal, A. & Vidnyánszky, Z. (2006). Electrophysiological correlates of visual adaptation to faces and body parts in humans. *Cerebral Cortex*, **16**, 742 –753. 97

Lee, K.J. & Perrett, D. (1997). Presentation-time measures of the effects of manipulations in colour space on discrimination of famous faces. *Perception*, **26**, 733–752, PMID: 9474343. 98

Leopold, D.A., Rhodes, G., Mueller, K. & Jeffery, L. (2005). The dynamics of visual adaptation to faces. *Proceedings. Biological Sciences / The Royal Society*, **272**, 897–904, PMID: 16024343. 131

Lewis, M.B. & Edmonds, A.J. (2003). Face detection: mapping human performance. *Perception*, **32**, 903–920, PMID: 14580138. 43

Li, L., Miller, E.K. & Desimone, R. (1993). The representation of stimulus familiarity in anterior inferior temporal cortex. *Journal of Neurophysiology*, **69**, 1918–1929, PMID: 8350131. 97

Linkenkaer-Hansen, K., Palva, J.M., Sams, M., Hietanen, J.K., Aronen, H.J. & Ilmoniemi, R.J. (1998). Face-selective processing in human extrastriate cortex around 120 ms after stimulus onset revealed by magneto- and electroencephalography. *Neuroscience Letters*, **253**, 147–150, PMID: 9792232. 45, 48, 49, 50, 89

Liu, J., Higuchi, M., Marantz, A. & Kanwisher, N. (2000). The selectivity of the occipitotemporal m170 for faces. *Neuroreport*, **11**, 337–341, PMID: 10674482. 44

Liu, J., Harris, A. & Kanwisher, N. (2002). Stages of processing in face perception: an MEG study. *Nature Neuroscience*, **5**, 910–916, PMID: 12195430. 43, 89

Liu, J., Harris, A. & Kanwisher, N. (2010). Perception of face parts and face configurations: An fMRI study. *Journal of cognitive neuroscience*, **22**, 203–211, PMID: 19302006 PMCID: 2888696. 1, 33, 34

Loffler, G., Yourganov, G., Wilkinson, F. & Wilson, H.R. (2005). fMRI evidence for the neural representation of faces. *Nat Neurosci*, **8**, 1386–1391. 31

Luck, S. & Handy, T. (2005). *Ten Simple Rules for Designing and Interpreting ERP Experiments*. 10

Luck, S.J. (2005). *An Introduction to the Event-Related Potential Technique*. The MIT Press, 1st edn. 10, 11

Macknik, S.L. (2006). Visual masking approaches to visual awareness. *Progress in Brain Research*, **155**, 177–215, PMID: 17027388. 161

Makeig, S., Westerfield, M., Jung, T.P., Enghoff, S., Townsend, J., Courchesne, E. & Sejnowski, T.J. (2002). Dynamic brain sources of visual evoked responses. *Science (New York, N.Y.)*, **295**, 690–694, PMID: 11809976. 20

Mangun, G.R. (1995). Neural mechanisms of visual selective attention. *Psychophysiology*, **32**, 4–18, PMID: 7878167. 12

Marotta, J.J., Genovese, C.R. & Behrmann, M. (2001). A functional MRI study of face recognition in patients with prosopagnosia. *Neuroreport*, **12**, 1581–1587, PMID: 11409720. 47

Mattson, A., Levin, H. & Grafman, J. (2000). A case of prosopagnosia following moderate closed head injury with left hemisphere focal lesion. *Cortex*, **36**, 125–137. 24, 25

Mayes, A.K., Pipingas, A., Silberstein, R.B. & Johnston, P. (2009). Steady state visually evoked potential correlates of static and dynamic emotional face processing. *Brain Topography*, **22**, 145–157. 129

Mazaheri, A. & Jensen, O. (2006). Posterior alpha activity is not phase-reset by visual stimuli. *Proceedings of the National Academy of Sciences of the United States of America*, **103**, 2948–2952, PMID: 16473952. 20

McCarthy, G., Puce, A., Belger, A. & Allison, T. (1999). Electrophysiological studies of human face perception. II: response properties of face-specific potentials generated in occipitotemporal cortex. *Cerebral Cortex (New York, N.Y.: 1991)*, **9**, 431–444, PMID: 10450889. 2, 30, 31, 33, 130

McCarthy, G., Puce, A., Gore, J.C. & Allison, T. (2011). Face-Specific processing in the human fusiform gyrus. *Journal of Cognitive Neuroscience*, **9**, 605–610. 1, 31

McCormick, D.A. & Bal, T. (1994). Sensory gating mechanisms of the thalamus. *Current Opinion in Neurobiology*, **4**, 550–556, PMID: 7812144. 94

Mcgeorge, A.P. (1978). Visual evoked potentials in man: New developments. *Journal of Neurology, Neurosurgery, and Psychiatry*, **41**, 579–579, undefinedPMCID: 493090. 92, 93

Meadows, J.C. (1974). The anatomical basis of prosopagnosia. *Journal of Neurology, Neurosurgery, and Psychiatry*, **37**, 489–501, PMID: 4209556. 180

Mentis, M.J., Alexander, G.E., Grady, C.L., Horwitz, B., Krasuski, J., Pietrini, P., Strassburger, T., Hampel, H., Schapiro, M.B. & Rapoport, S.I. (1997). Frequency variation of a pattern-flash visual stimulus during PET differentially activates brain from striate through frontal cortex. *NeuroImage*, **5**, 116–128, PMID: 9345542. 93, 95, 157, 161

Milner, B.A., Regan, D. & Heron, J.R. (1974). Differential diagnosis of multiple sclerosis by visual evoked potential recording. *Brain: A Journal of Neurology*, **97**, 755–772, PMID: 4434192. 92

Moeller, S., Freiwald, W.A. & Tsao, D.Y. (2008). Patches with links: A unified system for processing faces in the macaque temporal lobe. *Science*, **320**, 1355 –1359. 34

Morgan, S.T., Hansen, J.C. & Hillyard, S.A. (1996). Selective attention to stimulus location modulates the steady-state visual evoked potential. *Proceedings of the National Academy of Sciences of the United States of America*, **93**, 4770–4774, PMID: 8643478 PMCID: 39354. 129

Morris, J.S., Frith, C.D., Perrett, D.I., Rowland, D., Young, A.W., Calder, A.J. & Dolan, R.J. (1996). A differential neural response in the human amygdala to fearful and happy facial expressions. *Nature*, **383**, 812–815. 36

# REFERENCES


Mur, M., Ruff, D.A., Bodurka, J., Bandettini, P.A. & Kriegeskorte, N. (2010). Face-Identity change activation outside the face system: "Release from adaptation" may not always indicate neuronal selectivity. *Cerebral Cortex*, **20**, 2027 – 2042. 40

Naesaenen, R. (1999). Spatial frequency bandwidth used in the recognition of facial images. *Vision Research*, **39**, 3824–3833, PMID: 10748918. 53

Neuenschwander, S. & Singer, W. (1996). Long-range synchronization of oscillatory light responses in the cat retina and lateral geniculate nucleus. *Nature*, **379**, 728–732, PMID: 8602219. 94

Nicol, D.S., Hamilton, R., Shahani, U. & McCulloch, D.L. (2011). Monocular and binocular steady-state flicker VEPs: frequency–response functions to sinusoidal and square-wave luminance modulation. *Documenta Ophthalmologica*, **122**, 63–70. 15

Noss, R.S., Boles, C.D. & Yingling, C.D. (1996). Steady-state analysis of somatosensory evoked potentials. *Electroencephalography and Clinical Neurophysiology*, **100**, 453–461, PMID: 8893664. 12

Nuñez, A., Amzica, F. & Steriade, M. (1992). Intrinsic and synaptically generated delta (1-4 hz) rhythms in dorsal lateral geniculate neurons and their modulation by light-induced fast (30-70 hz) events. *Neuroscience*, **51**, 269–284, PMID: 1465192. 94

Nunez, P.L. & Srinivasan, R. (2005). *Electric Fields of the Brain: The Neurophysics of EEG, 2nd Edition*. Oxford University Press, USA, 2nd edn. 6, 8, 44, 45, 161, 189

O'Donnell, C. & Bruce, V. (2001). Familiarisation with faces selectively enhances sensitivity to changes made to the eyes. *Perception*, **30**, 755–764, PMID: 11464563. 98, 127

Oram, M.W. & Perrett, D.I. (1996). Integration of form and motion in the anterior superior temporal polysensory area (STPa) of the macaque monkey. *Journal of Neurophysiology*, **76**, 109–129, PMID: 8836213. 2

Orban de Xivry, J., Ramon, M., Lefevre, P. & Rossion, B. (2008). Reduced fixation on the upper area of personally familiar faces following acquired prosopagnosia. *Journal of Neuropsychology*, **2**, 245–268, PMID: 19334313. 26, 101

O'Toole, A.J., Vetter, T. & Blanz, V. (1999). Three-dimensional shape and two-dimensional surface reflectance contributions to face recognition: an application of three-dimensional morphing. *Vision Research*, **39**, 3145–3155, PMID: 10664810. 131

Parente, R. & Tommasi, L. (2008). A bias for the female face in the right hemisphere. *Laterality: Asymmetries of Body, Brain and Cognition*, **13**, 374–386. 128

Pascual-Marqui, R.D., Michel, C.M. & Lehmann, D. (1994). Low resolution electromagnetic tomography: a new method for localizing electrical activity in the brain. *International Journal of Psychophysiology: Official Journal of the International Organization of Psychophysiology*, **18**, 49–65, PMID: 7876038. 45

Pastor, M.A., Artieda, J., Arbizu, J., Valencia, M. & Masdeu, J.C. (2003). Human cerebral activation during steady-state visual-evoked responses. *The Journal of Neuroscience: The Official Journal of the Society for Neuroscience*, **23**, 11621–11627, PMID: 14684864. 93, 94

Pastor, M.A., Valencia, M., Artieda, J., Alegre, M. & Masdeu, J.C. (2007). Topography of cortical activation differs for fundamental and harmonic frequencies of the steady-state visual-evoked responses. an EEG and PET H215O study. *Cerebral Cortex (New York, N.Y.: 1991)*, **17**, 1899–1905, PMID: 17060366. 15, 162

Pei, F., Pettet, M.W. & Norcia, A.M. (2002). Neural correlates of object-based attention. *Journal of Vision*, **2**, 588–596, PMID: 12678630. 12

Perrett, D.I., Rolls, E.T. & Caan, W. (1982). Visual neurones responsive to faces in the monkey temporal cortex. *Experimental Brain Research. Experimentelle Hirnforschung. Expérimentation Cérébrale*, **47**, 329–342, PMID: 7128705. 30, 130

Perrett, D.I., Smith, P.A., Mistlin, A.J., Chitty, A.J., Head, A.S., Potter, D.D., Broennimann, R., Milner, A.D. & Jeeves, M.A. (1985). Visual analysis of body movements by neurones in the temporal cortex of the macaque monkey: a preliminary report. *Behavioural Brain Research*, **16**, 153–170, PMID: 4041214. 2

Phillips, M.L., Young, A.W., Scott, S.K., Calder, A.J., Andrew, C., Giampietro, V., Williams, S.C., Bullmore, E.T., Brammer, M. & Gray, J.A. (1998). Neural responses to facial and vocal expressions of fear and disgust. *Proceedings of the Royal Society B: Biological Sciences*, **265**, 1809–1817, PMID: 9802236 PMCID: 1689379. 36

Pikovsky, A., Rosenblum, M. & Kurths, J. (2003). *Synchronization: A Universal Concept in Nonlinear Sciences*. Cambridge University Press, 1st edn. 20

Pitcher, D., Walsh, V., Yovel, G. & Duchaine, B. (2007). TMS evidence for the involvement of the right occipital face area in early face processing. *Current Biology*, **17**, 1568–1573. 1, 34, 48

Pitcher, D., Walsh, V. & Duchaine, B. (2011). The role of the occipital face area in the cortical face perception network. *Experimental Brain Research. Experimentelle Hirnforschung. Expérimentation Cérébrale*, **209**, 481–493, PMID: 21318346. 1, 48

Pizzagalli, D.A., Lehmann, D., Hendrick, A.M., Regard, M., Pascual-Marqui, R.D. & Davidson, R.J. (2002). Affective judgments of faces modulate early activity (approximately 160 ms) within the fusiform gyri. *NeuroImage*, **16**, 663–677, PMID: 12169251. 45

Plourde, G. & Villemure, C. (1996). Comparison of the effects of enflurane/N2O on the 40-Hz auditory steady-state response versus the auditory middle-latency response. *Anesthesia and Analgesia*, **82**, 75–83, PMID: 8712429. 19

Podvigin, N.F., Bagaeva, T.V., Boykova, E.V., Zargarov, A.A., Podvigina, D.N. & Pöppel, E. (2004). Three bands of oscillatory activity in the lateral geniculate nucleus of the cat visual system. *Neuroscience Letters*, **361**, 83–85, PMID: 15135899. 162

Pourtois, G., Grandjean, D., Sander, D. & Vuilleumier, P. (2004). Electrophysiological correlates of rapid spatial orienting towards fearful faces. *Cerebral Cortex*, **14**, 619 –633. 11

Puce, A., Allison, T., Bentin, S., Gore, J.C. & McCarthy, G. (1998). Temporal cortex activation in humans viewing eye and mouth movements. *The Journal of Neuroscience: The Official Journal of the Society for Neuroscience*, **18**, 2188–2199, PMID: 9482803. 31, 33, 48

Puce, A., Allison, T. & McCarthy, G. (1999). Electrophysiological studies of human face perception. III: effects of top-down processing on face-specific potentials. *Cerebral Cortex (New York, N.Y.: 1991)*, **9**, 445–458, PMID: 10450890. 2, 30, 31, 130

Puce, A., Syngeniotis, A., Thompson, J.C., Abbott, D.F., Wheaton, K.J. & Castiello, U. (2003). The human temporal lobe integrates facial form and motion: evidence from fMRI and ERP studies. *NeuroImage*, **19**, 861–869, PMID: 12880814. 2, 36

Rager, G. & Singer, W. (1998). The response of cat visual cortex to flicker stimuli of variable frequency. *The European Journal of Neuroscience*, **10**, 1856–1877, PMID: 9751156. 12, 93, 94, 157

Ramon, M. & Rossion, B. (2010). Impaired processing of relative distances between features and of the eye region in acquired prosopagnosia–two sides of the same holistic coin? *Cortex; a Journal Devoted to the Study of the Nervous System and Behavior*, **46**, 374–389, PMID: 19589510. 25, 26

Ramon, M., Dricot, L., Goebel, R. & Rossion, B. (2009). The right FFA is sensitive to subtle physical changes between personally familiar faces. *Journal of Vision*, **9**, 463. 25, 40

Ramon, M., Busigny, T. & Rossion, B. (2010a). Impaired holistic processing of unfamiliar individual faces in acquired prosopagnosia. *Neuropsychologia*, **48**, 933–944, PMID: 19944710. 25, 85

Ramon, M., Dricot, L. & Rossion, B. (2010b). Personally familiar faces are perceived categorically in faceselective regions other than the fusiform face area. *European Journal of Neuroscience*, **32**, 1587–1598. 25

Reddy, L., Moradi, F. & Koch, C. (2007). Top-down biases win against focal attention in the fusiform face area. *NeuroImage*, **38**, 730–739, PMID: 17904388. 50

Regan, D. (1966). Some characteristics of average steady-state and transient responses evoked by modulated light. *Electroencephalography and Clinical Neurophysiology*, **20**, 238–248. 8, 12, 97, 129, 157

Regan, D. (1968a). Chromatic adaptation and steady-state evoked potentials. *Vision Research*, **8**, 149–158, PMID: 5729326. 12, 129, 157

Regan, D. (1968b). A high frequency mechanism which underlies visual evoked potentials. *Electroencephalography and Clinical Neurophysiology*, **25**, 231–237, PMID: 4176925. 91, 92, 157

Regan, D. (1972). *Evoked Potentials in Psychology Sensory Physiology and Clinical Medicine*. Springer, 1st edn. 92, 93, 97

Regan, D. (1989). *Human brain electrophysiology : evoked potentials and evoked magnetic fields in science and medicine*. Elsevier, New York. 8, 11, 12, 13, 15, 19, 91, 92, 93, 97, 129, 157

Regan, D. (2009). Some early uses of evoked brain responses in investigations of human visual function. *Vision Research*, **49**, 882–897, PMID: 18304602. 12, 92, 97, 129, 157

Regan, D. & Lee, B.B. (1993). A comparison of the 40-Hz response in man, and the properties of macaque ganglion cells. *Visual Neuroscience*, **10**, 439–445, PMID: 8494797. 92

Regan, M. & Regan, D. (1988). A frequency domain technique for characterizing nonlinearities in biological systems. *Journal of Theoretical Biology*, **133**, 293–317. 12, 19, 97

Renault, B., Signoret, J.L., Debruille, B., Breton, F. & Bolgert, F. (1989). Brain potentials reveal covert facial recognition in prosopagnosia. *Neuropsychologia*, **27**, 905–912, PMID: 2771029. 49

Rhodes, G. (1985). Perceptual asymmetries in face recognition. *Brain and Cognition*, **4**, 197–218, PMID: 4015874. 128

Rhodes, G., Michie, P.T., Hughes, M.E. & Byatt, G. (2009). The fusiform face area and occipital face area show sensitivity to spatial relations in faces. *The European Journal of Neuroscience*, **30**, 721–733, PMID: 19674084. 34

Righart, R., Andersson, F., Schwartz, S., Mayer, E. & Vuilleumier, P. (2010). Top-down activation of fusiform cortex without seeing faces in prosopagnosia. *Cerebral Cortex (New York, N.Y.: 1991)*, **20**, 1878–1890, PMID: 19939884. 50

Ringo, J.L. (1996). Stimulus specific adaptation in inferior temporal and medial temporal cortex of the monkey. *Behavioural Brain Research*, **76**, 191–197, PMID: 8734053. 97

Ritter, W., Simson, R., Vaughan, J., H G & Friedman, D. (1979). A brain event related to the making of a sensory discrimination. *Science (New York, N.Y.)*, **203**, 1358–1361, PMID: 424760. 12

Rosburg, T., Ludowig, E., Dümpelmann, M., Alba-Ferrara, L., Urbach, H. & Elger, C.E. (2010). The effect of face inversion on intracranial and scalp recordings of event-related potentials. *Psychophysiology*, **47**, 147–157, PMID: 19761525. 89

Rossion, B. (2003). A network of occipito-temporal face-sensitive areas besides the right middle fusiform gyrus is necessary for normal face processing. *Brain*, **126**, 2381–2395. 25, 26, 27, 33, 47, 48, 50, 84, 166, 168, 179, 180

Rossion, B. (2008). Constraining the cortical face network by neuroimaging studies of acquired prosopagnosia. *NeuroImage*, **40**, 423–426, PMID: 18086537. vii, 1, 25, 36, 37, 47, 48

Rossion, B. & Boremanse, A. (2011). Robust sensitivity to facial identity in the right human occipito-temporal cortex as revealed by steady-state visual-evoked potentials. *Journal of Vision*, **11**. 4, 5, 96, 97, 98, 99, 100, 128, 129, 130

# REFERENCES


Rossion, B. & Caharel, S. (2011). ERP evidence for the speed of face categorization in the human brain: Disentangling the contribution of low-level visual cues from face perception. *Vision Research*, **51**, 1297–1311, PMID: 21549144. 2, 11, 38, 44, 49, 51, 53, 58, 86, 99, 130, 162

Rossion, B. & Jacques, C. (2008). Does physical interstimulus variance account for early electrophysiological face sensitive responses in the human brain? ten lessons on the n170. *NeuroImage*, **39**, 1959–1979, PMID: 18055223. 67, 86, 99

Rossion, B. & Jacques, C. (2010). *The Oxford Handbook of Event-Related Potential Components*, chap. The N170: understanding the time course of face perception in the human brain. Oxford University Press, Oxford, UK. 39, 48, 49, 85

Rossion, B., Delvenne, J.F., Debatisse, D., Goffaux, V., Bruyer, R., Crommelinck, M. & Guérit, J.M. (1999). Spatio-temporal localization of the face inversion effect: an event-related potentials study. *Biological Psychology*, **50**, 173–189, PMID: 10461804. 2, 50

Rossion, B., Dricot, L., Devolder, A., Bodart, J.M., Crommelinck, M., De Gelder, B. & Zoontjes, R. (2000a). Hemispheric asymmetries for whole-based and part-based face processing in the human fusiform gyrus. *Journal of Cognitive Neuroscience*, **12**, 793–802, PMID: 11054921. 1, 25, 31, 33, 162

Rossion, B., Gauthier, I., Tarr, M.J., Despland, P., Bruyer, R., Linotte, S. & Crommelinck, M. (2000b). The n170 occipito-temporal component is delayed and enhanced to inverted faces but not to inverted objects: an electrophysiological account of face-specific processes in the human brain. *Neuroreport*, **11**, 69–74, PMID: 10683832. 2, 38, 99, 162

Rossion, B., Joyce, C.A., Cottrell, G.W. & Tarr, M.J. (2003a). Early lateralization and orientation tuning for face, word, and object processing in the visual cortex. *NeuroImage*, **20**, 1609–1624, PMID: 14642472. 2, 45, 85, 87, 99, 162, 166

Rossion, B., Schiltz, C. & Crommelinck, M. (2003b). The functionally defined right occipital and fusiform "face areas" discriminate novel from visually familiar faces. *NeuroImage*, **19**, 877–883, PMID: 12880816. 25, 26, 51, 84

Rossion, B., Dricot, L., Goebel, R. & Busigny, T. (2011). Holistic face categorization in higher order visual areas of the normal and prosopagnosic brain: toward a non-hierarchical view of face perception. *Frontiers in Human Neuroscience*, **4**, 225, PMID: 21267432. 25, 31, 36, 48, 84, 85, 166

Rotshtein, P., Henson, R.N.A., Treves, A., Driver, J. & Dolan, R.J. (2005). Morphing marilyn into maggie dissociates physical and identity face representations in the brain. *Nat Neurosci*, **8**, 107–113. 34

Rousselet, G.A., Mace, M.J. & Fabre-Thorpe, M. (2003). Is it an animal? is it a human face? fast processing in upright and inverted natural scenes. *Journal of Vision*, **3**, 440–455, PMID: 12901715. 43

Rousselet, G.A., Husk, J.S., Bennett, P.J. & Sekuler, A.B. (2005). Spatial scaling factors explain eccentricity effects on face ERPs. *Journal of Vision*, **5**, 755–763, PMID: 16441183. 53

Rousselet, G.A., Husk, J.S., Bennett, P.J. & Sekuler, A.B. (2007). Single-trial EEG dynamics of object and face visual processing. *NeuroImage*, **36**, 843–862, PMID: 17475510. 38

Russell, R., Biederman, I., Nederhouser, M. & Sinha, P. (2007). The utility of surface reflectance for the recognition of upright and inverted faces. *Vision Research*, **47**, 157–165, PMID: 17174375. 98

Sadeh, B. & Yovel, G. (2010). Why is the n170 enhanced for inverted faces? an ERP competition experiment. *NeuroImage*, **53**, 782–789. 86, 87

Sagiv, N. & Bentin, S. (2001). Structural encoding of human and schematic faces: holistic and part-based processes. *Journal of Cognitive Neuroscience*, **13**, 937–951, PMID: 11595097. 2, 38, 85

Sams, M., Hietanen, J.K., Hari, R., Ilmoniemi, R.J. & Lounasmaa, O.V. (1997). Face-specific responses from the human inferior occipito-temporal cortex. *Neuroscience*, **77**, 49–55, PMID: 9044373. 45

Sander, D., Andres, M., Grandjean, D., Reveret, L., Olivier, E., Vuilleumier, P. & Pourtois, G. (2004). Dissociable roles of the human somatosensory and superior temporal cortices for processing social face signals. *European Journal of Neuroscience*, **20**, 3507–3515. 31

Santarelli, R., Maurizi, M., Conti, G., Ottaviani, F., Paludetti, G. & Pettorossi, V.E. (1995). Generation of human auditory steady-state responses (SSRs). II: addition of responses to individual stimuli. *Hearing Research*, **83**, 9–18. 17, 19

Sauseng, P., Klimesch, W., Gruber, W.R., Hanslmayr, S., Freunberger, R. & Doppelmayr, M. (2007). Are event-related potential components generated by phase resetting of brain oscillations? a critical discussion. *Neuroscience*, **146**, 1435–1444, PMID: 17459593. 20

Sayers, B.M., Beagley, H.A. & Henshall, W.R. (1974). The mechansim of auditory evoked EEG responses. *Nature*, **247**, 481–483, PMID: 4818547. 20

Scherg, M. & Ebersole, J.S. (1994). Brain source imaging of focal and multifocal epileptiform EEG activity. *Neurophysiologie Clinique = Clinical Neurophysiology*, **24**, 51–60, PMID: 8121338. 45

Schiltz, C., Sorger, B., Caldara, R., Ahmed, F., Mayer, E., Goebel, R. & Rossion, B. (2006). Impaired face discrimination in acquired prosopagnosia is associated with abnormal response to individual faces in the right middle fusiform gyrus. *Cerebral Cortex (New York, N.Y.: 1991)*, **16**, 574–586, PMID: 16033923. 26, 31, 33, 36, 51, 84, 85, 166

Schuermann, M. & Basar, E. (1994). Topography of alpha and theta oscillatory responses upon auditory and visual stimuli in humans. *Biological Cybernetics*, **72**, 161–174, PMID: 7880920. 94

Schweinberger, S.R., Pfütze, E. & Sommer, W. (1995). Repetition priming and associative priming of face recognition: Evidence from Event-Related potentials. *Journal of Experimental Psychology: Learning, Memory, and Cognition*, **21**, 722–736. 99

Schweinberger, S.R., Pickering, E.C., Jentzsch, I., Burton, A.M. & Kaufmann, J.M. (2002). Event-related brain potential evidence for a response of inferior temporal cortex to familiar face repetitions. *Brain Research. Cognitive Brain Research*, **14**, 398–409, PMID: 12421663. 45

Sergent, J. & Signoret, J.L. (1992). Varieties of functional deficits in prosopagnosia. *Cerebral Cortex (New York, N.Y.: 1991)*, **2**, 375–388, PMID: 1422092. 1, 24, 30, 33, 47

Sergent, J., Ohta, S. & Macdonald, B. (1992). Functional neuroanatomy of face and object processing. *Brain*, **115**, 15 –36. 31, 35, 47

Shah, A.S., Bressler, S.L., Knuth, K.H., Ding, M., Mehta, A.D., Ulbert, I. & Schroeder, C.E. (2004). Neural dynamics and the fundamental mechanisms of event-related brain potentials. *Cerebral Cortex (New York, N.Y.: 1991)*, **14**, 476–483, PMID: 15054063. 20

Shea, S.J., Chandna, A. & Norcia, A.M. (1999). Oscillatory motion but not pattern reversal elicits monocular motion VEP biases in infantile esotropia. *Vision Research*, **39**, 1803–1811, PMID: 10343872. 12

Silberstein, R.B., Nunez, P.L., Pipingas, A., Harris, P. & Danieli, F. (2001). Steady state visually evoked potential (SSVEP) topography in a graded working memory task. *International Journal of Psychophysiology: Official Journal of the International Organization of Psychophysiology*, **42**, 219–232, PMID: 11587778. 97

Singer, W. (1977). Control of thalamic transmission by corticofugal and ascending reticular pathways in the visual system. *Physiological Reviews*, **57**, 386–420, PMID: 196301. 94

Singh, M., Kim, S. & Kim, T. (2003). Correlation between BOLD-fMRI and EEG signal changes in response to visual stimulus frequency in humans. *Magnetic Resonance in Medicine: Official Journal of the Society of Magnetic Resonance in Medicine / Society of Magnetic Resonance in Medicine*, **49**, 108–114, PMID: 12509825. 93, 94

Sinha, P. & Poggio, T. (1996). I think i know that face.. *Nature*, **384**, 404, PMID: 8945457. 98, 127

Sinha, P. & Poggio, T. (2002). 'United' we stand. *Perception*, **31**, 133, PMID: 11922119. 98, 127

Snodgrass, J.G. & Vanderwart, M. (1980). A standardized set of 260 pictures: norms for name agreement, image agreement, familiarity, and visual complexity. *Journal of Experimental Psychology. Human Learning and Memory*, **6**, 174–215, PMID: 7373248. 26

Sorger, B., Goebel, R., Schiltz, C. & Rossion, B. (2007). Understanding the functional neuroanatomy of acquired prosopagnosia. *NeuroImage*, **35**, 836–852, PMID: 17303440. 25, 26, 48, 50, 51, 52, 84, 85, 87, 88, 89, 166

Spekreijse, H. (1969). Rectification in the goldfish retina: analysis by sinusoidal and auxiliary stimulation. *Vision Research*, **9**, 1461–1472, PMID: 5367436. 19

Spekreijse, H., van Norren, D. & van den Berg, T.J. (1971). Flicker responses in monkey lateral geniculate nucleus and human perception of flicker. *Proceedings of the National Academy of Sciences of the United States of America*, **68**, 2802–2805, PMID: 5001396. 19

Spekreyse, H. & Tweel, L.H.V.D. (1965). Linearization of evoked responses to sine wave-modulated light by noise. *Nature*, **205**, 913–913. 19

Srinivasan, R. (2004). Internal and external neural synchronization during conscious perception. *International Journal of Bifurcation and Chaos in Applied Sciences and Engineering*, **14**, 825–842, PMID: 17898863. 97

Srinivasan, R., Russell, D.P., Edelman, G.M. & Tononi, G. (1999). Increased synchronization of neuromagnetic responses during conscious perception. *The Journal of Neuroscience: The Official Journal of the Society for Neuroscience*, **19**, 5435–5448, PMID: 10377353. 97, 103

Srinivasan, R., Bibi, F.A. & Nunez, P.L. (2006). Steady-state visual evoked potentials: distributed local sources and wave-like dynamics are sensitive to flicker frequency. *Brain topography*, **18**, 167–187, PMID: 16544207 PMCID: 1995016. 93

Stapells, D.R., Galambos, R., Costello, J.A. & Makeig, S. (1988). Inconsistency of auditory middle latency and steady-state responses in infants. *Electroencephalography and Clinical Neurophysiology/Evoked Potentials Section*, **71**, 289–295. 17

Steeves, J.K.E., Culham, J.C., Duchaine, B.C., Pratesi, C.C., Valyear, K.F., Schindler, I., Humphrey, G.K., Milner, A.D. & Goodale, M.A. (2006). The fusiform face area is not sufficient for face recognition: evidence from a patient with dense prosopagnosia and no occipital face area. *Neuropsychologia*, **44**, 594–609, PMID: 16125741. 36, 48

Steriade, M. & Amzica, F. (1996). Intracortical and corticothalamic coherency of fast spontaneous oscillations. *Proceedings of the National Academy of Sciences of the United States of America*, **93**, 2533–2538, PMID: 8637909. 94

Steriade, M., Gloor, P., Llinas, R.R., Lopes de Silva, F.H. & Mesulam, M.M. (1990). Report of IFCN committee on basic mechanisms. basic mechanisms of cerebral rhythmic activities. *Electroencephalography and Clinical Neurophysiology*, **76**, 481–508, PMID: 1701118. 94

Steriade, M., Dossi, R.C., Pare, D. & Oakson, G. (1991). Fast oscillations (20-40 hz) in thalamocortical systems and their potentiation by mesopontine cholinergic nuclei in the cat. *Proceedings of the National Academy of Sciences of the United States of America*, **88**, 4396–4400, PMID: 2034679. 94

Steriade, M., McCormick, D.A. & Sejnowski, T.J. (1993). Thalamocortical oscillations in the sleeping and aroused brain. *Science (New York, N.Y.)*, **262**, 679–685, PMID: 8235588. 94

Suzuki, T., Kobayashi, K. & Umegaki, Y. (1994). Effect of natural sleep on auditory steady state responses in adult subjects with normal hearing. *Audiology: Official Organ of the International Society of Audiology*, **33**, 274–279, PMID: 7818381. 19

Swithenby, S.J., Bailey, A.J., Braeutigam, S., Josephs, O.E., Jousmaeki, V. & Tesche, C.D. (1998). Neural processing of human faces: a magnetoencephalographic study. *Experimental Brain Research*, **118**, 501–510, PMID: 9504845. 45

# REFERENCES


Tanaka, J.W., Curran, T., Porterfield, A.L. & Collins, D. (2006). Activation of preexisting and acquired face representations: The n250 event-related potential as an index of face familiarity. *J. Cognitive Neuroscience*, **18**, 1488–1497, ACM ID: 1176423. 99

Tanskanen, T., Naesaenen, R., Montez, T., Paeaellysaho, J. & Hari, R. (2005). Face recognition and cortical responses show similar sensitivity to noise spatial frequency. *Cerebral Cortex (New York, N.Y.: 1991)*, **15**, 526–534, PMID: 15319307. 40, 43

Tarkiainen, A., Cornelissen, P.L. & Salmelin, R. (2002). Dynamics of visual feature analysis and object-level processing in face versus letter-string perception. *Brain: A Journal of Neurology*, **125**, 1125–1136, PMID: 11960901. 45

Tasman, M., William & Jaeger, M., Edward A. (2001). *Duane's Clinical Ophthalmology: 2001 Edition*. Lippincott Williams & Wilkins, cdr edn. 10

Taulu, S. & Simola, J. (2006). Spatiotemporal signal space separation method for rejecting nearby interference in MEG measurements. *Physics in Medicine and Biology*, **51**, 1759–1768, PMID: 16552102. 56

Taylor, M.J., Itier, R.J., Allison, T. & Edmonds, G.E. (2001). Direction of gaze effects on early face processing: eyes-only versus full faces. *Brain Research. Cognitive Brain Research*, **10**, 333–340, PMID: 11167057. 45

Thorpe, S.G., Nunez, P.L. & Srinivasan, R. (2007). Identification of wave-like spatial structure in the SSVEP: comparison of simultaneous EEG and MEG. *Statistics in Medicine*, **26**, 3911–3926, PMID: 17671957. 93

Thut, G. & Gross, J. (2011). Entrainment of perceptually relevant brain oscillations by non-invasive rhythmic stimulation of the human brain. *Frontiers in Perception Science*, **2**, 170. 21

Tranel, D., Damasio, A.R. & Damasio, H. (1988). Intact recognition of facial expression, gender, and age in patients with impaired recognition of face identity. *Neurology*, **38**, 690–696, PMID: 3362363. 23

Troje, N.F. & Buelthoff, H.H. (1996). Face recognition under varying poses: the role of texture and shape. *Vision Research*, **36**, 1761–1771, PMID: 8759445. 98, 100

Tsao, D.Y., Freiwald, W.A., Tootell, R.B.H. & Livingstone, M.S. (2006). A cortical region consisting entirely of face-selective cells. *Science (New York, N.Y.)*, **311**, 670–674, PMID: 16456083. 30

Tyler, C.W. & Kaitz, M. (1977). Movement adaptation in the visual evoked response. *Experimental Brain Research. Experimentelle Hirnforschung. Expérimentation Cérébrale*, **27**, 203–209, PMID: 838009. 129

van den Broek, S.P., Reinders, F., Donderwinkel, M. & Peters, M.J. (1998). Volume conduction effects in EEG and MEG. *Electroencephalography and Clinical Neurophysiology*, **106**, 522–534, PMID: 9741752. 3, 167

Van der Tweel, L.H. & Lunel, H.F. (1965). Human visual responses to sinusoidally modulated light. *Electroencephalography and Clinical Neurophysiology*, **18**, 587–598, PMID: 14296836. 91, 93, 129

Van Essen, D.C., Newsome, W.T., Maunsell, J.H. & Bixby, J.L. (1986). The projections from striate cortex (V1) to areas v2 and v3 in the macaque monkey: asymmetries, areal boundaries, and patchy connections. *The Journal of Comparative Neurology*, **244**, 451–480, PMID: 3958238. 36

Vaughan, H.G. (1972). Evoked potentials in psychology, sensory physiology and clinical medicine. d. regan. Wiley-Interscience, new york, 1972. xvi, 328 pp., illus. $15.95. *Science*, **178**, 150 –151. 8

Vinberg, J. & Grill-Spector, K. (2008). Representation of shapes, edges, and surfaces across multiple cues in the human visual cortex. *Journal of Neurophysiology*, **99**, 1380–1393, PMID: 18171705. 26, 179

Vinken, P.J. (1983). *Handbook of Clinical Neurology: Neurology, Neuroscience*. Elsevier Science Ltd, 1st edn. 22

Vogel, E.K. & Luck, S.J. (2000). The visual n1 component as an index of a discrimination process. *Psychophysiology*, **37**, 190–203, PMID: 10731769. 12

Vuong, Q.C., Peissig, J.J., Harrison, M.C. & Tarr, M.J. (2005). The role of surface pigmentation for recognition revealed by contrast reversal in faces and greebles. *Vision Research*, **45**, 1213–1223, PMID: 15733955. 98

Wang, Y., Wang, R., Gao, X., Hong, B. & Gao, S. (2006). A practical VEP-based brain-computer interface. *IEEE Transactions on Neural Systems and Rehabilitation Engineering: A Publication of the IEEE Engineering in Medicine and Biology Society*, **14**, 234–239, PMID: 16792302. 93, 103

Watanabe, S., Kakigi, R., Koyama, S. & Kirino, E. (1999). Human face perception traced by magneto- and electroencephalography. *Brain Research. Cognitive Brain Research*, **8**, 125–142, PMID: 10407202. 45, 49

Watanabe, S., Kakigi, R. & Puce, A. (2003). The spatiotemporal dynamics of the face inversion effect: A magneto- and electro-encephalographic study. *Neuroscience*, **116**, 879–895. 45, 53, 87, 89

Wernicke, C. (1874). *Der Aphasische Symptomencomplex: Eine Psychologische Studie Auf Anatomischer Basis*. Cohn und Weigert, Breslau. 22

Wigan, A.L. (2007). *A New View Of Insanity: The Duality Of The Mind Proved By The Structure, Functions And Diseases Of The Brain*. Kessinger Publishing, LLC. 23

Wilbrand, H. (2011). *Die Seelenblindheit: Als Herderscheinung Und Ihre Beziehungen Zur Homonymen Hemianopsie Zur Alexie Und Agraphie*. Nabu Press. 23

Winston, J.S., Henson, R., Fine-Goulden, M.R. & Dolan, R.J. (2004). fMRI-Adaptation reveals dissociable neural representations of identity and expression in face perception. *Journal of Neurophysiology*, **92**, 1830 –1839. 31, 40

Wright, H., Wardlaw, J., Young, A.W. & Zeman, A. (2006). Prosopagnosia following nonconvulsive status epilepticus associated with a left fusiform gyrus malformation. *Epilepsy & Behavior: E&B*, **9**, 197–203, PMID: 16777488. 24, 25

Yin, R.K. (1969). Looking at upside-down faces. *Journal of Experimental Psychology*, **81**, 141–145. 43

Young, A.W., Hay, D.C., McWeeny, K.H., Flude, B.M. & Ellis, A.W. (1985). Matching familiar and unfamiliar faces on internal and external features. *Perception*, **14**, 737–746, PMID: 3837875. 98, 127

Young, A.W., Hellawell, D. & Hay, D.C. (1987). Configurational information in face perception. *Perception*, **16**, 747–759, PMID: 3454432. 98

Yovel, G. & Kanwisher, N. (2004). Face perception: domain specific, not process specific. *Neuron*, **44**, 889–898, PMID: 15572118. 33

Yue, X., Cassidy, B.S., Devaney, K.J., Holt, D.J. & Tootell, R.B.H. (2011). Lower-level stimulus features strongly influence responses in the fusiform face area. *Cerebral Cortex (New York, N.Y.: 1991)*, **21**, 35–47, PMID: 20375074. 87